NORTHWESTERN UNIVERSITY

Extracellular Nucleotide Regulation of Airway Epithelial Cell Immunological Mediator Release

A DISSERTATION

SUBMITTED TO THE GRADUATE SCHOOL IN PARTIAL FULFILLMENT OF THE REQUIREMENTS

for the degree

DOCTOR OF PHILOSOPHY

Life Sciences

By

Timothy Kountz

EVANSTON, ILLINOIS

June 2022

Abstract

The airway epithelial cells (AECs) lining the conducting passageways of the lung secrete a variety of immunomodulatory factors. One interesting pair of molecules produces by AECs is IL-6 and prostaglandin E2 (PGE_2). PGE_2 limits lung inflammation and promotes bronchodilation. By contrast, IL-6 drives intense airway inflammation, remodeling, and fibrosis. The signaling that differentiates the production of these opposing mediators is not understood. In this thesis, we find that the production of PGE_2 and IL-6 following stimulation of AECs by the danger associated molecule pattern (DAMP), extracellular ATP, share a common requirement for Ca^{2+} release-activated Ca^{2+} (CRAC) channels. ATP-mediated synthesis of PGE_2 required activation of cell surface metabotropic $P2Y_2$ receptors and CRAC channel-mediated $cPLA_2$ signaling. By contrast, ATP-evoked synthesis of IL-6 occurred via activation of P2X receptors and CRAC channel-mediated calcineurin/NFAT signaling. In contrast to ATP, which elicited the production of both PGE_2 and IL-6, the uridine nucleotide, UTP, stimulated PGE_2 but not IL-6 production. These results reveal that AECs employ unique receptor-specific signaling mechanisms with CRAC channels as a signaling nexus to regulate release of opposing immunomodulatory mediators. Collectively, our results identify $P2Y_2$ receptors, CRAC channels, and P2X receptors as potential intervention targets for airway diseases.

The airway epithelial cells (AECs) lining the conducting airways of the lung form the first line of defense against a variety of inhaled pathogens, allergens and environmental irritants. When a respiratory virus infects cells within the airway epithelium, it provokes the release of numerous immunomodulatory mediators. One

essential component of a productive antiviral response is the production of interferons, a family of cytokines known to exhibit powerful antiviral influences. Cells derived from asthmatic patients are known to exhibit diminished interferon release. However, the cellular basis of this phenomenon is not well understood. In this thesis work, we find that two mediators known to be elevated in asthmatic airways, namely extracellular nucleotides and histamine, both potently inhibit the release of interferons from airway epithelial cells. Pharmacological evidence demonstrated that activation of G-protein coupled $P2Y_2$ and H_1 receptors elicited this effect. Differentiation of airway epithelial cells at an air-liquid interface confirmed that this phenotype is conserved following differentiation to develop mucociliary function. Mechanistically, receptor signaling through PKC was required to exert these inhibitory effects on interferon release. Significantly, histamine and ATP inhibited interferon release from airway cells infected with live influenza A virus. These results reveal a conserved role for G-protein coupled receptor signaling restraining release of interferons from airway epithelial cells. Collectively, our results provide a potential cellular and molecular basis for the observed limited interferon responses in asthmatic cells.

Acknowledgements

Isaac Newton is attributed with the quote, “If I have seen further it is by standing on the shoulders of giants”. During my time in graduate school, I may have seen a bit further in some areas of airway cell biology, but I would be remiss to claim the credit myself. First, I will thank my scientific mentors, then I will move to more personal mentors.

One memory early in my scientific training occurred in Mr. Betzler’s 8th grade science class. The homework was simple: jump rope for a set series of time and then measure your heart rate. Prior to the experiment, I had the unconscious hypothesis that as I jumped rope for longer periods of time, my heart rate would naturally increase. However, much to my dismay, the raw data did not precisely follow this trend and my heart rate slowed at the longest interval of jump roping. Without reflecting too much on the raw data, I altered the data to match my unconscious hypothesis. As I entered the classroom the next day to turn in the assignment, Mr. Betzler announced that he would know who had fabricated the experiment because he had asked us to take our pulse for 15 seconds and then multiple by four. Thus, all pulse values that were not multiples of four would be revealed to be fabricated. I was immediately dismayed. After class, I confessed my falsification of data to Mr. Betzler and he warned me that falsification of data was a serious offense and that I should steer clear of all such activity from that point on. Needless to say, the event had a long-term affect scientific outlook. Thank you Mr. Betzler for teaching me the importance of scientific integrity.

I had many great scientific teachers in high school, but time and space demands I focus on the major influencers. I came into college at the University of Washington intending to follow the pre-medicine route. At the end of my sophomore year, out of a

desire to strength my CV for medical school, I began volunteering in the laboratory of Dr. Chris Hague in the Pharmacology Department. Dr. Kyung-Soon Lee patiently trained me in lab techniques and Chris was an enthusiastic mentor. Chris has a deep love for training scientists and we connected quickly on a personal level. He was able to persuade me that graduate school and scientific research was a potential career tract that interested me. Chris gave me much autonomy in the lab and fanned into flame my passion for biological research.

Following graduation, my wife, Candace and I moved to Chicago and I worked as a technician in the laboratory of Dr. Philip Connell at the University of Chicago. Phil was an excellent mentor who spent hours training my mind to design efficient and effective experiments. It was in Phil's lab that my mind was resolved to enter upon graduate school training. I would also like to thank Brian Budke for how he trained me in my time at Dr. Connell's lab.

Upon my entrance at Northwestern, I was immediately drawn to Dr. Joan Cook-Mills' lab. It was here that I was introduced to immunology and the fantastic Allergy-Immunology Department. Joan encouraged me in my scientific interests and taught me many practical technical skills. I would like to thank Ashley Queener and Matthew Walker for their support and friendship in the lab.

I transition to Dr. Murali Prakriya's lab. Murali has been a fantastic supporter of my scientific training. I learned how to write scientifically from Murali. Murali granted me much independence in my scientific thinking. I particularly want to thank Murali for his willingness to allow me to pursue a project that was not directly related to CRAC channels. Collectively, Murali has been a huge component of my success as a graduate

student. My thesis committee has provided a plethora of scientific support over the years and I am indebted to Dr. Sergejs Berdnikovs, Dr. GR Scott Budinger, and Dr. Robert Schleimer. Dr. Robert Schleimer and Dr. Assel Biyasheva in particular provided scientific and technical support along the way. I would also like to thank Mehdi, Nisha, Mikki, Kate, Megumi, Kirill, Shogo, Kotoro, Martinna, Megan, Toneisha, Saki, Priscilla and Anna for their friendship and support over the years in the lab. We have shared many great scientific conversations and laughs over the years.

Moving to more personal acknowledgements, I would like to thank my family. My parents have always believed that I was intellectually capable, and over the years, this gave me great confidence to pursue academic pursuits. I would like to thank my two sisters for their witness to me over the years regarding my gifts and their friendship and support. I would like to thank all of my in-laws for their patience with me while I have kept their beloved Candace in Chicago these last two years. My wife Candace has been a steadfast pillar for me over the years. There have been innumerable times when I received encouragement and counseling from her in relation to my scientific pursuits. Needless to say, she has patiently listened to me discuss my scientific pursuits over the years. She is filled with much wisdom and I have leaned much on her over the years. Our marriage is certainly an uncommon union. Finally, the ultimate credit and acknowledgement belongs to God. I end my acknowledgements section with the Latin phrase, “*Soli Deo Gloria*”, “To God Alone be the Glory”.

Table of Contents

List of Figures

Chapter 1: Introduction

Asthma and Respiratory Viruses

Human airway diseases are a major burden on society and individuals. Airway diseases can be characterized as either chronic or acute. One chronic airway disease is asthma. Estimates are that approximately 10% of the world population suffers from asthma [2]. Asthma is a complex airway disease with hallmarks such as airway hyperresponsiveness, smooth muscle proliferation, decreased epithelial barrier function and goblet cell metaplasia [3, 4]. Inflammation is a common component of asthma as well, with approximately 50% of patients showing elevated type 2 inflammation [5]. Prototypical type 2 inflammation is linked to cell types such as Th2 and ILC2's releasing cytokines such as IL-4, IL-5, and IL-13 [5]. Type 2 inflammation is atopic, hence allergens play an important role. Common airway allergens implicated in asthma include house dust mite (HDM), pollen, cockroach, *Aspergillus fumigatus*, and ragweed [2]. HDM is the most common aeroallergen in humans [2]. Although historic therapeutic modalities include chronic treatment with inhaled corticosteroids and acute treatment with β_2-adrenergic receptor agonists, recent additions to the pharmacopoeia include modulators of interleukins and IgE [5, 6].

One genre of acute airway disease is infection with respiratory viruses. In the United States alone, estimates are that 29-59 million people are infected annually with influenza virus and approximately 36,000 die [7]. However, these numbers can significantly increase upon a pandemic such as in 1918, when estimates are that 50 million deaths occurred globally [8]. More recently, we have witnessed the emergence of the SARS-CoV-2 pandemic. Other respiratory viruses that cause the common cold,

such as human rhinovirus, also exact a significant economic burden on society [9]. Although vaccines do exist for some of these viruses, new therapies and understanding of molecular events that alter the course of infection are necessary.

Airway Epithelial Cells

In the context of human airway diseases, one essential cell type is the airway epithelial cell. The airway epithelial cells (AECs) lining the conducting airways of the lung form the first line of defense against a variety of inhaled pathogens, allergens and environmental irritants. The airway epithelium is pseudostratified and the cells are polarized [10]. In the upper airways, comprising trachea and bronchi, the dominant cell types include ciliated cells, goblet cells, club cells, and basal cells (Figure 1.1) [10]. In the lower airways and alveoli, type 1 and type 2 alveolar cells are predominant. Importantly, AECs are primary host target cells for infection by respiratory viruses [11, 12]. In the context of asthma, the epithelium contributes to disease through deficient barrier function and excessive goblet cell differentiation [3, 4]. Further, AECs not only provide a physical barrier but also actively orchestrate immune responses to inhaled substances through the production of a wide array of secreted factors that include alarmins, chemokines, cytokines, and eicosanoids [3]. The release of these immunomodulatory mediators can drive complex biological processes such as allergic sensitization [3, 4]. Additionally, AECs express many pattern recognition receptors (PRRs) that are activated by exogenous allergens or viruses [3, 4]. Activation of these receptors can then direct immune cells such as DCs and ILC2s to initiate a Th2-polarized response [4, 13].

However, many of the receptors and pathways in the epithelium orchestrating this inflammation are not well understood.

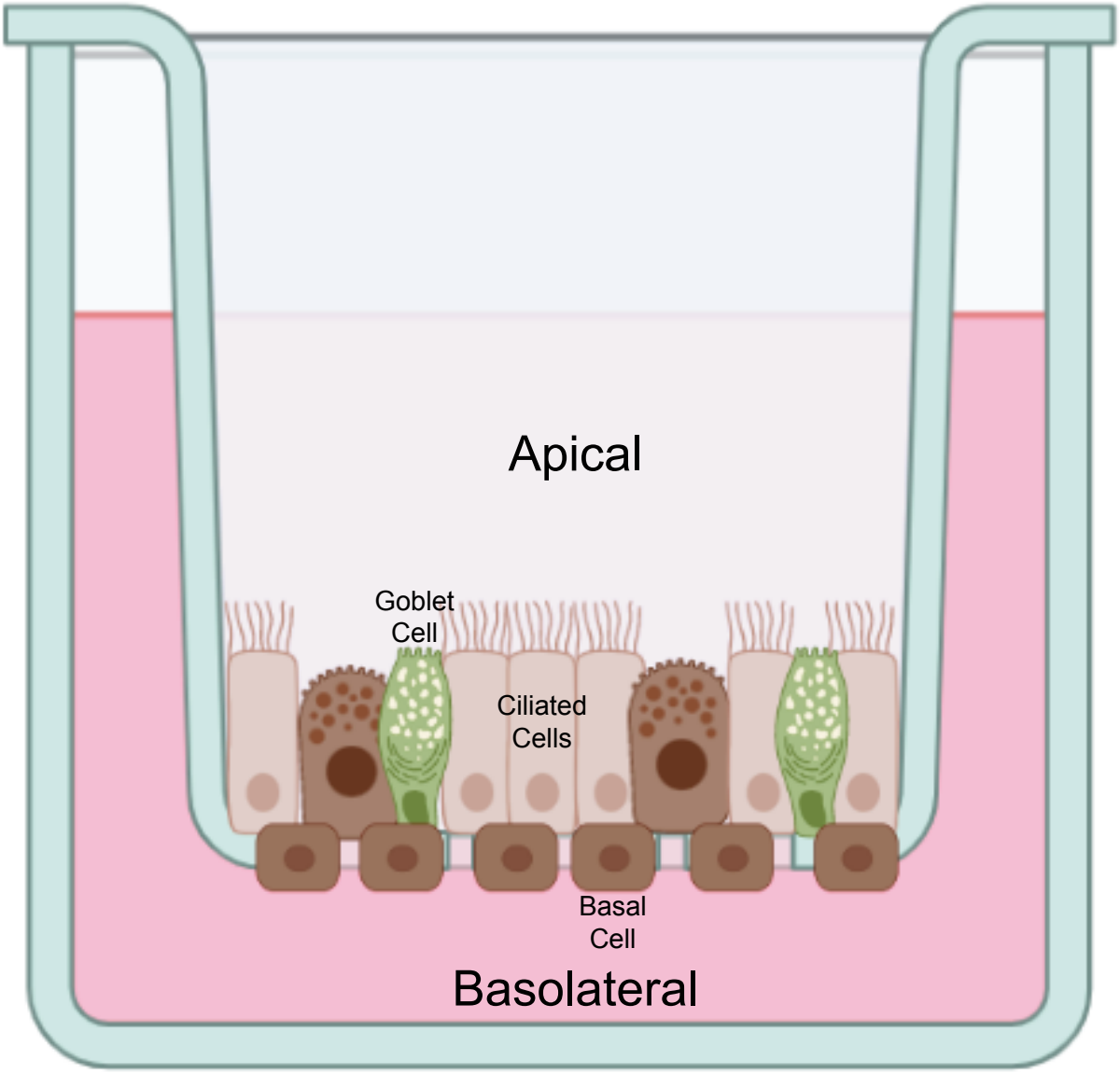

Figure 1.1 Air-liquid interface cultures of AECs. Normal human bronchial epithelial cells can be differentiated for 3 weeks at the air-liquid interface. Using this standard protocol, the bronchial epithelial cells differentiate into many of the cell types found in the upper airways such as ciliated cells, goblet cells, club cells, and basal cells. This system allows for the *in vitro* study of processes related to mucociliary clearance and mimics a more physiologically relevant system than submerged epithelial cultures, which are undifferentiated and not polarized.

One core function of the airway epithelium is mucociliary clearance (MCC). Human diseases such as cystic fibrosis and primary cilia dyskinesia are caused by mutations in genes essential for proper MCC, demonstrating the functional significance of MCC [14]. MCC is an indispensible innate host defense mechanism that comprises three components: 1) the cilia on ciliated cells 2) the airway surface liquid 3) the mucus layer [14]. The process begins when pathogens and particles become trapped in the mucus layer. Then, the mucus containing pathogen is shuttled up the respiratory tract through cilia beating, culminating in either swallowing or expectoration. One *in vitro* model that replicates many of the functional features of the intact airways is the air-liquid interface (ALI) model (Figure 1.1). Using this system, AECs can differentiate into ciliated and goblet cells and aspects of MCC biology can be investigated [15]. A deeper understanding of cilia and mucus may lead to helpful interventions in airway diseases.

Purinergic Signaling in the Airways

The airways harbor a plethora of small molecules and proteins that can interact with cellular receptors to drive dynamic responses. One small molecule in the airways that regulates physiology is adenosine triphosphate (ATP). Extracellular ATP in the airways is of growing interest due to its ability to drive airway inflammation [16-18]. Extracellular ATP is a damage- or danger-associated molecular pattern (DAMP) [16, 18]. Importantly, elevated ATP in the bronchoalveolar lavage (BAL) fluid is a key characteristic of many lung disorders including asthma, acute respiratory distress syndrome (ARDS), and chronic obstructive pulmonary disease (COPD) [16, 19-22]. Upon allergen challenge in the lungs, ATP levels in the bronchoalveolar lavage fluid increase dramatically [16, 18].

In the airways, ATP stimulates cytokine release, activates the inflammasome, and recruits immune cells [13, 16-18]. This extracellular ATP regulates allergic sensitization and inflammation through purinergic P2 receptors [16, 18]. However, the molecular identity of the purinergic receptors that drive the release of immunomodulatory mediators in the airways is unclear.

In contrast to its role in driving proinflammatory processes, ATP can also elicit protective responses. For instance, ATP signaling is linked to protective physiological processes in the lungs such as wound healing, rejection of tumors, killing of bacterial pathogens, and mucociliary clearance (MCC) [17, 23-27]. In addition to ATP, UTP is also released in the airways and increases MCC [28]. UTP can also stimulate numerous other physiologically important airway functions such as ion transport and mucin secretion [28]. However, how these nucleotides elicit both proinflammatory and protective effects on airway function is not well understood.

P2 receptors are a class of 15 purinergic receptors that are either P2Y metabotropic G-protein couple receptors (GPCRs) or P2X ionotropic ion channels (Figure 1.2) [29-31]. There are eight P2Y receptors including *P2RY1, 2, 4, 6, 11-14* [29]. P2Y ligands are diverse and include ATP, ADP, UTP, UDP, and UDP-glucose [29]. P2X channels comprise seven subtypes including *P2RX1-7* with ATP as the primary physiological agonist [31]. Another class of purinergic receptors are the four adenosine receptors termed P1 receptors [32]. P2 receptors have well known roles in inflammation. One well-described role is that ATP-evoked opening of P2X7 receptors drives inflammasome activation [17]. P2 receptors can also drive nuclease and cytokine release in eosinophils and dendritic cells [33, 34]. Many cell types express multiple P2

receptors. In some circumstances, cross talk can occur between receptors culminating in either synergy or antagonism at downstream endpoints such as cytokine release [35]. In AECs, P2 receptor activation evokes IL-6 secretion [36]. Collectively, purinergic receptors have diverse roles in the regulation of inflammatory processes.

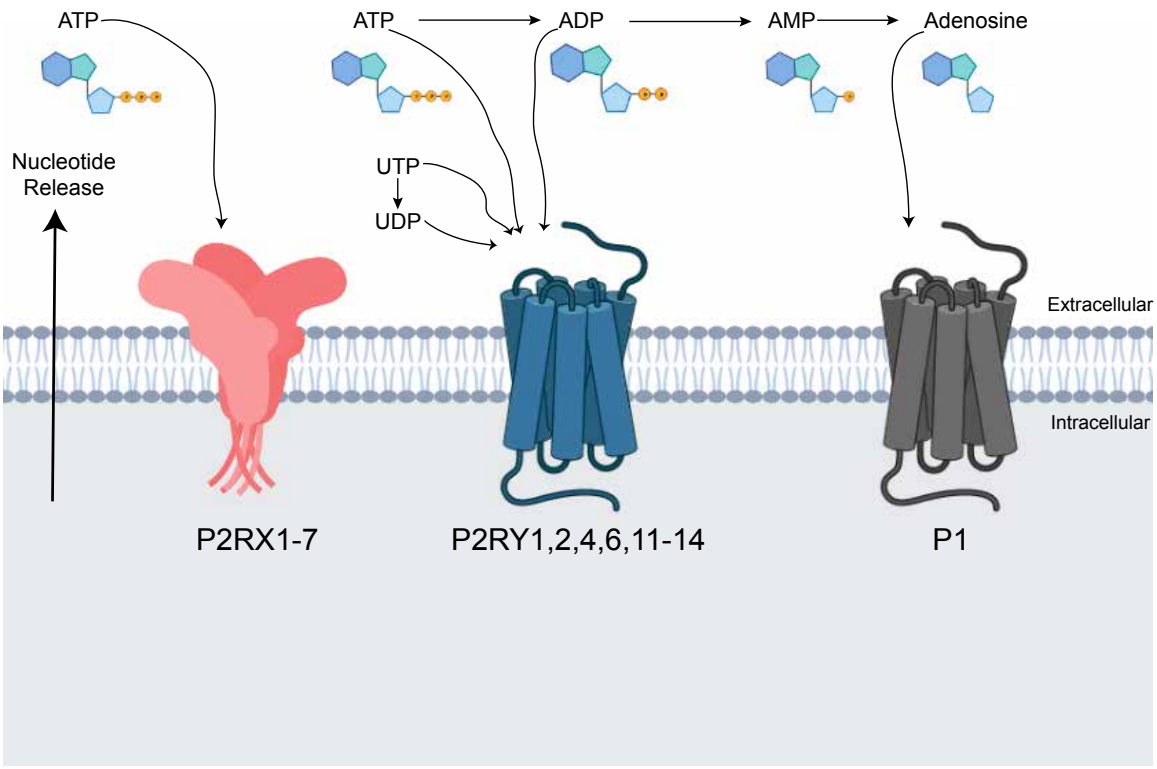

Figure 1.2 Purinergic Signaling. First, nucleotides are released from cells into the extracellular space. These extracellular nucleotides can then be degraded from ATP-ADP-AMP-Adenosine. A similar degradation process exists for uridine nucleotides. Three main classes of purinergic receptors exist. P2RX receptors are ion channels with ATP are the dominant physiological agonist. P2RY receptors are GPCRs with agonists that range from ATP, ADP, UTP, UDP, and UDP-glucose. P1 receptors are GPCRs with adenosine as their physiological agonist. Enzymes that degrade ATP/ADP into AMP are termed ecto-nucleoside triphosphate diphosphohydrolases (E-NTPDases), such as CD39. Enzymes that degrade AMP into Adenosine are termed ecto-5'-nucleotidase, such as CD73. Enzymes that degrade AMP into adenosine are termed purine nucleoside phosphorylase (PNP) [1]. Apyrase will degrade ATP/ADP into AMP. ARL 67156 prevents the degradation of ATP.

Nucleotides can be release from cells via lytic or non-lytic mechanisms. In general, there are three mechanisms whereby cells release nucleotides in a non-lytic fashion. The first is constitutive release through the ER-Golgi pathway. The second is a Ca^{2+} dependent exocytotic release. The third is pannexin- or connexin-mediated release of nucleotides [37]. AECs are known to release ATP via all three of these mechanisms [37]. Interestingly, goblet cell metaplasia, a phenomenon whereby the abundance of goblet cells in the epithelium increases, is linked to a greater release of ATP from AECs [38]. This release of ATP also contained other nucleotides such as ADP, AMP, and adenosine [38]. In AECs derived from cystic fibrosis patients, the inflammatory state of the cells has been linked to increased nucleotide release [39]. Respiratory virus infection of AECs can also increase nucleotide release [38, 40-42]. Toll-like receptor 3, a sensor for dsRNA, has been implicated in this virus-induced release of nucleotides [40, 42]. Airway allergens, such as Alternaria and cockroach also drive the release of nucleotides from AECs [13]. A further mechanism that elicits nucleotide release from AECs is cyclic compressive stress [43]. This cyclic compressive stress has been proposed to be a model for normal tidal breathing in humans suggesting that normal breathing rhythm may induce low levels of nucleotide release [43]. Importantly, the release of nucleotides from AECs is not limited to adenine derivatives but includes uridine nucleotides as well [44, 45]. Direct quantification suggests that ATP concentrations in cellular supernatants are approximately 3-5 fold higher than UTP concentrations, correlating strongly with intracellular nucleotide ratios [46, 47]. Collectively, an abundance of stimuli have been reported to induce the release of

nucleotides from AECs implying that AEC purinergic signaling may occur after a host of different physiological insults.

The two most well described purinergic receptors expressed in AECs are $P2Y_2$ receptors and A_{2B} receptors [48]. AECs are polarized cells and $P2Y_2$ receptors are reported to be expressed on both apical and basolateral surfaces [49, 50]. Agonists for $P2Y_2$ receptors include ATP and UTP while adenosine is the physiological agonist for A_{2B} receptors. Thus, when AECs release extracellular ATP, which is subsequently degraded into adenosine, both of these receptors may be simultaneously activated. Both of these purinergic receptors have essential roles in the regulation of mucociliary clearance (MCC). Specifically, $P2Y_2$ receptor activation can drive the rapid release of mucin proteins from goblet cells [51-53]. Further, both $P2Y_2$ receptor and A_{2B} receptor activation can elicit the opening of Cl^- channels on the apical surface of AECs [48]. This Cl^- channel activation is essential for proper hydration of the mucus. However, the underlying mechanisms for how these receptors induce this response are divergent. Activation of $P2Y_2$ receptors evokes Ca^{2+} signaling and leads to opening of the Ca^{2+} activated Cl^- channels (CACCs) [48]. On the other hand, activation of A_{2B} receptors evokes cAMP signaling and leads to opening of the cystic fibrosis transmembrane conductance regulator (CFTR), the Cl^- channel mutated in cystic fibrosis [48]. Another mechanism whereby these two receptors increase MCC is that they can induce an increase in cilia beat frequency [48]. Interestingly, a feedback mechanism exists between MCC and nucleotide release. Cilia can sense the viscosity of the mucus layer in the airways and when it is too viscous, cilia cause the release of ATP [24]. This ATP and subsequently adenosine then drives hydration of mucus through $P2Y_2$ receptor and

A_{2B} receptor activation of Cl^- channels [24]. Because $P2Y_2$ receptors drive activation of CACCs and not CFTR, activation of these receptors was proposed as a means to restore Cl^- channel function in cystic fibrosis patients [54]. Unfortunately, stable agonists of $P2Y_2$ receptors were ultimately abandoned in CF clinical trials due to low efficacy [55]. Altogether, $P2Y_2$ receptors and A_{2B} receptors are essential regulators of MCC in AECs. However, the role of P2 receptors in AEC release of immunological mediators is less clear.

There are some reports suggesting that ionotropic P2X receptors are expressed on AECs [56]. Activation of AEC P2X channels can enhance Ca^{2+} signaling [57]. Although not as dominant as $P2Y_2$ receptors, ATP gated P2X channels have been implicated in increasing both cilia beat frequency and mucin secretion in AECs [58, 59]. The biophysical properties of P2X channels in AECs suggest that both P2X7 and P2X4 channels are functional [60]. Further, P2X channel activation has been implicated in the release of IL-8 from AECs [61]. Interestingly, *P2rx4* knockout mice are protected in models of allergic lung inflammation [62]. Collectively, the roles of AEC P2X receptors are less well understood than P2Y receptors.

Histamine Signaling in AECs

Another important mediator in the airways is histamine. Histamine was the first mediator causally linked to allergic disease as it recapitulated many of the symptoms of allergy. Histamine is typically released from mast cells and basophils upon degranulation [63]. In the airways, histamine evokes vasodilation, smooth muscle contraction, and pruritus [63]. In airway epithelial cells, histamine induces a strong Ca^{2+} response [64]. Although

H_1 receptors are thought to be the dominant histamine receptor subtype in AECs, some reports suggest $H_{2\text{-}3}$ may also be expressed [64, 65]. Histamine can drive the release of cytokines from AECs [64]. It can also drive ROS signaling in AECs [66]. In polarized AECs, histamine receptors are predominantly expressed on the basolateral surfaces [67]. Decreased AEC barrier function is a hallmark of asthmatic disease and histamine receptor activation can transiently decrease AEC barrier function [68]. Altogether, histamine receptors are a classic regulator of allergic lung inflammation but how histamine modulates AEC immune responses are not clear.

Ca^{2+} signaling and CRAC Channels in AECs

One key-signaling mechanism in AECs is Ca^{2+}-dependent pathways. Ca^{2+} is a ubiquitous second messenger that drives numerous biological phenomena including transcription, exocytosis, and enzyme regulation [69-71]. Resting Ca^{2+} concentrations are approximately 100 nM in the cytosol, 300-400 μM in the ER, and 2 mM in the extracellular space thereby setting the stage for steep concentration gradients. One primary mechanism for Ca^{2+} entry into the cytosol is described as store-operated Ca^{2+} entry (SOCE). This occurs when the intracellular Ca^{2+} stores, such as the $[Ca^{2+}]_{ER}$ decrease, leading to Ca^{2+} entry across the plasma membrane from the extracellular space. The prototypic channel that is operated in a store-dependent manner is the Ca^{2+} release-activated Ca^{2+} (CRAC) channel.

CRAC channels are formed by the ORAI proteins, which comprise the pore subunits, and are activated by the ER Ca^{2+} sensing STIM proteins. STIM1 and STIM2 are single pass transmembrane proteins localized to the ER. The ER luminal portion of

STIM1 and STIM2 contains a Ca^{2+}-binding domain called an EF hand that acts as a $[Ca^{2+}]_{ER}$ sensor. When the $[Ca^{2+}]_{ER}$ decreases, Ca^{2+} is released from STIM1-2 causing oligomerization and the unveiling of a binding domain for ORAI proteins on the cytosolic portion of STIM. Activated STIM1-2 localize to the ER-PM junction and binding ORAI proteins, they cause ORAI pore opening and Ca^{2+} influx into the cytosol (Figure 1.3). Following channel opening, inactivation occurs through Ca^{2+}-dependent mechanisms and also the refilling of ER Ca^{2+} stores through the SERCA pump [70]. Interestingly, STIM1 binding to ORAI1 channels increases the Ca^{2+} selectively of ORAI1 channels [72]. The best understood ORAI and STIM proteins are ORAI1 and STIM1.

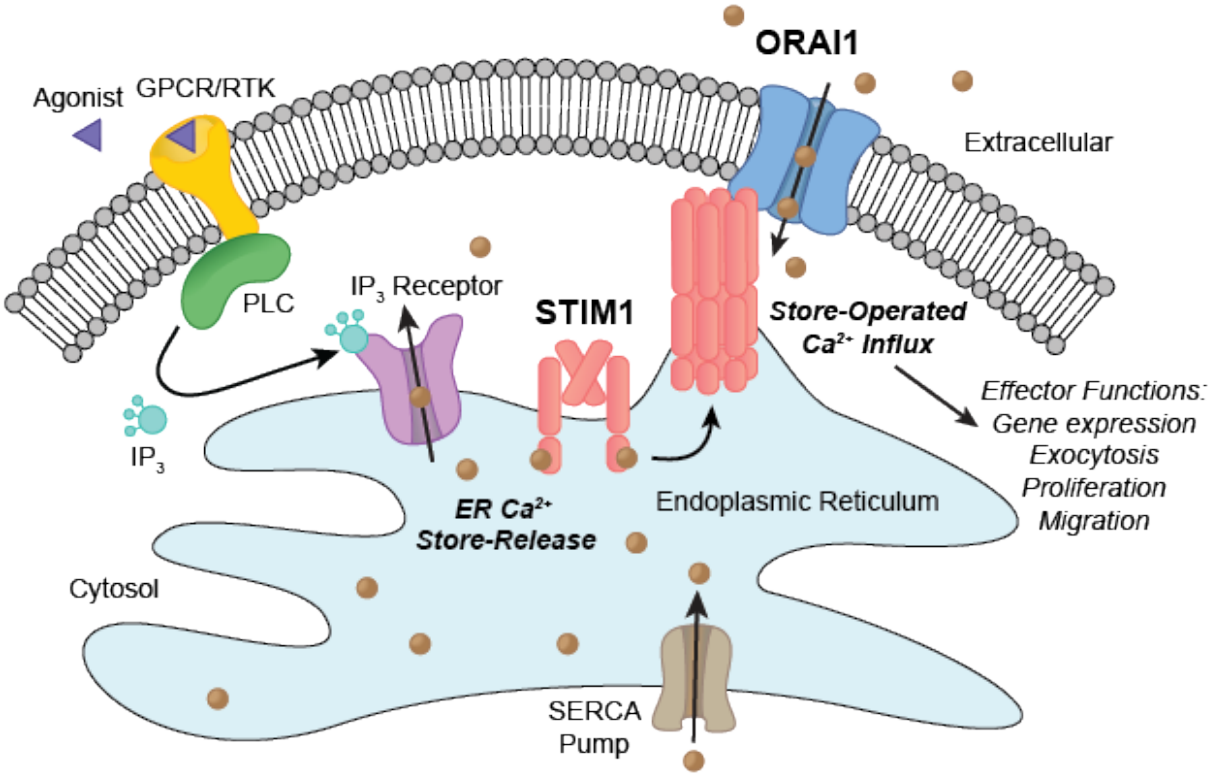

Figure 1.3 CRAC Channel Activation. Store-operated calcium entry through The CRAC channel occurs when $[Ca^{2+}]_{ER}$ decreases causing STIM1 to oligomerize. STIM1 then relocates to PM-ER junctions binding ORAI1 and causing pore opening. Image adapted from, *Yeung, P.S., M. Yamashita, and M. Prakriya, Molecular basis of allosteric Orai1 channel activation by STIM1. J Physiol, 2019.*

The CRAC channel is most well studied in immune cells, although the components ORAI1 and STIM1 are widely expressed in other tissues [70]. In T cells, CRAC channels regulate processes such as IL-2 production and proliferation [70, 73, 74]. The molecular identity of the channel was elucidated when *ORAI1* was discovered because of a human missense mutation, R91W, which leads to a severe combined immune deficiency (SCID) phenotype [74]. ORAI1 deficient patients are not only immunodeficient, but experience myopathy and ectodermal dysplasia as well [75]. ORAI1 deficient patients also have defects in dental enamel formation [76]. The list of clinical syndromes described for STIM1 deficient patients includes immunodeficiency, hepatosplenomegaly, autoimmune hemolytic anemia, thrombocytopenia, muscular hypotonia, and defective enamel formation [77]. However, CRAC channels are increasingly tied to diverse physiological processes. In T cells, *Orai1* deficiency in mice has been linked to mitochondrial metabolic defects [78]. In neutrophils, both *Stim1* and *Stim2* are necessary for full stimulus-evoked cytokine production [79]. In mast cells, CRAC channel function is essential for cysteinyl leukotriene production and degranulation [80-83]. In the nervous system, *Orai1* channels have been linked to long-term potentiation, astrocyte gliotransmitter and cytokine release [84-86]. Altogether, CRAC channels have established roles in immunity and a host of other physiological processes.

In recent years, CRAC channels have been linked to regulated exocytosis in secretory epithelium [87]. In lacrimal glands, loss of *Orai1* leads to less fluid and protein secretion in response to muscarinic receptor activation [88]. Within pancreatic acinar cells, loss of *Orai1* leads to decreased secretion of digestive enzymes and antimicrobial

peptides [89]. Similarly, in sweat glands, loss of *Orai1* leads to decreased chloride and fluid secretion [90]. Thus, CRAC channels are known regulators of exocytosis in secretory epithelial cells.

In airway epithelial cells (AECs), Ca^{2+} is known to regulate a host of biological processes. Mucociliary clearance is dynamically regulated by Ca^{2+} signaling. Specifically, Ca^{2+} can increase cilia beat frequency, enhance Cl^- channel activation, and induce mucin secretion [14, 48, 91, 92]. Ca^{2+} signaling in AECs can also drive the release of nucleotides into the extracellular space [44, 45]. Receptor-mediated Ca^{2+} signaling in AECs can also drive the release of immunomodulatory lipids such as PGE_2 [93, 94]. Finally, the synthesis and release of cytokines such as IL-6 and IL-33 is Ca^{2+} dependent [13, 36]. However, which of these Ca^{2+}-dependent processes are also CRAC channel dependent is unclear.

We have recently identified CRAC channels as a major route of calcium entry in airway epithelial cells [95]. In AECs, direct activation CRAC channels causes cytokine induction that is largely NFAT dependent [95]. These cytokines include TNF-α, IL-6, IL-8, GM-CSF, and TSLP [95]. Other genes reportedly regulated through direct CRAC channel activation include c-Fos and EGF [96]. Furthermore, PAR2 agonists have been shown to activate CRAC channels in AECs [95]. Indeed, CRAC channel activation is necessary for the production of IL-6, IL-8 and GM-CSF downstream of PAR2 activation (Figure 1.4) [95]. Allergens have also been shown to activate CRAC channels in AECs and drive IL-6 and IL-8 production [97]. In summary, CRAC channels in AECs have primarily been investigated for their role in the production of proinflammatory cytokines. However, a scarcity of information exists on how these channels regulate enzymes and

exocytosis. Additionally, how CRAC channel activation may contribute to the diverse functions of purinergic receptors in AECs is unknown.

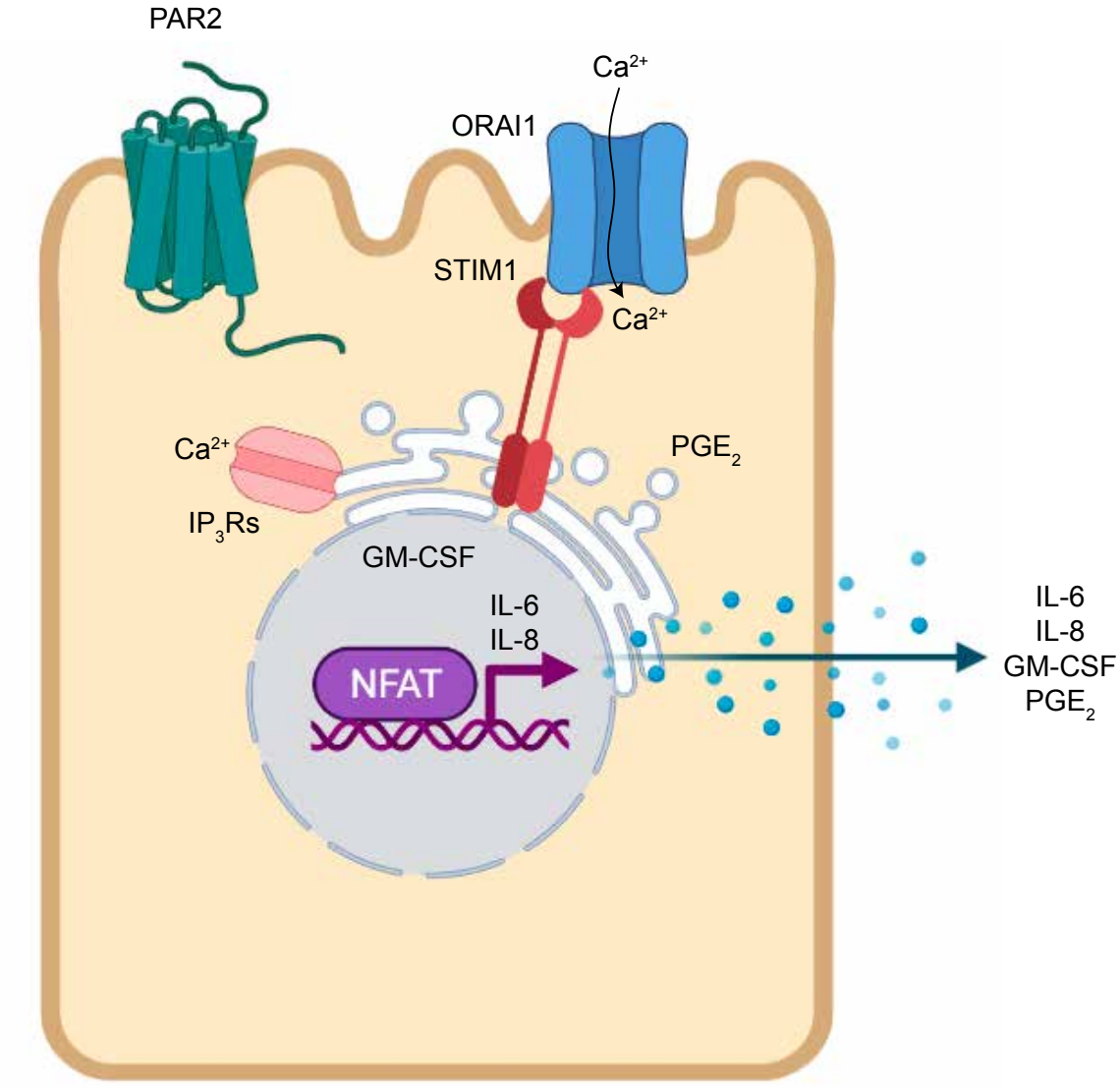

Figure 1.4 PAR2 activation in AECs evokes CRAC channel dependent production of proinflammatory cytokines, chemokines and eicosanoids. PAR2 activation leads to phospholipase C signaling and IP_3 generation. IP_3 elicits opening of IP_3Rs in the endoplasmic reticulum. A decrease in ER Ca^{2+} levels drives STIM1 activation and subsequent opening of plasma membrane ORAI1 channels. Ca^{2+} activates a host of Ca^{2+} dependent enzymes including calcineurin. The production of PGE_2 is CRAC channel dependent in this system but the mechanism for CRAC channel-mediated PGE_2 production is unclear. GM-CSF is also produced in a CRAC channel dependent manner. Calcineurin activation leads to NFAT transcription of IL-6 and IL-8. Thus, PAR2 activation leads to CRAC channels as a signaling nexus provoking the release of PGE_2, GM-CSF, IL-6, IL-8 from AECs.

Release of AEC Immunomodulatory mediators

Airway epithelial cells release a host of mediators that direct subsequent immune responses. These include lipid mediators such as prostaglandins as well as protein products such as cytokines, chemokines, mucin proteins, and antimicrobial peptides that direct immune responses in the context of allergic responses or antiviral responses. Thus, understanding the mechanisms that drive the synthesis and release of these mediators are essential for a deeper understanding of immunological responses in the lungs.

One prominent mediator released by AECs in PGE_2. [94, 98-100]. PGE_2 stimulates dilation of the lung airways thereby protecting the lung against severe bronchoconstriction that is a hallmark of diseases such as asthma [101, 102]. PGE_2 also inhibits several inflammatory processes, including the release of histamine and cysteinyl leukotrienes from mast cells [101], T-cell migration [103], ILC2 function [104], and the production of proinflammatory TNF-α and IL-12β by dendritic cells [105]. In addition to inhibiting proinflammatory signaling in the lungs, it also enhances the synthesis of the anti-inflammatory cytokine IL-10 [105] and promotes wound healing [106]. Further, growing evidence suggests that PGE_2 can drive reverse migration and removal of neutrophils from sites of inflammation to dissipate inflammation *in vivo [107]*. Failure of resolution of inflammation can lead to inflammatory diseases such as chronic obstructive pulmonary disease (COPD) and acute respiratory distress syndrome

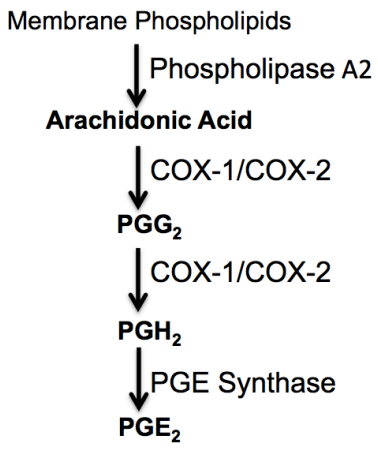

Figure 1.5 The biosynthetic pathway that culminates in the production of prostaglandin E2.

(ARDS). Altogether, within the lung, PGE_2 exerts predominantly bronchoprotective and anti-inflammatory effects [108].

The synthesis of PGE_2 is well studied (Figure 1.5)**.** The process begins when arachidonic acid (AA) is liberated from phospholipids in membranes via phospholipase activity. Cyclooxygenase (COX) enzymes then process AA in a two-step reaction into PGH_2 [109]. Prostaglandin E synthase enzymes then convert PGH_2 into PGE_2, which is subsequently transported out of cells via passive diffusion or the transporter MRP4 [110-112]. This enzyme cascade is tightly regulated and therapeutics to inhibit this pathway are a hallmark of modern medicine. The enzymes COX-2 and mPGES-1 are primarily regulated through increases in protein expression [109-111]. In contrast, regulation of $cPLA_2$ occurs posttranslationally through direct ERK1/2 phosphorylation of Ser505 and Ca^{2+}-dependent membrane translocation [98, 113]. Ca^{2+} binding to the Ca^{2+}-dependent phospholipid-binding domain of $cPLA_2$ is both necessary and sufficient for PGE_2 synthesis. However, the ion channels responsible for this influx of Ca^{2+} into the cytosol in AECs remain enigmatic. *The first hypothesis of my thesis dissertation is to determine how CRAC channel activation may be involved in PGE_2 synthesis.*

Mucin proteins, along with water and ions are an important component of mucus [114]. In the airways, mucus is used in the mucociliary escalator, a process in which ciliated cells pump mucus up and out of the airways to be either swallowed or expectorated [114]. Although this physiology is important for host pathogen protection, mucus hypersecretion and goblet cell metaplasia are hallmarks of both asthma and chronic obstructive pulmonary disease (COPD) [114-116]. Importantly, the most common cause of death in asthmatic patients is excessive mucus plugs [114]. Thus,

therapies that can attenuate mucin hypersecretion have vast potential to improve modern asthma treatment. In human airways, club (Clara) and goblet cells synthesize and secrete mucin proteins [114, 115]. The major secreted mucins of the airways are MUC5AC and MUC5B. These large glycoproteins are packaged into secretory granules [114]. Although some basal exocytosis of these granules occurs, secretion can rapidly increase in a receptor dependent manner [115, 117, 118]. These receptors are numerous but include P2Y, PAR2, and EGFR [53, 118-120]. One conserved mechanism for inducing mucin secretion is Ca^{2+} signaling [116]. Although it is understood that IP_3Rs are involved in mucin secretion from AECs, it remains unclear if Ca^{2+} influx from the extracellular space is also required. If so, inhibiting these Ca^{2+} channels may prove a novel mechanism to selectively reduce mucus plugs in airway diseases. *The second hypothesis of my thesis dissertation is to investigate the role of CRAC channels in goblet cell exocytosis and the secretion of mucin proteins.*

A key cytokine released from AECs is IL-6. IL-6 is a potent inflammatory cytokine that elicits a wide-range of inflammatory effects including T-cell expansion, pulmonary neutrophil infiltration, airway mucus secretion, lung fibrosis, and the hyperplasia and hypertrophy of airway smooth muscle cells [121-124]. Further, IL-6 is linked to numerous airway diseases from asthma to COPD [121-124]. Investigations with patients suffering from severe COVID-19 have revealed massive increases in IL-6 in the lung airways, a feature thought to contribute to microvascular thrombosis in the lung and multiple organ dysfunction in these patients [125]. Importantly, blockade of IL-6 signaling in mouse models of asthma protects against airway inflammation [122, 126], and early reports indicate that targeting IL-6 may be a viable therapy to decrease

mortality in severe COVID-19 patients [127]. In AECs, P2 receptor activation induces IL-6 secretion [36]. Understanding the mechanisms that provoke IL-6 release from AECs may uncover novel therapeutic modalities for use in both allergic inflammation and severe COVID-19. *The third hypothesis of my thesis dissertation is to determine the role of CRAC channels in purinergic receptor-driven IL-6 production.*

When a respiratory virus infects AECs, one essential class of antiviral cytokines that is produced is interferons (Figure 1.6) [12, 128, 129]. Interferons (IFNs) are classified as type 1 (IFN-α/β), 2 (IFN-γ), or 3 (IFN-λ). Respiratory virus-infected AECs produce predominantly type 1 and type 3 IFN [130]. While both of these cytokines have antiviral activity, important distinctions exist. Type 3 IFN receptors are restricted to mucosal surfaces while type 1 IFN receptors are considered ubiquitous [12, 128]. Thus, IFN-λ is a mucosal specific mechanism for antiviral defense. Although, AECs generally make higher quantities of type 3 IFN than type 1 IFN following infection [130], type 1 is more potent at inducing an antiviral state in cells [131]. Both type 1 and type 3 IFN signaling induces the expression of interferon-stimulated genes (ISGs) that enhance antiviral defense of cells [12, 128].

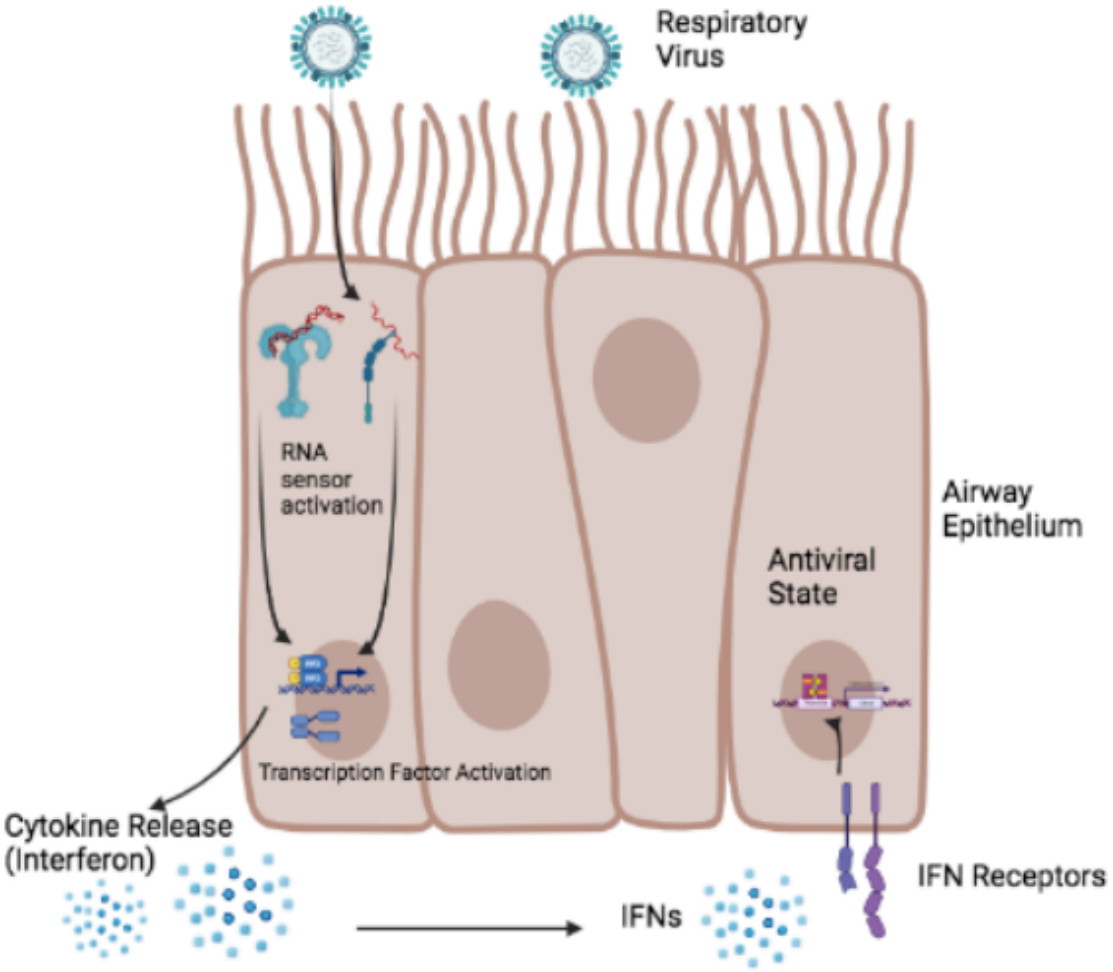

Figure 1.6 Respiratory Virus infection of AECs drives Interferon release. Respiratory viruses in the airways are most often RNA viruses. The virus infects AECs and as the virus replicates, dsRNA is synthesized and dsRNA sensors such as TLR3 and RLRs are activated. Activation of these sensors then drives activation of transcription factors such as NF-kB and IRF family members. One of the key mediators that is released is the antiviral cytokines termed interferons. AECs release both type 1 and type 3 IFN. IFNs signal through IFN receptors to induce the transcription of interferon stimulated genes (ISGs) that induce an antiviral state in the neighboring cells.

IFN production can be regulated in a host of manners. Respiratory viruses themselves often exhibit a capacity to inhibit IFN production or downstream IFN signaling [128]. This capacity to dampen host IFN responses is often critical for successful viral infection and replication. However, many host receptors and signaling pathways can also enhance or inhibit interferon pathways. In macrophages, CCL2 has been shown to dampen IFN-α release [132]. In plasmacytoid dendritic cells (pDCs), ligands such as histamine and nucleotides have been shown to inhibit IFN-α release [133, 134]. In AECs, EGFR activation can decrease IFN-λ production thereby enhancing viral infection [135, 136]. The cytokines IL-4,13, and IL-17 have also been shown to dampen IFN production from AECs [137-139]. Cigarette smoke can also dampen AEC IFN production [140, 141]. Interestingly, allergens such as aspergillus, alternaria, and house dust mite, have further been shown to inhibit IFN production from AECs [142-144]. This reduction of IFN production has been proposed to be a potential mechanism whereby the airway milieu is skewed towards a Th2 phenotype upon exposure to these allergens [143, 145]. Mechanistically, both aspergillus and alternaria have been shown to activate proteinase-activated receptor 2 (PAR2) on AECs and signaling from this receptor limits the release of Th1 chemokines and IFNs [143, 146]. Altogether, understanding the signaling mechanisms that regulate AEC IFN production may enable the development of novel antiviral therapies.

Acute respiratory viral infections can also aggravate underlying chronic airway diseases and visa versa. For example, asthma may be a risk factor for severe influenza A virus (IAV) infection during IAV pandemics [11]. Furthermore, there is a strong correlation between children experiencing rhinovirus (RV) or respiratory syncytial virus

(RSV) induced wheezing episodes early in life with later development of asthma [147]. Although the exact mechanisms remain unclear, this may be related to a viral interaction with allergic sensitization [148]. Importantly, acute RV or RSV infections are responsible for most exacerbations of asthma [9, 147, 149, 150]. While asthmatics are not prone to greater incidence of respiratory tract infections, they are prone to more severe and longer lasting lower respiratory tract symptoms during the course of infection compared to healthy controls [151]. There are also correlations between asthma and the production of the key antiviral cytokines interferons. On a cellular level, most [137, 149, 152-157], but not all [158], studies have suggested that cells or tissue derived from patients with asthma or chronic obstructive pulmonary disease (COPD) have an intrinsic defect in IFN production following viral infections. Mechanisms to explain how asthmatics may come to have deficient IFN production are not clear.

Two mediators present in the airways during asthma are histamine and extracellular nucleotides [16, 63]. However, whether there may be a causative relationship between nucleotides, histamine and deficient IFN production is unclear. It is also important to note that nucleotides are released following viral infection of AECs [38, 40-42]. Thus, nucleotide signaling may regulate not only allergic sensitization [16] but also antiviral responses in the airways. Dissecting these hypotheses using cellular models may be of the upmost importance for understanding the clinical observations regarding asthmatics and IFN production. *The fourth hypothesis of my thesis dissertation is that nucleotides and histamine regulate AEC IFN production.*

Summary

Understanding how airway epithelial cells produce immunomodulatory factors such as cytokines and eicosanoids will lead to a better understanding of host immune responses against allergens and viruses. In Chapter 2, I focus on investigating receptors that elicit the activation of Ca^{2+} signaling and CRAC channels in AECs. Chapter 3 and 4 are devoted to interrogating mechanisms AECs employ to produce PGE_2 or IL-6. Chapter 5 and 6 are an investigation of mechanisms whereby nucleotides and histamine suppress the release of interferons from AECs. Chapter 7 is devoted to studying AEC function at the air-liquid interface, particularly with a focus on validating previous findings in submerged NHBEs and testing the CRAC channel dependence of mucin secretion. Chapter 8 is a short pilot study using the CRAC channel inhibitor CM4620 in an animal model of allergic lung disease. Chapter 9 is a brief conclusion followed by materials and methods in chapter 10. Overall, this thesis work uncovers novel mechanisms whereby AECs may orchestrate downstream immune responses in the lungs through mediator release.

Chapter 2: G-protein Coupled Receptor Activation elicits Ca^{2+} signaling and Store-Operated Ca^{2+} Entry in Human Airway Epithelial Cells

Introduction

Calcium is a ubiquitous second messenger that encodes for numerous biological phenomena including transcription, exocytosis, and enzyme regulation [69, 70]. One critical set of proteins for cellular calcium signaling are ORAI and STIM [70, 159]. These two proteins comprise the Calcium Release-Activated Calcium (CRAC) channel, the prototypic store-operated calcium channel [70, 159]. The CRAC channel component STIM functions as a sensor for ER calcium levels such that when $[Ca^{2+}]_{ER}$ decreases, STIM binds to ORAI in the plasma membrane. STIM thereby acts as a ligand for ORAI, the pore subunit, ultimately leading to sustained calcium entry into the cytosol from the extracellular space. Many receptors and pathways lead to a decrease in $[Ca^{2+}]_{ER}$ and subsequent CRAC channel opening. The most well studied role for ORAI is in T cells where loss of function mutations leads to defective T cell function and ultimately severe combined immunodeficiency (SCID) syndrome [74].

In human airway epithelial cells, G-protein coupled receptors (GPCRs) and allergens elicit the activation of CRAC channels [95, 97]. CRAC channel activation in AECs has been shown to evoke the release of numerous immunomodulatory mediators [95, 97]. Although the proteinase-activated receptor 2 (PAR2) has been demonstrated to drive CRAC channel dependent release of mediators [95], the other receptor subtypes that induce CRAC channel activation in AECs remain unclear. Here we set out to investigate the scope of GPCRs that evoke Ca^{2+} signaling and CRAC channel

activation. Purinergic ligands such as ATP and UTP have previously been demonstrated to activate CRAC channels, yet the subtype responsible was unknown [95]. Histamine is also a biologically relevant ligand in the context of allergic airway diseases [63]. We tested purinergic ligands and histamine for their ability to drive CRAC channel activation in AECs. Both sets of ligands substantially evoked Ca^{2+} signaling and CRAC channel activation, albeit purinergic ligands consistently elicited stronger responses. Purinergic ligands ATP and UTP elicited the activation of $P2Y_2$ receptors while histamine activated H_1 receptors in AECs. This data suggests that purinergic ligands and histamine may induce the release of inflammatory mediators from human AECs through their harnessing of CRAC channel dependent Ca^{2+} signaling.

Results

The $P2Y_2$ receptor mediates ATP- and UTP-induced Ca^{2+} signals in AECs

ATP acts on numerous membrane receptors including metabotropic P2Y receptors along with ionotropic P2X receptors [31, 160]. Previous literature suggests AECs express $P2Y_2$, $P2Y_6$ and P2X receptors [48, 60, 61, 161]. All of these receptors then elicit Ca^{2+} signaling. Thus, we sought to identify the receptor subtypes that drive ATP-induced Ca^{2+} elevations. We used primary human airway epithelial cells and the ratiometric dye, Fura-2 as previously described [95] to interrogate the receptor identity. Our experiments revealed that a saturating dose of ATP (100μM) evoked a rapid increase in $[Ca^{2+}]_i$ followed by a sustained phase (Figure 2.1A). When extracellular Ca^{2+} was removed, the rapid rise in $[Ca^{2+}]_i$ was preserved while the sustained phase was lost (Figure 2.1B). This data was highly suggestive that the initial rise in $[Ca^{2+}]_i$ was driven by

Ca^{2+} store-release while the sustained phase required Ca^{2+} entry across the plasma membrane.

Next, we utilized the selective metabotropic P2Y receptor agonist, uridine triphosphate (UTP) [28]. When primary AECs were stimulated with ATP and UTP the Ca^{2+} signals elicited were nearly identical (Figure 2.1C). This is highly reminiscent of the pharmacological footprint of the $P2Y_2$ receptor [29, 160]. Thus, we tested the selective $P2Y_2$ antagonist AR-C 118925XX (hereby "AR-C") [53]. AR-C pretreatment abolished both ATP- and UTP- evoked Ca^{2+} signals (Figure 2.1D-F). The PAR2 activating peptide SLIGKV was still capable of mounting a Ca^{2+} response in the presence of AR-C suggesting that AR-C is indeed selective for $P2Y_2$ receptors (Figure 2.1D-E). These results indicate that the nucleotides ATP and UTP evoke Ca^{2+} signals in AECs primarily through the activation of metabotropic $P2Y_2$ receptors.

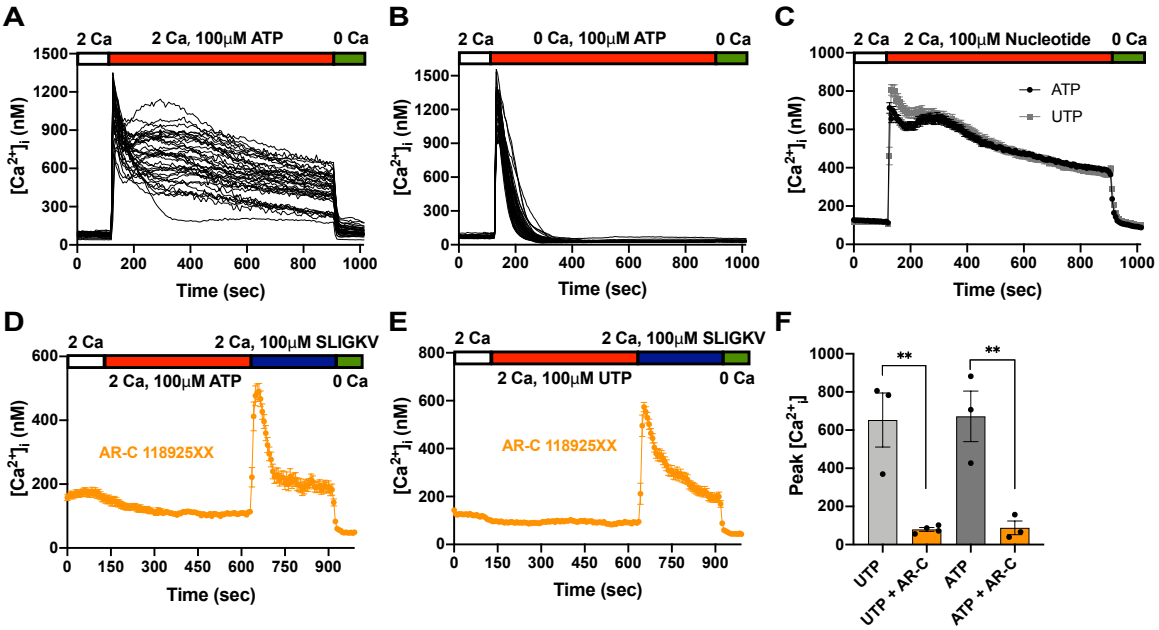

Figure 2.1 The $P2Y_2$ receptor mediates ATP- and UTP-induced Ca^{2+} elevations in AECs. A) ATP (100 μM) stimulates a bi-phasic $[Ca^{2+}]_i$ rise in primary human AECs consisting of an initial rapid, transient Ca^{2+} peak followed by a sustained $[Ca^{2+}]_i$ elevation in the presence of extracellular Ca^{2+} (2 mM). $[Ca^{2+}]_i$ was measured using Fura-

2 AM as previously described [95]. Each trace shows response of single cells in the imaging field. **B)** The removal of extracellular Ca^{2+} abolishes the sustained phase of the ATP-induced $[Ca^{2+}]_i$ elevation without affecting the initial transient $[Ca^{2+}]_i$ rise. **C)** The uridine nucleotide UTP (100 μM) evokes a Ca^{2+} rise that is similar in amplitude and kinetics to the ATP-evoked signal. Data are mean ± SEM of n = 35-37 cells. **D)** The selective $P2Y_2$ receptor antagonist, AR-C 118925XX (10 μM), completely abrogates ATP (100 μM)-induced Ca^{2+} rise but does not affect the ability of the PAR2 peptide, SLIGKV, to induce Ca^{2+} signaling. Data are mean ± SEM of n = 21 cells. **E)** Likewise, AR-C 118925XX (10 μM) abrogates UTP (100 μM)-induced Ca^{2+} rises but does not affect the Ca^{2+} rises stimulated by the PAR2 agonist, SLIGKV. Data are mean ± SEM of n = 23 cells. **F)** Summary of peak Ca^{2+} signal following agonist addition. Each data point is the mean peak Ca^{2+} signal (averaged over approximately 20-30 cells) for a given experiment (one dish) and the bar graph is mean ± SEM of n = 3-4 independent experiments. **p<0.01

CRAC channel inhibitors block the $P2Y_2$-evoked Ca^{2+} elevations

The sustained $[Ca^{2+}]_i$ phase elicited upon $P2Y_2$ receptor activation lead us to probe whether CRAC channels are activated in this signal. We employed the ORAI1 inhibitor, CM4620 [162], and measured ATP-induced Ca^{2+} signals. Pretreatment of cells with CM4620 strongly abrogated the ATP-induced sustained $[Ca^{2+}]_i$ phase but left intact the rapid $[Ca^{2+}]_i$ rise (Figure 2.2A and Figure 2.2C). Next, we used the well-studied CRAC channel inhibitor BTP2 [163-165]. BTP2 also inhibited the UTP-induced sustained $[Ca^{2+}]_i$ phase but left intact the rapid $[Ca^{2+}]_i$ rise (Figure 2.2B-C). To confirm this finding, we performed a Ca^{2+} add-back experiment where intracellular Ca^{2+} stores are first depleted in the absence of extracellular Ca^{2+}, and then extracellular Ca^{2+} is reintroduced allowing for more accurate measurement of Ca^{2+} entry across the plasma membrane. Pretreatment of cells with CM4620 stifled the Ca^{2+} entry following reintroduction without altering intracellular Ca^{2+} store release (Figure 2.2D-E). Collectively, this data suggests that $P2Y_2$ receptor activation elicits activation of CRAC channel mediated Ca^{2+} signals in AECs.

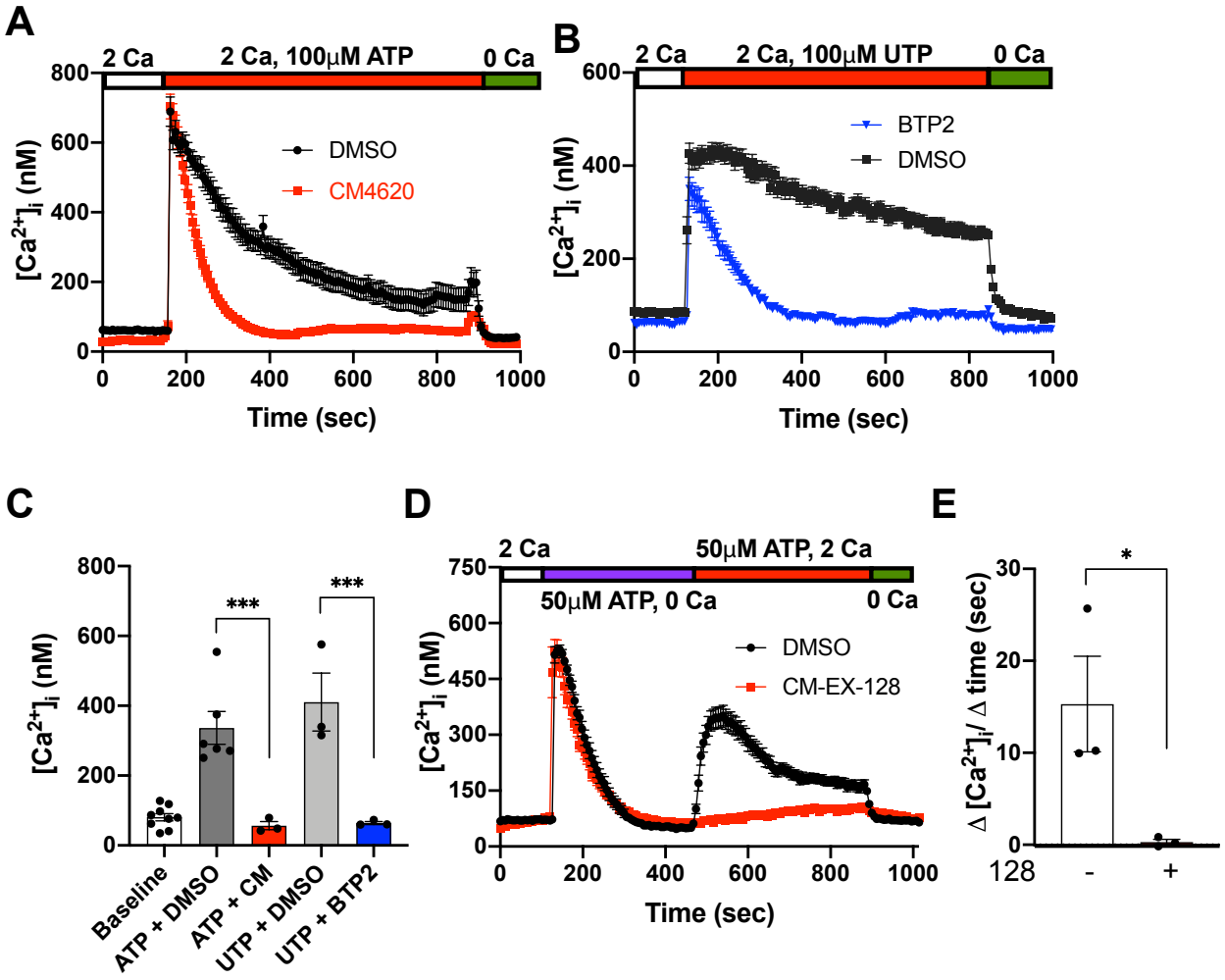

Figure 2.2 CRAC channel inhibitors block the P2Y$_2$-evoked Ca^{2+} elevations.
A) Pretreatment of NHBE cells with the CRAC channel inhibitor, CM4620 (1 μM, 2 hrs) abolishes the sustained entry evoked by 100 μM ATP. Data are mean ± SEM of n = 18-27 cells per trace. **B)** Likewise, pretreatment of cells with BTP2 (1 μM, 2 hrs) abolished the sustained entry elicited by 100 μM UTP. Data are mean ± SEM of n = 23-31 cells per trace. **C)** Quantification of $[Ca^{2+}]_i$ from A-B taken 5 minutes after agonist addition. Each data point is the mean $[Ca^{2+}]_i$ (averaged over 20-30 cells) for a given experiment (one dish) and the bar graph is mean ± SEM of n = 3-6 independent experiments. **D)** ATP-induced Ca^{2+} influx is inhibited by pretreatment (2hrs) with the ORAI1 inhibitor CM4620 (1 μM). Cells were treated with ATP (50 μM) in Ca^{2+} free Ringers solution to allow for store release followed by perfusion of Ringers contained 2mM Ca^{2+}. Data are mean ± SEM of n = 14-21 cells. **E)** Quantification of the rate of Ca^{2+} influx in D. Rate of

influx was calculated for the 24 seconds immediately following extracellular Ca^{2+} addition. Each data point is the mean Ca^{2+} influx rate for a given experiment (one dish) and the graph is the mean ± SEM of n = 3 independent tests *p<0.05, ***p<0.001

ORAI1 and STIM1 are the molecular components of $P2Y_2$ activated CRAC channels

Multiple ORAI and STIM isoforms exist that have the potential to form CRAC channels [70, 166]. Thus, we set out to identify the molecular identity of $P2Y_2$ receptor activated CRAC channels. ORAI1 and STIM1 were selectively knocked down using siRNA. Knockdown of either ORAI1 or STIM1 abrogated the ATP-induced sustained $[Ca^{2+}]_i$ phase but left intact the rapid $[Ca^{2+}]_i$ rise (Figure 2.3A-B). These results strongly suggest ORAI1 and STIM1 are predominant CRAC channel protein isoforms involved in $P2Y_2$ receptor signaling.

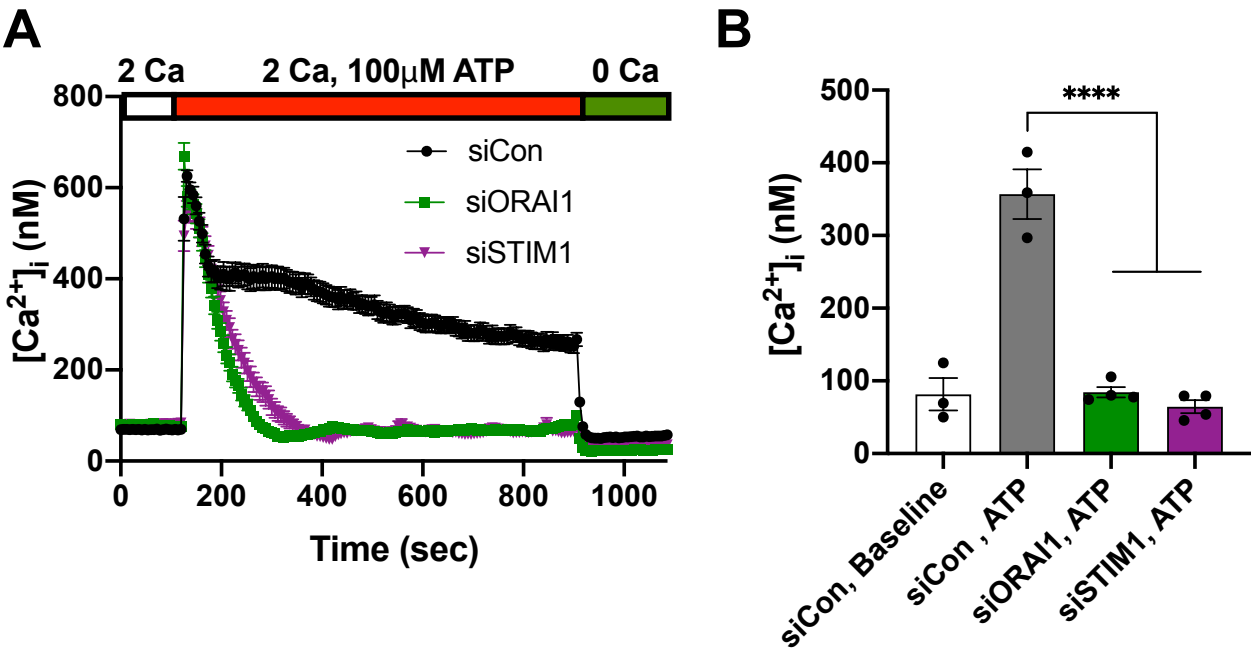

Figure 2.3 ORAI1 and STIM1 are the molecular components of $P2Y_2$ activated CRAC channels. A) siRNA constructs targeting ORAI1 (10 nM) or STIM1 (10 nM) block the sustained Ca^{2+} entry stimulated by ATP without affecting the initial Ca^{2+} release from intracellular stores. Data are mean ± SEM of n = 21-31 cells per trace. **B)** Quantification of $[Ca^{2+}]_i$ from *A*. $[Ca^{2+}]_i$ was measured 5 minutes after agonist addition. Each data point is the mean $[Ca^{2+}]_i$ (averaged over 20-30 cells) for a given experiment (one dish) and the bar graph is the mean ± SEM of n = 3-4 independent experiments.

Histamine activates CRAC channels in AECs

Previous data had implicated PAR2 receptors in CRAC channel mediated Ca^{2+} signaling [95]. Histamine is another inflammatory mediator in the airways and we tested whether histamine could elicit Ca^{2+} signals in primary human AECs. Histamine evoked a similar initial Ca^{2+} rise as UTP and the PAR2 activator SLIGKV (Figure 2.4A-B). However, the sustained Ca^{2+} elevations were much more substantial for UTP than for either histamine or the PAR2 activator SLIGKV (Figure 2.4C). Next, we employed the ORAI1 inhibitor CM4620 to test whether histamine activates CRAC channels. CM4620 strongly inhibited the histamine-induced sustained $[Ca^{2+}]_i$ phase but left intact the rapid $[Ca^{2+}]_i$ rise (Figure 2.4D). Altogether, these findings suggest that while AECs express $P2Y_2$ receptors, histamine receptors, and PAR2 receptors, $P2Y_2$ receptor activation elicits the strongest Ca^{2+} signals. Furthermore, all three of these receptors have the capacity to activate CRAC channels in AECs.

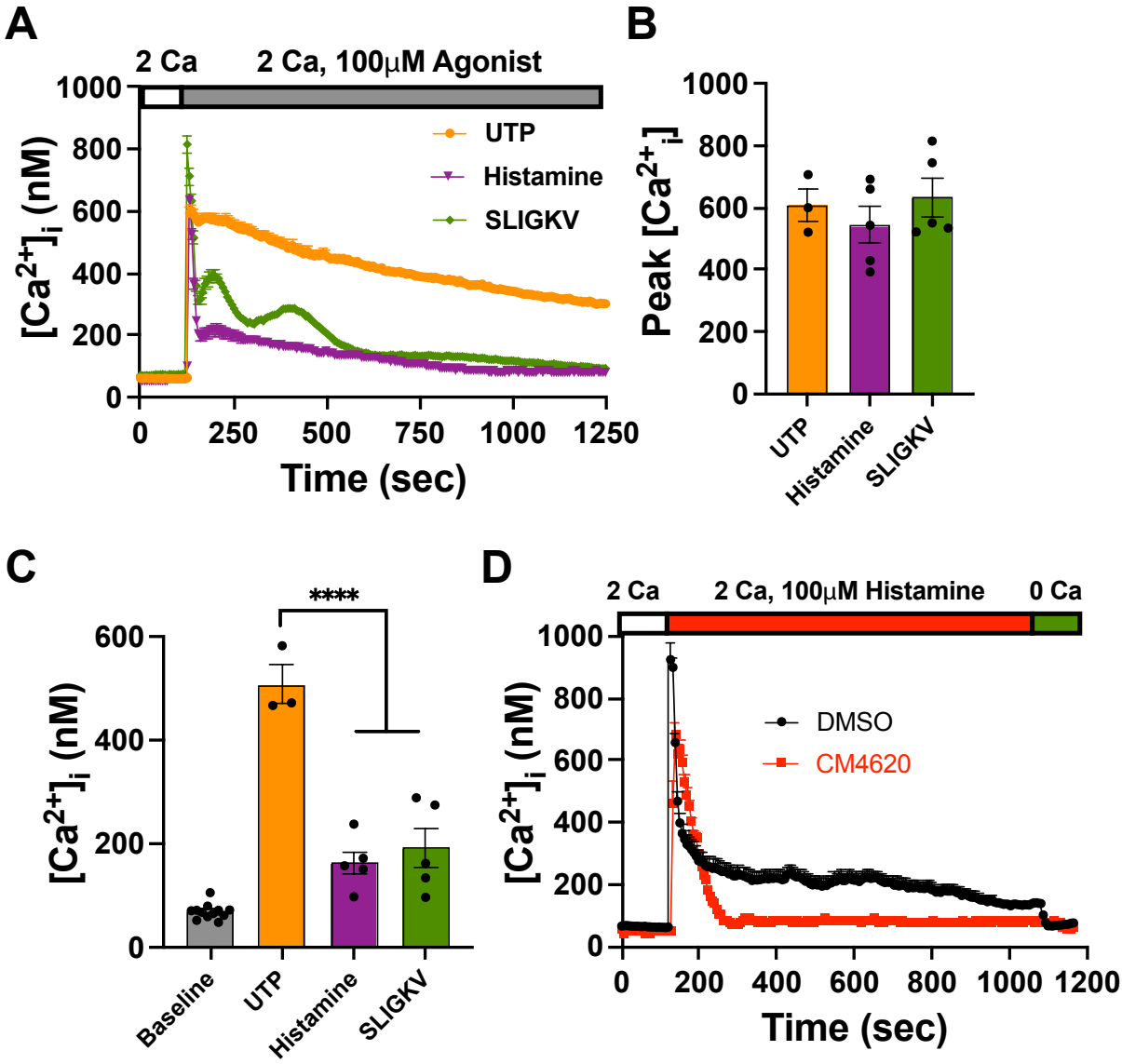

Figure 2.4 Histamine activates CRAC channels in AECs. A) The GPCR agonists UTP, histamine, and the PAR2 activator SLIGKV all elicit a $[Ca^{2+}]_i$ elevation. $[Ca^{2+}]_i$ was measured using Fura-2 AM as previously described [162]. Data are mean ± SEM of n = 40-50 cells. **B)** Summary of peak Ca^{2+} signal following agonist addition. Each data point is the mean peak Ca^{2+} signal (averaged over approximately 30-50 cells) for a given experiment (one dish) and the bar graph is mean ± SEM of n = 3-5 independent experiments. **C)** Quantification of $[Ca^{2+}]_i$ measured 5 minutes after agonist addition. Each data point is the mean $[Ca^{2+}]_i$ (averaged over 30-50 cells) for a given experiment (one dish) and the bar graph is the mean ± SEM of n = 3-5 independent experiments. **D)** Pretreatment of NHBE cells with the CRAC channel inhibitor, CM4620 (1 μM, 2 hrs) abolishes the sustained entry evoked by 100 μM histamine. Data are mean ± SEM of n = 27-32 cells per trace.

Discussion

Extracellular ATP is a damage-associated molecular pattern [18]. Upon allergen challenge in the lungs, ATP levels in the bronchoalveolar lavage fluid increase dramatically [16, 18]. This extracellular ATP regulates allergic sensitization and inflammation through purinergic P2 receptors [16, 18]. Histamine is also linked to airway inflammation [63]. However, it was unknown if nucleotides or histamine drive CRAC channel activation in AECs. Here we demonstrate that the nucleotides ATP and UTP both activate $P2Y_2$ receptors in AECs, eliciting Ca^{2+} signaling and CRAC channel activation through ORAI1 and STIM1. Likewise, histamine also activates CRAC channels in AECs through H_1 receptors. However, $P2Y_2$ receptor activation elicits more sustained Ca^{2+} signaling than H_1 receptor activation. The discovery that both ligands activate AEC CRAC channels leads us to speculate that CRAC channels may be a signaling nexus driving airway inflammation. Nonetheless, the function ramifications of nucleotide or histamine signaling and subsequent CRAC channel activation in AECs remain to be elucidated.

Chapter 3: Nucleotides evoke PGE_2 synthesis through $P2Y_2$ receptors, CRAC channels, MEK1/2-ERK1/2, and ultimately $cPLA_2$ signaling

Introduction

One of the most prominent mediators produced by AECs is Prostaglandin E2 (PGE_2). PGE_2 is synthesized through an enzymatic cascade tied to the activities of phospholipase A2, the COX-1 and COX-2 enzymes, and a terminal PGE synthase [109]. PGE_2 stimulates dilation of the lung airways thereby protecting the lung against severe bronchoconstriction that is a hallmark of diseases such as asthma [101, 102]. PGE_2 also inhibits several inflammatory processes, including the release of histamine and cysteinyl leukotrienes from mast cells [101], T-cell migration [103], ILC2 function [104], and the production of proinflammatory TNF-α and IL-12β by dendritic cells [105], while also enhancing the synthesis of the anti-inflammatory cytokine IL-10 [105] and promoting wound healing [106]. Further, growing evidence suggests that PGE_2 can drive reverse migration and removal of neutrophils from sites of inflammation to dissipate inflammation *in vivo [107]*. Failure of resolution of inflammation can lead to inflammatory diseases such as COPD and ARDS. Thus, within the lung, PGE_2 exerts predominantly bronchoprotective and anti-inflammatory effects [108].

The mechanism(s) by which ATP and UTP signaling engages the synthesis of PGE_2 in AECs is largely unclear. There is compelling evidence, however, that CRAC channel dependent cytosolic Ca^{2+} elevations are necessary [95]. As a multifunctional second messenger, Ca^{2+} activates distinct genetic programs to regulate many cellular functions including gene transcription, cytokine production and activation of numerous enzymes [167]. Other important signaling pathways such as the MEK1/2-ERK1/2

pathway and reactive oxygen species (ROS) have also been implicated in PGE_2 synthesis [93, 113, 168-170]. Here we find that nucleotides activate $P2Y_2$ receptors in AECs, initiating signaling culminating in CRAC channel dependent activation of $cPLA_2$ and subsequent PGE_2 release. Both the MEK1/2-ERK1/2 pathway and ROS from NADPH oxidases appear necessary for full production of PGE_2. These findings reveal the key nucleotide signaling checkpoints that mediate the synthesis of PGE_2 involving Ca^{2+} signals through CRAC channels as a key signaling nexus. We speculate that engaging these pathways may elicit bronchoprotective responses in the human airways.

Results

$P2Y_2$ receptor stimulation evokes PGE_2 synthesis

Prostaglandin E2 (PGE_2) is a major mediator released from AECs eliciting anti-inflammatory effects and limiting bronchoconstriction in the lungs [101, 102]. Nucleotides are known to elicit PGE_2 synthesis from AECs, but the receptors and signaling pathways responsible for this are largely unknown. Thus, we set out to identify the molecular mediators driving PGE_2 synthesis in AECs. To begin, we performed a time course analysis of PGE_2 in the supernatant following ATP stimulation. ATP-evoked a rapid increase in PGE_2 within 1 hour, which was sustained for several hours (Figure 3.1A). Next, we performed a dose-response analysis for ATP-mediated PGE_2 synthesis. Our analysis revealed an ATP-induced PGE_2 response with an EC_{50} of approximately 7 μM (Figure 3.1B). When we tested ATP and UTP in parallel, both caused release of PGE_2 to a similar degree (Figure 3.1C). This was highly suggestive of a common nucleotide membrane receptor driving the PGE_2 response. Therefore, we tested the

$P2Y_2$ receptor antagonist, AR-C 118925XX (hereby termed, "AR-C"), for its ability to inhibit the nucleotide driven PGE_2 response [53]. AR-C strongly abrogated the ATP- and UTP-mediated PGE_2 response (Figure 3.1C). To verify the involvement of $P2Y_2$ receptors using an RNAi-based method, we utilized siRNA to knockdown *P2RY2* mRNA. siRNA targeting *P2RY2* strongly decreased the mRNA levels (Figure 3.1D). *P2RY2* siRNA also abrogated the ATP-induced PGE_2 response, confirming the involvement of $P2Y_2$ receptors (Figure 3.1E). Interestingly, AR-C and siRNA targeting *P2RY2* both effectively inhibited the basal PGE_2 release, suggesting that $P2Y_2$ receptors exhibit a low-level, basal activation (Figure 3.1F-G). Collectively, these findings demonstrate that nucleotides drive PGE_2 release through the activation of AEC $P2Y_2$ receptors.

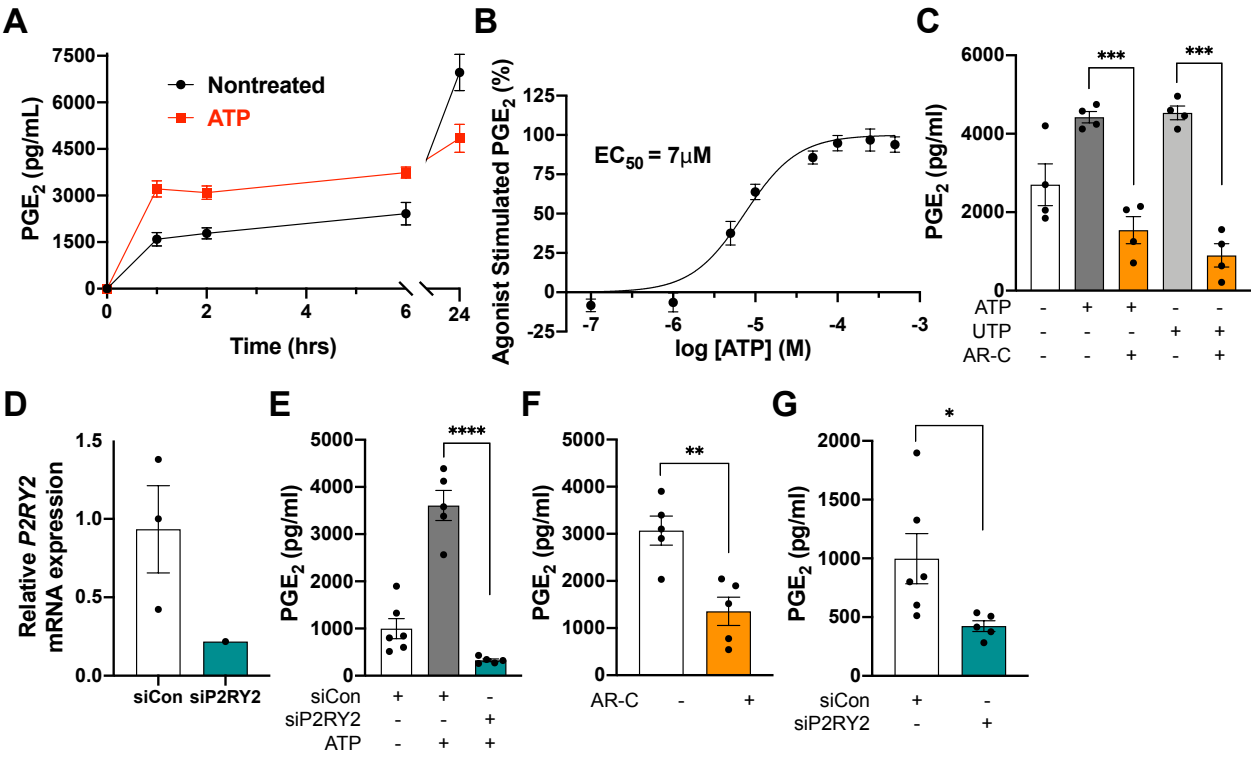

Figure 3.1 $P2Y_2$ receptor stimulation evokes PGE_2 synthesis. A) Time course of PGE_2 induction elicited by 250 μM ATP. Data are mean ± SEM of n = 6 samples/time

point. **B)** Dose-response of PGE_2 synthesis by ATP. PGE_2 was measured in the cell culture supernatant 2 hrs following agonist addition. The solid line is a four-parameter nonlinear regression fit of the Hill equation (*response= 1/(1 + $(EC_{50}/[agonist])^n$]*) with EC_{50} = 7.4 μM and Hill Slope = 1.35. Baseline PGE_2 was set to 0% and maximal agonist-evoked response was set at 100% for the fitting procedure. Data are mean ± SEM of n = 5-17 samples from 3 independent experiments. **C)** The selective $P2Y_2$ antagonist, AR-C 118925XX (10 μM), abrogates nucleotide (50 μM)-induced PGE_2 synthesis. Cells were pretreated with the antagonist for 1 hr prior to agonist stimulation (2 hr). Data are mean ± SEM of n = 4 samples. **D)** *siP2RY2* decreases *P2RY2* mRNA expression. Expression was normalized to the housekeeping gene *RPLP0*. Data are mean ± SEM of n = 1-3 samples. **E)** siRNA knockdown of *P2RY2* blocks ATP (100 μM)-induced PGE_2 synthesis. Data are mean ± SEM of n = 5-6 samples. **F)** The $P2Y_2$ antagonist AR-C 118925XX (10μM) inhibits basal PGE_2 synthesis. Data are mean ± SEM of n = 5 samples. **G)** siRNA against *P2RY2* lowers basal PGE_2 synthesis. Data are mean ± SEM of n = 5-6 samples. *p<0.05, **p<0.01, ***p<0.001, ****p<0.0001

Media change induces transient ATP release into the supernatant

Reports suggest mechanical strain can cause ATP release from cells *in vitro* [46, 47]. We tested whether a media change could evoke the release of ATP in NHBEs. ATP levels were very low in the supernatant of undisturbed cells whereas a media change provoked a rapid increase in extracellular ATP levels that decreased over time (Figure 3.2).

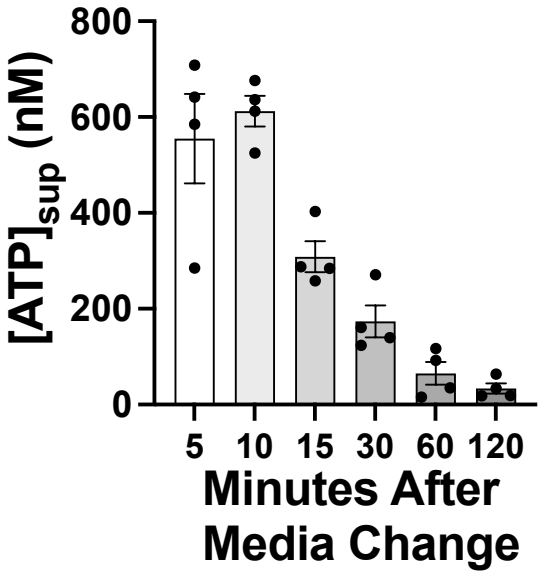

Figure 3.2 Media change evoked ATP release from NHBEs. A) Media was changed and ATP concentrations were measured in the supernatant at the indicated time points. Data are mean ± SEM of n = 4 samples/time point.

CRAC channel activation is essential for receptor-evoked PGE_2 synthesis

CRAC channels are activated upon $P2Y_2$ receptors activation (Figure 2.2). CRAC channels have also been implicated in other cell types in the production of prostaglandins and leukotrienes [80, 171]. Thus, we tested whether CRAC channels composed of ORAI1 and STIM1 were necessary for $P2Y_2$ receptor-evoked PGE_2 synthesis. Indeed, knockdown of either ORAI1 or STIM1 via siRNA inhibited the ATP-induced PGE_2 response (Figure 3.3A). To confirm the involvement of CRAC channels using an alternative method, we utilized the CRAC channel inhibitors CM4620 and BTP2. Both CRAC channel inhibitors strongly repressed the nucleotide-induced PGE_2 release (Figure 3.3B-C). This data implicates AEC CRAC channels are necessary for nucleotide-mediated PGE_2 responses.

Local Ca^{2+} signaling in the immediate proximity of the Ca^{2+} channel pore drives many Ca^{2+} dependent processes [84, 172]. Therefore, we tested whether CRAC channel-mediated PGE_2 synthesis exhibits this phenomenon of local Ca^{2+} signaling. We employed the Ca^{2+} chelators EGTA and BAPTA to assess this endpoint. Interestingly, BAPTA, which binds Ca^{2+} with much faster kinetics than EGTA [173], was much more effective at inhibiting the ATP-induced PGE_2 response (Figure 3.3D). BAPTA also inhibited the basal PGE_2 release while EGTA did not (Figure 3.3E). Altogether, this observed difference between BAPTA and EGTA is highly suggestive that the Ca^{2+} dependent machinery driving PGE_2 synthesis is spatially coupled to CRAC channels.

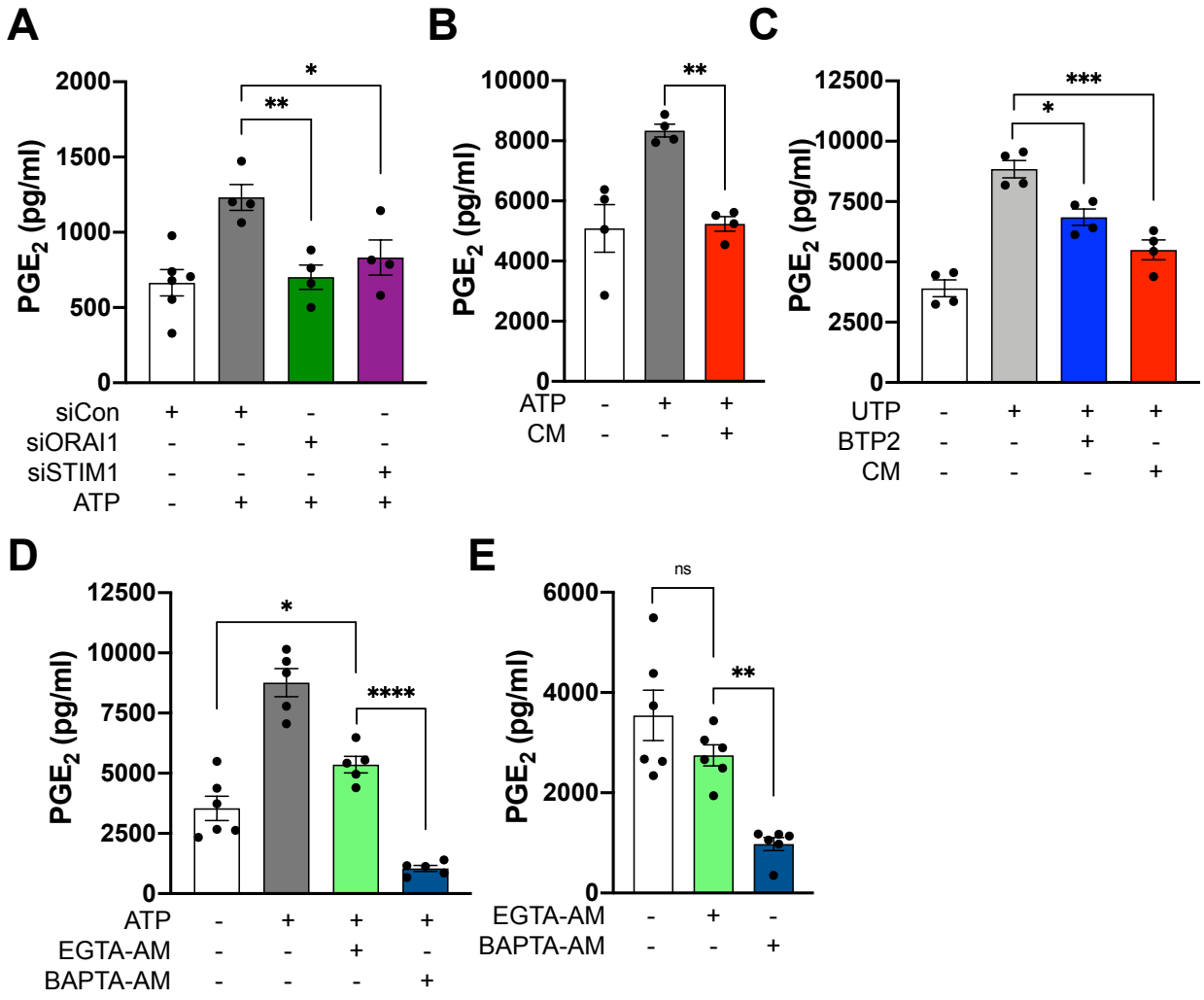

Figure 3.3 CRAC channels activation is essential for receptor-evoked PGE_2 synthesis. A) siRNA knockdown of ORAI1 and STIM1 blocks ATP (100 μM)-induced PGE_2 synthesis. Data are mean ± SEM of n = 4-5 samples. **B)** The ORAI1-selective CRAC channel inhibitor, CM4620, (1μM pretreated for 2 hrs; referred in the figure as "CM") abolishes ATP (100μM) induced PGE_2 synthesis. Data are mean ± SEM of n = 4 samples. **C)** CM4620 (1 μM) and the CRAC channel inhibitor, BTP2 (1 μM), inhibit UTP (50 μM)-induced PGE_2 synthesis. Data are mean ± SEM of n = 4 samples. **D)** PGE_2 synthesis induced by ATP (50 μM) persists in cells loaded with EGTA-AM (25 μM) but not in cells loaded with BAPTA-AM (25 μM). Cells were loaded with EGTA-AM or BAPTA-AM for 50 min prior to agonist stimulation. Data are mean ± SEM of n = 5-6 samples. **E)** Likewise, the baseline PGE_2 synthesis persists in cells loaded with the slow Ca^{2+} chelator, EGTA, but is abolished by the rapid Ca^{2+} chelator, BAPTA. Cells were loaded with EGTA-AM (25 μM) or BAPTA-AM (25 μM) for 50 min prior to 2 hr basal measurement. *p<0.05, **p<0.01, ***p<0.001, ****p<0.0001.

The MEK1/2-ERK1/2 kinase pathway is essential for PGE_2 synthesis

The MEK1/2-ERK1/2 pathway has been implicated downstream of receptor activation and in the production of PGE_2. Therefore, we examined whether $P2Y_2$ receptor activation could elicit ERK1/2 activation. ATP-induced a transient increase in ERK1/2 activation, which was blocked by the $P2Y_2$ receptor antagonist AR-C (Figure 3.4A-B). In contrast, CRAC channel inhibition did not prevent this ATP-mediated increase in ERK1/2 activation (Figure 3.4C). Next, we used the selective MEK1/2 inhibitor, U0126 [174], to block ERK1/2 activation. As expected, U0126 completely blocked the phosphorylation of ERK1/2, indicative of decreased ERK1/2 activity (Figure 3.4D). U0126 also strongly abrogated nucleotide-mediated increases in PGE_2 (Figure 3.4E-F). Collectively, these results implicate $P2Y_2$ receptor-mediated activation of the MEK1/2-ERK1/2 pathway as an essential step for PGE_2 synthesis.

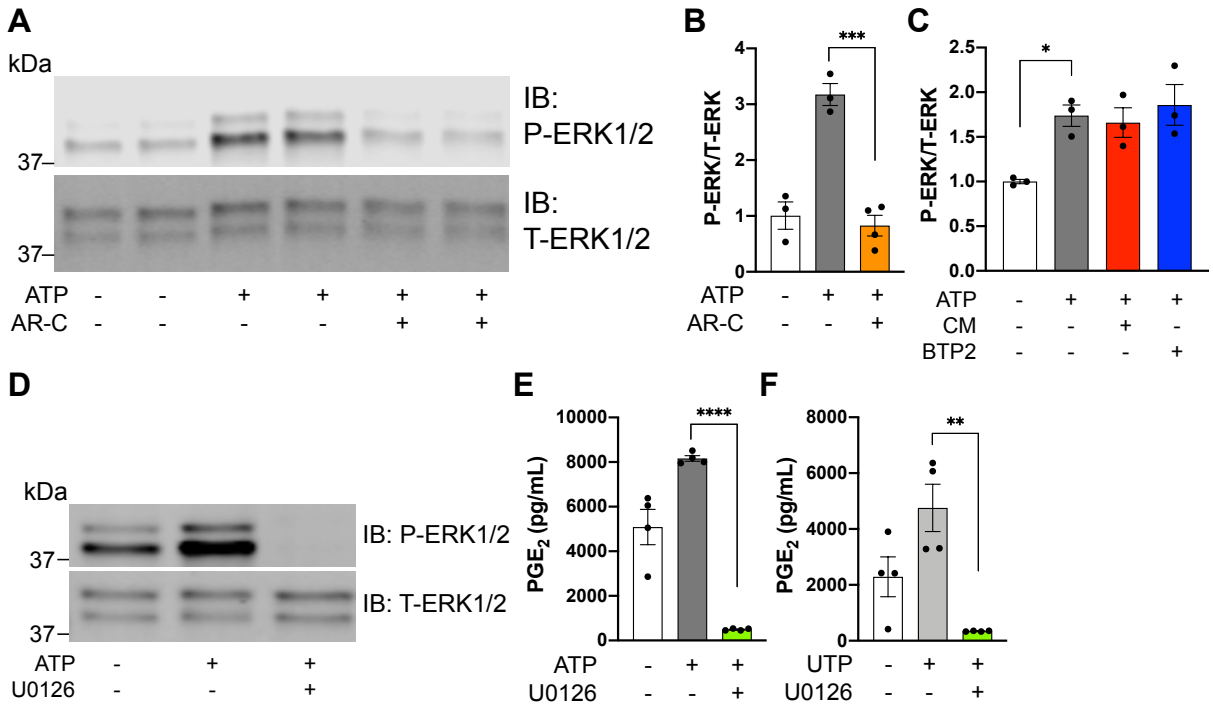

Figure 3.4 The MEK1/2-ERK1/2 kinase pathway is essential for PGE_2 synthesis. A) Western blot illustrating ATP (100 μM)-mediated induction of ERK1/2 phosphorylation in NHBE cells (15 min following agonist treatment). This is abolished by the selective $P2Y_2$ receptor antagonist AR-C 118925XX (10 μM). Cells were pretreated with AR-C 118925XX for 1 hour. (P-ERK: phospho-ERK; T-ERK: Total ERK). **B)** Densitometry analysis of the Western blot data from A. Data are mean ± SEM of n = 3-4 samples. **C)** CRAC channel inhibitors CM4620 (1μM) and BTP2 (1μM) do not alter ATP induced ERK1/2 activation (100 μM, 15min stimulation). Data are mean ± SEM of n = 3 samples and densitometry was performed for quantification. **D)** Pretreatment of cells with the MEK1/2 inhibitor U0126 (20μM) inhibits ATP (100μM) induced ERK1/2 phosphorylation. **E)** The MEK1/2 inhibitor, U0126 (20 μM), abolishes ATP (50 μM)-induced PGE_2 synthesis. Data are mean ± SEM of n = 4-5 samples. **F)** Likewise, UTP (50 μM)-induced PGE_2 synthesis is abolished by U0126 (20 μM). Cells were pretreated with U0126 for 1 hour. Data are mean ± SEM of n = 4-5 samples. *p<0.05, **p<0.01, ***p<0.001, ****p<0.0001

$P2Y_2$ receptor-mediated PGE_2 synthesis requires COX-2 activity but not COX-2 induction

One set of enzymes essential for PGE_2 synthesis is the COX-1/2 enzymes. Therefore, we tested whether COX-1 or COX-2 enzyme activity was necessary for AEC PGE_2 synthesis. The COX-1 inhibitor, FR122047, as well as the COX-2 inhibitor, Celecoxib, abolished AEC PGE_2 synthesis (Figure 3.5A). Previous work in a lung cancer cell line revealed that nucleotides could increase COX-2 protein levels [169]. Therefore, we measured COX-2 protein levels following ATP stimulation of AECs. ATP-induced a transient and modest increase in COX-2 protein levels that quickly returned to baseline (Figure 3.5B). We examined whether this modest increase in COX-2 protein levels was dependent on $P2Y_2$ receptor activation. The $P2Y_2$ receptor antagonist AR-C trended towards limiting this COX-2 induction (Figure 3.5C-D). The CRAC channel inhibitors CM and BTP2 did not inhibit this increase in COX-2 levels (Figure 3.5E). We also examined whether MEK1/2-ERK1/2 signaling was involved in this transient increase in COX-2 protein. The MEK1/2 inhibitor U0126 failed to inhibit the small increase in COX-2 protein levels (Figure 3.5F-G). Collectively, these findings suggest that the increase in COX-2 protein levels following nucleotide treatment is minimal whereas COX-2 activity is essential for AEC PGE_2 synthesis.

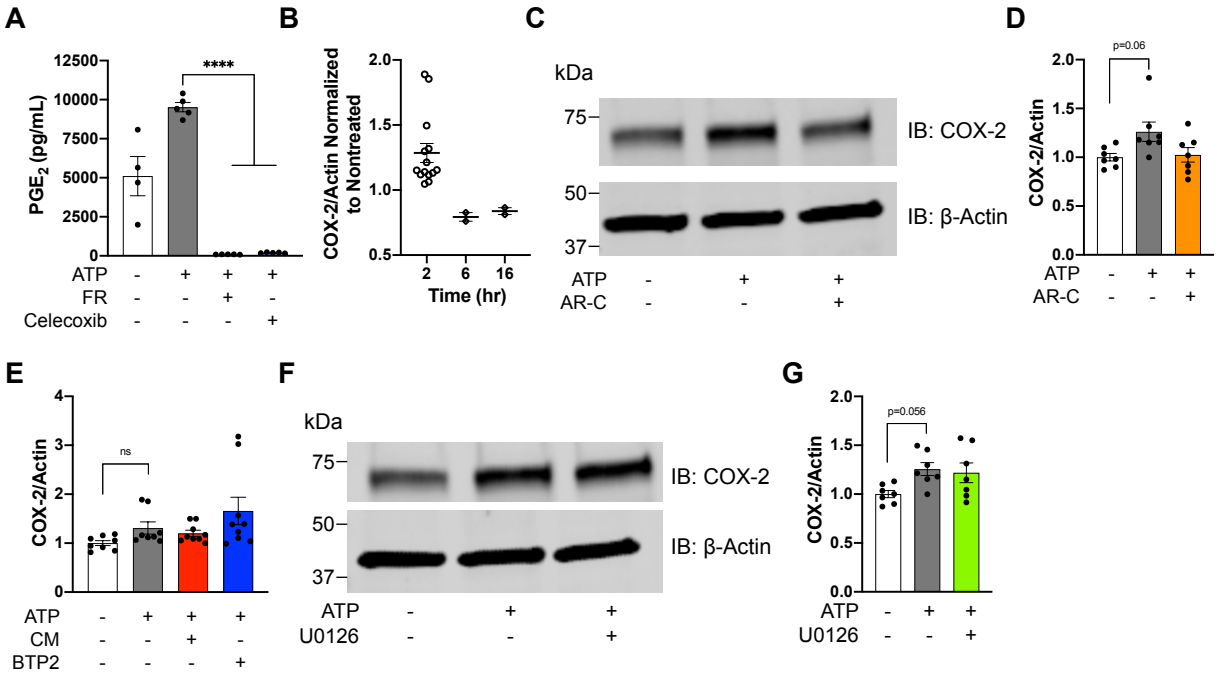

Figure 3.5 $P2Y_2$ receptor-mediated PGE_2 synthesis requires COX-2 activity but not COX-2 induction. A) PGE_2 synthesis induced by ATP (100 μM) is abolished with the COX-1 inhibitor FR122047 (1μM) and by the COX-2 inhibitor Celecoxib (1μM). Cells were pretreated for 1 hr prior to agonist stimulation. Data are mean ± SEM of n = 4-5 samples. **B)** Time course for ATP (100μM)-mediated COX-2 upregulation. Data are mean ± SEM of n = 2-14 samples. **C)** ATP (100μM, 2hrs) induces only a small extent of COX-2 upregulation, which is inhibited by AR-C 118925XX (10μM). **D)** Summary of COX-2 upregulation using densitometry analysis. Data are mean ± SEM of n = 7 samples. **E)** CRAC channel inhibitors CM4620 (1μM) and BTP2 (1μM) do not alter ATP (100μM) induced COX-2 upregulation (2hr stimulation duration). Data are mean ± SEM of n = 7-9 samples and densitometry was performed for quantification. **F)** ATP (100 μM, 2hrs) induces a low level of COX-2 upregulation, which is not inhibited by MEK1/2 inhibitor, U0126 (20μM). **G)** Densitometry analysis of the Western blot data illustrated in *F*. Data are mean ± SEM of n = 7 samples. ****p<0.0001

Inhibition of NADPH oxidase occludes ATP- and UTP- induced synthesis of PGE_2

Reactive oxidation species (ROS) has also been implicated in PGE_2 synthesis. The two primary sources of ROS in cells are plasma membrane associated NADPH oxidase enzymes and the mitochondria [175]. Therefore, we employed the NADPH oxidase

inhibitor, apocynin, and the mitochondrial ROS inhibitor S3QEL-2 [176], to interrogate whether ROS from either of these sources is involved in PGE_2 synthesis. Interestingly, apocynin strongly inhibited nucleotide-mediated PGE_2 release while S3QEL-2 was completely ineffective (Figure 3.6A-B). ROS has been linked to activation of the MEK1/2-ERK1/2 pathway. Thus, we investigated whether apocynin blocks ATP-induced ERK1/2 activation. Apocynin had no effect on ATP-mediated ERK1/2 activation (Figure 3.6C-D). Altogether, these results suggest that NADPH oxidase derived ROS is necessary for nucleotide-evoked PGE_2 synthesis in AECs.

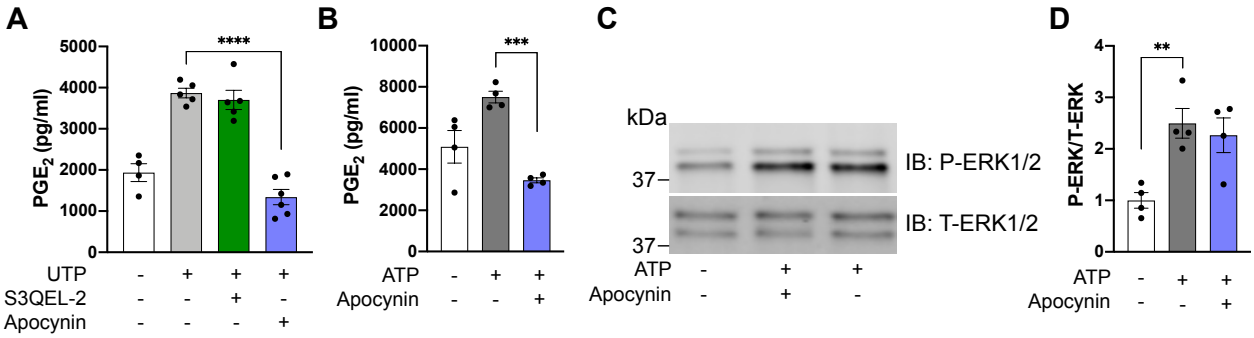

Figure 3.6 Inhibition of NADPH oxidase occludes ATP- and UTP- induced synthesis of PGE_2. A) Apocynin (200μM), an inhibitor of NADPH oxidase, abrogates UTP (50μM) induced PGE_2 synthesis. By contrast, the mitochondrial complex III inhibitor S3QEL-2 (20μM) does not affect the UTP (50μM)- induced PGE_2 response. Data are mean ± SEM of n = 4-6 samples. **B)** Likewise, apocynin (200μM) abrogates ATP (50μM)-induced PGE_2 synthesis. Data are mean ± SEM of n = 4 samples. **C)** Pretreatment of cells with the apocynin (200μM) does not inhibit ATP (100μM)-induced ERK1/2 phosphorylation (15min stimulation). **D)** Densitometry to quantify experiments shown in *C*. Data are mean ± SEM of n = 4 samples. **p<0.01, ***p<0.001, ****p<0.0001.

$P2Y_2$ receptor activation of CRAC channels elicits $cPLA_2$ activation

We next investigated the role of Ca^{2+}-dependent enzymes in the production of PGE_2. One key Ca^{2+}-dependent enzyme implicated in agonist-evoked responses is calcineurin. Therefore, we tested the calcineurin inhibitor, FK-506, for its role in the synthesis of PGE_2. FK-506 had no effect on ATP-induced PGE_2 release (Figure 3.7A). Another Ca^{2+}-dependent enzyme downstream of the COX enzymes and linked to PGE_2 synthesis is $cPLA_2$ [98]. Thus, we tested the $cPLA_2$ inhibitor, $AACOCF_3$, for its role in PGE_2 release. $AACOCF_3$ significantly inhibited ATP-evoked PGE_2 production (Figure 3.7B). Activation of $cPLA_2$ prompts its accumulation at intracellular membranes, where it liberates arachidonic acid from the phospholipid membrane [98, 177]. To interrogate this step more closely, we performed a nuclear versus cytosolic fractionation protocol followed by western blotting to assess $cPLA_2$ activation [80]. ATP-induced a rapid enrichment of $cPLA_2$ in the nuclear fraction (Figure 3.7C). The selective $P2Y_2$ receptor antagonist, AR-C, completely blocked $cPLA_2$ recruitment to the nuclear fraction (Figure 3.7C-D). Next, we investigated whether CRAC channel activation was required for $cPLA_2$ enrichment in the nuclear fraction. The CRAC channel inhibitors CM4620 and BTP2 both inhibited nucleotide-stimulated $cPLA_2$ recruitment to the nuclear fraction (Figure 3.7E-H). Collectively, these findings demonstrate that $P2Y_2$ receptor activation elicits CRAC channel-induced activation of $cPLA_2$.

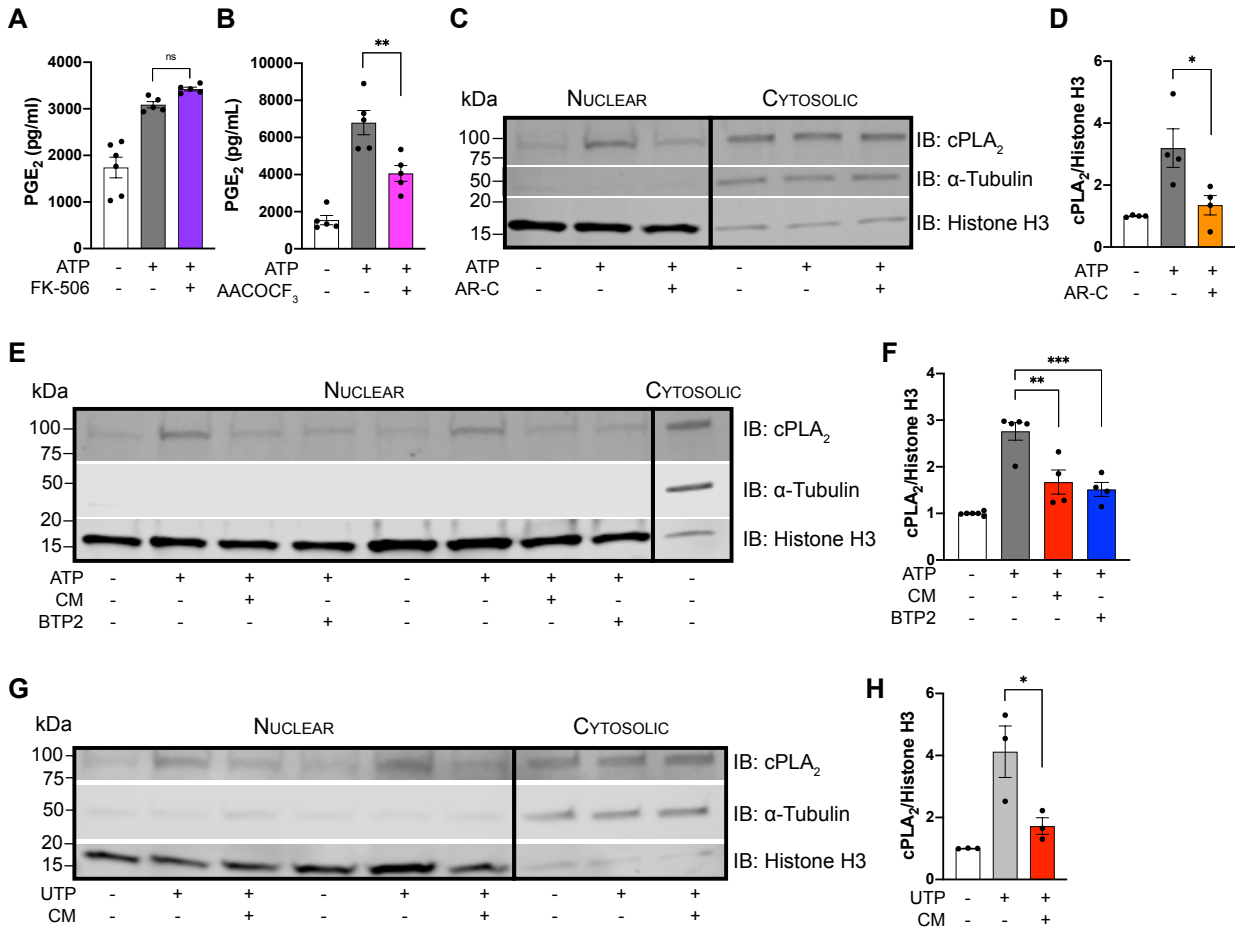

Figure 3.7 $P2Y_2$ receptor activation of CRAC channels elicits $cPLA_2$ activation. A) FK-506 (1 μM) does not inhibit ATP (100μM)-induced PGE_2 synthesis. Data are mean ± SEM of n = 5-6 samples. **B)** ATP (100 μM)-induced PGE_2 synthesis is inhibited with pretreatment of cells with $cPLA_2$ inhibitor $AACOCF_3$ (5 μM). Data are mean ± SEM of n = 5 samples. **C)** The $P2Y_2$ receptor antagonist AR-C 118925XX (10 μM) blocks ATP-induced enrichment of $cPLA_2$ in the nuclear fraction. **D)** Densitometry analysis of the Western blot data illustrated in *C*. Data are mean ± SEM of n = 4 samples. **E,F)** The CRAC channel inhibitors, CM4620/CM-EX-128 (1 μM referred as "CM") and BTP2 (1 μM), block ATP (100 μM)-induced enrichment of $cPLA_2$ in the nuclear fraction. Data are mean ± SEM of n = 4-5 samples. **G)** Likewise, CM4620 (1 μM) also blocks UTP (100 μM)-induced enrichment of $cPLA_2$ in the nuclear fraction. **H)** Densitometry to quantify experiments shown in *G*. Data are mean ± SEM of n = 3 samples. *p<0.05, **p<0.01, ***p<0.001

Airway Epithelial Cell passage number regulates PGE_2 production

Throughout our experiments examining PGE_2 release from AECs, we observed significant variability in the basal PGE_2 depending on the experiment. Thus, we pooled data from many experiments to compare the basal PGE_2 release levels. Our data was highly suggestive that higher passage number of cells leads to higher levels of basal PGE_2 release (Figure 3.8).

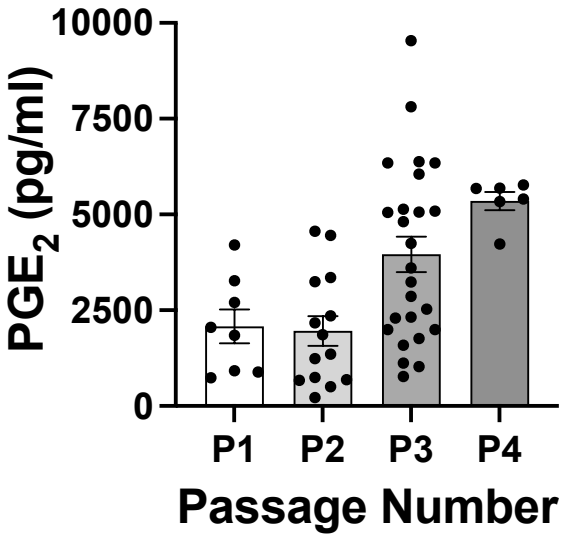

Figure 3.8 NHBE passage number correlates with basal PGE_2 production. Basal PGE_2 production of NHBEs sorted by passage number. Data are mean ± SEM of n = 6-25 samples.

Discussion

PGE_2 is a protective mediator in the airways. Specifically, it can protect against bronchoconstriction, a hallmark of diseases such as asthma [101, 102]. PGE_2 also

inhibits several inflammatory processes, such as the release of inflammatory mediators from mast cells [101], T-cell migration [103], ILC2 function [104], and the production of proinflammatory TNF-α and IL-12β by dendritic cells [105]. Moreover, PGE_2 can also promote the production of the anti-inflammatory cytokine IL-10 [105]. Understanding mechanisms that contribute to PGE_2 production in the airways may unveil pathways that can be harnessed in the context of lung inflammation.

Here we discover a multistep signaling pathway that culminates in PGE_2 release from AECs. The pathway begins with extracellular nucleotides activating the $P2Y_2$ receptor on AECs. $P2Y_2$ receptor activation elicits CRAC channel activation leading to rapid $cPLA_2$ recruitment to intracellular membranes, the liberation of arachidonic acid, and COX-2 dependent synthesis of PGE_2. The MEK1/2-ERK1/2 pathway is also activated by $P2Y_2$ receptors and is necessary for PGE_2 release. ROS from NADPH oxidases is also a necessary component for receptor-mediated production of PGE_2. Interestingly, we observed an increase in basal PGE_2 release with increasing passage number of NHBEs. This suggests that cellular senescence may lead to higher basal PGE_2 production.

An interesting feature of PGE_2 synthesis is that it's exquisite sensitivity to blockade by the rapid Ca^{2+} buffer BAPTA but not the slower buffer EGTA (Figure 3.3D-E). This result suggests that PGE_2 synthesis relies on local Ca^{2+} signaling likely through Ca^{2+} microdomains near CRAC channels that are functionally linked to $cPLA_2$ activation. Previous studies have shown that Ca^{2+} microdomains arising from CRAC channels can stimulate arachidonic acid release and leukotriene production in mast cells [80]. Ca^{2+} microdomains around CRAC channels are also linked to NFAT-dependent gene

transcription and exocytosis in neuronal stem cells and astrocytes [172, 178]. Thus, the finding that local Ca^{2+} signals around CRAC channels are essential for $cPLA_2$-mediated synthesis of PGE_2 broadens the role of Ca^{2+} microdomains linked to enzyme activation in different cell types.

Nucleotides are well known to be a danger-associated molecular pattern (DAMP) and are present in the context of asthma and COPD [16, 18, 21]. This suggests that the purinergic pathway culminating in PGE_2 release may be active in the context of ongoing lung inflammation. However, it may be therapeutically beneficial to enhance pathway activation even further with a selective $P2Y_2$ receptor agonist. Indeed, airway $P2Y_2$ receptors have attracted significant interest for therapeutics in recent years. A stable $P2Y_2$ receptor agonist (denufosol) was rigorously investigated in cystic fibrosis patients based on its ability to stimulate mucociliary clearance (MCC) [54]. Unfortunately, long-term treatment with denufosol showed no improvement of lung function in cystic fibrosis patients [55]. More studies may be warranted to test denufosol in the context of ongoing lung inflammation in patients with asthma or COPD.

Chapter 4: ATP evokes IL-6 release through P2X receptors and CRAC channel dependent Calcineurin-NFAT pathways

Introduction

Airway epithelial cells (AECs) can be induced to release interleukin-6 (IL-6). IL-6 is a proinflammatory cytokine that elicits a wide-range of inflammatory effects including T-cell expansion, pulmonary neutrophil infiltration, airway mucus secretion, lung fibrosis, and the hyperplasia and hypertrophy of airway smooth muscle cells [121-124]. Recent studies have linked IL-6 to numerous airway diseases such as asthma to COPD [121-124]. Importantly, patients with severe COVID-19 have revealed massive increases in IL-6 in the lung airways, a feature thought to contribute to microvascular thrombosis in the lung and multiple organ dysfunction in these patients [125]. Conversely, blockade of IL-6 signaling in mouse models of asthma protects against airway inflammation [122, 126], and early reports indicate that targeting IL-6 may be a viable therapy to decrease mortality in severe COVID-19 patients [127]. Collectively, understanding the signaling mechanisms orchestrating AEC release of IL-6 may prove beneficial for a host of human airway diseases.

One stimulus that is reported to elicit the release of IL-6 from AECs is extracellular nucleotides [36]. Recent discoveries in our lab have also highlighted AEC CRAC channels as essential for IL-6 production [95, 97]. Ca^{2+} is a multifaceted second messenger that coordinates distinct genetic programs to regulate many cellular functions including gene transcription, cytokine production and enzyme activation [167]. How nucleotides and Ca^{2+} signals combine to evoke the release of IL-6 from AECs

remains unclear. Here we discover that extracellular ATP activates ionotropic P2X receptors to provoke IL-6 release from AECs. In contrast to ATP, the uridine nucleotide UTP showed no efficacy for IL-6 release. CRAC channel activation and subsequent calcineurin/NFAT signaling was necessary for ATP-mediated IL-6 production. Similar to PGE_2 synthesis, the MEK1/2-ERK1/2 pathway was also necessary for full IL-6 release. Altogether, these findings highlight CRAC channels as a key signaling hub employed by purinergic receptor signaling.

Results

ATP drives IL-6 release through a pathway distinct from $P2Y_2$ receptors

ATP is known to elicit IL-6 release from AECs yet the receptor signaling mechanisms are largely unknown. To begin, we performed a time course analysis of ATP-induced IL-6 release. The majority of the IL-6 was released at overnight time points (Figure 4.1A). Next, we performed a dose-response analysis, which revealed that ATP-elicited release of IL-6 with an EC_{50} of approximately 16 μM (Figure 4.1B). Notably, this was significantly higher than the EC_{50} of approximately 7 μM for PGE_2 release (Figure 4.1B). To verify that ATP, and not a downstream metabolite of ATP, was increasing IL-6 secretion, we utilized the ATP variant, ATPγS, which is resistant to ecto-ATPase degradation. ATPγS evoked IL-6 release at similar doses seen for ATP (Figure 4.1C). As a complementary method to elucidate the active nucleotide driving IL-6 release, we employed the enzyme apyrase, which degrades ATP and ADP into AMP. When ATP was pretreated with apyrase prior to cellular stimulation, the IL-6 release was significantly decreased (Figure 4.1D). These findings strongly implicate ATP is the bona

fide ligand that elicits IL-6 release. Furthermore, we tested whether the $P2Y_2$ receptor antagonist, AR-C, blocked ATP-induced IL-6 release. AR-C showed no effect on ATP-mediated IL-6 release (Figure 4.1E). In agreement with this data, the $P2Y_2$ receptor agonist UTP did not elicit IL-6 release (Figure 4.1E). Altogether, these results imply that ATP drives IL-6 release through a pathway distinct from $P2Y_2$ receptors.

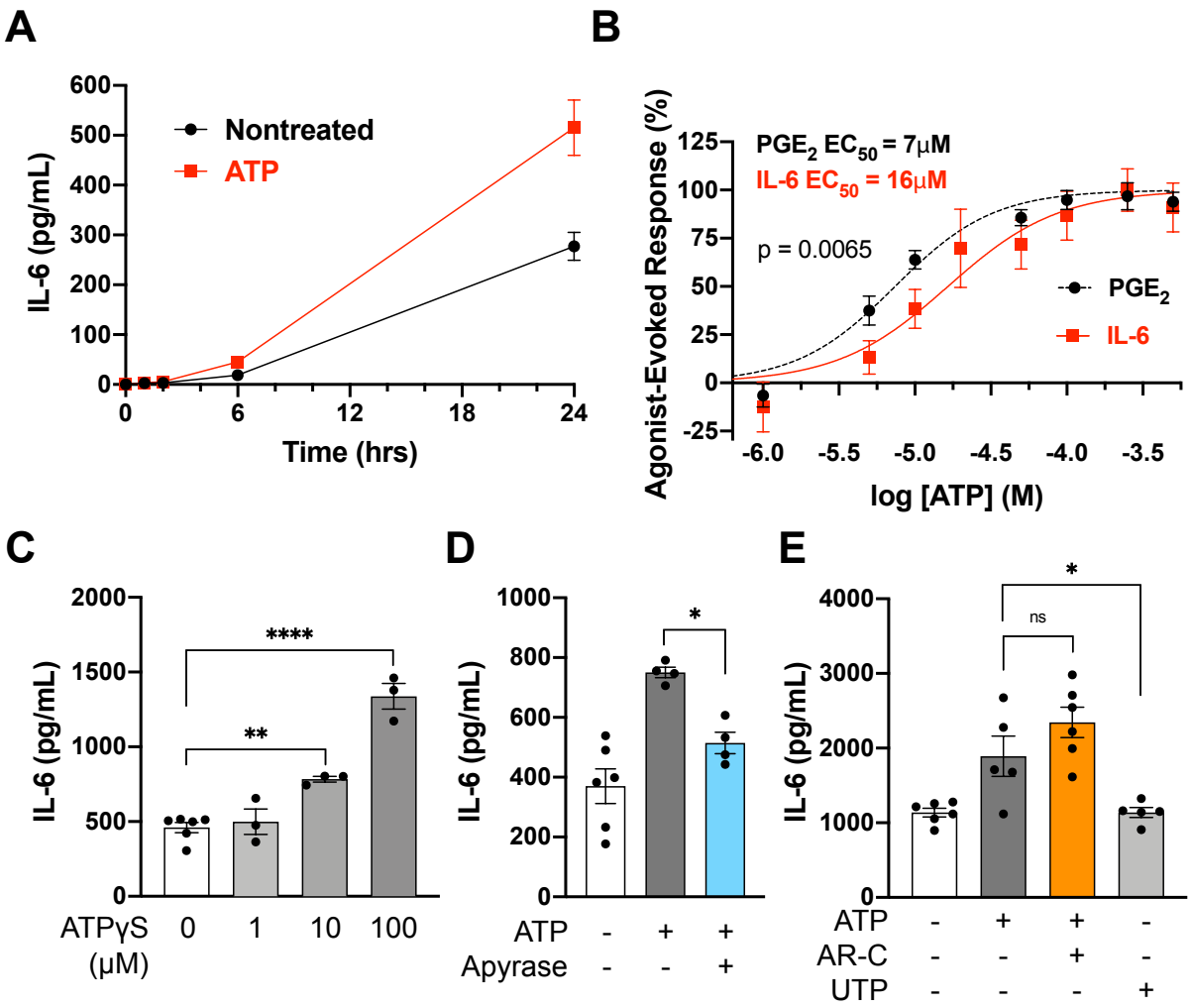

Figure 4.1 ATP drives IL-6 release through a pathway distinct from $P2Y_2$ receptors. A) Time course of ATP-induced IL-6 secretion from NHBE cells. Cells were stimulated with 250 μM ATP for the indicated times. Data are mean ± SEM of n = 6 samples/time point. **B)** Dose-response of IL-6 induction by ATP. IL-6 was measured in the cell culture supernatant 20 hrs following addition of ATP (red). The dose-response of ATP-induced PGE_2 (grey) from Figure 3.1B is shown for comparison. The data was fit with the Hill equation with EC_{50} = 16.5 μM and Hill Slope = 1.2. The extra sum-of-squares F-Test used to statistically compare the two dose-response curves. IL-6 data are mean ± SEM of n = 6-12 samples from two independent experiments. **C)** ATPγS stimulates IL-6 secretion. NHBE cells were treated with the indicated concentrations of ATPγS, and IL-6 was measured 16 hours following stimulation. Data are mean ± SEM of n = 3-6 samples. **D)** Pretreating ATP with apyrase (5U/mL) inhibits the ATP (250 μM)-induced IL-6 induction. Data are mean ± SEM of n = 4-6 samples. **E)** The ATP-induced IL-6 induction is not mediated by $P2Y_2$ receptors. The $P2Y_2$ receptor antagonist, AR-C 118925XX (10 μM), does not affect ATP (250 μM)-induced IL-6 secretion. Importantly, the P2Y receptor agonist, UTP (250 μM), fails to induce IL-6 secretion. Data are mean ± SEM of n = 5-6 samples.

P2Y receptors do not drive IL-6 release

To test whether an alternative P2Y receptor may elicit IL-6 release, we compared the efficacy of ATPγS and ADPβS in IL-6 secretion. ATPγS was much more effective at eliciting IL-6 secretion than ADPβS, ruling out ADP receptor involvement (Figure 4.2A). Next, we tested whether the $P2Y_6$ agonist UDP and the $P2Y_{11}$ agonist NF546 caused IL-6 release. Neither UDP nor NF546 induced IL-6 release (Figure 4.2B-C). In agreement with this, the $P2Y_{11}$ antagonist, NF157, did not inhibit IL-6 secretion (Figure 4.2D). Collectively, this data excludes all known subtypes of P2Y receptors in the ATP-induced IL-6 release.

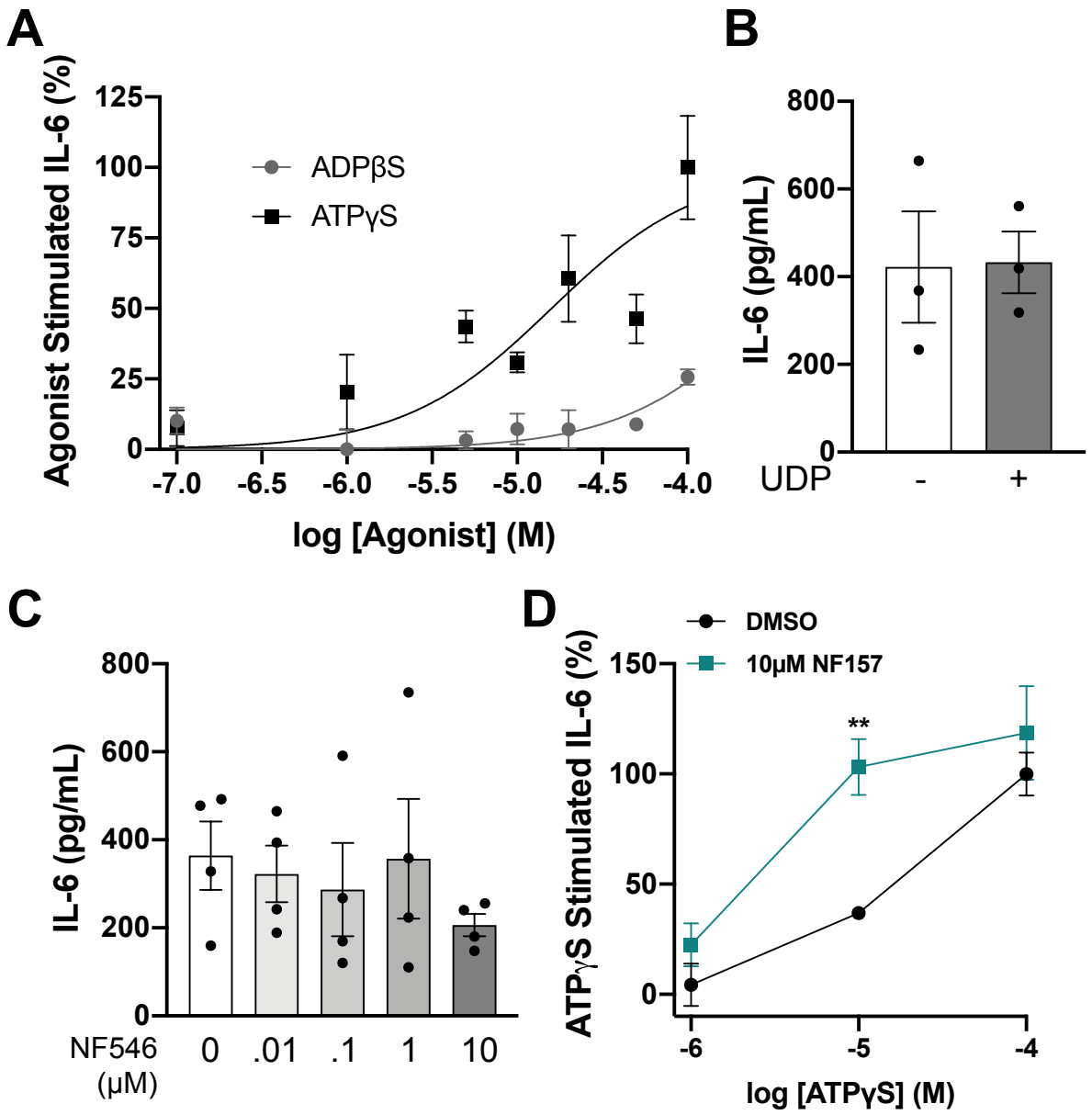

Figure 4.2 P2Y receptors do not drive IL-6 release. A) Dose-response for ATPγS versus ADPβS induced IL-6 secretion measured in cell culture supernatant 16 hrs following agonist addition. Data are mean ± SEM of n = 4-6 samples. **B)** UDP ($P2Y_6$ receptor agonist) does not elicit IL-6 secretion. Data are mean ± SEM of n = 3 samples. **C)** NF546 ($P2Y_{11}$ receptor agonist) fails to elicit IL-6 secretion. Data are mean ± SEM of n = 4 samples. **D)** NF157 (an antagonists of $P2Y_{11}$ and P2X1 receptors) enhances low dose ATPγS induced IL-6 secretion. Data are mean ± SEM of n = 3 samples.

P2X receptors drive IL-6 secretion

We examined primary human AECs for their expression of P2X receptors via RT-qPCR. In two independent donors, we were able to detect expression of *P2RX4,5,7* (Figure 4.3A). We employed the broad-spectrum P2X receptor antagonists PPADS and suramin. Both antagonists strongly inhibited IL-6 secretion (Figure 4.3B). Then, we tested a series of P2X subtype selective antagonists. The antagonist of P2X1, P2X3, and P2X2/3 receptors, TNP-ATP, did not block IL-6 secretion (Figure 4.3C). Likewise, the P2X4 receptor antagonist, 5-BDBD, did not block IL-6 release (Figure 4.3D). Similarly, the P2X7 receptor antagonist, A740003, also did not inhibit IL-6 secretion (Figure 4.3E). Finally, we used shRNA to knockdown *P2RX4* mRNA. The knockdown showed low efficacy and did not inhibit IL-6 secretion (Figure 4.3F-G). These findings suggest that multiple P2X receptors may simultaneously engage to evoke IL-6 release.

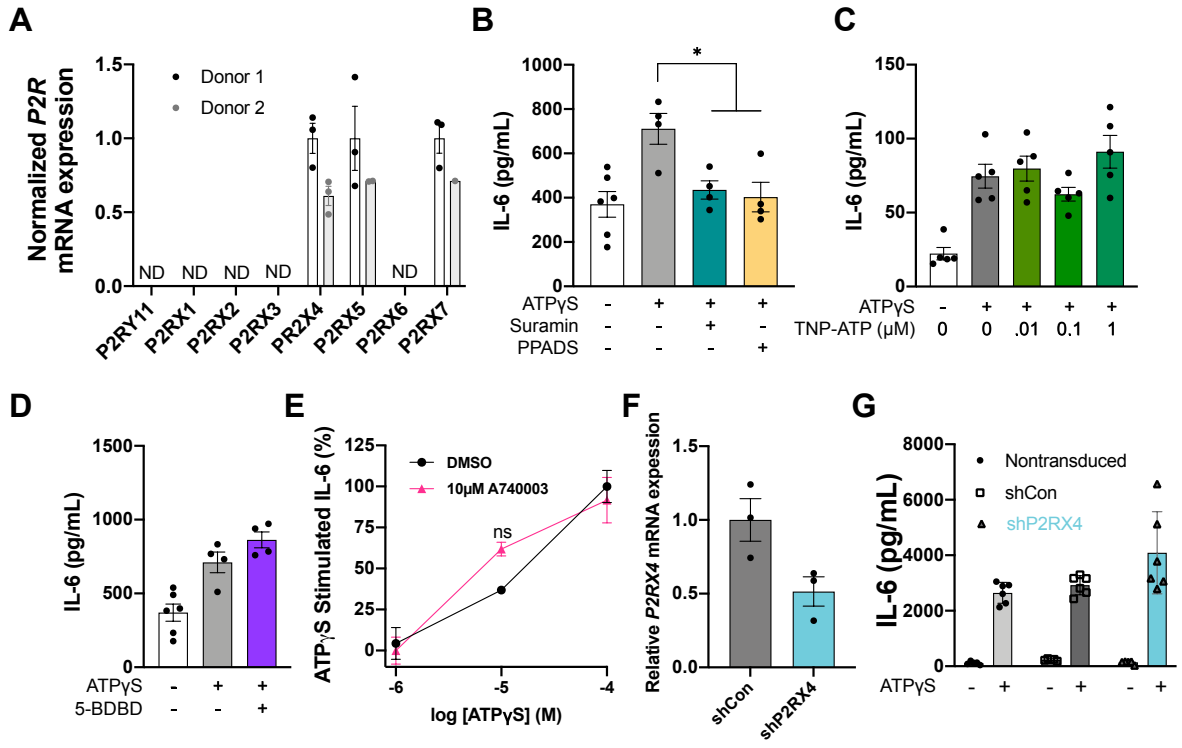

Figure 4.3 P2X receptors drive IL-6 secretion. A) Two independent donors (NHBE cells) were examined for P2R expression via RT-qPCR. *P2RX4,5,7* were detected while *P2RY11, P2RX1-3,6* were not detected. **B)** The broad-spectrum P2X antagonists PPADS (100 μM) and suramin (100 μM) abrogate ATPγS (10 μM)-induced IL-6. Data are mean ± SEM of n = 4-6 samples. **C)** TNP-ATP, an antagonist of P2X1, P2X3, and P2X2/3 receptors does not inhibit ATPγS-induced (10 μM) IL-6 secretion. Data are mean ± SEM of n = 5 samples. **D)** The P2X4 receptor antagonist, 5-BDBD (5 μM), does not inhibit ATPγS-induced (10 μM) IL-6 secretion. Data are mean ± SEM of n = 4-6 samples. **E)** The P2X7 receptor antagonist A740003 (10 μM) also does not inhibit ATPγS-induced IL-6 secretion. Data are mean ± SEM of n = 3-6 samples. **F)** *P2RX4* mRNA knockdown using shRNA quantified via RT-qPCR. Expression was normalized to the housekeeping gene *RPLP0*. Data are mean ± SEM of n = 3 samples. **G)** Knockdown of *P2RX4* does not affect ATPγS-evoked IL-6 synthesis. Data are mean ± SEM of n = 5-6 samples.

CRAC channels drive IL-6 release through a calcineurin-NFAT pathway

CRAC channel activation in AECs has been linked to IL-6 secretion [95, 97]. Therefore, we tested whether the CRAC channel inhibitors CM4620 and BTP2 inhibited ATPγS-induced IL-6 secretion. Indeed, both inhibitors significantly inhibited IL-6 release (Figure 4.4A). One Ca^{2+}-dependent enzyme CRAC channels activate is $cPLA_2$. However, the $cPLA_2$ inhibitor, $AACOCF_3$, did not inhibit IL-6 secretion (Figure 4.4B). Another enzyme downstream of CRAC channels is the Ca^{2+}-dependent phosphatase calcineurin. The calcineurin inhibitor, FK-506, strongly abrogated ATPγS-induced IL-6 secretion (Figure 4.4C). These results are strongly suggestive that CRAC channel dependent calcineurin-NFAT pathways are necessary for IL-6 release.

A host of stimuli have the capacity to elicit IL-6 release from AECs. Surprisingly, the CRAC channel inhibitor CM4620 inhibited basal IL-6 release in AECs (Figure 4.4D). This result did depend somewhat on the donor and the basal levels of IL-6 release (data not shown). For example, conditions where basal IL-6 release was high were more likely to exhibit this CRAC channel dependence on the basal release. We tested whether CRAC channels are necessary for stimulus-induced IL-6 release from an array of ligands. CM4620 inhibited house dust mite (HDM)-induced IL-6 release (Figure 4.4E). Similarly, CM4620 blocked TNF-α-driven IL-6 secretion (Figure 4.4F). Moreover, both CM4620 and BTP2 abrogated IL-1β-driven IL-6 release (Figure 4.4G). Altogether, these discoveries highlight that AEC CRAC channel activity is broadly necessary for stimulus-evoked IL-6 secretion.

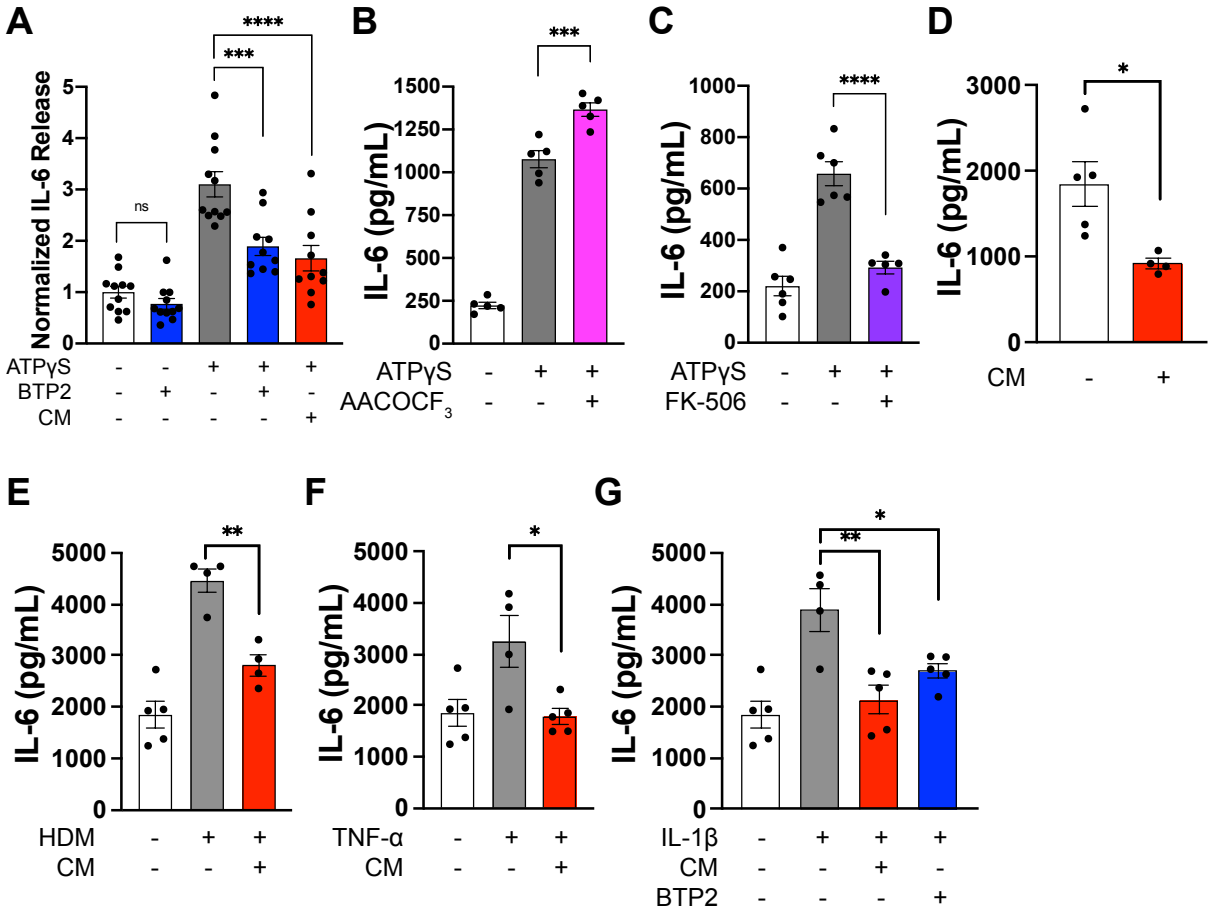

Figure 4.4 CRAC channels drive IL-6 release through a calcineurin-NFAT pathway. **A)** CM4620 (1 μM) and BTP2 (1 μM) block ATPγS (100μM)-induced IL-6 secretion. Due to variability in basal IL-6 release between different human donors, the data shown here are normalized to the levels found in unstimulated cells. The absolute concentrations of IL-6 in unstimulated cells ranged from 100 to 700 pg/mL. Data are mean ± SEM of n = 10-11 samples. **B)** IL-6 release induced by ATPγS (100 μM) is not affected by $AACOCF_3$ (5μM). Data are mean ± SEM of n = 5 samples. **C)** The calcineurin inhibitor FK-506 (1 μM) blocks ATPγS-induced IL-6 secretion. Data are mean ± SEM of n = 5-6 samples. **D)** CM4620 (2 μM) can block basal IL-6 release. **E)** CM4620 (2 μM) also blocks HDM (100μg/mL)-induced IL-6 secretion. **F)** CM4620 (2 μM) blocks TNF-α (10ng/mL)-induced IL-6 secretion. **G)** CM4620 (2 μM) and BTP2 (5 μM) also block IL-1β (10ng/mL)-induced IL-6 secretion. *p<0.05, **p<0.01, ***p<0.001, ****p<0.0001,

Reactive Oxygen Species are necessary for IL-6 induction

Reactive oxygen species (ROS) have been linked to IL-6 from AECs. Therefore, we set out to interrogate whether plasma membrane-associated ROS, from NADPH oxidases, or mitochondrial-associated ROS were necessary for IL-6 secretion. Interestingly, the NADPH oxidase inhibitor, apocynin, and the mitochondrial ROS inhibitor, S3QEL-2, both showed partial blockade of ATPγS-induced IL-6 secretion (Figure 4.5). This suggests that ROS from both the plasma membrane-associated NADPH oxidases and mitochondria may regulate AEC IL-6 release.

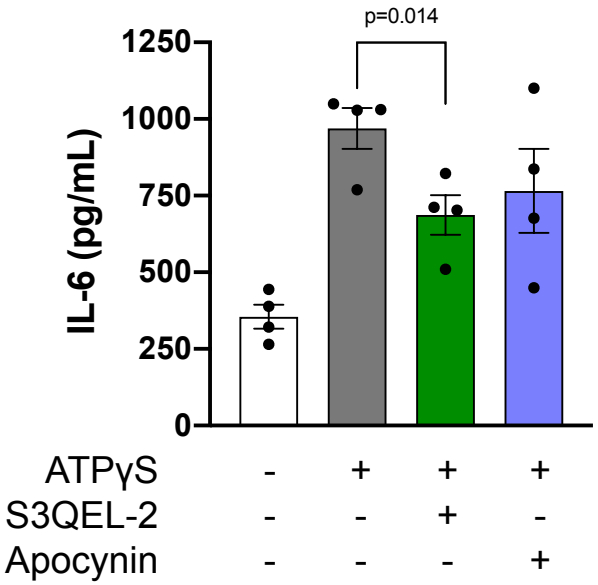

Figure 4.5 Reactive Oxygen Species are necessary for IL-6 induction. Inhibition of NADPH oxidase with apocynin (200μM) or the mitochondrial complex III inhibitor S3QEL-2 (20μM) have only modest effects on ATPγS (100μM) induced IL-6 synthesis. Data are mean ± SEM of n = 4 samples.

ROS from mitochondrial complex III does not activate NFAT in BEAS-2B cells

Reports suggest that ROS from mitochondrial complex III are implicated in NFAT activation and IL-6 release in immune cells [179, 180]. We utilized the NFAT firefly luciferase plasmid to dissect NFAT signaling in BEAS-2B cells. The NFAT promoter sequence in this plasmid is taken from the human IL-2 gene [181, 182]. As expected, the calcineurin inhibitor FK-506 blocked the induction of the luciferase (Figure 4.6A) confirming the calcineurin-NFAT pathway is necessary for luciferase production. The mitochondrial complex III ROS inhibitor S3QEL-2 [176] also dramatically blocked the production of the NFAT luciferase (Figure 4.6B) suggesting a role for ROS in the synthesis the luciferase. We assayed NFAT activation directly employing a NFAT4-GFP construct. Although FK-506 strongly blocked TG-induced NFAT4 nuclear translocation, S3QEL-2 did not inhibit translocation (Figure 4.6C) indicating mitochondrial complex III ROS does not directly activate NFAT4 downstream of CRAC channels. Finally, although TG-mediated IL-6 secretion from AECs is NFAT dependent [95], S3QEL-2 had no affect on TG-evoked IL-6 secretion (Figure 4.6D). It is likely that the S3QEL-2 impact on the NFAT luciferase is a result of the IL-2 NFAT promoter sequence also containing an AP-1 site [182, 183]. Altogether, mitochondrial ROS does not appear to be necessary for CRAC channel dependent IL-6 secretion in BEAS-2B cells.

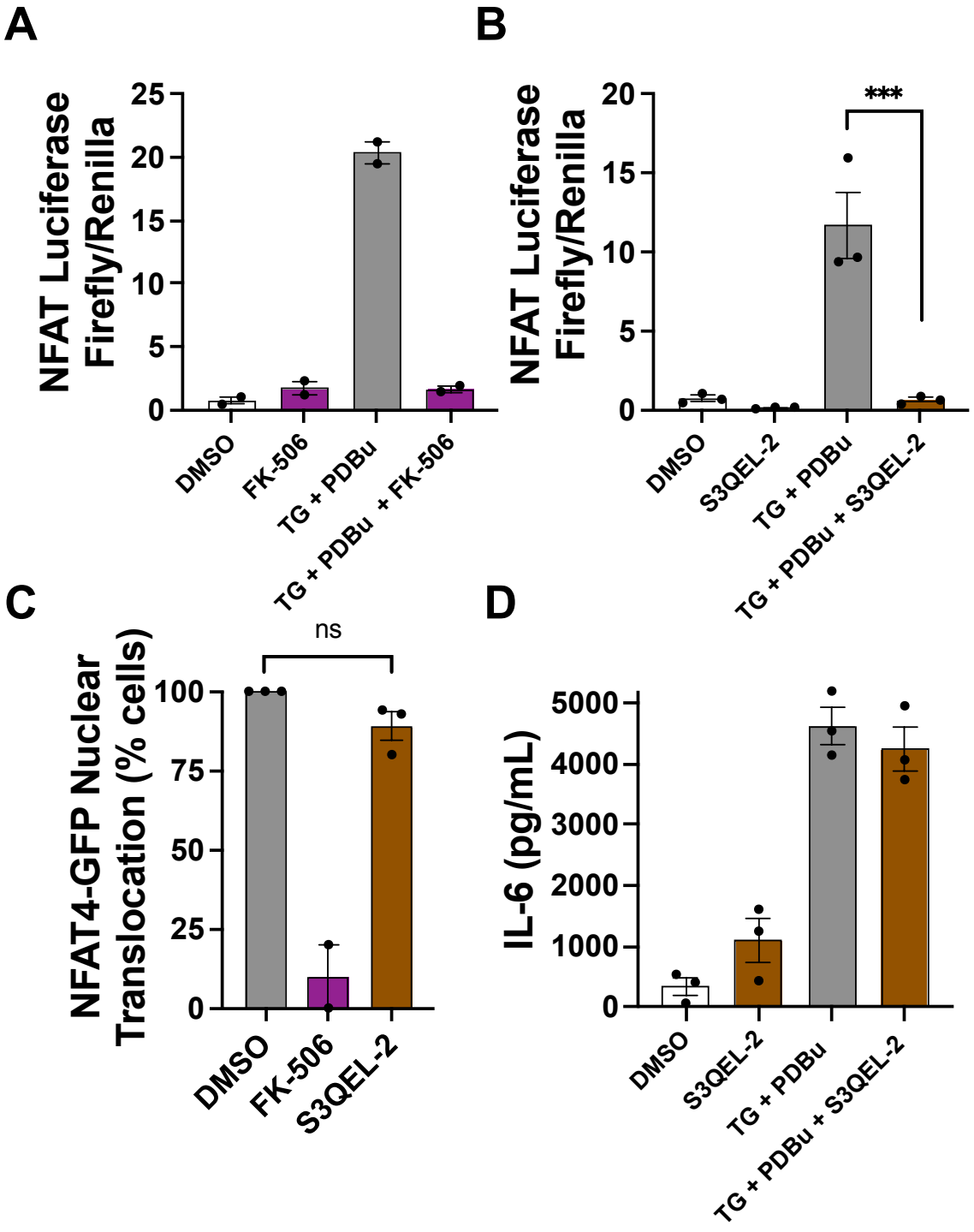
A
NFAT Luciferase Firefly/Renilla
25
20
15
10
5
0
DMSO
FK-506
TG + PDBu
TG + PDBu + FK-506
B
NFAT Luciferase Firefly/Renilla
20
15
10
5
0
***
DMSO
S3QEL-2
TG + PDBu
TG + PDBu + S3QEL-2
C
NFAT4-GFP Nuclear Translocation (% cells)
ns
100
75
50
25
0
DMSO
FK-506
S3QEL-2
D
IL-6 (pg/mL)
5000
4000
3000
2000
1000
0
DMSO
S3QEL-2
TG + PDBu
TG + PDBu + S3QEL-2

Figure 4.6 Complex III ROS does not activate NFAT downstream of CRAC channels in BEAS-2B cells. A-B) NFAT and mitochondrial complex III ROS are both required from activation of NFAT luciferase construct. BEAS-2B cells were transfected with NFAT luciferase plasmids and treated with compounds for 6 hours prior to analysis. **C)** S3QEL-2 does not block NFAT4-GFP translocation in BEAS-2B. Cells were treated with TG for 20 minutes prior to analysis of nuclear translocation. **D)** S3QEL-2 does not block TG-induced IL-6 secretion in BEAS-2Bs.
***p<0.001

MEK1/2-ERK1/2 signaling is necessary for IL-6 induction

MEK1/2-ERK1/2 signaling has also been linked to AEC IL-6 release. Indeed, the MEK1/2 inhibitor U0126 strongly abrogated the ATPγS-evoked IL-6 secretion (Figure 4.7). This data implicates the MEK1/2-ERK1/2 signaling pathway in ATPγS-evoked IL-6 secretion in AECs.

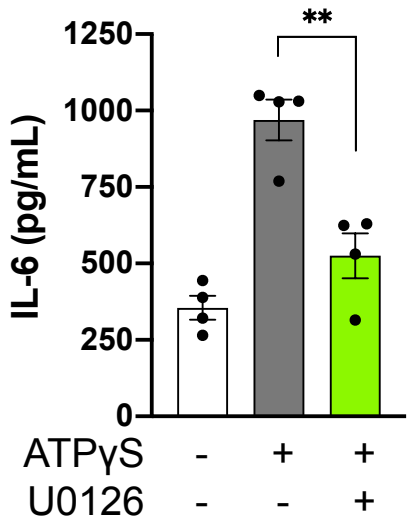

Figure 4.7 MEK1/2-ERK1/2 signaling is necessary for IL-6 induction.
The ATPγS (100 μM)-induced IL-6 secretion is abolished by the MEK1/2 inhibitor U0126 (20μM). Data are mean ± SEM of n = 4 samples. **p<0.01

Airway Epithelial Cell passage number regulates IL-6 production

Throughout our experiments examining IL-6 release from AECs, we observed significant variability in the basal IL-6 secretion depending on the experiment. Thus, we pooled data from many experiments to compare the basal IL-6 release levels. Our data was highly suggestive that higher passage number of cells leads to higher levels of basal IL-6 release (Figure 4.8).

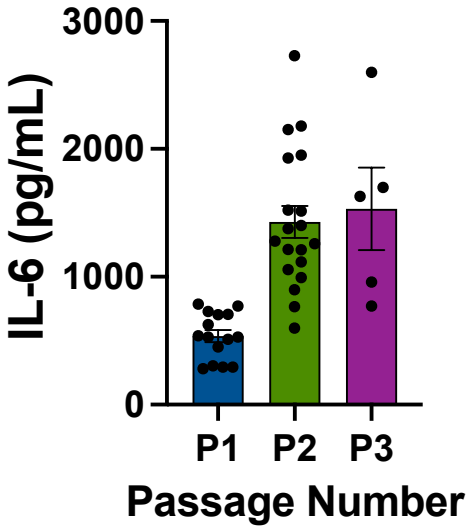

Figure 4.8 NHBE passage number correlates with basal IL-6 production. Basal IL-6 production of NHBEs sorted by passage number. Data are mean ± SEM of n = 5-20 samples.

Discussion

In the airways, nucleotide signaling is linked to a wide range of immune effects. High concentrations of extracellular ATP are linked to the production of inflammatory

cytokines leading to immune cell infiltration, airway remodeling, and hyperresponsiveness [13, 16, 18, 36]. Patients with asthma, COPD, and ARDS show increased airway ATP levels in the BAL fluid and elevated extracellular ATP is thought to contribute to disease pathology [16, 21, 22]. However, while high concentrations of extracellular ATP are considered pro-inflammatory, ATP (and UTP) can also stimulate many anti-inflammatory [184], and physiologically beneficial effects in the lung including mucociliary clearance (MCC), PGE_2 synthesis, and wound healing [23-25, 27, 94]. The differential cellular pathways mediating these potentially beneficial and harmful effects are not well understood.

Here we describe the cell signaling mechanisms underlying the purinergic IL-6 production from AECs. It is worth comparing the purinergic pathways that drive IL-6 versus PGE_2 as the first pathway is potentially proinflammatory while the second is bronchoprotective. Our results indicate that ATP/UTP signaling through $P2Y_2$ receptors activates CRAC channels and ERK1/2, and subsequently $cPLA_2$, resulting in rapid synthesis of PGE_2, which is known to evoke bronchoprotective and immune suppressive effects (Figure 4.9) [101-105, 108, 185]. To our knowledge, this is the first identification of AEC $P2Y_2$ receptors in stimulating protective PGE_2 synthesis. By contrast, ATP-mediated induction of IL-6, which is implicated in proinflammatory responses in the airways [121-124, 126, 127], appears to occur through stimulation of P2X receptors through a process requiring CRAC channels, ERK1/2 activation, but also distinctly involving calcineurin/NFAT activation (Figure 4.9).

Several key features both upstream and downstream of CRAC channels underscore the differences in the two pathways. First, although UTP strongly induces

PGE_2, it is completely ineffective in evoking IL-6 synthesis (Figure 3.1C versus 4.1E). In contrast, ATP evokes both PGE_2 and IL-6 synthesis, albeit at different potencies (7μM versus ~16μM; Figure 4.1B) and over significantly different time courses (Figure 3.1A versus 4.1A). As noted above, this difference is related to the different receptors ($P2Y_2$ versus P2X receptors) involved in stimulating PGE_2 and IL-6. Second, the Ca^{2+}-dependent signaling pathways downstream of receptor activation significantly differ: $P2Y_2$ receptor-driven PGE_2 synthesis involves Ca^{2+} activation of $cPLA_2$ whereas P2X-driven IL-6 secretion requires Ca^{2+}-dependent transcription via the calcineurin/NFAT pathway. As well, distinct sources of ROS appear to be involved in regulating the production of these mediators.

What are the functional implications of these findings and under what conditions could these differing outcomes become apparent? Although speculative, we can envision two scenarios. First, the observation that PGE_2 synthesis by ATP occurs at lower ATP doses than that required for IL-6 suggests that the protective versus proinflammatory outcomes for ATP may be dictated in part by the concentration and duration of ATP signaling in the airways. In the healthy lung, low micromolar levels of ATP over short time scales may selectively evoke PGE_2, whereas higher levels of ATP occurring over longer durations such as those found under conditions of intense inflammation and/or cellular necrosis would be predicted to elicit robust IL-6 synthesis. Although it is worth noting that studies that have quantified purine concentrations in sputum or BALf of diseased human patients tend to find concentrations in the high nM or low μM range [21, 186]. Second, extracellular UTP secretion would be predicted to exclusively induce PGE_2. Growing evidence points to UTP as a physiologically relevant

signaling molecule linked to numerous cellular processes including ion transport, ciliary beat frequency, and mucin release [28]. Although regulated secretion of UTP is very poorly understood likely due to lack of tools to easily detect extracellular UTP [187], release of UTP *in vitro* following mechanical stress, apoptosis, and solution exchange has been demonstrated using HPLC from a number of tissues including airway epithelial cells [46, 47, 50, 188]. UTP release under these conditions would be expected to preferentially evoke bronchoprotective responses in the lung. Future *in vivo* studies using mouse models in which $P2Y_2$ receptors are selectively deleted in the lung epithelium could shed light on this important question.

Two important mechanistic questions raised by our study that remain to be addressed relate to the nature of the Ca^{2+} signal activated by CRAC channels that drives IL-6 induction, and the mechanism of how P2X receptor stimulation is coupled to activation of CRAC channels. The data indicate that antagonism of $P2Y_2$ receptors blocks both ATP- and UTP-evoked Ca^{2+} elevations to similar extents (Figure 2.1D-F). Yet, unlike ATP, UTP is completely ineffective in inducing IL-6 (Figure 4.1E). Because CRAC channel blockade strongly inhibits induction of IL-6 by ATP (Figure 4.4A), this result suggests that ATP-mediated induction of IL-6 requires Ca^{2+} influx reliant on CRAC channels that is not readily detected by Fura-2. We speculate that P2X receptor activation of CRAC channels occurs over much longer time periods than was evaluated in our experiments and may be sufficiently local so as to evade detection by the bulk Ca^{2+} indicator, Fura-2. The functional coupling between P2X receptors and CRAC channels could involve localized ryanodine receptor-mediated Ca^{2+}-induced Ca^{2+} release events of the type that have been described in skeletal muscle and T-cells [189,

190]. Additional mechanistic studies using low-affinity and membrane-tethered Ca^{2+} indicators and genetic tools to manipulate specific P2X receptors are needed to help address the unknown links between P2X receptors, CRAC channels, and IL-6 induction.

Although P2X receptors have been widely investigated in many physiological contexts, their physiological roles and effector signaling mechanisms in airway epithelial cells are not well understood. One study described a key role for P2X receptor activation in inducing IL-8 production via Ca^{2+} signaling and NF-κB [61], suggesting that P2X receptors may have an important role in AECs to drive proinflammatory responses. Our finding that the P2X receptor antagonists suramin and PPADS strongly suppress ATP-evoked synthesis of IL-6 in airway epithelial cells is in agreement with this suggestion and expands the potential roles of P2X receptors in the airways to include the inflammatory cytokine IL-6.

Finally, airway CRAC channels have attracted significant interest for therapeutics in recent years. CRAC channel inhibitors have shown efficacy in preclinical models of asthma [73, 191-196]. Moreover, the CRAC channel inhibitor CM4620 is currently being tested in human patients for relieving the cytokine storm in seriously ill COVID-19 patients [197]. Our results showing that CM4620 is very effective in occluding IL-6 production may provide the mechanistic explanation for the benefits of this small molecule in improving patient survival. Although CRAC channels also play a key role in agonist-evoked PGE_2 synthesis, this may be counterbalanced under chronic inflammatory conditions *in vivo* due to its role in driving proinflammatory cytokine production, thus providing a therapeutic window to dampen chronic inflammation in the

lung airways. More studies are needed to address these scenarios but the results of this study provide a framework for testing these and other models.

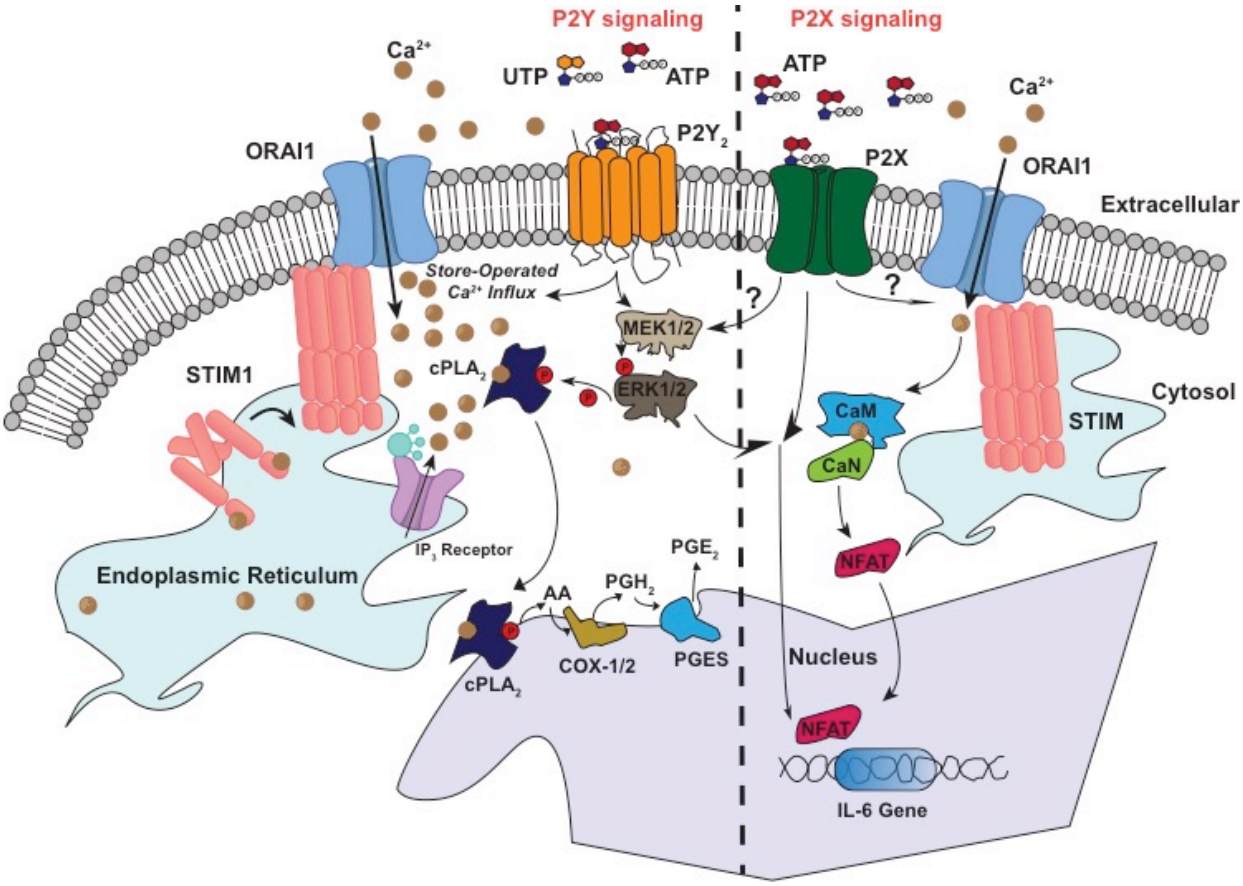

Figure 4.9 A model for divergent mechanisms driving PGE_2 and IL-6 synthesis in bronchial epithelial cells. The airway-derived nucleotides UTP and ATP stimulate production of PGE_2 via activation of cell surface $P2Y_2$ receptors, leading to activation of CRAC channels, ERK1/2, and $cPLA_2$. At higher doses, ATP will additionally also recruit activation of P2X receptors, leading to IL-6 induction via CRAC channels and ERK1/2 activation. In contrast to PGE_2 synthesis, the IL-6 synthesis cascade requires calcineurin-NFAT signaling.

Chapter 5: GPCR signaling inhibits IFN production in submerged AECs

Introduction

Airway epithelial cells (AECs) are primary host target cells for infection by respiratory viruses [11, 12]. Although AECs were once thought to be exclusively involved in barrier function, they have increasingly been understood to orchestrate downstream immune and inflammatory responses through the production of various classes of inflammatory mediators [3]. When a respiratory virus infects AECs, one essential class of antiviral cytokines that is produced is interferons [12, 128, 129]. Interferons (IFNs) are classified as type 1 (IFN-α/β), 2 (IFN-γ), or 3 (IFN-λ). Respiratory virus-infected AECs produce predominantly type 1 and type 3 IFN [130]. While both of these cytokines have antiviral activity, important distinctions exist. Type 3 IFN receptors are restricted to mucosal surfaces while type 1 IFN receptors are considered ubiquitous [12, 128]. Thus, IFN-λ is a mucosal specific mechanism for antiviral defense. Although, AECs generally make higher quantities of type 3 IFN than type 1 IFN following infection [130], type 1 is more potent [131]. Both type 1 and type 3 IFN signaling induces the expression of interferon-stimulated genes (ISGs) that enhance antiviral defense of cells [12, 128]. Altogether, understanding the signaling mechanisms that regulate AEC IFN production may enable the development of novel antiviral therapies.

Acute respiratory viral infections can aggravate underlying chronic airway diseases and visa versa. For instance, there is a strong correlation between children experiencing wheezing episodes early in life induced by rhinovirus (RV) or respiratory syncytial virus (RSV) with later development of asthma [147]. Furthermore, acute RV or RSV infections are responsible for most exacerbations of asthma [9, 147, 149, 150].

Asthma may also be a risk factor for severe IAV infections during IAV pandemics [11]. On a cellular level, most [137, 149, 152-157], but not all [158], studies have suggested that cells or tissue derived from patients with asthma or chronic obstructive pulmonary disease (COPD) have an intrinsic defect in IFN production following viral infections. Mechanisms to explain how asthmatics may come to have deficient IFN production are not clear.

IFN production can be regulated in a host of manners. Respiratory viruses themselves often exhibit a capacity to inhibit IFN production or downstream IFN signaling [128]. However, many host receptors and signaling pathways can enhance or inhibit interferon pathways. In macrophages, CCL2 has been shown to dampen IFNα release [132]. In AECs, EGFR activation can decrease IFN-λ production thereby enhancing viral infection [135, 136]. The cytokines IL-4,13, and IL-17 have also been shown to dampen IFN production from AECs [137-139]. Cigarette smoke can also dampen AEC IFN production [140, 141]. Interestingly, allergens such as aspergillus, alternaria, and house dust mite, have further been shown to inhibit IFN production from AECs [142-144]. This reduction of IFN production has been proposed to be a potential mechanism whereby the airway milieu is driven towards a Th2 phenotype upon exposure to these allergens [143, 145]. Mechanistically, both aspergillus and alternaria have been shown to activate proteinase-activated receptor 2 (PAR2) on AECs and signaling from this receptor limits the release of Th1 chemokines and IFNs [143, 146]. However, whether this also pertains to other cell surface receptors on AECs remains unknown.

Histamine and extracellular nucleotides are elevated during asthma and chronic airway diseases [16, 18, 21, 63]. In plasmacytoid dendritic cells (pDCs), ligands such as histamine and nucleotides have been shown to inhibit IFNα release [133, 134]. However, whether these ligands have the capacity to regulate IFN responses in AECs is unknown. Here we set out to screen these ligands for their ability to regulate IFN production. We identify both histamine receptors and nucleotide receptors that reduce the release of both IFN-β and IFN-λ from AECs. Pharmacological evidence demonstrated $P2Y_2$ and H_1 receptor activation was responsible for the inhibition by nucleotides and histamine, respectively. Our findings uncover an additional potential mechanism by which asthmatic patients manifest diminished IFN responses.

Results

Poly(I:C) drives IFN release through TLR3 signaling

AECs express multiple pattern-recognition receptors (PRRs) that can participate in the production of interferons following viral infection. One common mimic for the dsRNA produced during viral replication is poly(I:C). We began our study of interferon pathways in submerged AECs by performing a time course analysis following extracellular poly(I:C) stimulation. Poly(I:C) treatment evoked the release of both type 1 (IFN-β) and type 3 (IFN-λ1/3) IFN (Figure 5.1A-B). Notably, type 1 IFN was released much faster than type 3 IFN, which is in accordance with known properties of type 1 IFN (ref). Extracellular poly(I:C) is thought to predominantly activate the dsRNA sensor TLR3 (Kato 2007). We tested whether shRNA-mediated knockdown of TLR3 would inhibit poly(I:C) IFN responses. Two independent shRNA sequences targeting TLR3 both had

high knockdown efficiency as measured by qPCR (Figure 5.1C). Functionally, both shRNA also strongly abrogated poly(I:C)-mediated type 1 and type 3 IFN release (Figure 5.1D-E). This strongly suggests that extracellular poly(I:C) provokes TLR3 signaling culminating in IFN release from AECs.

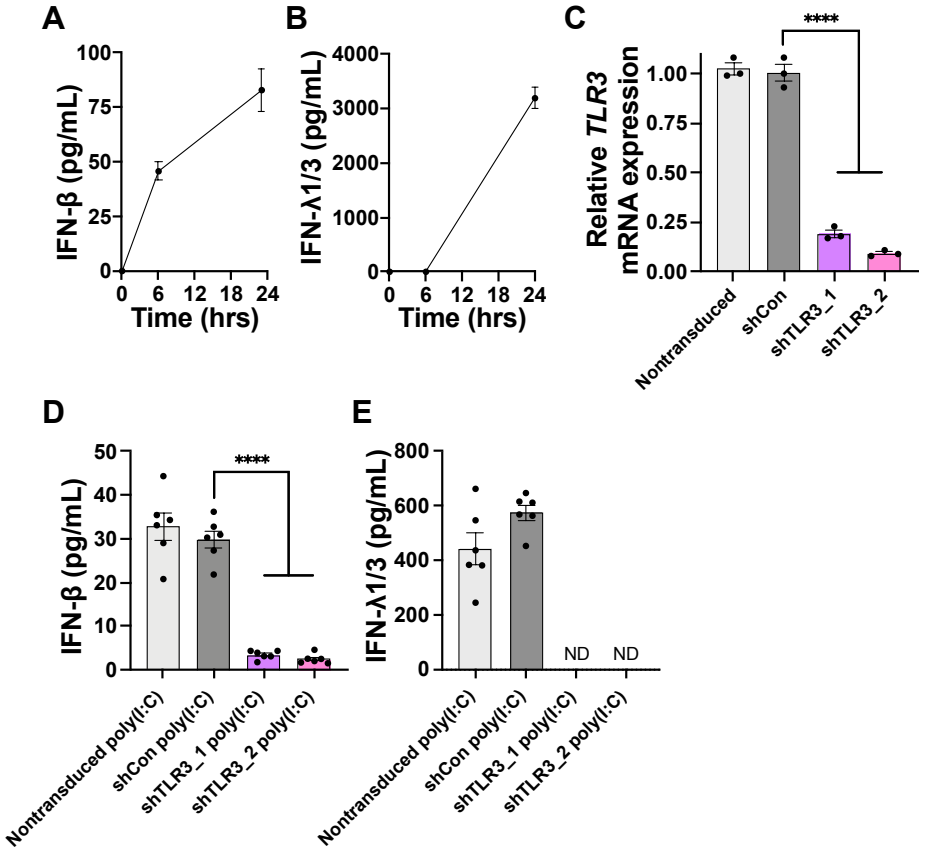

Figure 5.1 Poly(I:C) drives IFN release through TLR3 signaling. A) Normal human bronchial epithelial (NHBE) cells were stimulated with 10μg/mL poly(I:C) and IFN-β was measured in the supernatant at the given time points. Data are mean ± SEM of n = 4 samples/time point. **B)** Normal human bronchial epithelial (NHBE) cells were stimulated with 10μg/mL poly(I:C) and IFN-λ1/3 was measured in the supernatant at the given time points. Data are mean ± SEM of n = 4 samples/time point. **C)** shTLR3 decreases *TLR3* mRNA expression. Expression was normalized to the housekeeping gene *RPLP0*. Data are mean ± SEM of n = 3 samples. **D)** shRNA targeting TLR3 abrogated poly(I:C)-induced (10μg/mL) IFN-β release. Data are mean ± SEM of n = 6 samples/time point. **E)** shRNA targeting TLR3 abrogated poly(I:C)-induced (10μg/mL) IFN-λ1/3 release. Data are mean ± SEM of n = 6 samples/time point. Type 1 and 3 IFN levels were below the limit of detection in the supernatant without the presence of a stimulus such as poly(I:C)**.** ****p<0.0001

GPCR agonists inhibit IFN release

G-protein coupled receptor (GPCR) signaling has been shown to inhibit IFN responses in a wide variety of cell types. We screened three agonists that all induce Ca^{2+} signaling in AECs: UTP, histamine and the PAR2 activator SLIGKV. All three agonists effectively inhibited the poly(I:C)-mediated release of IFN-β (Figure 5.2A). The rank order of efficacy was UTP > histamine > SLIGKV. We also interrogated the release of IFN-λ1/3 and measured significantly less in the presence of UTP and histamine (Figure 5.2B). The PAR2 activator was ineffective at inhibiting the poly(I:C)-mediated release of IFN-λ1/3 (Figure 5.2B). ATP also suppressed the release of type 1 IFN (Figure 5.2C). The long acting β_2 adrenergic receptor agonist, fomoterol, did not significantly inhibit type 1 or type 3 IFN release (data not shown). These results suggest that GPCR agonists that provoke Ca^{2+} signaling in AECs dampen IFN production.

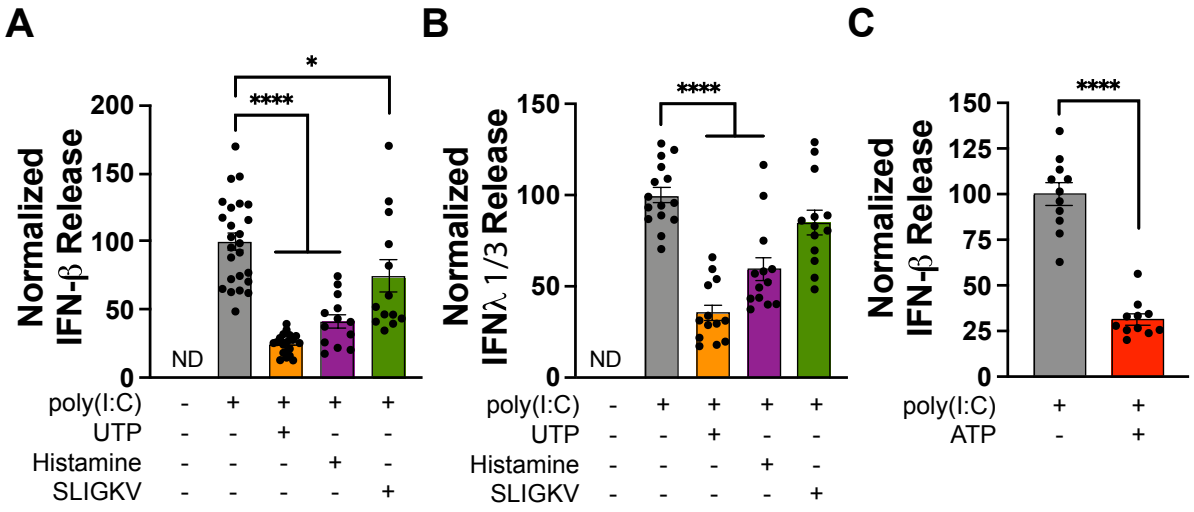

Figure 5.2 GPCR agonists inhibit IFN release.
A) The GPCR agonists (100μM) UTP, histamine, and to a lesser degree SLIGKV inhibit poly(I:C)-induced (10μg/mL) IFN-β release into the supernatant (24hr time point). Data are mean ± SEM of n = 13-25 samples. **B)** The GPCR agonists (100μM) UTP and histamine inhibit poly(I:C)-induced (10μg/mL) IFN-λ1/3 release into the supernatant (24hr time point). Data are mean ± SEM of n = 5-15 samples. **(C)** ATP (10μM) inhibits poly(I:C)-induced (10μg/mL) IFN-β release into the supernatant (6-hour time point). Data are mean ± SEM of n = 11 samples. *p<0.05, ****p<0.0001

ATP and UTP show opposing effects on IFN release in submerged AECs

Two nucleotides in the airways that both elicit Ca^{2+} signaling in AECs are ATP and UTP [162]. We performed a dose-response analysis for these two nucleotides in regulation of poly(I:C)-mediated IFN release. UTP showed a classic inhibitory dose-response curve for both type 1 and type 3 IFN (Figure 5.3A-B). In contrast, ATP showed a more complex dose-response curve. For type 1 IFN, ATP showed a biphasic response with low doses of ATP (< 10μM) inhibiting IFN similarly to UTP while dose higher than 10μM began to be less effective (Figure 5.3A). For type 3 IFN, low dose of ATP (< 10μM) had no effect on IFN release, while higher doses of ATP (100μM) showed potentiation of IFN release. UTP is a selective agonist of metabotropic P2Y receptors while ATP is an agonist at metabotropic P2Y receptors and ionotropic P2X receptors [29]. Both UTP and ATP elicit the activation of $P2Y_2$ receptors (Figure 2.1). While many potential models immerge from this data, a likely scenario is that UTP receptors inhibit IFN release while ATP receptors can potentiate IFN release. ATP may also activate the UTP receptors leading to the biphasic response in type 1 IFN release.

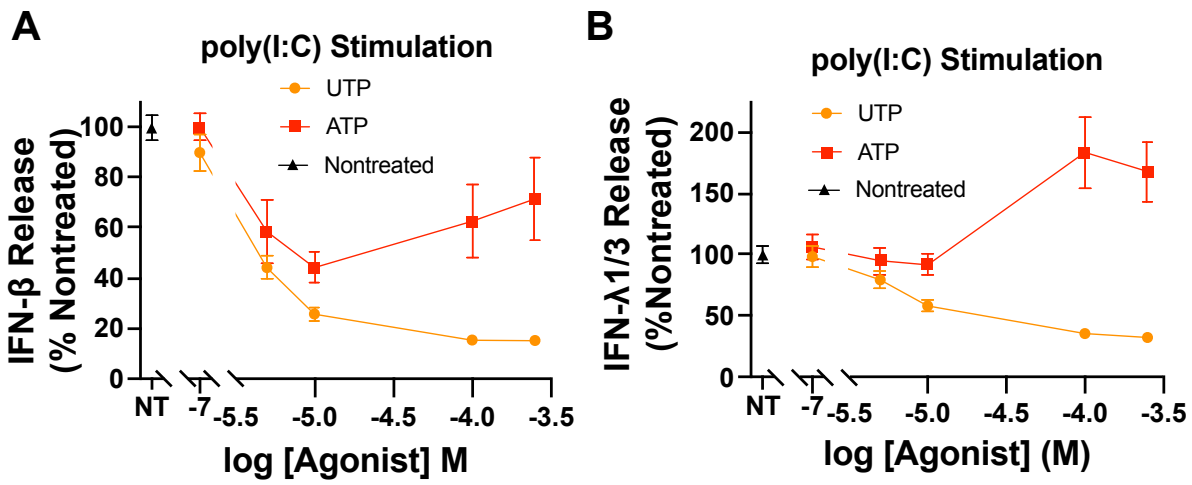

Figure 5.3 ATP and UTP show opposing effects on IFN release in submerged AECs. A-B) UTP inhibits IFN release while ATP is either less effective at inhibiting (IFN-β) or potentiates (IFN-λ1/3) release. Cells were stimulated with 10μg/mL poly(I:C) +/- ATP/UTP and supernatants were collected 16hrs later and IFN levels were measured. Data are mean ± SEM of n = 4 samples.

Pharmacological analysis of histamine and UTP responses reveals H_1 and $P2Y_2$ receptor activation

To begin unraveling the molecular identity of the UTP and histamine receptors driving inhibition of IFN responses, we performed a dose-response analysis of IFN release. UTP was ten times more potent than histamine in inhibiting the release of IFN-β (0.34μM versus 3.4μM) (Figure 5.4A). Regarding IFN-λ1/3, UTP was six times more potent than histamine in inhibiting the release (1μM versus 6μM) (Figure 5.4A). Both agonists were more potent in inhibiting the release of type 1 IFN than type 3 IFN. The Hill-slope for histamine was also much more steep for both type 1 and type 3 IFN release (Figure 5.4A-B). Next, we employed the selective $P2Y_2$ receptor antagonist AR-C. AR-C blocked the UTP-mediated inhibition of IFN-β (Figure 5.4C). We tested the

selective H_1 receptor antagonist cetirizine in reversing the histamine responses. Cetirizine effectively reversed the histamine-mediated inhibition of both type 1 and type 3 IFN release (Figure 5.4D-E). These findings strongly implicate $P2Y_2$ receptors and H_1 receptors in the UTP- and histamine-induced inhibition of IFN release.

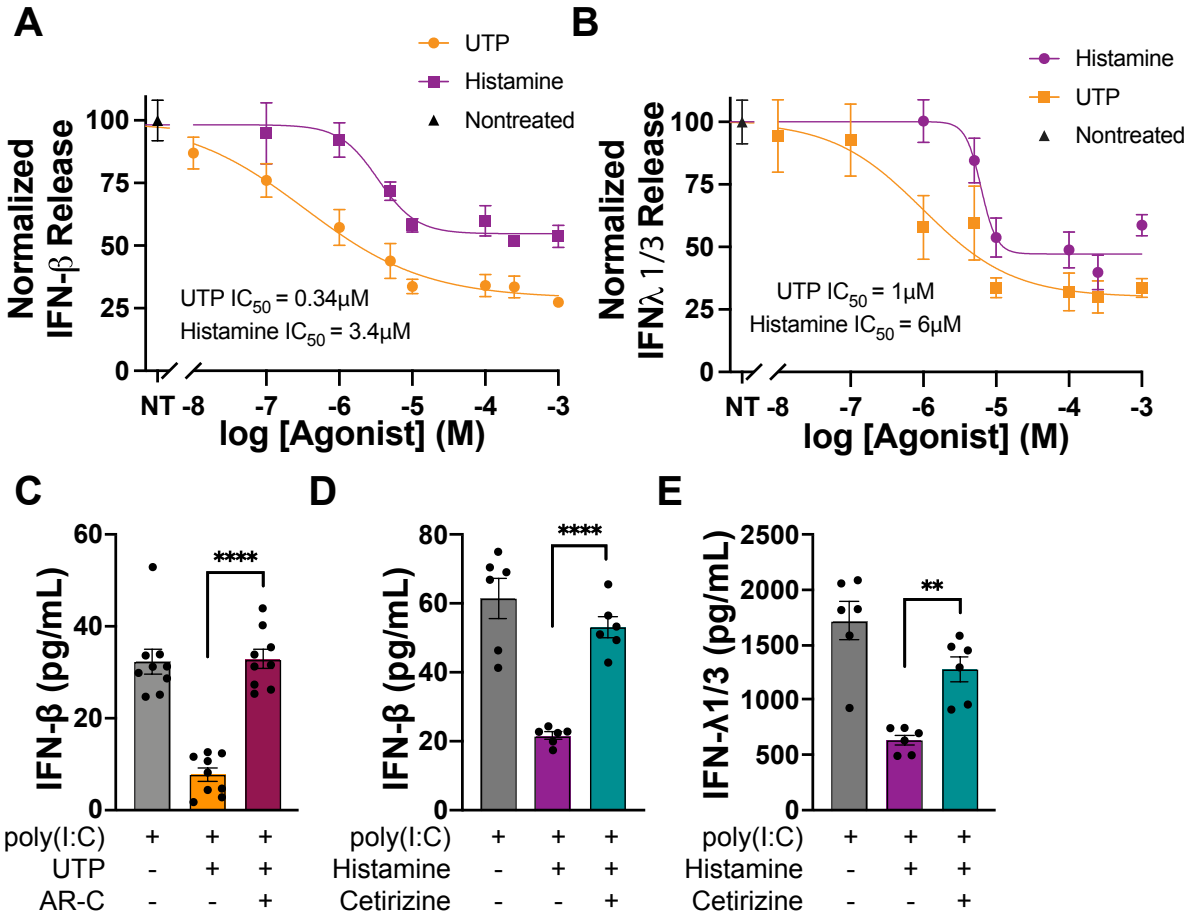

Figure 5.4 Pharmacological analysis of histamine and UTP responses reveals H_1 and $P2Y_2$ receptor activation. A) Dose-response of IFN-β release inhibition by UTP and histamine. IFN-β was measured in the cell culture supernatant 24 hrs following

simultaneous addition of poly(I:C) (10μg/mL) and UTP/histamine. The solid line is a four-parameter nonlinear regression fit of the Hill equation with IC_{50} = 0.34 μM and Hill Slope = -0.52 for UTP and IC_{50} = 3.4 μM and Hill Slope = -1.65 for histamine. IFN-β was undetectable without a stimulus and thus 0 pg/ml was set to 0% and maximal poly(I:C)-evoked response was set at 100% for the fitting procedure. Data are mean ± SEM of n = 4-18 samples from 2 independent experiments. **B)** Dose-response of IFN-λ1/3 release inhibition by UTP and histamine IFN-λ1/3 was measured in the cell culture supernatant 24 hrs following simultaneous addition of poly(I:C) (10μg/mL) and UTP/histamine. The solid line is a four-parameter nonlinear regression fit of the Hill equation with IC_{50} = 1 μM and Hill Slope = -0.7 for UTP and IC_{50} = 6 μM and Hill Slope = -4.09 for histamine. IFN-λ1/3 was undetectable without a stimulus and thus 0 pg/ml was set to 0% and maximal poly(I:C)-evoked response was set at 100% for the fitting procedure. Data are mean ± SEM of n = 4-18 samples from 2 independent experiments. **C)** The $P2Y_2$ antagonist AR-C 118925XX (10μM) reverses UTP-mediated (100μM) inhibition of IFN-β release. Data are mean ± SEM of n = 9 samples. **D)** The H_1 antagonist cetirizine (10μM) reverses histamine-mediated (100μM) inhibition of IFN-β release. Data are mean ± SEM of n = 6 samples. **E)** The H_1 antagonist cetirizine (10μM) reverses histamine-mediated (100μM) inhibition of IFN-λ1/3 release. Data are mean ± SEM of n = 6 samples. **p<0.01, ****p<0.0001

GPCR signaling inhibits cGAS-STING-mediated IFN release

In addition to dsRNA sensors, AECs also express functional dsDNA sensors that elicit IFN synthesis [198]. One such dsDNA sensor is cGAS, which signals through the adaptor protein STING to drive IFN responses [199, 200]. We compared the kinetics of IFN-β release evoked by extracellular poly(I:C) versus transfected 2,3 cGAMP (a STING agonist). Both ligands induced IFN-β with similar kinetics and abundances (Figure 5.5A). We tested UTP and histamine for the capacity to inhibit 2,3 cGAMP-mediated IFN release. Both UTP and histamine significantly inhibited 2,3 cGAMP-mediated IFN release, with a greater degree of inhibition measured for type 1 compared to type 3 IFN (Figure 5.5B-C). To activate cGAS upstream of STING, we employed the dsDNA sequence known as interferon stimulatory DNA (ISD). UTP alone inhibited ISD-dependent type 1 IFN responses while histamine was without effect (Figure 5.5D).

Neither agonist significantly inhibited ISD-mediated type 3 IFN responses (Figure 5.5E). Altogether, these findings imply that UTP and histamine have the capacity to inhibit cGAS-STING-mediated IFN release, although the magnitude of the inhibition appears weaker than that observed for TLR3-mediated release.

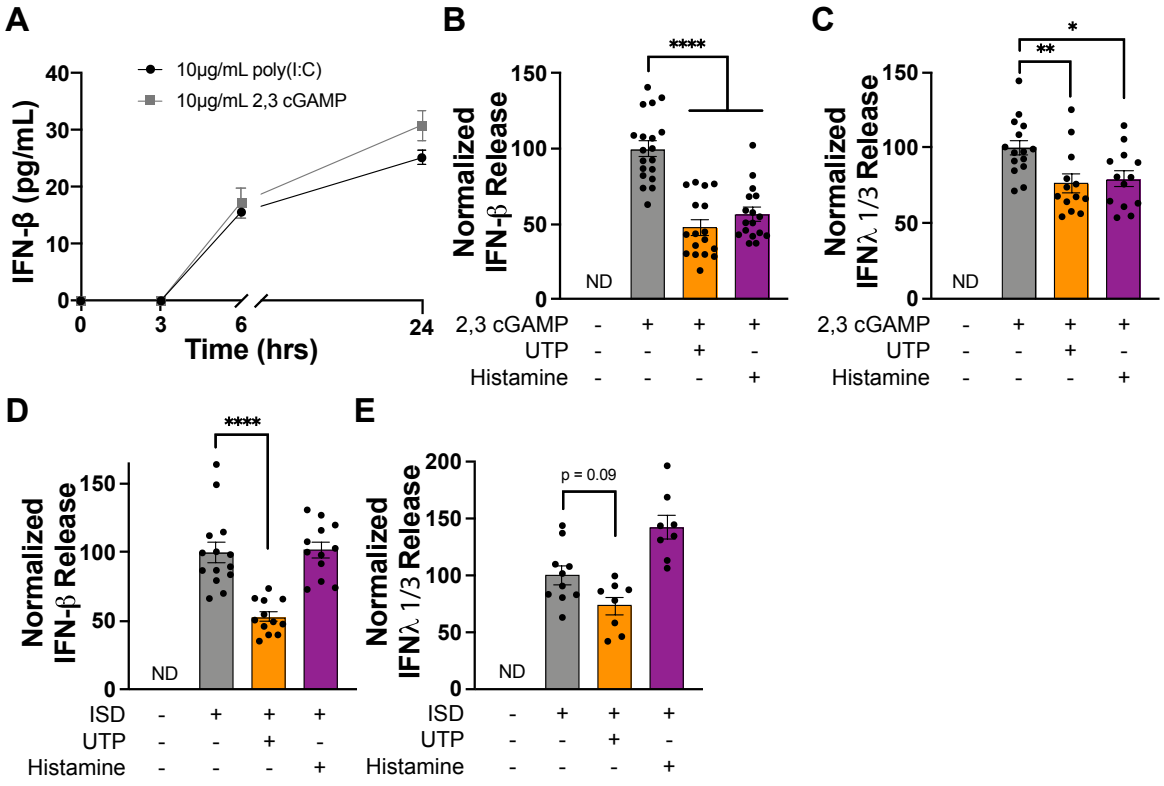

Figure 5.5 GPCR signaling inhibits cGAS-STING-mediated IFN release. A) Normal human bronchial epithelial (NHBE) cells were stimulated with 10μg/mL poly(I:C) or transfected with 10μg/mL 2,3 cGAMP and IFN-β was measured in the supernatant at the given time points. Data are mean ± SEM of n = 4 samples/time point. **B)** The GPCR agonists (100μM) UTP and histamine inhibit 2,3 cGAMP-induced (10μg/mL) IFN-β release into the supernatant (24hr time point). Data are mean ± SEM of n = 17-19 samples. **C)** The GPCR agonists (100μM) UTP and histamine inhibit 2,3 cGAMP-induced (10μg/mL) IFN-λ1/3 release into the supernatant (24hr time point). Data are mean ± SEM of n = 13-15 samples. **D)** The GPCR agonist (100μM) UTP inhibits ISD-induced (1μg/mL) IFN-β release into the supernatant (24hr time point). Data are mean ± SEM of n = 12-14 samples. **E)** The GPCR agonists (100μM) do not significantly inhibit

ISD-induced (1μg/mL) IFN-λ1/3 release into the supernatant (24hr time point). Data are mean ± SEM of n = 8-10 samples. *p<0.05, **p<0.01, ****p<0.0001

Agonists inhibit RIG-I-dependent IFN release

TLR3 is a dsRNA sensor that resides in endosomes while RIG-I-like receptors (RLRs) reside in the cytosol similar to cGAS [201, 202]. To test if GPCR agonists inhibit RLR-mediated IFN responses, we employed the RIG-I agonist 3p-hpRNA. Transfection of 3p-hpRNA evoked a powerful induction of type 1 IFN (Figure 5.6A). At the early time point of 6 hours, all three GPCR modulators, ATP, UTP, and histamine suppressed RIG-I-mediated IFN-β release (Figure 5.6B), ATP showing the strongest inhibition. UTP and histamine also suppressed the induction of IFN-β release but to a lesser extent (Figure 5.6B). However, at later time points (24 hours), ATP and histamine retained their efficacy to suppress 3p-hpRNA-mediated IFN-β, while UTP was ineffective (Figure 5.6C). These results indicate that ATP is highly effective at inhibiting RIG-I-induced IFN-β release stimulated by 3p-hpRNA while histamine and UTP exhibit lower efficacy. At the early time point, the $P2Y_2$ receptor antagonist AR-C partially reversed the ATP-mediated inhibition of 3p-hpRNA-mediated IFN-β (Figure 5.6D). Interestingly, both ATP and adenosine suppressed 3p-hpRNA-mediated IFN release (Figure 5.6E-F), suggesting that at least part of ATP's suppression may stem from ATP metabolites like adenosine. In agreement with this interpretation, the NTPDase inhibitor, ARL 67156, which inhibits the enzymes that degrade ATP, blocked ATP-mediated IFN suppression (Figure 5.6G). However, the adenosine receptor agonist NECA did not suppress IFN release suggesting that a classical adenosine receptor may not be involved (Figure

5.6G). Collectively, these findings suggest that ATP and its metabolites strongly suppress RIG-I-induced IFN release.

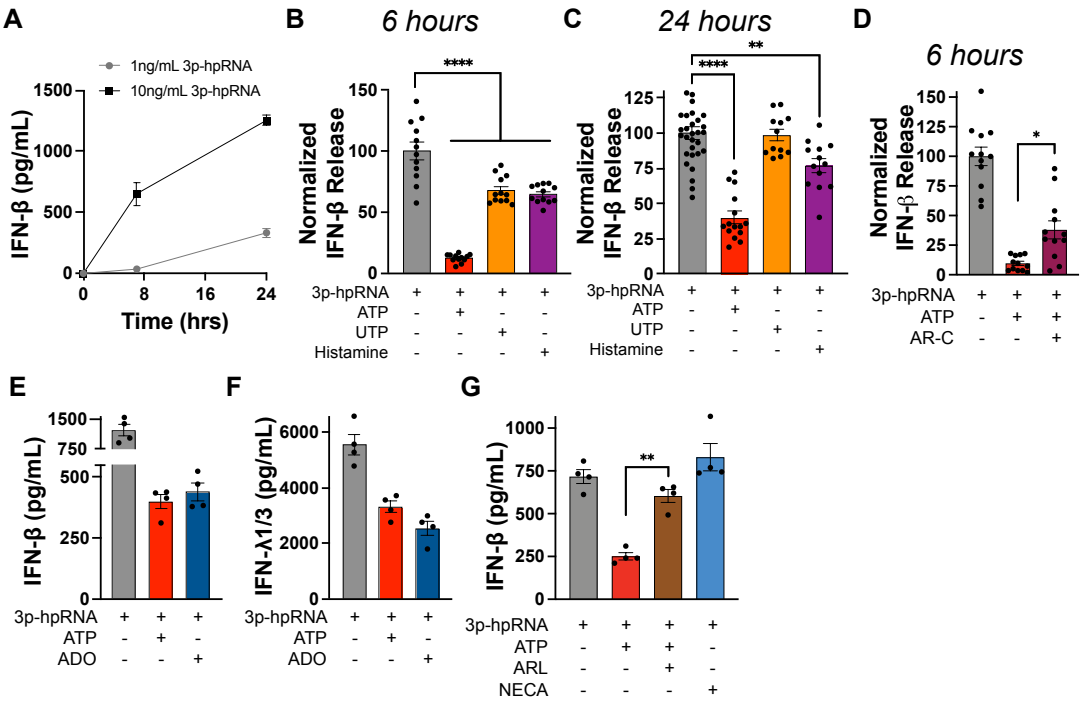

Figure 5.6 Agonists inhibit RIG-I-dependent IFN release. A) Transfection of NHBEs with 3p-hpRNA elicits IFN-β release into the supernatant. Data are mean ± SEM of n = 3 samples. **(B)** ATP (100μM) strongly while UTP (100μM) and histamine (100μM) mildly inhibit 3p-hpRNA-induced (10ng/mL) IFN-β release into the supernatant. Supernatants were collected at a 6-hour time point. The absolute concentrations of IFN-β ranged from 12.9-321 pg/mL. Data are mean ± SEM of n = 12 samples from two independent experiments. **(C)** ATP (100μM) and histamine (100μM) inhibit 3p-hpRNA-induced (10ng/mL) IFN-β release into the supernatant. Supernatants were collected at a 24-hour time point. The absolute concentrations of IFN-β ranged from 156-1552 pg/mL. Data are mean ± SEM of n = 13-30 samples. **(D)** The $P2Y_2$ antagonist, AR-C 118925XX (10μM), partially reverses ATP-mediated (100μM) inhibition of 3p-hpRNA-evoked (10ng/mL) IFN-β release. Supernatants were collected 6 hours after stimulation. Data are mean ± SEM of n = 12 samples. **(E and F)** ATP (100μM) and Adenosine, labeled as ADO, (50μM) inhibits 3p-hpRNA-induced (10ng/mL) IFN-β *(E)* and IFN-λ1/3 *(F)* release into the supernatant. Cell supernatants were collected at a 16-hour time point. Data are mean ± SEM of n = 4 samples. **(K)** The NTPDase inhibitor, ARL 67156 (100μM), reverses ATP-mediated (100μM) inhibition of 3p-hpRNA-evoked (10ng/mL) IFN-β

release. The adenosine receptor agonist NECA (10μM) did not inhibit 3p-hpRNA-evoked (10ng/mL) IFN-β release. Supernatants were collected at a 16-hour time point. Data are mean ± SEM of n = 4 samples. *p<0.05, **p<0.01, ****p<0.0001

Influenza A virus drives IFN responses partially through TLR3

We transitioned to a live respiratory virus, influenza A virus (IAV), to measure functional IFN responses. Infection of AECs with IAV elicited type 1 IFN release in a multiplicity of infection (MOI) dependent manner (Figure 5.7A). To interrogate if TLR3 was necessary for IAV-induced IFN responses, we again utilized shRNA lentiviral transduction. Knockdown of TLR3 partially inhibited IAV-induced release of both type 1 and type 3 IFN (Figure 5.7B-C). Thus, although TLR3 is necessary in IAV-mediated IFN responses, other dsRNA sensors such as RLRs are likely involved.

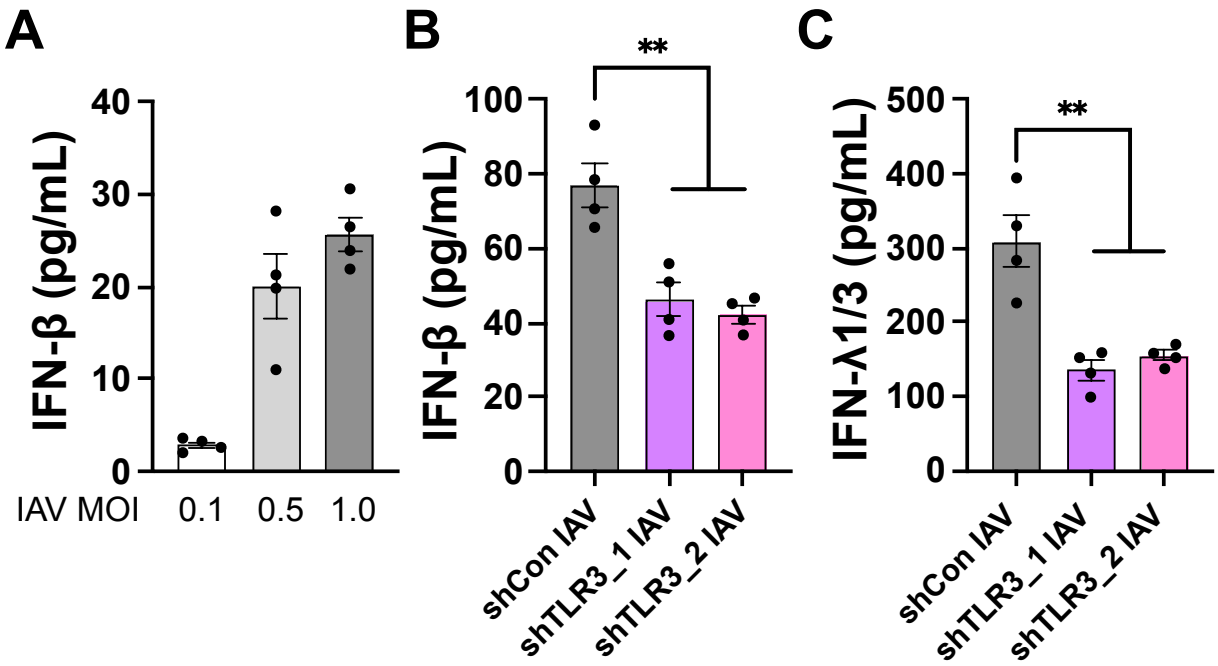

Figure 5.7 Influenza A virus drives IFN responses partially through TLR3.
A) Influenza A virus strain A/WSN/33(H1N1) was used to infect NHBEs at a multiplicity of infection (MOI) of 0.1, 0.5, or 1.0 and IFN-β release into the supernatant was measured 24 hrs after infection. Data are mean ± SEM of n = 4 samples. **B)** shRNA-mediated knockdown of TLR3 partially blocks IAV-induced (MOI 0.5) IFN-β release into the supernatant. Data are mean ± SEM of n = 4 samples. **C)** shRNA-mediated knockdown of TLR3 partially blocks IAV-induced (MOI 0.5) IFN-λ1/3 release into the supernatant. Data are mean ± SEM of n = 4 samples. **p<0.01

Histamine, ATP, and Adenosine inhibits respiratory virus-mediated IFN production

We tested histamine and UTP for their ability to inhibit IFN release induced by the live respiratory virus IAV. Histamine significantly inhibited IAV-mediated release of both type 1 and type 3 IFN (Figure 5.8A-B). In contrast, UTP was completely ineffective (Figure 5.8A-B). ATP much more powerfully inhibited IAV-induced IFN release (Figure 5.8C-D). This data is highly reminiscent of the discoveries related to the RIG-I agonist 3p-hpRNA. The infections and agonists did not dramatically alter cellular cytotoxicity or cellular ATP levels (Figure 5.8E-F). In agreement with the discoveries related to the RIG-I activator, adenosine also suppressed IAV-induced IFN release (Figure 5.8G-H), suggesting ATP and its metabolites may both contribute to the inhibition of IAV-mediated IFN release.

Rhinovirus, a family of viruses that contribute to the common cold, is another important family of viruses that can contribute to asthma exacerbation [9]. Thus, we infected airway cells with rhinovirus strain 1B (RV1B) and measured IFN release. Type 1 IFN release into the supernatant was low and difficult to accurately quantify so we quantified *IFNB1* mRNA levels. Importantly, ATP strongly suppressed RV1B-induced *IFNB1* mRNA levels (Figure 5.8I). These results indicate that histamine and particularly ATP are powerful suppressors of RIG-I-, IAV-, and RV1B-induced IFN production from

AECs and suggest that these agonists may be responsible for the well-described suppression of IFN responses in asthmatics (Figure 5.8J).

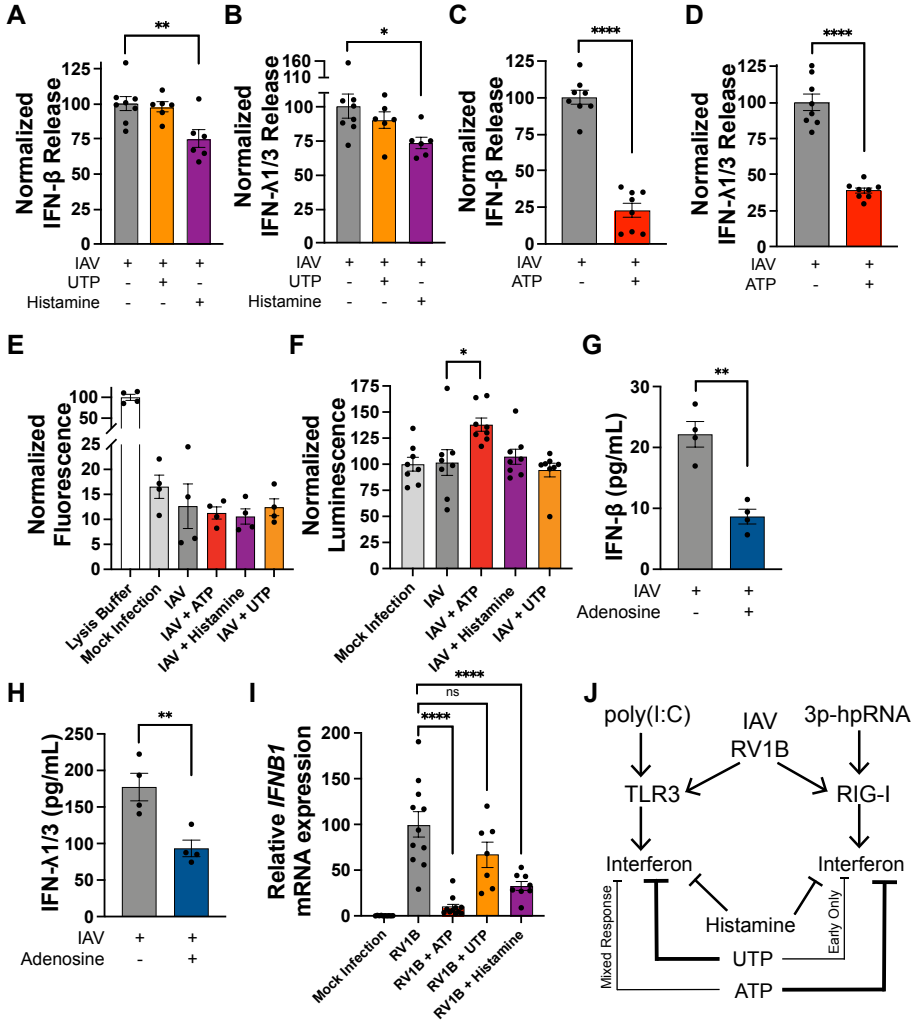

Figure 5.8 Histamine, ATP, and Adenosine inhibits respiratory virus-mediated IFN production. A) Histamine (100μM) inhibits IAV-induced (MOI 1) IFN-β release into the supernatant. Data are mean ± SEM of n = 6 samples from two independent experiments. **B)** Histamine (100μM) inhibits IAV-induced (MOI 1) IFN-λ1/3 release into the supernatant. Data are mean ± SEM of n = 6 samples from two independent experiments. (**C and D)** ATP (100μM) inhibits IAV-induced (MOI 0.5) IFN-β *(C)* and IFN-λ1/3 *(D)* release into the supernatant. Cell supernatants were collected at a 24-hour time point. Concentrations of IFN-β ranged from 2-81 pg/mL. Concentrations of IFN-λ1/3 ranged from 68-836 pg/mL. Data are mean ± SEM of n = 8 samples from two

independent experiments. **(E)** IAV (MOI 0.5) and agonists (100μM) do not strongly induce cytotoxicity as measured via CellTox assay. Data are mean ± SEM of n = 4 samples. **(F)** IAV (MOI 0.5) and agonists (100μM) do not strongly inhibit cellular metabolism/proliferation as measured via CellTiter-Glo assay. Data are mean ± SEM of n = 8 samples. (**G and H)** Adenosine (50μM) inhibits IAV-induced (MOI 0.5) IFN-β *(G)* and IFN-λ1/3 (*H)* release into the supernatant. Cell supernatants were collected at a 24-hour time point. Data are mean ± SEM of n = 4 samples. (**I)** ATP and histamine (both 100μM) inhibit RV1B-induced (MOI 10) *IFNB1* mRNA expression. Expression was normalized to the housekeeping gene RPLP0. RNA was collected 24 hours after infection. Within a given experiment, expression was normalized to mock infection. The data are displayed as normalized between experiments with the mean RV1B-induced expression set to 100 and all other treatments scaled proportionally. Data are mean ± SEM of n = 7-11 samples from three independent experiments. **(J)** Summary model: poly(I:C) drives TLR3-mediated IFN release while 3p-hpRNA drives RIG-I-mediated IFN release. IAV and likely RV activate both TLR3 and RIG-I pathways to induce IFN release. Histamine dampens IFN release from both pathways. UTP strongly inhibits poly(I:C)-mediated IFN release but only inhibits early release of RIG-I-induced IFN. ATP shows modest inhibition of poly(I:C)-mediated type 1 IFN but powerfully suppresses RIG-I-, IAV-, and RV1B-induced IFN production. *p<0.05, **p<0.01, ****p<0.0001

Discussion

Interferons are powerful antiviral cytokines induced upon viral infection. One mechanism IFNs employ to evoke antiviral responses is the upregulation of interferon-stimulated genes (ISGs). While not all ISGs have established roles in viral defense, many are classic antiviral genes. Type 1 IFNs are also involved in adaptive immune responses, particularly due to their role in dendritic cell-mediated T-cell activation and antibody responses [203, 204]. Airway viruses, especially RV and RSV, are also well known to induce exacerbations of asthma [9, 147, 149, 150]. In the context of chronic airway disease like asthma, both histamine and nucleotides are elevated [16, 18, 21, 63]. Yet, the crosstalk between histamine and nucleotide signaling and IFN responses in AECs is unclear.

Here we demonstrate that histamine and nucleotides are able to inhibit the stimulus-evoked release of type 1 and type 3 IFNs from AECs. Our results demonstrate

that UTP activates $P2Y_2$ receptors and thereby reduce poly(I:C) and cGAS-STING-induced IFN release. Likewise, we show that histamine activates H_1 receptors and also limits poly(I:C) and RIG-I-induced IFN release. UTP was more potent than histamine as an inhibitor of poly(I:C)-mediated IFN release. Importantly, histamine and ATP also diminished IAV- and RV1B-induced IFN release. To our knowledge, this is the first report that $P2Y_2$ receptors and H_1 receptors on AECs have the capacity to dampen IFN release.

Our data illustrates how infection of AECs with respiratory viruses is a much more complex phenomenon than poly(I:C) treatment. Interestingly, while UTP inhibited poly(I:C)-mediated IFN release, it proved less capable at inhibiting RIG-I- or IAV-induced IFN release (Figure 5.2A-B, 5.6C, 5.8A-B). However, histamine had efficacy in inhibiting IFN release induced by poly(I:C), RIG-I, and IAV (Figure 5.2A-B, 5.6B-C, 5.8A-B). On the other hand, ATP powerfully inhibited both RIG-I and IAV-induced IFN secretion (Figure 5.6E-F, 5.8C-D). These differences are likely due to the fact that IAV activates multiple RNA sensors, including TLR3 and RLRs [205, 206] while extracellular poly(I:C) exclusively activates TLR3 (Figure 5.7B-C vs. Figure 5.1D-E). Another explanation for this data is found in that the ATP metabolite adenosine also suppresses RIG-I- and IAV-induced IFN release (Figure 5.6E-F, 5.8G-H). Thus, it seems likely that ATP activates two distinct pathways, the first adenosine-mediated, the second $P2Y_2$ receptor-mediated, both contributing to suppression of IFN. UTP on the other hand, selectively activates $P2Y_2$ and does not produce adenosine metabolites and is therefore insufficient to powerfully inhibit respiratory virus-induced IFN. Collectively, these discoveries suggest caution when interpreting IFN response data generated from

stimulation with the model viral agonist poly(I:C) alone without confirmation using live respiratory viruses.

Histamine is a classic allergic mediator in the context of Th2 inflammation [63]. In contrast, IFNs are known to inhibit Th2 bias and mast cell degranulation [207-209]. Thus, our discovery that histamine can inhibit IFN release by AECs may reveal a positive feedback loop in which histamine reinforces Th2 inflammation. Clinically, pediatric atopic patients often progress from atopic dermatitis (AD) towards asthma later in childhood [210]. This progression of disease has long been termed the “atopic march” [210]. Interestingly, there have been multiple reports that treatment of atopic infants with an H_1 receptor antagonist can decrease the likelihood of subsequent development of asthma [211, 212]. One of these studies showed that infants with atopy to house dust mite (HDM) or grass pollen had lower incidence of later asthma development if they were given cetirizine [213]. Our discovery that histamine can inhibit the release of IFNs from AECs, thereby potentially skewing the environment further towards a Th2 milieu, may provide some mechanistic basis for these clinical observations.

Asthmatic cells have been shown to have deficient IFN responses [137, 149, 152-155]. This impairment may contribute to the well-known ability of respiratory viruses to trigger acute asthma exacerbations. Insofar as IFNs counter-regulate allergic responses, this deficiency may also allow unchecked allergic responses in asthmatics. One report has demonstrated that treatment with omalizumab, a monoclonal antibody that inhibits IgE activation of allergic cells, can partially restore the *ex vivo* IFN response and decrease the incidence of asthma exacerbations [214]. Thus, IFN may decrease exacerbations through its antiviral activity. Another group has shown that nebulized IFN-

β following cold symptoms could protect against worsening lung symptoms in asthmatics with poorly controlled disease [215]. This same group reported that inhaled IFN-β improves outcomes of infection with SARS-CoV2 reinforcing the antiviral effects of intrapulmonary IFN-β [216]. It is reasonable to conclude that IFN responses in asthmatics during respiratory tract infections are important for the preservation of lung function and prevention of exacerbations. Our present finding that histamine and nucleotides, which are known to be in the airways following allergen exposure [16, 18, 63], inhibit IFN release from AECs may provide a mechanism for the deficient IFN responses found in asthmatics. Finally, although data is limited suggesting that H_1 antagonists alone can improve lung function during asthma, our data suggests that H_1 antagonists should be tested for their ability to restore IFN production in asthmatics, as has been found with omalizumab, an antibody that reduces the release of histamine from mast cells and basophils [214, 217].

Recent studies have also suggested that IAV can directly provoke mast cells to release proinflammatory cytokines, chemokines and mediators such as histamine [218, 219]. Indeed, in multiple animal models of IAV infection, histamine levels were elevated in the airways during infection [220, 221]. There is also some evidence suggesting that H_1 antagonists may decrease pneumonia and inflammatory mediators in the context of IAV infection [220]. Therefore, histamine may actively inhibit the ability of IAV to induce the expression of protective IFN during *in vivo* IAV infection. However, further *in vivo* studies utilizing a conditional knockout of H_1 receptors in AECs would be necessary to test this hypothesis.

ATP is released at sites of many forms of inflammation [16, 18, 21]. IFNs can be damaging in some contexts of severe inflammation [222]. Thus, the ability of ATP to inhibit AEC IFN release may comprise a negative feedback loop preventing excessive tissue damage in the context of severe inflammation. On the other hand, ATP and purinergic receptor signaling has been identified as a driver of allergic lung inflammation [16, 18]. Given the antagonist relationship between IFN and allergic asthma, our finding that ATP powerfully inhibits IAV-induced IFN secretion may provide a cellular basis for the observation that P2 receptor antagonists reverse allergic airway inflammation [16, 18]. With regards to viral infection, multiple reports have suggested that infection of AECs can elicit nucleotide release [38, 40, 41]. Thus, our discovery that ATP strongly suppresses the virus-induced IFN release may be a novel mechanism viruses employ to dampen host IFN responses. Altogether, these findings suggest ATP may modulate the immune response during respiratory virus infection and allergic inflammation. Nevertheless, further *in vivo* studies utilizing a conditional knockout of P2 receptors in AECs would be necessary to test these hypotheses and investigate the physiological significance of these discoveries.

Chapter 6: Mechanisms underlying GPCR-mediated inhibition of IFN secretion

Introduction

Interferons are an essential class of antiviral cytokines. The stimulus that evokes the release of IFNs is typically either dsDNA or dsRNA. Both of these chemical moieties are sensed by intracellular receptors. These sensors, such as TLR3, RLRs, cGAS-STING, then evoke a signaling response that activates transcription factors such as NF-kB or IRF3 and other IRFs [128]. The transcription factors drive the transcription of various interferon genes, culminating in their synthesis and release from the infected cells. Due to the importance of IFNs for host defense against viruses, many studies have investigated how their production is regulated. Some of these mechanisms include Ca^{2+} or cAMP signaling [223-225]. Furthermore, β-arrestin signaling has also been implicated in the inhibition of IFN responses [132, 226]. The pathway that culminates in the synthesis of IFNs includes many kinases and not surprisingly, multiple phosphatases have been shown to regulate IFN production [227, 228]. Reactive oxygen species (ROS) have also been implicated in the inhibition of IFN responses [137, 140]. PKC signaling downstream of nucleotide receptors in plasmacytoid dendritic cells has been shown to inhibit IFN responses [133]. Another family of proteins that regulate interferons are the suppressor of cytokine signaling (SOCS) proteins [139]. Altogether, a host of receptors and signaling pathways converge on IFN production to fine-tune the antiviral response.

Results

$P2Y_2$ receptors inhibit IFN release through Gq signaling

GPCRs that evoke Ca^{2+} signaling often do so through a heterotrimeric G-protein subunit termed Gq [229]. We tested the Gq inhibitor YM-254890 [229] (hereby termed "YM") for its ability to inhibit UTP-meditated Ca^{2+} signaling. YM completely abrogated UTP-evoked Ca^{2+} signaling (Figure 6.1A). We next tested YM for its ability to reverse UTP-induced inhibition of IFN responses. YM significantly reversed UTP-mediated inhibition of both type 1 and type 3 IFN release (Figure 6.1B-C). These findings suggest that Gq signaling is necessary for $P2Y_2$ receptors to dampen AEC IFN responses.

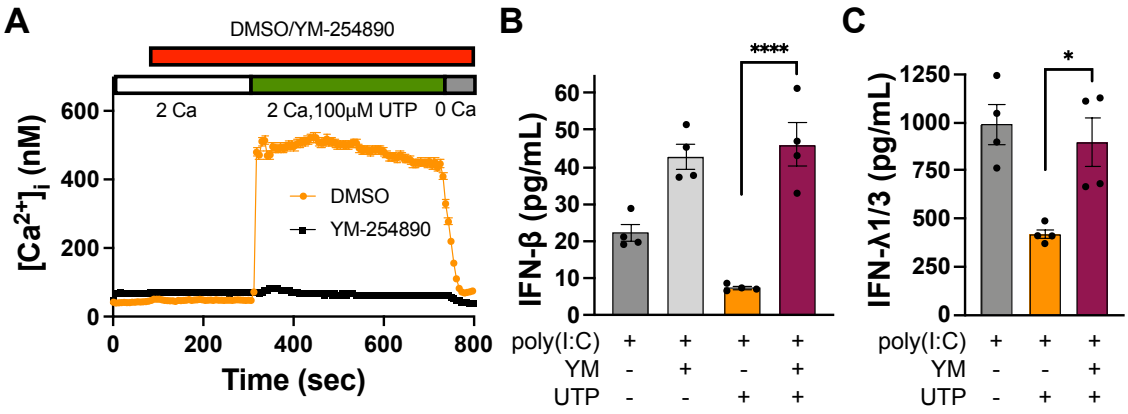

Figure 6.1 $P2Y_2$ receptors inhibit IFN release through Gq signaling. A) The Gq inhibitor YM-254890 (1μM) abrogates UTP-induced $[Ca^{2+}]_i$ elevations. $[Ca^{2+}]_i$ was measured using Fura-2 AM as previously described [95, 97]. Data are mean ± SEM of n = 27-37 cells. **B)** The Gq inhibitor YM-254890 (1μM) reverses UTP-mediated (100μM) inhibition of IFN-β release. Supernatants were collected 6 hrs after stimulation. Data are mean ± SEM of n = 4 samples. **C)** The Gq inhibitor YM-254890 (1μM) reverses UTP-mediated (100μM) inhibition of IFN-λ1/3 release. Supernatants were collected 20 hrs after stimulation. Data are mean ± SEM of n = 4 samples. *p<0.05, ****p<0.0001

PKC signaling is necessary for GPCR-mediated inhibition of IFN production

Another signaling mediator downstream of GPCRs coupled to Gq is PKC. One report has suggested that PKC activation in pDCs can dampen type 1 IFN responses [133]. We tested the broad-spectrum PKC inhibitor, Gö 6983, for its ability to reverse GPCR responses. Gö 6983 reversed both UTP- and histamine-mediated inhibition of type 1 IFN release (Figure 6.2A). The reversal appeared stronger for histamine than UTP. Similar to UTP, ATP-mediated suppression of type 1 IFN release was inhibited by the PKC inhibitor, Gö 6983, and the Gq inhibitor, YM-254890 (Figure 6.2B). A second PKC inhibitor GF 109203X also partially reversed UTP-mediated inhibition of IFN release (Figure 6.2C). Turning to type 3 IFN, Gö 6983 reversed only the histamine-induced inhibition while the UTP-induced inhibition was left larger intact (Figure 6.2D). This data suggests that while both receptors utilize PKC signaling to inhibit type 1 IFN responses, type 3 IFN responses appear more complex. To confirm that PKC activation is sufficient to dampen type 1 IFN responses, we employed two PKC activators, the phorbol esters PDBu and PMA. Both PDBu and PMA strongly abrogated the poly(I:C)-mediated release of type 1 IFN (Figure 6.2E). Likewise, PMA strongly suppressed 3p-hpRNA-mediated type 1 IFN release (Figure 6.2F). Thus, PKC activation is sufficient to inhibit type 1 IFN secretion.

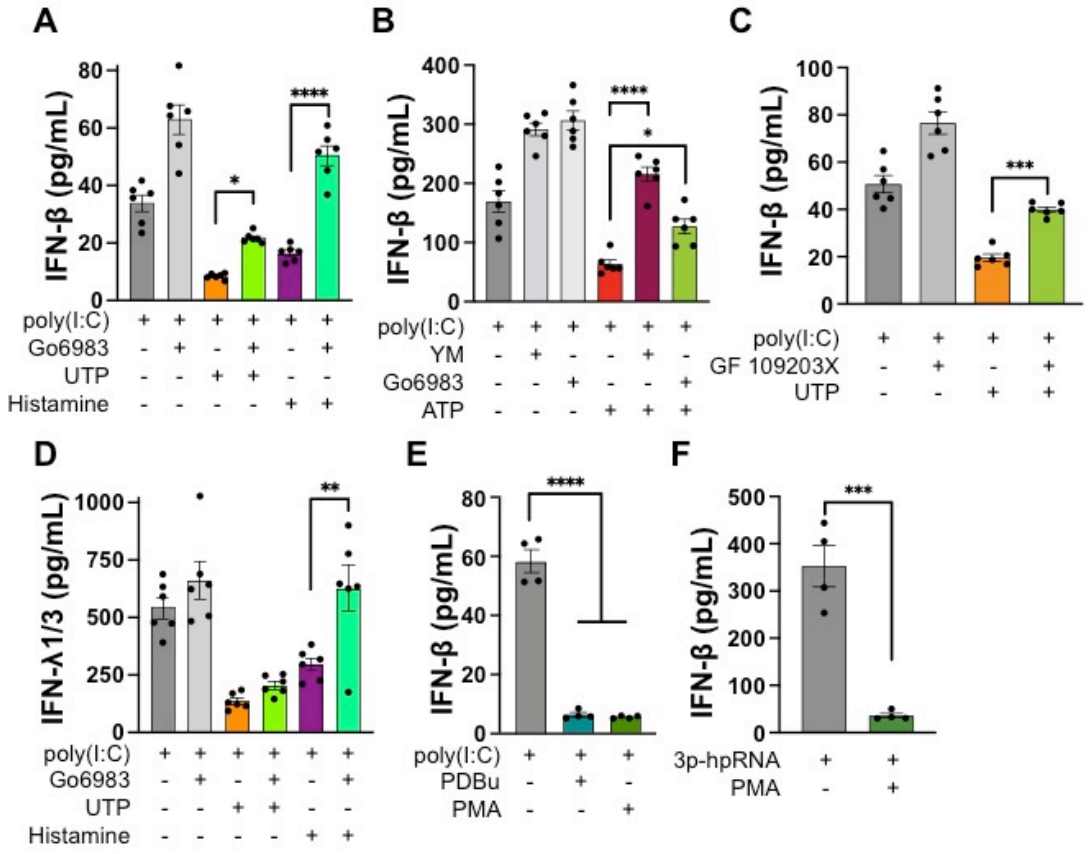

Figure 6.2 PKC signaling is necessary for GPCR-mediated inhibition of IFN-β production. A) The PKC inhibitor Gö 6983 (2.5μM) reverses UTP and histamine-mediated (100μM) inhibition of IFN-β release. Supernatants were collected 20 hrs after stimulation. Data are mean ± SEM of n = 6 samples. **(B)** The PKC inhibitor Gö 6983 (2.5μM) and the Gq inhibitor YM-254890 (1μM) reverses ATP-mediated (10μM) suppression of IFN-β release. Supernatants were collected 6 hours after cell stimulation with poly(I:C). Data are mean ± SEM of n = 6 samples. . **(C)** The PKC inhibitor GF 109203X (5μM) reverses UTP-mediated (100μM) inhibition of IFN-β release. Supernatants were collected 20 hours after stimulation. Data are mean ± SEM of n = 6 samples. **D)** The PKC inhibitor Gö 6983 (2.5μM) reverses histamine-mediated (100μM) inhibition of IFN-λ1/3 release. Supernatants were collected 20 hrs after stimulation. Data are mean ± SEM of n = 6 samples. **E)** The phorbol esters PDBu and PMA (100nM) inhibit IFN-β release. Supernatants were collected 6 hrs after stimulation. Data are mean ± SEM of n = 4 samples. **F)** PMA (100nM) blocks 3p-hpRNA (10ng/mL) evoked

IFN-β release into the supernatant. Supernatants collected 6 hours after stimulation. Data are mean ± SEM of n = 4 samples. *p<0.05, **p<0.01, ***p<0.001, ****p<0.0001

GPCR signaling inhibits *IFNB1* mRNA levels

We turned to examine if agonist stimulation inhibited *IFNB1* mRNA levels. Importantly, at a four hour time point, all the agonists suppressed poly(I:C)-driven *IFNB1* mRNA levels (Figure 6.3A). In contrast, the agonists were less effective at regulating the mRNA levels of the Th2 cytokine TSLP (Figure 6.3B). Collectively, this data suggests that the agonist regulation of type 1 IFN is primarily at the level of mRNA.

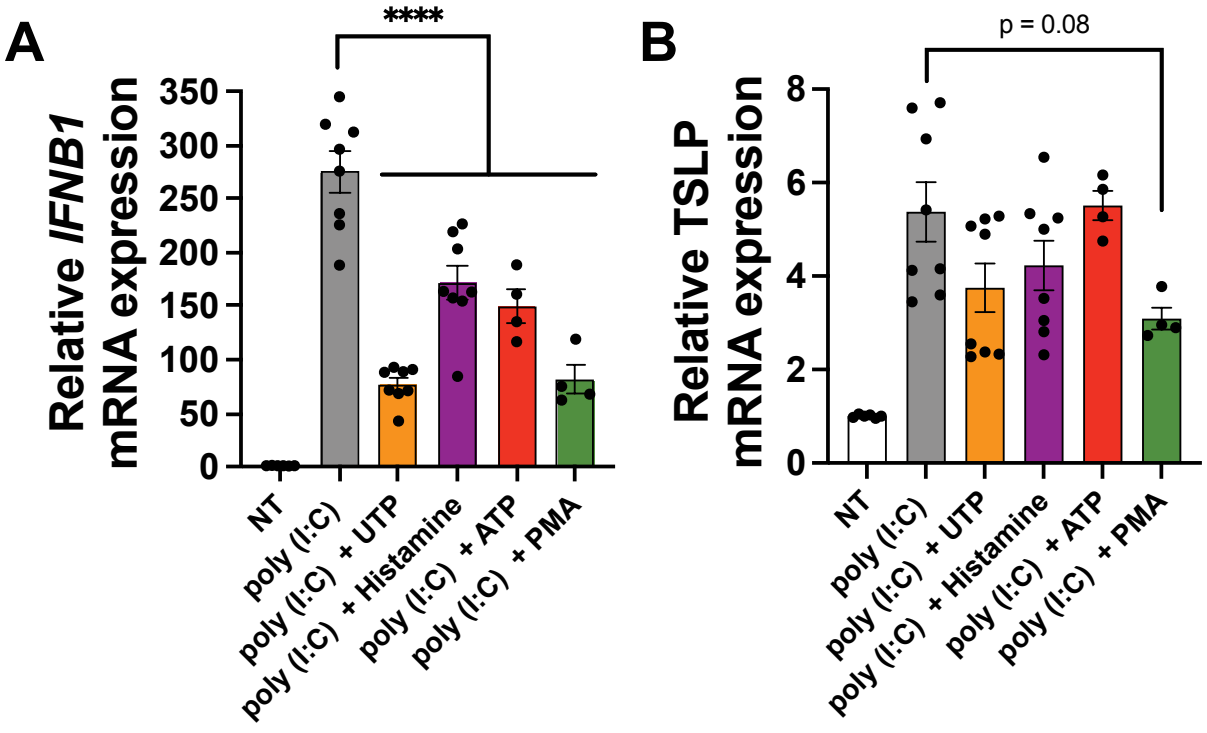

Figure 6.3 Agonists inhibit *IFNB1* mRNA levels but not *TSLP* mRNA levels. (A) UTP (100μM), histamine (100μM), ATP (10μM), PMA (100nM) suppress poly(I:C)-induced (10μg/mL) *IFNB1* mRNA expression. Expression was normalized to the

housekeeping gene RPLP0. RNA was collected 4 hours after stimulation. Data are mean ± SEM of n = 4-8 samples. **(B)** UTP (100μM), histamine (100μM), ATP (10μM), PMA (100nM) do not suppress poly(I:C)-induced (10μg/mL) *TSLP* mRNA expression. Expression was normalized to the housekeeping gene RPLP0. RNA was collected 4 hours after stimulation. Data are mean ± SEM of n = 4-8 samples. ****p<0.0001

UTP does not inhibit IFN receptor signaling

Some reports suggest that IFN signaling can drive IFN synthesis and release in a positive feedback loop [139]. We therefore tested whether UTP can directly inhibit IFN signaling. We first utilized the JAK inhibitor ruxolitinib to abrogate IFN signaling and measured IFN release. While ruxolitinib did modestly inhibit IFN release at longer time points (24hrs), UTP inhibited IFN release at earlier time points (6hrs) as well, suggesting two distinct mechanisms of action (Figure 6.4A-B). Next, we speculated that IFN-λ1/3 production might depend on IFN-β due to the faster release of IFN-β (Figure 6.4A-B). If this is the case, UTP induced inhibition of IFN-β may be responsible for the decrease in IFN-λ1/3 production by UTP. To test this, we applied exogenous IFN-β to rescue the deficient production of IFN-β in the context of UTP stimulation. However, exogenous IFN-β was not able to rescue the UTP-mediated inhibition of IFN-λ1/3 (Figure 6.4C). Finally, we pretreated cells with UTP and stimulated them with exogenous IFN-β to measure IFN signaling directly. UTP did not inhibit the phosphorylation of STAT1, or the induction of STAT1 and IRF1 (Figure 6.4D). These results suggest that UTP does not directly inhibit IFN signaling.

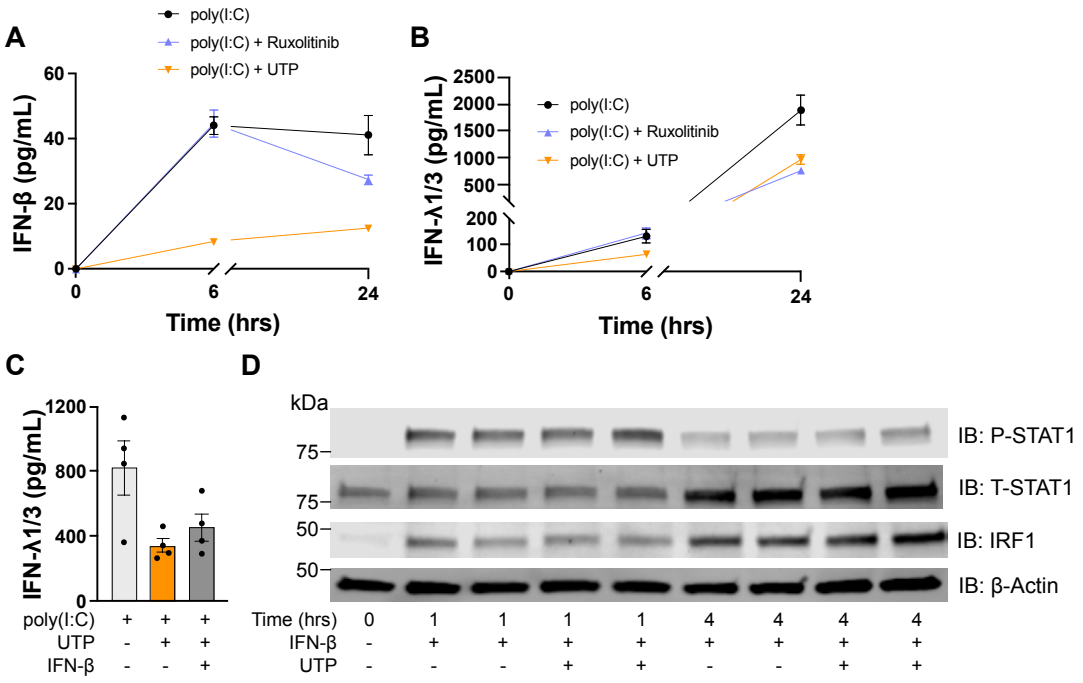

Figure 6.4 UTP does not inhibit IFN receptor signaling. A-B) The time course of JAK1/2 inhibitor ruxolitinib (1μM) and UTP (100μM)-mediated inhibition of IFN release does not phenocopy. Cells were stimulated with 10μg/mL poly(I:C) and supernatants were collected at 6 hrs or 24 hrs later for IFN analysis. Data are mean ± SEM of n = 4 samples. **C)** Exogenous IFN-β does not rescue the UTP-dependent IFN-λ1/3 release deficiency. Exogenous IFN-β (100pg/mL) was added to cells 2 hrs after simultaneous poly(I:C) (10μg/mL) and UTP (100μM) stimulation. Samples were collected at a 20 hrs time point and accessed for IFN analysis. Data are mean ± SEM of n = 4 samples. **D)** Western blot showing UTP does not inhibit exogenous IFN-β signaling. Cells were pretreated with UTP (100μM) 2 hrs prior to IFN-β stimulation (1000 IU/mL). Cells were lysed 1 or 4 hrs after IFN-β addition. (P-STAT: phospho-STAT1; T-STAT1: total-STAT1).

UTP does not inhibit activation of TBK1 or nuclear import of IRF3 and p65

Activation of TLR3 drives activation of the kinase TBK1, leading to nuclear import of the

transcription factors IRF3 and NF-κB [202]. We next tested whether UTP inhibits phosphorylation of TBK1. UTP had no effect on poly(I:C)-mediated phosphorylation of TBK1 (Figure 6.5A). We then determined whether UTP inhibited nuclear import of either IRF3 or the important NF-κB subunit p65. UTP had no clear effect on the nuclear translocation of either of these transcription factors (Figure 6.5B). These findings suggest that UTP does not inhibit the activation of TBK1, IRF3 or p65.

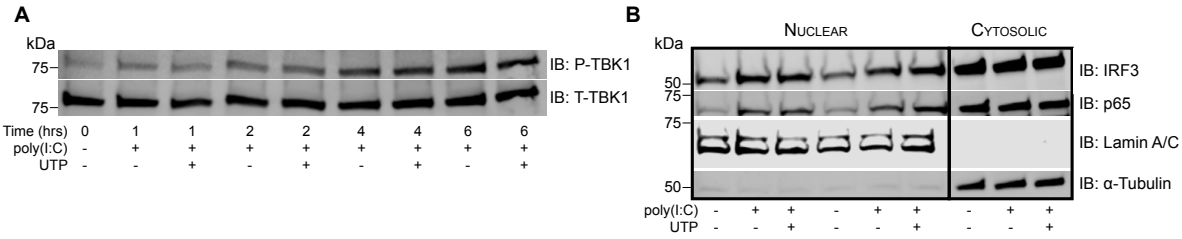

Figure 6.5 UTP does not inhibit activation of TBK1 or nuclear import of IRF3 and p65. A) Western blot showing UTP does not inhibit activation of TBK1. Cells were simultaneously stimulated with UTP (100μM) and poly(I:C) (10μg/mL) and lysed at the indicated time points. (P-TBK1: phospho-TBK1; T-TBK1: total-TBK1). **B)** Western blot showing UTP does not inhibit nuclear import of IRF3 or p65 (NF-κB subunit). Cells were simultaneously stimulated with UTP (100μM) and poly(I:C) (10μg/mL) and cells were lysed for nuclear vs. cytosolic fraction 3 hrs later.

CRAC channel activation is not necessary for GPCR-mediated inhibition of IFN release

UTP consistently inhibited IFN release more powerfully than histamine or SLIGKV with all stimuli besides RIG-I agonists and IAV (Figure 5.2 and Figure 5.5). UTP also elicited the most sustained Ca^{2+} signal (Figure 2.4A,C). We hypothesized that Ca^{2+} signaling and more specifically CRAC channels may be involved in GPCR-mediated inhibition of IFN secretion. We tested the CRAC channel inhibitor BTP2, which showed no efficacy for reversing the UTP-mediated inhibition of 2,3 cGAMP-induced IFN-β (Figure 6.6A).

BTP2 had no effect on the 2,3 cGAMP-mediated release of IFN-β either (Figure 6.6A). We also tested the CRAC channel inhibitor, CM4620, for its role in the regulation of IFN release. Neither BTP2 nor CM4620 had any effect on the release of IFN regardless of PRR activated or nucleotide used to suppress IFN (Figure 6.6B-G). Thus, we conclude that CRAC channel activation is not necessary for PRR-mediated IFN release or nucleotide-mediated suppression of IFN release.

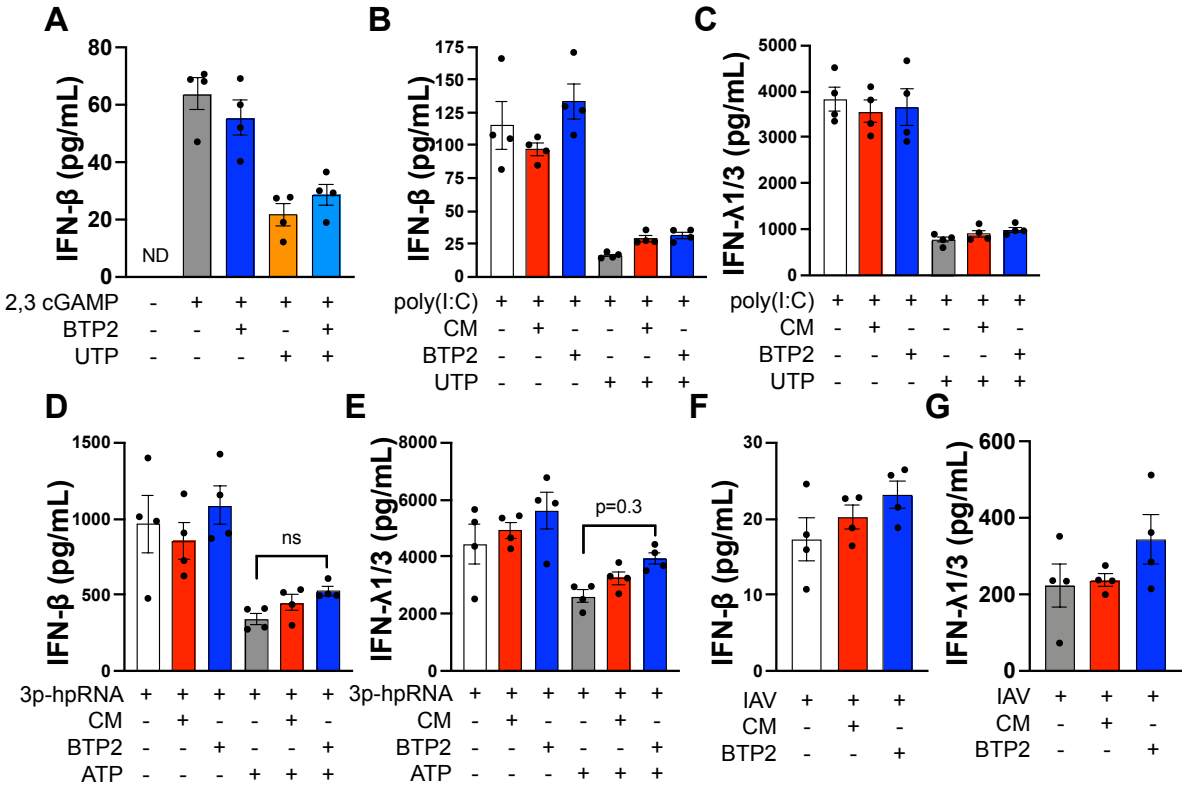

Figure 6.6 CRAC channel activation is not necessary for agonist-mediated inhibition of IFN release. A) The CRAC channel inhibitor BTP2 (1μM) does not reverse UTP-mediated (100μM) inhibition of 2,3 cGAMP-driven (10μg/mL) IFN-β release into the supernatant (24hr time point). Data are mean ± SEM of n = 4 samples. **(B-G)** The CRAC channel inhibitors CM4620 (1μM) and BTP2 (1μM) do not reverse UTP-mediated (100μM) inhibition of poly(I:C)-driven (10μg/mL) IFN release into the

supernatant (24hr time point) *(B-C)* or ATP-mediated (100μM) inhibition of 3p-hpRNA-driven (10ng/mL) IFN release into the supernatant (24hr time point) *(D-E)* or IAV-driven (MOI 1) IFN release into the supernatant (24hr time point) *(F-G)*. Data are mean ± SEM of n = 4 samples.

EGF inhibits IFN release from airway epithelial cells

Multiple reports suggest a role for EGFR signaling in the suppression of IFN release from AECs [135, 136]. Purinergic receptor signaling has also been linked to transactivation of EGFR in AECs [230]. We first replicated the prior findings, demonstrating that EGF powerfully inhibits the release of both type 1 and type 3 IFN induced by poly(I:C) from AECs (Figure 6.7A-B). The strength of the inhibition was similar to a saturating dose of UTP (Figure 6.7A-B). Then, we utilized the EGFR kinase inhibitor AG 1478 [231]. AG 1478 partially reversed the UTP-mediated inhibition of type 1 IFN, but showed little effect on UTP-mediated suppression of type 3 IFN (Figure 6.7C-D). This result was similar to the broad spectrum PKC inhibitors that were tested prior (Figure 6.2A,D) and suggests that EGFR signaling downstream of $P2Y_2$ receptors may be partially involved in the suppression of type 1 IFN but are unlikely to contribute to the suppression of type 3 IFN.

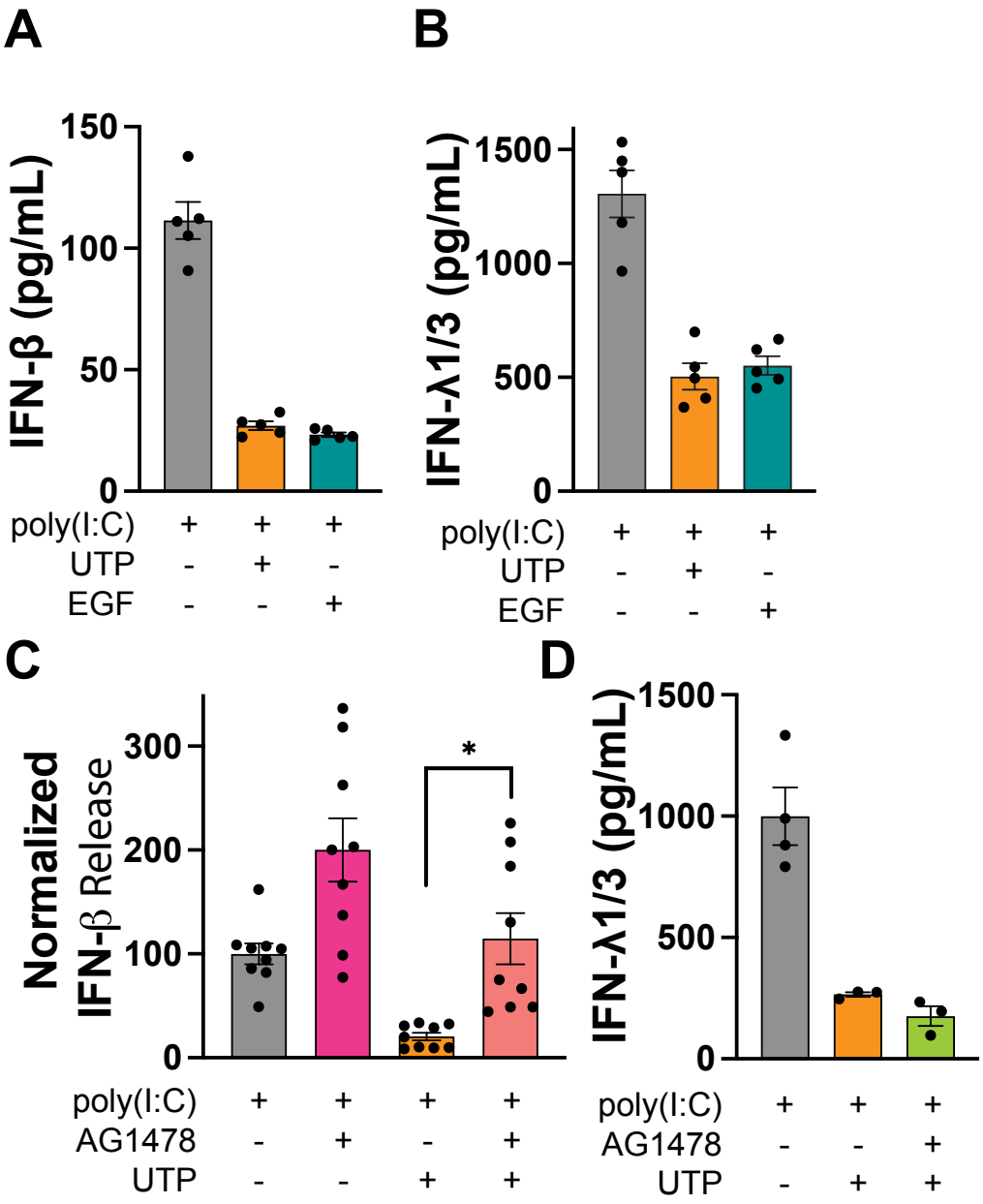

Figure 6.7 EGF signaling inhibits IFN release. (A-B) EGF (10ng/mL) inhibits poly(I:C)-induced (10μg/mL) IFN-β release (A) and IFN-λ1/3 release (B) to a similar degree as UTP (100μM). IFN in the supernatant was quantified 16 hours post stimulation. Data are mean ± SEM of n = 4 samples. **(C-D)** The EGFR inhibitor AG1478 (1μM) partially reverses UTP-mediated (100μM) inhibition of poly(I:C)-driven (10μg/mL) IFN-β release into the supernatant (6 hour time point) but leaves the inhibition of IFN-λ1/3 release intact (20 hour time point). Data are mean ± SEM of n = 4 samples. *p<0.05

Discussion

Numerous studies have demonstrated that G-protein coupled receptor signaling inhibits IFN secretion [133, 134]. Here we demonstrate that Gq signaling is necessary for the inhibition of IFN release by $P2Y_2$ receptors. We interrogated poly(I:C)-dependent activation of TBK1, as well as nuclear import of the transcription factors IRF3 and the NF-kB subunit p65. However, we found no clear inhibition of any of these endpoints by UTP (Figure 6.5). However, when we quantified the synthesis of *IFNB1* mRNA directly all agonist suppressed type 1 IFN (Figure 6.3A). This suggests a model where the agonist-directed inhibition occurs downstream of transcription factor import into the nucleus. This is likely at the point of transcriptional activation of the relevant transcription factors. We measured *IFNB1* mRNA half-life in the presence of UTP and saw no differences (data not shown). We also investigating whether UTP disrupted IFN receptor signaling and no clear inhibition was observed (Figure 6.4). Collectively, the agonist-mediated suppression appears to be at a transcriptional level, although the precise mechanism remains to be determined.

One study in pDCs has demonstrated that strong PKC activation can inhibit type 1 interferon production [133]. Here we demonstrate that in AECs, PKC activation was necessary for agonist-mediated suppression of type 1 IFN (Figure 6.3A-C). Additionally, phorbol esters directly inhibited IFN-β release (Figure 6.2D-E). This suggests that PKC is both necessary and sufficient to drive the suppression of type 1 IFN, likely at the level of transcription (Figure 6.3A). Further studies will be required to uncover the complex mechanisms behind PKC regulation of type 1 IFN production in AECs.

Chapter 7: GPCR and CRAC channel function in AECs following mucociliary differentiation

Introduction

Submerged cultures of primary human airway cells lack many of the features of the differentiated airways such as motile cilia and goblet cells producing mucus [115, 117]. Following differentiation, many of the receptors that activate CRAC channels, such as $P2Y_2$ receptors, H_1 receptors, PAR2 are also functional [49, 67, 232, 233]. These receptors have functions such as the activation of the Ca^{2+} activated Cl^- channel (CACC), increasing cilia beat frequency, mucin secretion, barrier function, and cytokine release [26, 48, 51-53, 94, 115, 118]. Interestingly, GPCR expression in differentiated AECs is reported to be polarized such that $P2Y_2$ receptors are often found on the apical and basolateral surfaces while H_1 receptors and PAR2 receptors are restricted to basolateral surfaces [49, 67, 232-234].

Mucin proteins, along with water and ions are an important component of mucus [114]. In the airways, mucus is used in the mucociliary escalator, a process in which ciliated cells pump mucus up and out of the airways to be either swallowed or coughed up [114]. Although this physiology is important for host pathogen protection, mucus hypersecretion and goblet cell metaplasia are hallmarks of both asthma and chronic obstructive pulmonary disease (COPD) [114-116]. The most common cause of death in asthmatic patients is excessive mucus plugs [114]. Thus, therapies that can attenuate mucin hypersecretion have vast potential to improve modern asthma treatment. In human airways, club (Clara) and goblet cells synthesize and secrete mucin proteins [114, 115]. The major mucins of the airways are MUC5AC and MUC5B. These large

glycoproteins are packaged into secretory granules [114]. Although some basal exocytosis of these granules occurs, secretion can rapidly increase in a receptor dependent manner [115, 117, 118]. These receptors are numerous but include P2Y, PAR2, and EGFR [53, 118-120]. One conserved mechanism for inducing mucin secretion is Ca^{2+} signaling [116].

Ca^{2+} signaling is also known to be elevated in cells derived from cystic fibrosis patients [234]. Although Ca^{2+} signaling is essential for differentiated AEC function, which of these may be attributed to CRAC channel activation is unknown. To dissect the signaling pathways and CRAC channel function in AECs following differentiation, we utilized an air-liquid interface system. To our surprise, we found that ATP-evoked PGE_2 synthesis became CRAC channel independent in AECs following mucociliary differentiation. Similarly, ATP-evoked MUC5AC release was not inhibited with the CRAC channel inhibitor CM4620. This could be explained in part by a diminished sustained phase of Ca^{2+} entry following GPCR activation in AECs that have been differentiated. However, GPCR agonists largely retained their ability to suppress interferon release in ALI cultures. This further validates that the mechanism of interferon suppression is CRAC channel independent. Collectively, we see large scale rewiring of Ca^{2+} signaling in AECs following mucociliary differentiation.

Results

ATP evoked PGE_2 synthesis is independent of extracellular Ca^{2+} entry following mucociliary differentiation

We tested whether agonists and activators of CRAC channels evoke PGE_2 synthesis in AECs following mucociliary differentiation. Both ATPγS and TG evoked release of PGE_2 to both the apical and basolateral compartments (Figure 7.1A). When ATP and ATPγS were compared directly, ATP seemed less effective than ATPγS at inducing release to the apical surface (Figure 7.1B). Higher doses of ATP (500μM) replicated ATPγS. This suggests that the apical surface may have high expression of ecto-ATPases that degrade ATP. Next, we tested whether the CRAC channel inhibitors CM4620 and BTP2 inhibited ATP-mediated PGE_2 synthesis. Surprisingly, both inhibitors had no effect (Figure 7.1C). This is in contrast to the results in submerged NHBE cultures (Figure 3.2). However, in agreement with the submerged cultures, the ATP-mediated PGE_2 release was abrogated in the presence of AR-C (Figure 7.1C). This suggests that $P2Y_2$ receptors drive PGE_2 synthesis in ALI cultures as well as submerged cultures. Finally, we tested whether extracellular Ca^{2+} was required for ATP-mediated PGE_2 synthesis. Chelation of all extracellular Ca^{2+} did not inhibit ATP-evoked PGE_2 synthesis (Figure 7.1D). This data strongly suggests that extracellular Ca^{2+} entry is not required for ATP-driven PGE_2 synthesis following mucociliary differentiation. Altogether, this data suggests that the Ca^{2+} dependence of PGE_2 synthesis alters following AEC differentiation likely switching from Ca^{2+} entry through CRAC channels to Ca^{2+} release from intracellular stores.

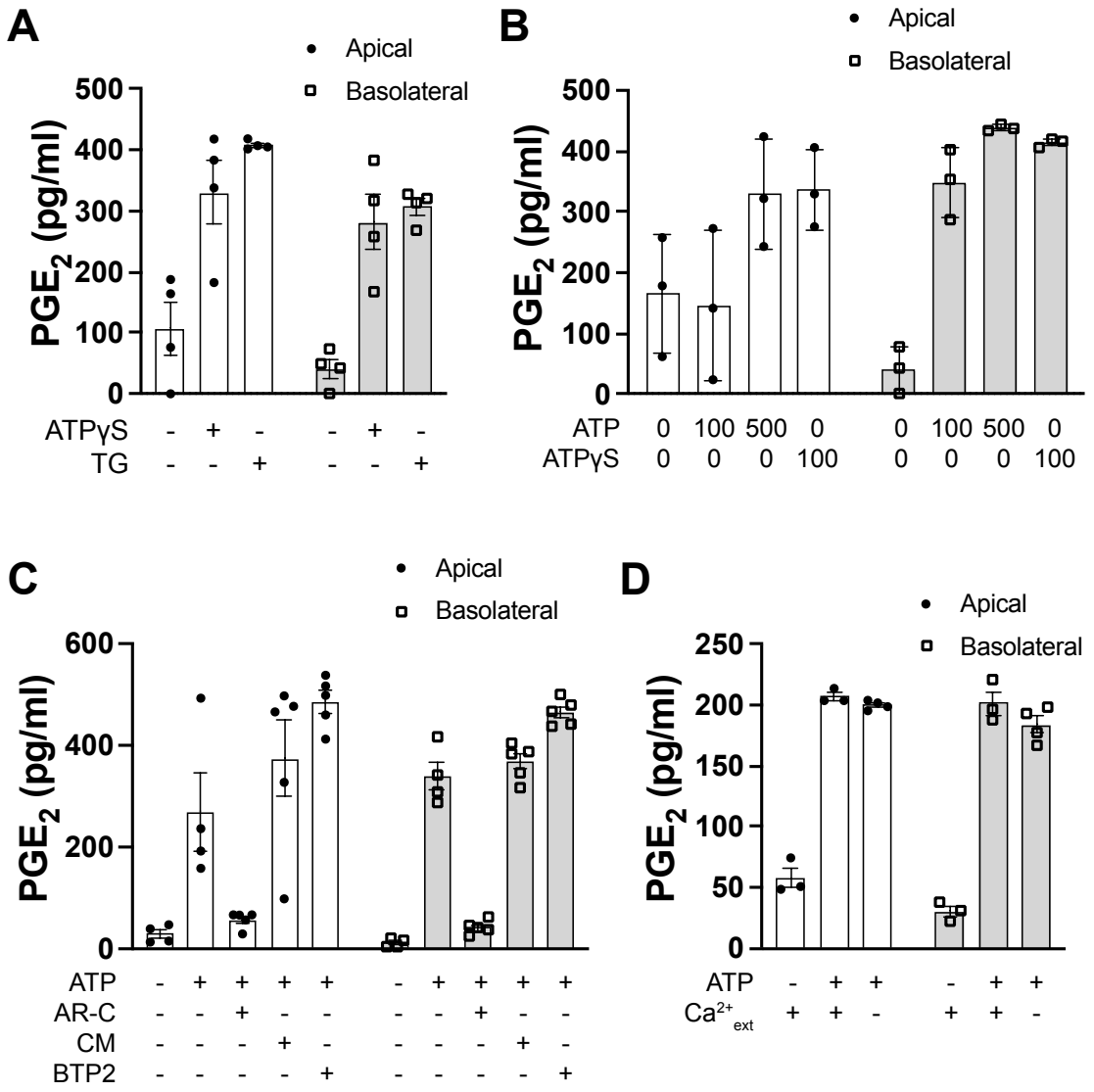

Figure 7.1 ATP evoked PGE_2 synthesis is independent of extracellular Ca^{2+} entry following mucociliary differentiation. A-D) NHBEs were differentiated using LifeLine ALI media. The day before stimulation, basolateral ALI media was replaced with 2 Ca BEBM media to remove hydrocortisone. All drugs were added to both apical and basolateral compartments and PGE_2 levels were measured independently for both compartments. **A)** ATPγS (100μM) and TG (500nM) evoke PGE_2 synthesis (2 hrs) in ALI cultures. Data are mean ± SEM of n = 4 samples. **B)** ATPγS (100μM) and ATP (100 or 500μM) evoke PGE_2 synthesis (2 hrs) in ALI cultures. Data are mean ± SEM of n = 3 samples. **C)** CRAC channel inhibitors do not block ATP (500μM) evoked PGE_2

synthesis (2 hrs) in ALI cultures. Cells were pretreated with CM4620 (1μM), BTP2 (5μM), or AR-C (10μM) for 2 hrs prior to ATP stimulation. Data are mean ± SEM of n = 4-5 samples. **D)** Ca^{2+}_{ext} is not necessary for ATP (500μM) evoked PGE_2 synthesis (2 hrs) in ALI cultures. BEBM media with 2mM Ca^{2+} or 0mM Ca^{2+} (adjusted using EGTA) was used for stimulation phase. Data are mean ± SEM of n = 4-5 samples.

Agonists evoke mild IL-6 release into the basolateral compartment

We tested whether agonists such as the PAR2 activator, SLIGKV, histamine, or ATP induce an increase in IL-6 release in the ALI cultures. When cultures were stimulated with agonists, an apical wash showed no induction of IL-6 by the PAR2 activator (Figure 7.2A). However, the basolateral compartment showed small increases in IL-6 levels upon treatment with the PAR2 activator and high doses of ATP (Figure 7.2B). When ALI cultures were differentiated using the StemCell Technologies media, IL-6 in the basolateral compartment was not detectable (data not shown). This suggests that ALI cultures produce much less IL-6 than submerged cultures, similar to the results comparing PGE_2 production in these two models.

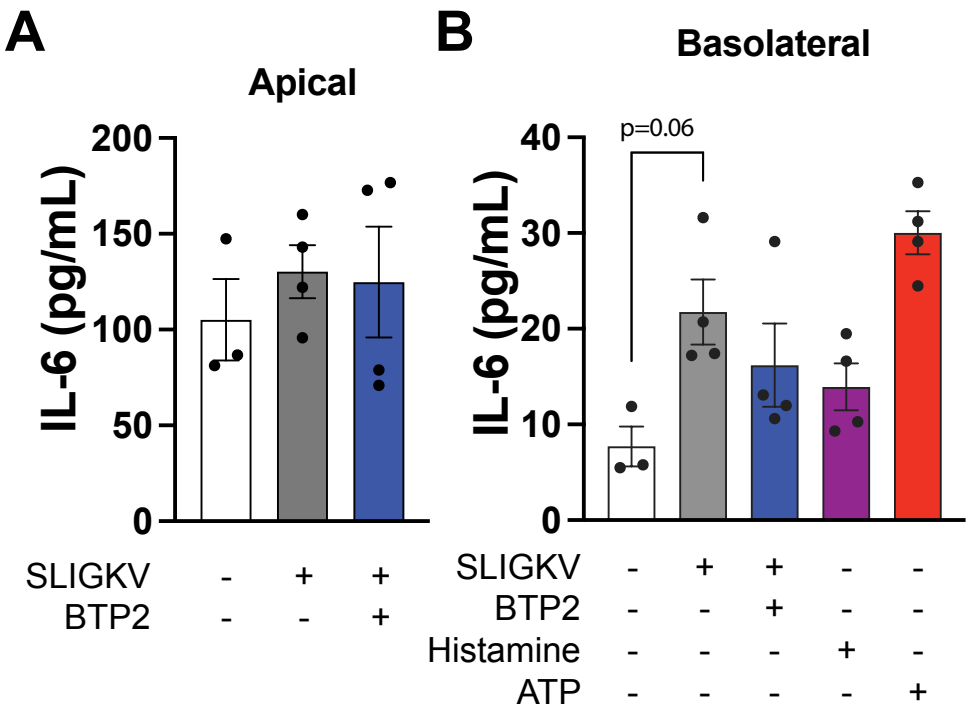

Figure 7.2 Agonists evoke mild IL-6 release into the basolateral compartment. NHBEs were differentiated using LifeLine ALI media. The day before stimulation, basolateral ALI media was replaced with 2 Ca BEBM media to remove hydrocortisone. All drugs were added to both apical and basolateral compartments and IL-6 levels were measured independently for both compartments. **A-B)** Agonists evoke modest IL-6 secretion to basolateral compartment but not to the apical compartment. IL-6 was quantified via ELISA from either an apical wash or the basolateral media 20 hours following stimulation. Concentrations for compounds were SLIGKV (100μM), BTP2 (5μM), Histamine (100μM), and ATP (500μM). Data are mean ± SEM of n = 3-4 samples.

Store-operated Ca^{2+} entry is diminished following mucociliary differentiation

This alteration in the Ca^{2+} dependence of PGE_2 synthesis following differentiation led us to test whether Ca^{2+} signaling itself alters. In ALI cultures, ATP evoked a rapid Ca^{2+} rise followed by a swift decay back to baseline (Figure 7.3A). Importantly, neither CRAC channel inhibitor CM4620 (also known as CM-EX-128) or BTP2 dramatically decreased the ATP-mediated Ca^{2+} signal (Figure 7.3A). To test if cytokines or house dust mite

(HDM) could restore the sustained Ca^{2+} signal, we treated cells overnight with IL-1β, IL-13, or HDM. However, none of these molecules had any effect on the ATP-mediated Ca^{2+} signal (Figure 7.3B). Therefore, we conclude that during the process of mucociliary differentiation, a rewiring of Ca^{2+} signaling occurs causing the sustained Ca^{2+} signal attributed to CRAC channels in submerged cultures (Figure 2.2) to diminish.

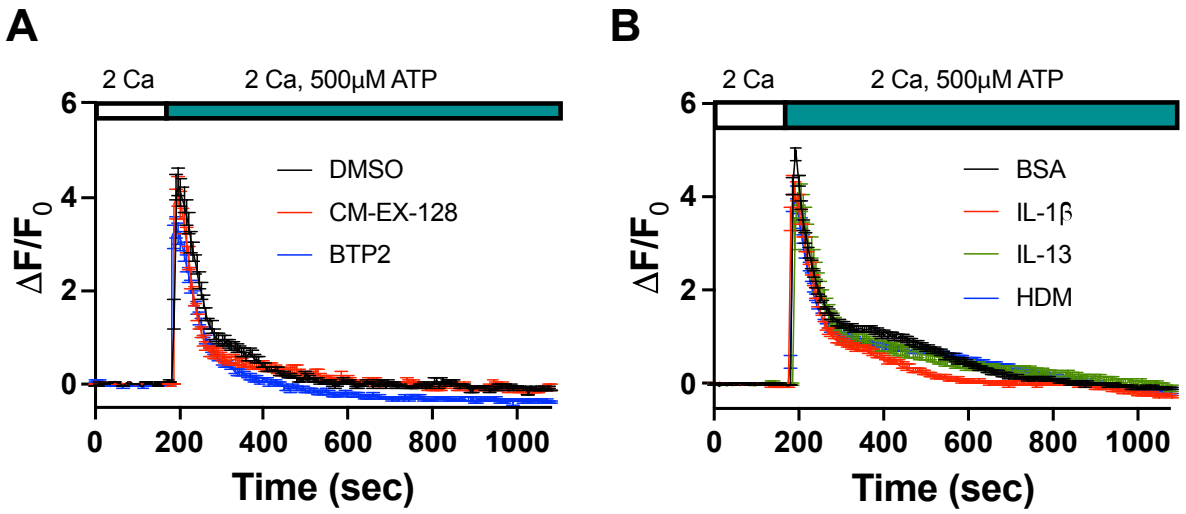

Figure 7.3 Store-operated Ca^{2+} entry is diminished following mucociliary differentiation. A-B) NHBEs were differentiated using LifeLine ALI media. The day before stimulation, basolateral ALI media was replaced with 2 Ca BEBM media to remove hydrocortisone. Cells were loaded with 5µM Fluo-4 for 1 hr on the apical compartment and Ca^{2+} signaling was measured from the apical side. **A)** CRAC channel inhibitors (CM4620 = CM-EX-128 used at 1µM and BTP used at 5µM) do not inhibit ATP-mediated Ca^{2+} signaling in ALI cultures. **B)** Cytokines and house dust mite (HDM) do not restore SOCE in ALI cultures. Treated cells basolaterally with cytokines or HDM 24 hrs prior to experiment. 72 hr pretreatment showed the same lack of effect. Bovine Serum Albumin (0.1%) was used as a control for the cytokines. IL-1β (10ng/mL), IL-13 (10ng/mL), HDM (100µg/mL) were used.

Histamine evokes Ca^{2+} signaling on basolateral cells exclusively following mucociliary differentiation

Polarized GPCR expression has been reported following AEC differentiation [49, 232-234]. To test if this occurred with histamine receptors, we measured Ca^{2+} signals in ALI cultures when histamine was perfused over either the basolateral or apical cells. Strikingly, histamine evoked a rapid Ca^{2+} signal when perfused over the basolateral cells but was incompetent when perfused over the apical cells (Figure 7.4A-B). This finding strongly suggests that histamine receptors are exclusively functional on the basolateral surface of ALI cultures.

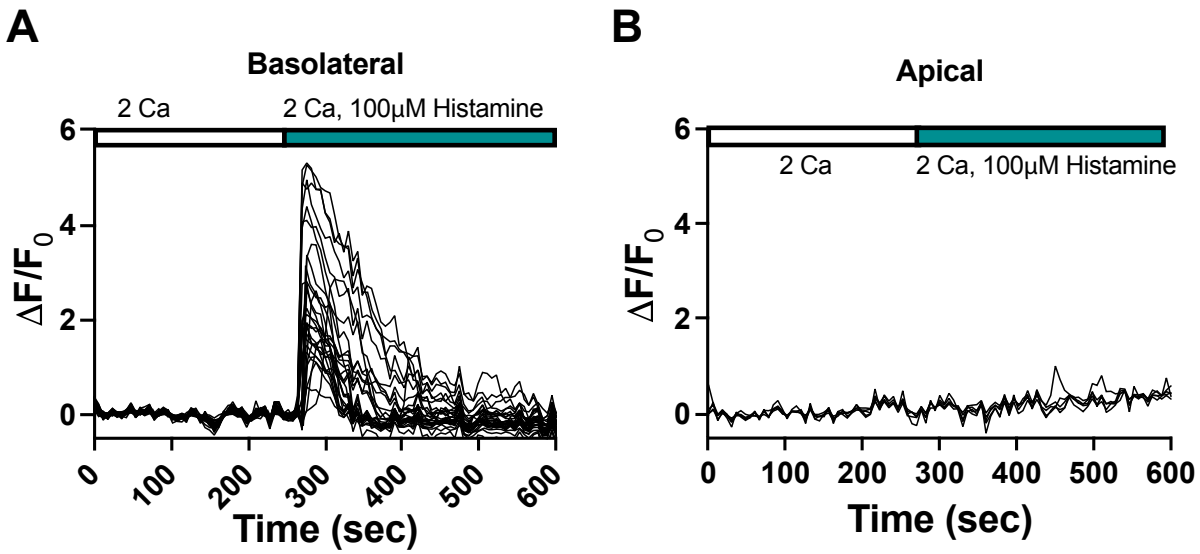

Figure 7.4 Histamine evokes Ca^{2+} signaling on basolateral cells exclusively following mucociliary differentiation. A-B) NHBEs were differentiated using LifeLine ALI media. The day before stimulation, basolateral ALI media was replaced with 2 Ca BEBM media to remove hydrocortisone. Cells were loaded with 5μM Fluo-4 for 1 hr on the apical compartment and Ca^{2+} signaling was measured from the basolateral side (A) or apical side (B). **A)** Histamine (100μM) induces a rapid Ca^{2+} signal when applied on the basolateral compartment. **B)** Histamine (100μM) induces no Ca^{2+} signal when applied on the apical compartment.

The CRAC channel inhibitor CM4620 does not inhibit nucleotide-evoked MUC5AC release following mucociliary differentiation

Ca^{2+} signaling has been implicated in the release of mucins from goblet cells [53]. To test if CRAC channels were involved in ATP-mediated MUC5AC release in goblet cells, we first optimized a protocol for the measurement of MUC5AC. MUC5AC measurements have historically been difficult, as no validated commercial kits exist. Successive washing of the apical surface is necessary to measure nucleotide-evoked MUC5AC release. In agreement with prior reports [53, 115, 235, 236], the protocol demonstrated the majority of the MUC5AC is removed during the wash steps, while ATPγS induced a 2.5 fold increase in release during the stimulation phase (Figure 7.5A). We tested the ORAI1 inhibitor CM4620 for its ability to regulated ATPγS-mediated MUC5AC release. CM4620 did not inhibit MUC5AC release when MUC5AC was measured via an ELISA or via a Dot Blot (Figure 7.5B-C). This data suggests that CRAC channel function is dispensable for nucleotide-induced MUC5AC secretion from goblet cells.

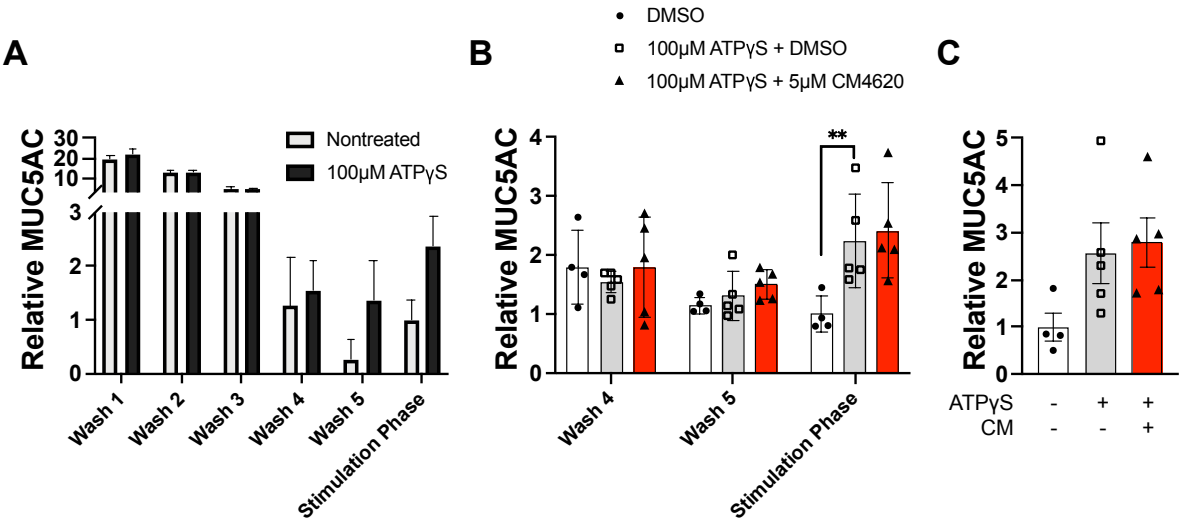

Figure 7.5 The CRAC channel inhibitor CM4620 does not inhibit nucleotide-evoked MUC5AC release following mucociliary differentiation. A-C) NHBEs were differentiated using LifeLine ALI media. **A)** ATPγS (100μM) evokes MUC5AC secretion. ALI cultures were apically washed five times to remove excess mucins. During the stimulation phase, ATPγS was added to some transwells and MUC5AC levels were measured via ELISA. Data are mean ± SEM of n = 5 samples. **B)** CM4620 (5μM) does not inhibit ATPγS (100μM) evoked MUC5AC secretion. ALI cultures were apically washed five times to remove excess mucins. During the stimulation phase, ATPγS was added to some transwells and MUC5AC levels were measured via ELISA. Cells were pretreated with CM 2 hrs prior to stimulation phase. Data are mean ± SEM of n = 4-5 samples. **C)** CM4620 (5μM) does not inhibit ATPγS (100μM) evoked MUC5AC secretion. ALI cultures were apically washed five times to remove excess mucins. During the stimulation phase, ATPγS was added to some transwells and MUC5AC levels were measured via Dot Blot. Cells were pretreated with CM 2 hrs prior to stimulation phase. Samples are from same experiment as (B). Data are mean ± SEM of n = 4-5 samples.

Polarized release of Interferons following mucociliary differentiation

We transitioned to test how GPCR-mediated inhibition of IFN release may alter following mucociliary differentiation. We performed a time course analysis of poly(I:C)-dependent IFN secretion in ALI cultures. Interestingly, IFN release was consistently higher to the basolateral compartment than the apical compartment (Figure 7.6A-B). This may be attributed to type 1 IFN receptors being exclusively expressed on the basolateral surface [237]. Another possible explanation was that the apical surface was pulsed with poly(I:C) for 2 hours, while the basolateral compartment was left in poly(I:C) for the length of the experiment. This difference in treatment was performed to limit squamous de-differentiation of the cells that has been shown to occur during the presence of long-term liquid in the apical compartment [232]. It is also interesting to note that the type 1 IFN release to the apical compartment was very rapid (peaking within 6 hrs). This suggests that upon viral infection, AECs may release type 1 IFN into the apical compartment rapidly to limit the spread of virus within the lumen of the airways. It is also striking that following differentiation, AECs produce significantly more

type 3 IFN than type 1 IFN (approximately 1,000 fold more). Collectively, this data suggests that following differentiation, AECs maintain sensors for poly(I:C) that elicit type 1 and type 3 IFN release.

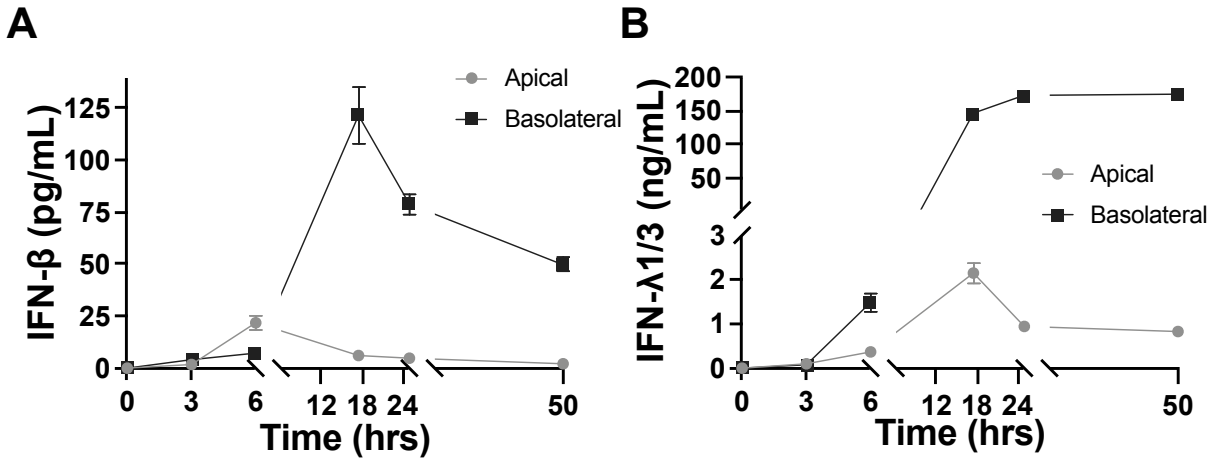

Figure 7.6 Polarized Release of Interferons following mucociliary differentiation. A-B) NHBEs were differentiated at the air-liquid interface (ALI) for 4 weeks and then stimulated with 10μg/mL poly(I:C) on both apical and basolateral sides. StemCell Technologies ALI media was used for this experiment. **A)** ALI cultures were stimulated with poly(I:C), then apical and basolateral supernatant samples were collected at the indicated time points and measured for IFN-β release via ELISA. To normalize for the difference in volumes collected from apical and basolateral compartments, basolateral concentrations were multiplied by 3.2. Data are mean ± SEM of n = 4-5 samples. **B)** ALI cultures were stimulated with poly(I:C), then apical and basolateral supernatant samples were collected at the indicated time points and measured for IFN-λ1/3 release via ELISA. To normalize for the difference in volumes collected from apical and basolateral compartments, basolateral concentrations were multiplied by 3.2. Data are mean ± SEM of n = 4-5 samples.

GPCR agonists inhibit Interferon release following mucociliary differentiation

We tested whether the agonists regulated poly(I:C)-mediated IFN release following differentiation. All the agonists (ATP, UTP, histamine, SLIGKV) inhibited the release of type 1 and type 3 IFN to the basolateral compartment (Figure 7.7B, 7.7D). In contrast, only ATP and UTP suppressed the release of type 1 IFN to the apical compartment

(Figure 7.7C). None of the agonists dampened type 3 IFN release to the apical compartment (Figure 7.7E). Collectively, these results show that GPCR-mediated signaling can inhibit interferon release from AECs that have undergone mucociliary differentiation, although the phenotypes are much more complex (Figure 7.7F).

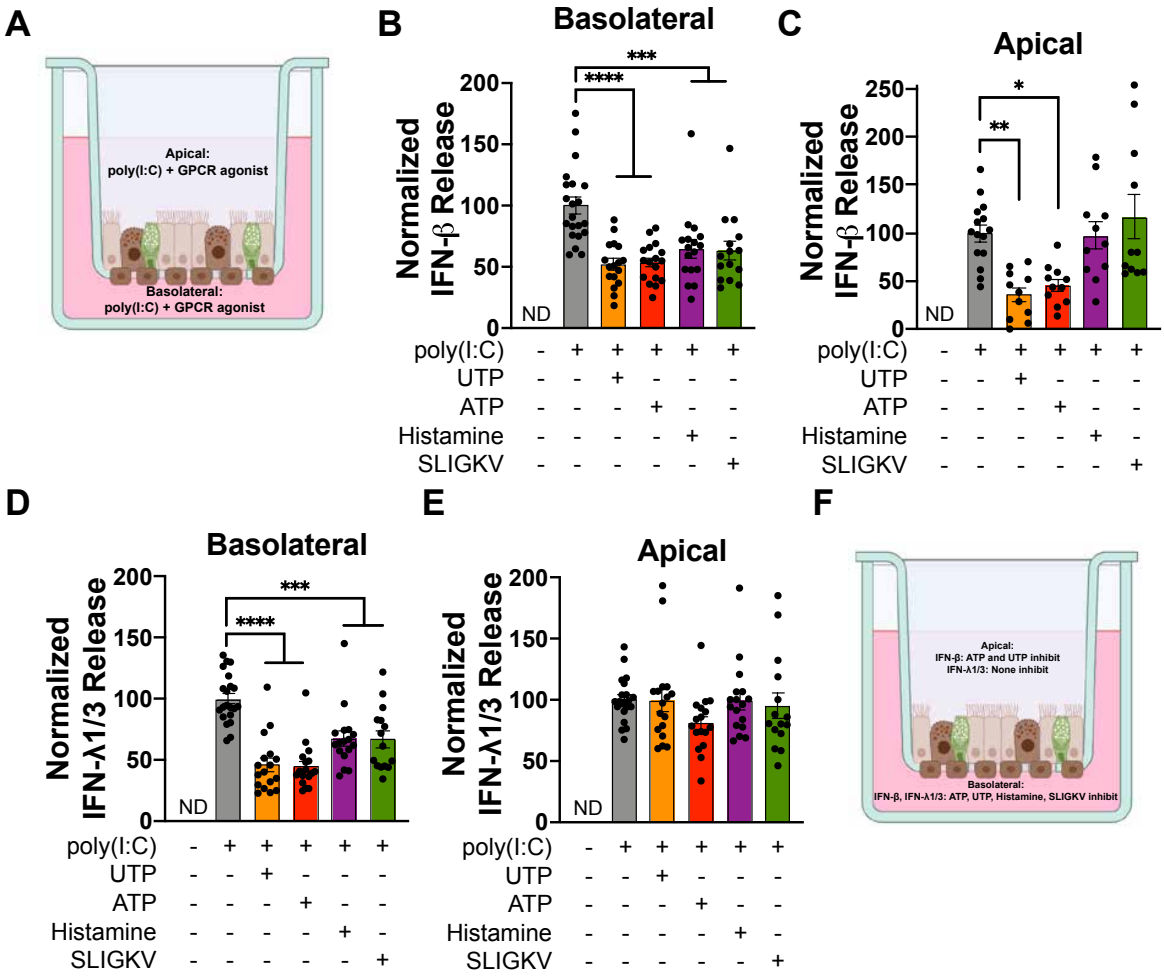

Figure 7.7 GPCR agonists inhibit Interferon release following mucociliary differentiation. A) NHBEs were differentiated at the air-liquid interface (ALI) for 4 weeks and then stimulated with 10μg/mL poly(I:C) +/- 100μM GPCR agonists on both apical and basolateral sides. StemCell Technologies ALI media was used for this experiment. **B-E)** GPCR agonists inhibit IFN release from dsRNA-stimulated ALI cultures. ALI cultures were stimulated with simultaneously with 10μg/mL poly(I:C) and 100μM GPCR agonist on both apical and basolateral sides. Apical and basolateral

supernatant samples were collected 20 hrs later and measured for IFN-β (B-C) or IFN-λ1/3 (D-E) release via ELISA. Apical cytokine levels are shown in C,E while basolateral levels are shown in B,D. Data are mean ± SEM of n = 11-21 samples. **F)** The nucleotides ATP and UTP inhibit the release of IFN-β to both apical and basolateral compartments while histamine and SLIGKV exclusively inhibit basolateral IFN-β. In contrast, all agonists effectively inhibit basolateral release of IFN-λ1/3 but do not inhibit apical IFN-λ1/3 release. *p<0.05, **p<0.01, ***p<0.001, ****p<0.0001

The $P2Y_2$ receptor antagonist AR-C reverses ATP-mediated inhibition of IFN release following mucociliary differentiation

ATP shows divergent effects on IFN release depending on the dose and differentiation state of the AECs. We tested the $P2Y_2$ receptor antagonist AR-C for its ability to modulate the ATP-mediated inhibition of IFN in ALI cultures. AR-C significantly reversed the ATP-driven inhibition of both type 1 and type 3 IFN (Figure 7.8A-B). This finding suggests that $P2Y_2$ receptor activation inhibits IFN secretion following mucociliary differentiation.

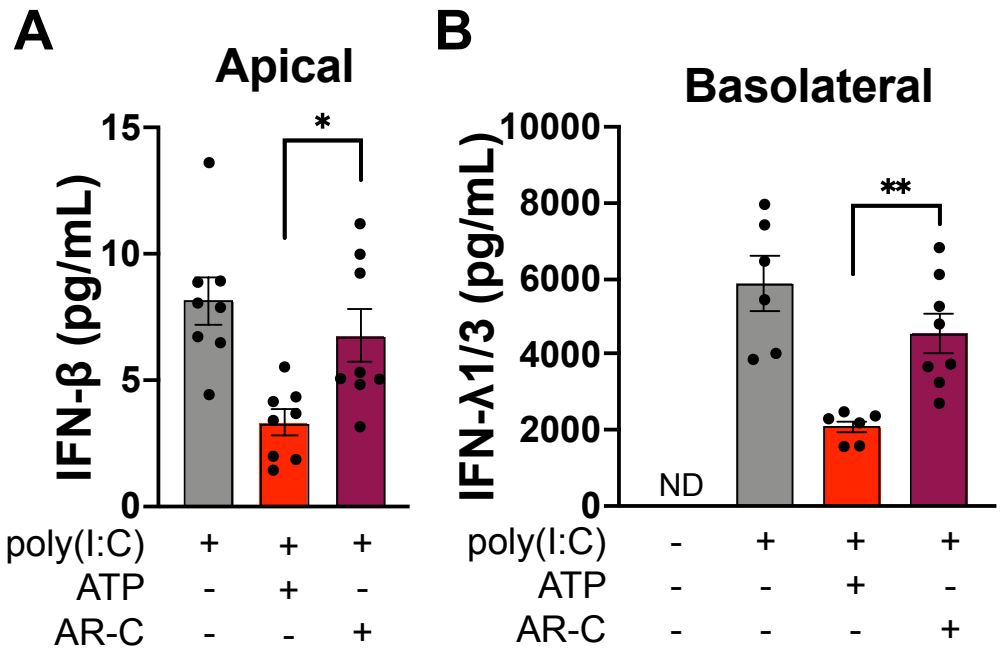

Figure 7.8 The $P2Y_2$ receptor antagonist AR-C reverses ATP-mediated inhibition of IFN release following mucociliary differentiation. A-B) NHBEs were differentiated at the air-liquid interface (ALI) for 4 weeks and then stimulated with 10μg/mL poly(I:C) +/- 100μM GPCR agonists on both apical and basolateral sides. StemCell Technologies ALI media was used for this experiment. **A)** The $P2Y_2$ antagonist AR-C 118925XX (10μM) reverses ATP-mediated (100μM) inhibition of IFN-β release. ALI cultures were stimulated simultaneously with 10μg/mL poly(I:C) and 100μM ATP on both apical and basolateral sides. Apical supernatant samples were collected 7 hrs later and measured for IFN-β. Data are mean ± SEM of n = 8 samples. **B)** The $P2Y_2$ antagonist AR-C 118925XX (10μM) reverses ATP-mediated (100μM) inhibition of IFN-λ1/3 release. ALI cultures were stimulated simultaneously with 10μg/mL poly(I:C) and 100μM ATP on both apical and basolateral sides. Basolateral supernatant samples were collected 24 hrs later and measured for IFN-λ1/3. Data are mean ± SEM of n = 6-8 samples. *p<0.05, **p<0.01

GPCR agonists are incapable of inhibiting STING-mediated IFN release following mucociliary differentiation

Little is known about the cGAS-STING pathway in AECs following mucociliary differentiation. Lipofectamine did not enhance 2,3 cGAMP-mediated type 1 IFN release

in ALI cultures (Figure 7.9A) This indicates that ALI cultures are resistant to transfection by lipids. The cGAS ligand interferon stimulatory DNA (ISD) did not elicit IFN release in ALI cultures (data not shown). This is likely due to the inability of lipofectamine to transfect the dsDNA across the plasma membrane into the cytosol in AECs that have been differentiated. We tested the GPCR agonists for their ability to modulate STING-evoked IFN release following mucociliary differentiation. None of the agonists tested showed significant inhibitory ability on type 1 IFN release (Figure 7.9B-C). Altogether, these findings imply that while STING is functional in AECs following differentiation, the GPCR-mediated inhibitory effects disappear (Figure 5.5 vs. Figure 7.9).

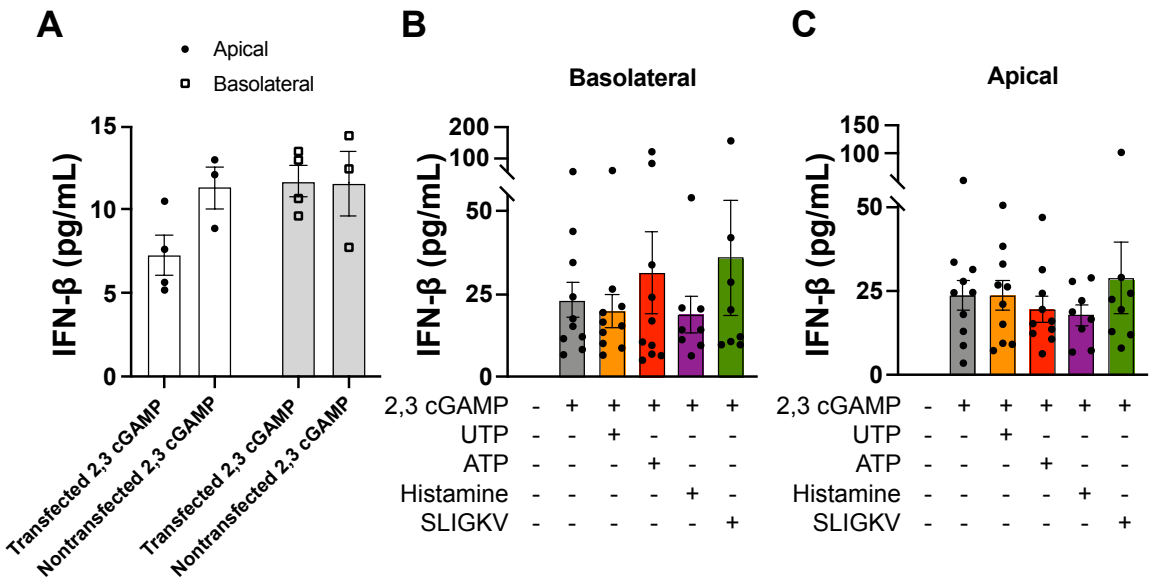

Figure 7.9 GPCR agonists are incapable of inhibiting STING-mediated IFN release following mucociliary differentiation. A-C) NHBEs were differentiated at the air-liquid interface (ALI) for 4 weeks and then stimulated with 40μg/mL 2,3 cGAMP +/- 100μM GPCR agonists on both apical and basolateral sides. StemCell Technologies ALI media was used for this experiment. **A)** Lipofectamine does not enhance 2,3 cGAMP-mediated

IFN-β release. Data are mean ± SEM of n = 3-4 samples. **B-C)** GPCR agonists do not inhibit 2,3 cGAMP-mediated IFN-β release. Basolateral IFN-β release (B) and apical IFN-β release (C) were measured via ELISA. Data are mean ± SEM of n = 8-10 samples.

Discussion

CRAC channel activity appears to be significantly diminished in AECs following mucociliary differentiation. This is demonstrated in the weak sustained Ca^{2+} entry following agonist stimulation (Figure 7.3) and the data demonstrating ATP-evoked PGE_2 synthesis is recalcitrant to CRAC channel inhibitors (Figure 7.1). However, this data is not conclusive that CRAC channel function is inherently decreased in differentiated cultures. It is possible that GPCR signaling itself is weaker in differentiated cultures and hence store depletion is not sufficient to elicit CRAC channel activation. It is also possible that ORAI1 and STIM1 possess polarized expression such that activation is only seen in particular stimulation contexts. However, available expression data suggests that upon ALI differentiation of submerged cultures, ORAI1 expression decreases while ORAI2 expression increases [238]. Bulk RNA-Seq data from Assel Biyasheva in the Schleimer lab corroborates these changes in ORAI1 and ORAI2 expression (data not shown). Hence, the most likely scenario is that as AECs differentiate, ORAI1 expression decreases and ORAI2 expression increases, radically restructuring the subunit composition of CRAC channels. It will be interesting future work to decipher what is the function of ORAI2 dominant CRAC channels in differentiated AECs.

One interesting discovery was the divergent effects of extracellular ATP in the

context of submerged, highly proliferative primary cell cultures versus an ALI culture that has undergone mucociliary differentiation. In the submerged cultures, ATP induced mild inhibition of IFN-β release regardless of concentration, yet high concentrations of ATP (100μM) potentiated IFN-λ1/3 release (Figure 5.3). However, in the ALI cultures, ATP and UTP showed identical pharmacological effects at 100μM (Figure 7.7). There are multiple potential explanations for this discrepancy. The first is that the purinergic receptor repertoire may change upon mucociliary differentiation, such that the ATP (or ATP metabolite) receptor driving the potentiation in the submerged cultures is lost upon differentiation. It is also possible that differentiation decreases expression of a downstream component of the signaling processes that is necessary for potentiation. An alternative explanation is that nucleotide metabolism may be altered by differentiation, leading to stronger activation of $P2Y_2$ receptors that override the other ATP (or ATP metabolite) receptors that seem to be driving the potentiation we have observed. Further investigation will be necessary to determine the mechanism responsible for this divergent effect and which response predominates in intact human airways.

In ALI differentiated primary cells, ATP, UTP, histamine, and SLIGKV all effectively inhibited the release of both type 1 and type 3 IFN to the basolateral compartment (Figure 7.7B, 7.6D). However, only nucleotides were able to inhibit the apical release of IFN-β while both histamine and the PAR2 activator SLIGKV were incompetent (Figure 7.7C). While many possible explanations exist, it is worth mentioning that this correlates well with the polarized localization of the respective receptors. $P2Y_2$ receptors are expressed on both apical and basolateral surfaces of differentiated cultures while both H_1 and PAR2 receptors typically reside exclusively on

basolateral surfaces [49, 67, 232-234]. However, recent data suggests that in the context of inflammation, such as after exposure to IL-13 or cigarette smoke, PAR2 can lose its restricted localization and gain access to the apical membrane [239]. Thus, in the context of chronic airway diseases where IL-13 is elevated or cigarette smoke is present, AEC PAR2 may gain the capacity to inhibit apical IFN-β release. It remains unclear whether a similar insult may induce the H_1 receptor to lose its polarized localization.

Chapter 8: Preclinical studies utilizing CM4620 in a murine HDM model of allergic disease

Introduction

CRAC channels are essential for proper immune responses [70, 74]. Specifically, both mast cells and T cells are known to heavily rely on CRAC channels for processes such as degranulation, cysteinyl leukotriene synthesis, IL-2 production and proliferation of T cells [70, 73, 74, 80, 82, 83]. Furthermore, *Orai1* knockdown in murine airways can protect against allergic rhinitis [240]. However, the role of CRAC channels in airway epithelial cell biology remains enigmatic. The airway epithelium regulates and orchestrates lung immune responses, especially in the context of asthma [3]. Recently, we have discovered that airway epithelial cells express CRAC channels [95, 97]. These CRAC channels are activated downstream of PAR2, HDM, Cockroach, and chitinase [95, 97]. They are responsible for the production of proinflammatory cytokines such as IL-6, IL-8, TNF-α, GM-CSF [95, 97]. However, the role of AEC CRAC channels in the development and chronic inflammation in asthma is unknown. To begin this investigation, we induced airway inflammation in C57BL/6 mice using HDM. We recently obtained CM4620, also known in our lab as CM-EX-128, a potent CRAC channel inhibitor currently in clinical trials for acute pancreatitis, courtesy of CalciMedica [241]. At the challenge phase of the protocol, mice were treated intranasally with either placebo or CM-EX-128 prior to HDM. We collected serum and BALf and performed Th2 cytokine arrays. Although the induction of these cytokines was modest, intranasal CM4620 abolished the cytokine induction both in the BALf and the serum. This data

provides further evidence that AEC CRAC channels may coordinate immune responses.

Results

We performed a standard house dust mite (HDM) sensitization protocol to model allergic airway disease in mice (Figure 8.1A-B). A few specific elements of the protocol are worth highlighting. First, only a small cohort of mice was used so the data is all very preliminary. Second, the CM4620 (also known as CM-EX-128) was a lipid emulsion and the placebo was that same lipid emulsion from CalciMedica. The volumes of placebo and CM4620 were limited to prevent excessive accumulation of liquid in the lungs. This protocol induced strong allergic inflammation in the airways as demonstrated by accumulation of eosinophils in the BALf (Figure 8.2), strong cellular infiltration (Figure 8.3), and mucin staining (Figure 8.3). However, CM4620 treatment did not influence any of these endpoints (data not shown). We measured cytokine and chemokine levels in either BALf or the serum via an array. Remarkably, CM4620 did reduce many cytokine and chemokines that were measured in both the BALf and the serum (Figure 8.4). This data is highly suggestive that intranasal CM4620 treatment may dampen cytokine and chemokine production in the airways. Altogether, more sustained treatment with CM4620 may be necessary to see more global decreases in inflammation as seen in BALf analysis and lung histology.

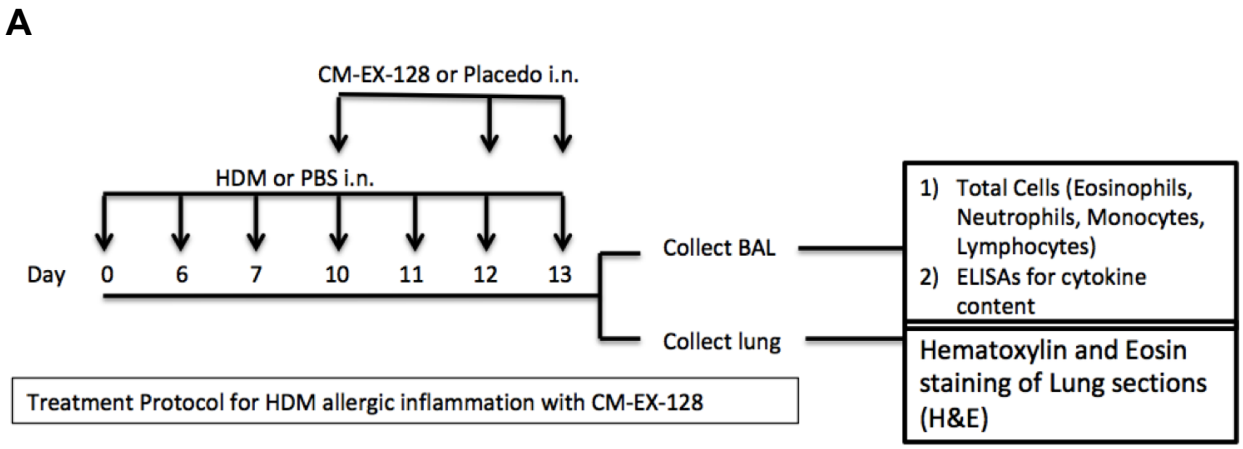

B

Day 0: HDM or Saline (50ul)
Day 6: HDM or Saline (50ul)
Day 7: HDM or Saline (50ul)
Day 10: CM-EX-128 or Placebo (50ul i.n.); CM-EX-128 i.p. (200ul)
Day 11: HDM or Saline (50ul)
Day 12: CM-EX-128 or Placebo (25ul i.n.), CM-EX-128 i.p. (200ul) at 9am; HDM or Saline (40ul) at 6pm
Day 13: CM-EX-128 or Placebo (25ul i.n.), CM-EX-128 i.p. (200ul) at 9am; HDM or Saline (40ul) at 5pm
Day 14: Harvest

Figure 8.1 HDM Protocol. A) Three month old C57BL/6 mice were treated intranasally (i.n.) with either house dust mite (HDM) or PBS. At later time points, mice were also treated with either CM-EX-128 (also known as CM4620) or placebo. **B)** Volumes and kinetics for the treatments are given. HDM was used at a concentration of 50 µg / 50 µl. CM-EX-128 was received from CalciMedica at a stock concentration of 1.6 mg/mL.

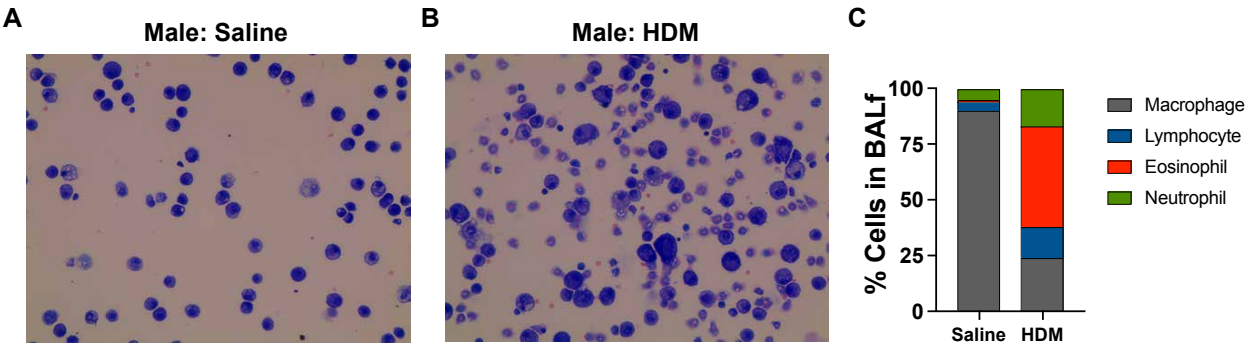

Figure 8.2 BALf Analysis. A-C) Bronchoalveolar lavage fluid (BALf) was collected on day 14 and cytospins were performed. Mice treated with HDM had a much greater percentage of Lymphocytes, Eosinophils and Neutrophils in the BALf than Saline treated mice.

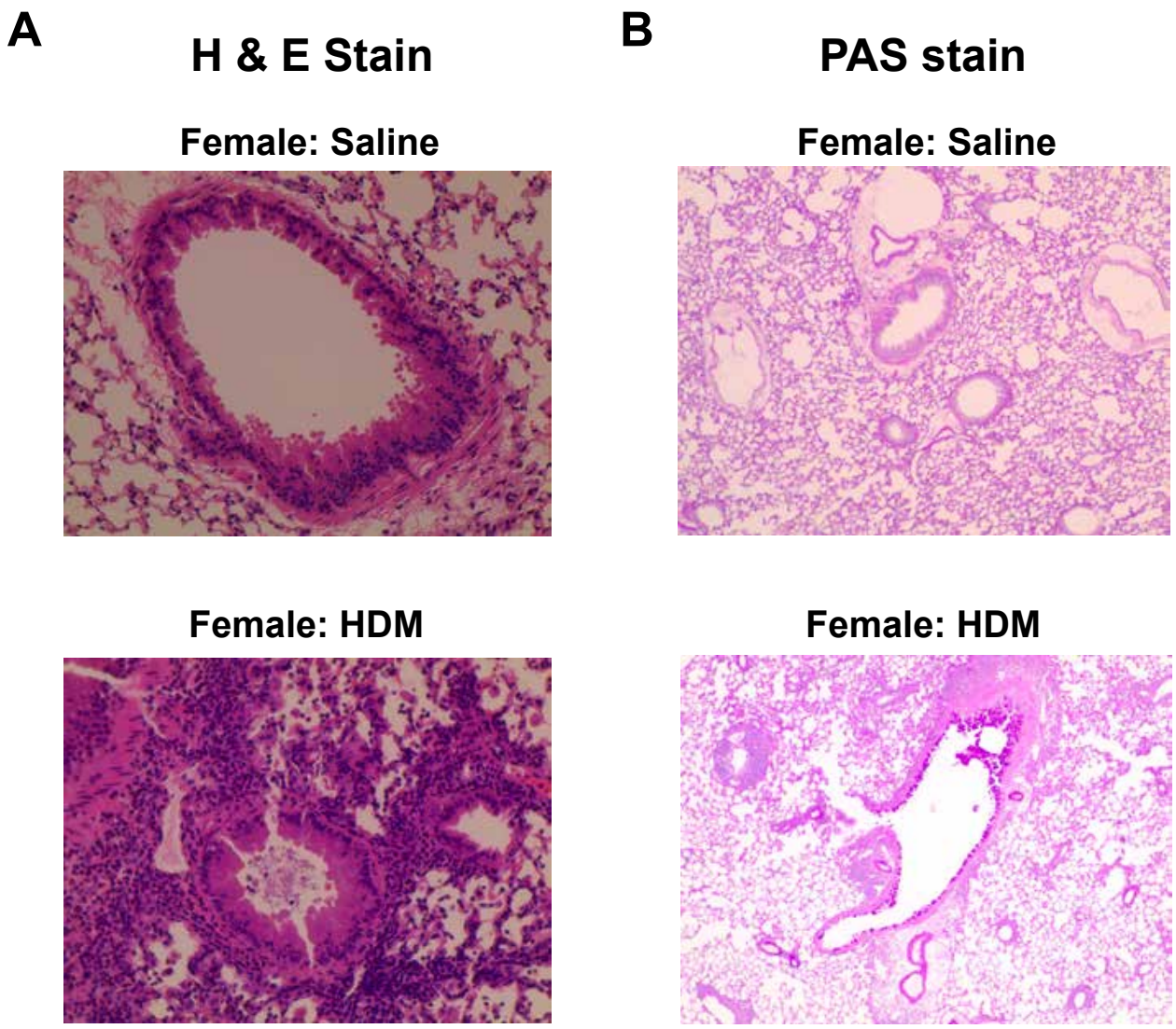

Figure 8.3 Histological Analysis. A-B) Lung sections were stained at the mouse phenotyping core with either H &E staining or PAS staining. HDM treated mice showed greater cellular infiltration via H & E and greater mucins via PAS.

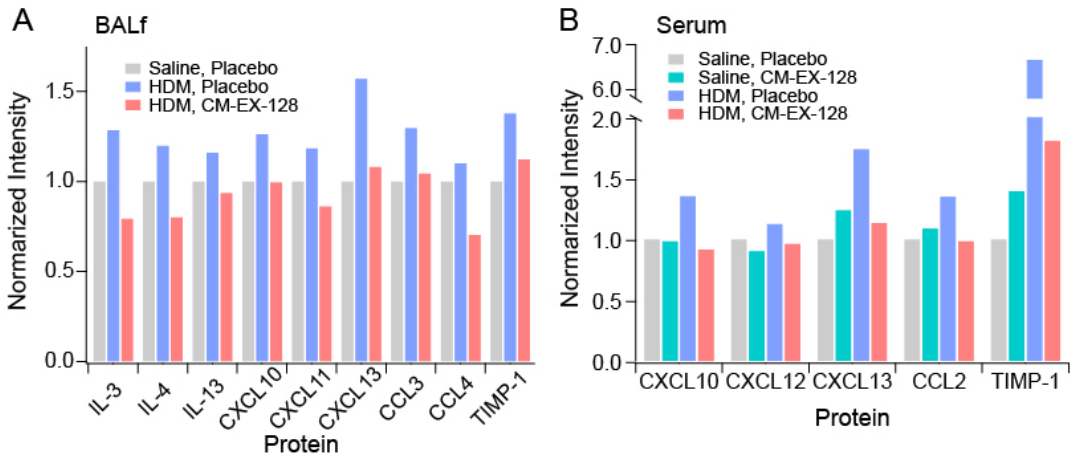

Figure 8.4 CM4620 reduces chemokine and cytokine expression. A) CM4620 (also known as CM-EX-128) reduced cytokine and chemokine expression in the BALf of male mice. Data are one mouse per group. **B)** CM4620 (also known as CM-EX-128) reduced cytokine and chemokine expression in the serum of female mice. Data are one mouse per group.

Discussion

Here we demonstrate that intranasal treatment of the novel ORAI1 inhibitor CM4620 reduces the chemokine and cytokine induction in a HDM model of allergic inflammation. However, we did not see marked differences in either BALf cellular analysis or lung histology. This may be due to the relatively brief treatment with CM4620. It should be noted that many reports have highlighted CRAC channel function is necessary for allergic asthma in murine models [73, 191-196, 240]. However, the advantage of our study was the local administration of the CRAC channel inhibitor while most of the previous studies introduced the pharmacological agent systemically. Since CRAC channel function is so essential to proper immune responses, we hypothesize that local inhibition of airway CRAC channels may allow systemic CRAC channel function to

persist, leading to a greater therapeutic index. Nonetheless, further studies are necessary to confirm this hypothesis.

Chapter 9: Conclusions and Future Directions

Within this thesis dissertation, we have thoroughly characterized the interaction between AEC purinergic signaling and CRAC channel function in the release of immunomodulatory mediators. These findings provide further novel targets for airway disease such as activation of $P2Y_2$ receptors to elicit production of PGE_2, inhibition of P2X and CRAC channels to block IL-6 secretion from AECs as well as inhibition of purinergic signaling to enhance IFN production.

It is worth noting that all of these studies were performed in cells derived from healthy adults from both sexes and multiple ethnic backgrounds. Increasingly, complexities driven by sex, disease state, ethnicity, and age are being linked to metabolic and airway epithelial function [242, 243]. Therefore, future studies to interrogate how AEC CRAC channel or IFN production varies dependent on these characteristics would be important advances for the field.

One further line of investigation involves cGAS-STING signaling in AECs. Our data suggests that STING is functional in AECs differentiated at the ALI (Figure 7.8). Recent data suggests that the endogenous STING agonist 2,3 cGAMP can be released and imported from cells via LRCC8 channels [244, 245]. It would be interesting to

interrogate if LRCC8 channels are functional in AECs differentiated at the ALI and allow for this transport of 2,3 cGAMP into the cells. Our preliminary data suggests that lipofectamine did not enhance type 1 IFN production suggesting active transport of 2,3 cGAMP across cell membranes. Another possible set of experiments would be to test if mice with *Sting* selectively knocked out in AECs exhibit phenotypes in models of respiratory virus infection. It may be that intranasal 2,3 cGAMP would prove to be a useful antiviral therapy.

Another interesting further line of experiments is whether inflammatory insults can restore SOCE function in ALI cultures. SOCE was markedly diminished in ALI cultures (Figure 7.2A) and decreased ORAI1 expression and increased ORAI2 expression has been reported in ALI cultures [238]. Bulk RNA-Seq data from Assel Biyasheva in the Schleimer lab corroborates these changes in ORAI1 and ORAI2 expression (data not shown). However, this is all indicative of the healthy, unperturbed state of ALI cultures. In a disease context, ORAI1 and ORAI2 expression may very well revert back to levels more closely resembling submerged NHBE cultures. When IL-13, IL-1β, and HDM were tested none of these inflammatory insults were capable of restoring SOCE in ALI cultures (Figure 7.2B). However, other inflammatory insults for longer treatment times may restore SOCE function in ALI cultures.

Numerous reports demonstrate that CRAC channel inhibition protects in models of allergic lung inflammation [73, 191, 193-196]. These studies administered the CRAC channel inhibitors in routes leading to systemic delivery. Therefore, the contribution of AEC CRAC channel inhibition to this disease protection remains uncertain. Indeed, we have recently shown that AEC CRAC channels cause GM-CSF production, a cytokine

essential for dendritic cell maturation and Th2 polarization [4, 95]. If deletion of AEC CRAC channels protects in murine models of asthma, this will provide further rationale for the use of CRAC channel inhibitors in asthma. A useful Cre line to induce this would be SPC-Cre, a line that we have recently generated in the lab [246]. Although it is worth mentioning that undesirable side effects have been noted in this Cre line [247]. Systemic inhibition of the CRAC channel is likely to cause unacceptable side effects such as global immunosuppression. Therefore, local delivery of CRAC channel inhibitors through an inhaler may prove a route with a greater therapeutic index. This route would also lead to more efficient inhibition of AEC CRAC channels. Thus, future studies that interrogate the role of AEC CRAC channels in allergic inflammation and whether local delivery of CRAC channel inhibitors may alleviate local inflammation while leaving host immunity intact are essential hypotheses to test.

Chapter 10: Materials and Methods

Cells, media and solutions: Normal human bronchial epithelial (NHBE) cells were purchased from Lonza (CC-2540) and were grown in bronchial epithelial growth media (BEGM, CC-3170). All experiments that used media for the stimulation phase utilized Lonza BEBM (CC-3171) media supplemented with Ca^{2+} to bring the total concentration up to 2mM. Cells were grown in 37°C and 5% CO_2. Ringers solutions were as follows: 2mM Ca^{2+} Ringers solution: 155mM NaCl, 4.5mM KCl, 10mM D-glucose, 5mM HEPES,

2mM $CaCl_2$, 1mM $MgCl_2$. 0mM Ca^{2+} Ringers solution: 155mM NaCl, 4.5mM KCl, 10mM D-glucose, 5mM HEPES, 1mM EGTA, 3mM $MgCl_2$.

Antibodies and Pharmacological Tools: Primary antibodies were as follows: COX-2 (CST 12282), β-actin (CST 3700), P-ERK (CST 4370), T-ERK (CST 9102), $cPLA_2$ (CST 2832), STIM1 (Feske Lab #3917), α-Tubulin (Abcam ab52866), P-STAT1 (CST 7649), β-actin (CST 3700), T-STAT1 (CST 9172), IRF1 (CST 8478), P-TBK1 (CST 5483), IRF3 (CST 11904), p65 (CST 8242), LaminA/C (CST 4777), T-TBK1 (Abcam ab40676). Pharmacological tools were as follows: UTP (Sigma U6875), SLIGKV-NH2 (Tocris 4153), FK-506 (Tocris 3631), BTP2 (Sigma 203890), ATP (Sigma A6419), Diclofenac (Tocris 4454), Apocynin (Tocris 4663), NAC (Sigma 106425), U0126 (Tocris 1144), ATPγS (Tocris 4080), AACOCF3 (Tocris 1462), AR-C 118925XX (Tocris 4890), NF546 (Tocris 3892), S3QEL 2 (Tocris 5735), ADPβS (Sigma A8016), UDP (Sigma U4125), NF157 (Tocris 2450), Apyrase (Sigma A6410 Grade VI, High ATPase/ADPase activity), TNP-ATP (Tocris 2464), 5-BDBD (Tocris 3579), A740003 (Tocris 3701), Suramin (ACROS Organics-Fisher AC328540500), PPADS (Tocris 0625), SLIGKV-NH2 (Tocris 4153), histamine (Tocris 3545), cetirizine (Tocris 2577), YM-254890 (Cayman Chemical 29735), Gö 6983 (Tocris 2285), PDBu (Tocris 4153), PMA (Tocris 1201), ruxolitinib (Tocris 7054), AG 1478 (Tocris 1276), IFN-β (R & D systems 8499-IF), EGF (R & D systems 236-EG), poly(I:C) (Invivogen tlrl-picw), 2,3 cGAMP (Invivogen tlrl-nacga23), ISD (Invivogen tlrl-isdn), 3p-hpRNA (Invivogen tlrl-hprna), CM4620 (also known as CM-EX-128) was a kind gift from CalciMedica.

siRNA or shRNA Knockdowns: On day 0, NHBE cells were plated onto 24 well plates in the morning in BEGM media lacking antibiotics. In the afternoon, cells were transfected

using RNAi Max and siRNA at final concentrations of 10nM. On day 1, cells were given fresh BEGM media lacking antibiotics and re-transfected using identical conditions as day 0. On day 2, cells were given fresh BEGM media lacking antibiotics and lacking hydrocortisone and retransfected using identical conditions as day 0. On day 3 (72 hrs after initial transfection), cells were either collected for analysis of protein levels, mRNA levels, or were stimulated with ATP for 2hrs for PGE_2 analysis according to the standard PGE_2 stimulation protocol (see PGE_2 measurement section). siRNA used included "siRNA Universal Negative Control #1" SICOO1 (Sigma) hereby termed "siCon", *siSTIM1*: SASI_Hs01_00107803 (Sigma), *siORAI1*: 4392420 assay ID s228396 (Thermofisher). On day 0, NHBE cells were thawed into T-25 flasks at approximately 25,000 cells/flask. On day 1, cells were infected with lentivirus harboring control or gene targeting sequences at MOI of 10. On day 2, fresh BEGM media was given to each flask. On day 3, puromycin was added to the culture media at a final dose of 4μg/ml and selection was allowed to occur for 3 days. Nontransduced cells were always handled in parallel to confirm puromycin's ability to induce selection. On day 6 or 7, cells were then plated for experiments and maintained in 1μg/ml puromycin until the time of stimulation when puromycin was removed from the culture media and cells were stimulated in BEBM without growth factors. Lentiviral particles expressing shRNA were purchased from Sigma: shCon (SHC202V), shTLR3_1 (TRCN0000056851), shTLR3_2 (TRCN0000358585), shP2RX4 (TRCN0000044962).

Intracellular Ca^{2+} measurements: NHBE cells were grown on poly-L-lysine coated glass-bottom dishes purchased from MatTek. Cells were loaded with 2μM Fura-2-AM (Thermofisher F1221) in BEGM with 5% FBS added to increase loading. Cells were

loaded for 40 min at room temperature in the dark. Cells were washed 3X with 2mM Ca^{2+} Ringers solution and then incubated for an additional 15 min in the dark before initiating Ca^{2+} imaging. Experiments were performed at room temperature. Dishes were mounted on the stage of an Olympus IX71 inverted microscope. Images were acquired every 6 seconds at excitation wavelengths of 340nm and 380nm and an emission wavelength of 510nm. Image acquisition and analysis were performed using SlideBook software. For data analysis, regions of interest were drawn around individual cells, background fluorescence was subtracted, and the F_{340}/F_{380} ratios were calculated for each timepoint. An increase in the ratio of F_{340}/F_{380} indicates a rise in $[Ca^{2+}]_i$. The F_{340}/F_{380} ratios were then converted to an estimate of $[Ca^{2+}]_i$ through the equation: $[Ca^{2+}]_i = \beta*K_d*(R-R_{min})/(R_{max}-R)$, where R is the F_{340}/F_{380} ratio and the values of β, $R_{min,}$ R_{max} were determined from an *in vitro* calibration with Fura-2 pentapotassium salt. β is determined from the F_{min}/F_{max} ratio at 380nm and K_d is the dissociation constant of Fura-2 binding to Ca^{2+} (135nM). The determined values were β= 23.152, R_{min}=0.2092, R_{max}=6.954.

ATP release assays: On day 0, NHBE cells were plated onto 24 well plates. On day 1, BEGM media was replaced with BEGM media lacking hydrocortisone. On day 2, media changes were performed and supernatants were collected at the indicated time points. ATP concentrations were quantified using Sigma Catalogue Number FLAA (FLAAM and FLAAB). Product FLAAM was diluted 25-fold with FLAAB prior to use. An ATP standard curve was used to determine absolute concentrations.

NFAT Dual Luciferase Assays: On day 0, BEAS-2B cells were plated onto 96 well plates (costar 3610) to allow analysis within plates. On day 1, cells were transfected

with 190 ng of NFAT plasmid and 10 ng of Renilla plasmid. Transfection allowed for 150 µl of media and 50 µl of optimum/lipofectamine/plasmid cocktail. On day 2, cells were stimulated in 2mM Ca^{2+} BEAS-2B media using the relevant compounds and Promega E1910 kits were used for analysis of luciferase levels. Data are displayed as firefly luciferase signal divided by renilla luciferase signal. Firefly luciferase is driven by the NFAT:AP-1 promoter sequence and renilla luciferase is driven by a thymidine kinase promoter.

NFAT4-GFP Nuclear Translocation Assays: On day 0, BEAS-2B cells were plated onto 3.5mM glass coverslips. On day 1, BEAS-2B cells were transfected with 200 ng/plate of NFAT4-GFP plasmid for 6 hours, then optimum/lipofectamine/plasmid cocktail was removed and fresh media was given to cells. Twenty four to forty eight hours later, experiments were performed. Images were taken of NFAT4-GFP localization prior to TG addition and 20 minutes following TG addition and analysis was done in a binary manner (either translocation did occur or translocation did not occur).

ALI PGE_2 stimulation experiments: NHBEs were differentiated using LifeLine ALI media (LM-0050). The day before stimulation, basolateral ALI media was replaced with 2 Ca BEBM media to remove hydrocortisone. Through my time working with ALI cultures, I transitioned to Promocell ALI media because it had better performed. The Promocell media also allows for the remove of hydrocortisone. See “Air-liquid interface (ALI) differentiation and stimulation” section for a fuller description of the Promocell ALI method. Washed apical side 2X prior to stimulation phase to remove excess mucus. All drugs were added to both apical and basolateral compartments and PGE_2 levels were measured independently for both compartments.

Fluo-4 ALI Ca^{2+} experiments: NHBEs were differentiated using LifeLine ALI media (LM-0050). The day before stimulation, basolateral ALI media was replaced with 2 Ca BEBM media to remove hydrocortisone. On the day of experiment, wash apical side 3X with 300 µl of 2 Ca BEBM. Load apical side only with 5 µM Fluo-4. Load for 1 hour at 37C. At time of loading, give fresh 2 Ca BEBM to basolateral side with DMSO, BTP2, or CM4620. Included DMOS, BTP2, or CM4620 in apical side. After loading wash apical side 2X with fresh 2 Ca BEBM. Remove the membrane with a 22-gauge syringe and forceps and gently place in 2 Ca Ringers (with DMSO, BTP2, 128) with apical side facing up. Imaged using confocal microscopy with a "harp" to hold the cells in position under the microscope.

MUC5AC experiments: Quantification of MUC5AC secretion is notoriously difficult. Thus, the methods from Dr. William Davis's group were followed closely [236]. NHBEs were differentiated using LifeLine ALI media (LM-0050). The day before stimulation, basolateral ALI media was replaced with 2 Ca BEBM media to remove hydrocortisone. On the day of experiment, wash apical side 5X with 300 µl of 2 Ca BEBM.

To analyze MUC5AC via ELISA, the follow method was performed.

1. Plated 100ul of sample diluted in PBS in 96 well plate (Costar 3590), incubate overnight at 4C on shaker
2. Wash 4X in PBST (0.1% tween) using 200ul
3. Block with 5% NFDM in PBST for 1hr at 37 C in the humidified chamber using 200ul
4. Incubate with 45M1 (Invitrogen MA5-12178) primary (dissolved 1:500 in 1% NFDM in PBST) using 100ul/well for 2hr at 37 C in humidified chamber
5. Wash 4X in PBST (0.1% tween) using 200ul
6. Incubate with anti-mouse biotinylated secondary (dissolved 1:1000 in PBST) using 100ul/well for 1hr at 37 C in humidified chamber
7. Wash 4X in PBST (0.1% tween) using 200ul
8. Incubate with streptavidin-HRP tertiary antibody (Thermofisher N100) (dissolved 1:1000 in PBST) using 100ul/well for 1hr at 37 C in humidified

chamber
9. Wash 4X in PBST (0.1% tween) using 200ul
10. Develop with 150ul/well OPD substrate (1mg/mL in 1X Stable Peroxide Substrate Buffer) for 10-15 min at RT in dark, stop reaction with 50ul/well of 4M H_2SO_4
11. Determine OD at 490nM

To measure MUC5AC via Dot Blot technique, the following protocol was followed:

1. Make grid on nitrocellulose membrane using pencil and pipette on indicated amounts of cell culture supernatant
2. Let membrane dry completely at RT (approx. 1 hr)
3. Block for 1hr at RT in 5% BSA dissolved in TBST
4. Incubate with primary antibody overnight at 4C (Used Thermofisher 45M1 MA5-12178 at 1:500 dilution)
5. Wash 3X with TBST 5-10min each
6. Incubate with secondary antibody for anti-mouse biotin labeling (same one using for MUC5AC ELISA, 1:1000) for 4hrs at 4C
7. Wash 3X with TBST 5-10min each
8.Incubate with tertiary antibody (HRP-Strept from LiCor, 1:5000) for 1hr at RT
9. Wash 3X with TBST 5-10min each
10. Image

HDM model of allergic inflammation: HDM was from Greer item number XPB70D3A25 and lot number 343205. It was used at a final concentration of 50 µg protein / 50 µl. 50 µl of either saline or HDM were given to each mouse. Stock HDM came as 37.40 mg protein/vial and is dissolved in sterile saline at a concentration of 500 µg / 50 µl (10X stock) and stored in glass vials from agilent technologies (5182-0714 and 5182-0717) in the -80C. Prior to administration, 450 µl of sterile saline was added to the HDM stock to adjust the concentration to the working concentration of 50 µg protein / 50 µl. CM-EX-128 (CM4620) was an emulsion solution at 1.6 mg/mL concentration. Histology was performed through the mouse phenotyping core facility. The cytokine and chemokine screen was conducted using R & D kit ARY006.

COX-2 and ERK1/2 activation assays: On day 0, NHBE cells were plated onto 24 well plates. On day 1, BEGM media was replaced with BEGM media lacking hydrocortisone. On day 2, cells were stimulated. If cells were pretreated with drugs, half of the BEGM media lacking hydrocortisone was taken off the cells, the drug was added to that media at 2X final concentration, vortexed, and added back to the relevant wells. Cells were activated for either 15min. (for ERK1/2 measurements) or 2 hr. to overnight (for COX-2 upregulation measurements) as indicated in the Figure legends. Following stimulation, cells were lysed using 1X Cell Signaling Lysis Buffer (9803S) containing protease and phosphatase inhibitors (PPIs) (Thermofisher 78440). Cell lysates were incubated on ice for 30 minutes and vortexed every 10 minutes. Samples were spun at 12,000rpm for 15min at 4°C and supernatants were collected and analyzed via western blotting.

Western Blots: Following stimulation, cells were lysed using 1X Cell Signaling Lysis Buffer (9803S) containing protease and phosphatase inhibitors (PPIs) (Thermofisher 78440). Lysates were boiled for 5 min in 1X Laemmli Sample Buffer (Bio-Rad 1610747) containing 2-ME. Samples were then subjected to SDS-PAGE. Transfer occurred at 4°C for 1.5 hrs and at 100V. PVDF membranes were used for the transfer. Following transfer, membranes were washed in TBST (0.1% Tween 20), blocked for 1 hr at RT using 5% BSA dissolved in TBST, then incubated overnight at 4°C with primary antibodies. All dilutions for primary antibodies were 1:1000 besides anti-β-actin: 1:2000, anti-phospho ERK1/2: 1:2000, anti-α-Tubulin: 1:5000. The following day, membranes were washed 3X for 5 min each using TBST and incubated with secondary antibodies for 1 hr at RT in 5% BSA dissolved in TBST. Li-Cor secondary antibodies were used (IRDye 800 CW or IRDye 680 RD) at dilutions of 1:10000. Membranes were washed 3X

for 5 min each using TBST and immediately imaged using an Odyssey CLx imaging system.

Nuclear and Cytosolic Fractionation assays: On day 0, NHBE cells were plated onto 6 well plates. On day 1, BEGM media was replaced with BEGM media lacking hydrocortisone. On day 2, cells were stimulated. If cells were pretreated with drugs, half of the BEGM media lacking hydrocortisone was taken off the cells, the drug was added to that media at 2X final concentration, vortexed, and added back to the relevant wells. This protocol was adapted from Chang et al. [80]. Cells were stimulated for 5 minutes in BEBM media lacking all growth factors. Media was immediately aspirated, cells were placed on ice, and cells were scrapped in hypotonic lysis buffer containing protease and phosphatase inhibitors (PPIs) (Thermofisher 78440) and collected into prechilled eppendorf tubes. Lysates from two wells were combined into one tube to ensure sufficient protein content. Samples were incubated on ice for 10min. Samples were then spun at 1,000rpm for 4min at 4°C. The supernatant was collected as the crude cytosolic fraction and the pellet was resuspended in hypertonic lysis buffer containing PPIs. Both the crude cytosolic fractions and the resuspended pellet were incubated on ice for another 30min, and periodically vortexed every 10min to ensure full lysis. Next, both crude cytosolic fraction samples and the resuspended pellet samples were centrifuged at 12,000rpm for 10min at 4°C and the supernatants were collected and termed “cytosolic fraction” and “nuclear fraction”. The hypotonic buffer consisted of: 10mM Hepes pH 7.9, 10mM KCl, 1.5mM $MgCl_2$, 0.5mM EDTA, PPIs added fresh. The hypertonic buffer consisted of: 20mM Hepes pH 7.9, 420mM NaCl, 1.5mM $MgCl_2$, 0.2mM EDTA, 25% glcyerol, PPIs added fresh.

PGE_2 measurements: On day 0, NHBE cells were plated onto 24 well plates. On day 1, BEGM media was replaced with BEGM media lacking hydrocortisone. On day 2, cells were stimulated. If cells were pretreated with drugs, half of the BEGM media lacking hydrocortisone was taken off the cells, the drug was added to that media at 2X final concentration, vortexed, and added back to the relevant wells. At the time of stimulation, media was removed and cells were stimulated for 2 hours in BEBM media lacking all growth factors. Following this stimulation phase, the supernatants were collected, spun at 300g for 4min to remove cellular debris, and the supernatant from this sample was then collected and stored at -80°C until the time of analysis. To perform analysis of PGE_2 levels, the Cayman Chemical kit (514010) was used and the manufacturers protocols were followed. All samples were diluted at least 10-fold in ELISA buffer prior to analysis. All samples that were compared statistically had the same concentration of organic solvents (such as DMSO and ethanol) as organic solvents can interfere with the assay.

IL-6 ELISAs: On day 0, NHBE cells were plated onto 24 well plates. On day 1, BEGM media was replaced with BEGM media lacking hydrocortisone. On day 2, cells were stimulated. If cells were pretreated with drugs, half of the BEGM media lacking hydrocortisone was taken off the cells, the drug was added to that media at 2X final concentration, vortexed, and added back to the relevant wells. At the time of stimulation, media was removed and cells were stimulated overnight (16hrs) in BEBM media lacking all growth factors. Following this stimulation phase, the supernatants were collected, spun at 300g for 4min to remove cellular debris, and the supernatant from this sample was then collected and stored at -80°C until the time of analysis. To perform analysis of

IL-6 levels, the RayBiotech Human IL-6 ELISA kit (ELH-IL6-1) was used and the manufacturers protocols were followed. All samples were diluted typically 5-fold in ELISA buffer prior to analysis. Samples that were compared statistically had the same concentration of organic solvents (DMSO).

Transfection of NHBEs: NHBEs were transfected with 2,3 cGAMP, ISD, or 3p-hpRNA using Lipofectamine 2000 (Thermofisher Scientific 11668019) at a constant volume of 2.5µl Lipofectamine/well of 24 well plate. Transfection cocktails were mixed containing ligand (2,3 cGAMP, ISD, 3p-hpRNA), Lipofectamine 2000, and Opti-MEM media (Thermofisher Scientific 31985062) and were gently vortexed and allowed to sit 10 minutes prior to transfecting NHBEs. Using 24 well plates, 50µl of transfection cocktail was added to 450µl of BEBM media (containing 2mM Ca^{2+}) to initiate transfection. Cells were incubated with transfection cocktail for the length of the experiment.

Influenza A virus infection of NHBEs: Influenza A virus strain A/WSN/33(H1N1) was used for all IAV experiments. NHBEs were plated onto 24 well plates and infected at MOI 0.1, 0.5 or 1.0 for 24 hours. Cells were washed with PBS prior to infection, 200µl of BEBM (containing 2mM Ca^{2+}) with IAV was added to the respective wells and cells were incubated on shaker (approximately 30 rpm) inside an incubator set to 37°C and 5% CO_2. Infection was allowed to occur for 1 hour then virus was aspirated and fresh BEBM (containing 2mM Ca^{2+}) was added to the respective wells. RV1B was purchased from ATCC (VR-1645) and was used at an MOI of 10 for all experiments. Cells were washed with PBS prior to infection, 200µl of BEBM (containing 2mM Ca^{2+}) with RV1B was added to the respective wells and cells were incubated on shaker (approximately 30 rpm) inside an incubator set to 33°C and 5% CO_2. Infection was allowed to occur for

2 hours then virus was aspirated and fresh BEBM (containing 2mM Ca^{2+}) was added to the respective wells. For treatments including UTP, ATP, or histamine, agonist (100μM) was added at the time of initial infection and fresh agonist was added following infection.

IFN ELISAs: On day 0, NHBE cells were plated onto 24 well or 48 well plates. On day 1, BEGM media was replaced with BEGM media lacking hydrocortisone. On day 2, cells were stimulated. If cells were pretreated with drugs, half of the BEGM media lacking hydrocortisone was taken off the cells, the drug was added to that media at 2X final concentration, vortexed, and added back to the relevant wells. At the time of stimulation, media was removed and cells were stimulated in BEBM media lacking all growth factors. Poly(I:C) and GPCR agonists were added simultaneously. Following this stimulation phase, the supernatants were collected and stored at -80°C until the time of analysis. To perform analysis of IFN-β levels, the PBL Assay Science kit (41435-1) was used and the manufacturers protocols were followed. To perform analysis of IFN-λ1/3 levels, the R & D systems kits (DY1598B and DY008) were used and the manufacturers protocols were followed. Samples that were compared statistically had the same concentration of organic solvents (DMSO).

Air-liquid interface (ALI) differentiation and stimulation: NHBEs were plated onto costar 3460 transwells (coated with 0.03 mg/mL collagen) at 110,000 cells/well in BEGM media on day 0. BEGM media was on both apical and basolateral sides from day 0 until day 2. On day 1, fresh BEGM media was given on both apical and basolateral sides. On day 2, the media was removed from the apical side and the basolateral side media was replaced with differentiation media. Two different differentiation medias were used in this thesis work. The first media was LifeLine ALI media (LM-0050) and the second was

from StemCell Technologies (05001) supplemented with hydrocortisone (07925) and heparin (07980) and Gibco gentamicin/amphotericin (R-015-10). The early studies were done using LifeLine ALI media as that was the media that the Berdnikovs lab uses. However, this media comes with hydrocortisone already dissolved in it. Hence, for the experiments done with this media, 24 hours prior to the experiment, differentiation media was replaced with 2mM Ca^{2+} BEBM media. Discussion with other labs about the ALI media they used led me to the StemCell Technologies media where the hydrocortisone was supplemented instead of predissolved. Overall, I noticed that the experiments done with the LifeLine media were stronger produces of cytokines and prostaglandins, but this is likely because they had the differentiation media replaced with 2mM Ca^{2+} BEBM media 24 hours prior to the experiment. I think the StemCell Technologies media is the preferred media choice. Regardless of which media was used, differentiation media was replaced Monday, Wednesday, and Friday and differentiated was allowed to occur for at least 28 days until experiments were performed. Once cells began releasing mucus around day 14, the apical surface was washed once weekly with PBS to remove excess mucus until the time of the experiment. On the day of the experiment, the apical side was washed 3X with 2mM Ca^{2+} BEBM media and cells were stimulated with all drugs on both the apical side (300µl) and the basolateral side (800µl). Two hours later, the apical side media was aspirated out to reestablish the air interface as long-term media on the apical side has been shown to cause de-differentiation [239]. At the time of collection, the apical side was washed with 2mM Ca^{2+} BEBM (250µl/well) and collected and the basolateral media

was collected as well. Supernatants were then used for downstream applications such as IFN analysis.

CellTox and CellTiter-Glo assays: CellTox Green Cytotoxicity Assay (G8741) and CellTiter-Glo 2.0 Assay (G9241) were purchased from Promega and manufacturers instructions were followed for experimentation. NHBEs were plated in 96 well plates (costar 3610) and infected with IAV at an MOI of 0.5 as described in the virus infection methods section. The sequential multiplexing protocol was followed such that both CellTox and CellTiter-Glo could be performed using the same plate of cells.

RT-qPCR analysis: Total RNA was extraction was performed using RNeasy Plus Mini Kit (Qiagen 74134). cDNA generation was performed using iScript Reverse Transcription Supermix for RT-qPCR (Biorad 1708841). qPCR was performed using PowerUp SYBR Green Master Mix (A25741). For qPCR, final concentration of primers was 500nM and cDNA was used at 6ng/well. Primer sequences used were as follows: *RPLP0* Forward 5' AGCCCAGAACACTGGTCTC 3', *RPLP0* Reverse 5' ACTCAGGATTTCAATGGTGCC 3', *IFN-B1* Forward 5' GAAACTGAAGATCTCCTAGCCT 3', *IFN-B1* Reverse 5' GCCATCAGTCACTTAAACAGC 3' (IDT Assay Name Hs.PT.58.39481063.g), TLR3 (IDT Assay Name Hs.PT.58.25887499.g), *ORAI1* Forward 5' GATGAGCCTCAACGAGCACT 3', *ORAI1* Reverse 5' ATTGCCACCATGGCGAAGC 3', *P2RY2* Forward 5' CCGCTTCAACGAGGACTTCAA 3', *P2RY2* Reverse 5' GCGGGCGTAGTAATAGACCA 3', *P2RX4* Forward 5' CTACCAGGAAACTGACTCCGT 3', *P2RX4* Reverse 5' GGTATCACATAATCCGCCACAT 3', HPRT1 Forward 5' ACCCTTTCCAAATCCTCAGC 3', *HPRT1* Reverse 5' GTTATGGCGACCCGCAG 3',

RPLP0 Forward 5' AGCCCAGAACACTGGTCTC 3', *RPLP0* Reverse 5' ACTCAGGATTTCAATGGTGCC 3', *PPIA* Forward 5' CCCACCGTGTTCTTCGACATT 3', *PPIA* Reverse 5' GGACCCGTATGCTTTAGGATGA 3', *P2RY11* Forward 5' GTAGCAGACACAGGCTGA 3', *P2RY11* Reverse 5' CCTGGAACCCACTGAGTTTG 3', *P2RX1* Forward 5' CGTTATCTTCCGACTGATCCAG 3', *P2RX1* Reverse 5' CACAGAGACACTGCTGATGAG 3', *P2RX2* Forward 5' GAGGTGTTCGGCTGGTG 3', *P2RX2* Reverse 5' GGTAGTGGATGCTGTTCTTGA 3', *P2RX3* Forward 5' CAACATCATCCCCACCATCA 3', *P2RX3* Reverse 5' CTCATTCACCTCCTCAAACTTCT 3', *P2RX5* Forward 5' GGAAGCAGCAGTCAGAAGG 3', *P2RX5* Reverse 5' AAAGGCATGGGATCACTGG 3', *P2RX6* Forward 5' TGGCCTCACTACTCCTTCC 3', *P2RX6* Reverse 5' ATGTCGAAGCGGATTCCATAG 3', *P2RX7* Forward 5' CCCTGTGTGTGGTCAACGAAT 3', *P2RX7* Reverse 5' TGCAGACTTCTCCCTAGTAGC 3'.

Data Analysis: All bar graphs summarizing data are represented as mean ± SEM. Individual points are always indicative of biological replicates. For a data set involving more than two groups, an initial one-way ANOVA was performed followed by Tukey's multiple comparison tests. For data sets with only two groups, a two-tailed unpaired Student t-test was performed. Dose-response curves were created using a four parameter (variable slope) nonlinear regression. Extra sum-of-squares F-Test used to statistically compare the PGE_2 and IL-6 dose-response curves. Statistical analysis and data analysis was performed using Prism 8 or 9 (GraphPad Software). *p<0.05, **p<0.01, ***p<0.001, ****p<0.0001 when statistical comparisons are made.

References:

1. Kaebisch, C., D. Schipper, P. Babczyk, and E. Tobiasch, *The role of purinergic receptors in stem cell differentiation.* Comput Struct Biotechnol J, 2015. **13**: p. 75-84.
2. Chapman, D.G., J.E. Tully, J.D. Nolin, Y.M. Janssen-Heininger, and C.G. Irvin, *Animal models of allergic airways disease: where are we and where to next?* J Cell Biochem, 2014. **115**(12): p. 2055-64.
3. Lambrecht, B.N. and H. Hammad, *The airway epithelium in asthma.* Nat Med, 2012. **18**(5): p. 684-92.
4. Lambrecht, B.N. and H. Hammad, *Allergens and the airway epithelium response: gateway to allergic sensitization.* J Allergy Clin Immunol, 2014. **134**(3): p. 499-507.
5. Lambrecht, B.N., H. Hammad, and J.V. Fahy, *The Cytokines of Asthma.* Immunity, 2019. **50**(4): p. 975-991.
6. Galli, S.J., M. Tsai, and A.M. Piliponsky, *The development of allergic inflammation.* Nature, 2008. **454**(7203): p. 445-54.
7. Hodinka, R.L., *Respiratory RNA Viruses.* Microbiol Spectr, 2016. **4**(4).
8. Monto, A.S. and K. Fukuda, *Lessons From Influenza Pandemics of the Last 100 Years.* Clin Infect Dis, 2020. **70**(5): p. 951-957.
9. Jacobs, S.E., D.M. Lamson, K. St George, and T.J. Walsh, *Human rhinoviruses.* Clin Microbiol Rev, 2013. **26**(1): p. 135-62.
10. Camelo, A., R. Dunmore, M.A. Sleeman, and D.L. Clarke, *The epithelium in idiopathic pulmonary fibrosis: breaking the barrier.* Front Pharmacol, 2014. **4**: p. 173.
11. Herold, S., C. Becker, K.M. Ridge, and G.R. Budinger, *Influenza virus-induced lung injury: pathogenesis and implications for treatment.* Eur Respir J, 2015. **45**(5): p. 1463-78.
12. Lazear, H.M., T.J. Nice, and M.S. Diamond, *Interferon-lambda: Immune Functions at Barrier Surfaces and Beyond.* Immunity, 2015. **43**(1): p. 15-28.
13. Kouzaki, H., K. Iijima, T. Kobayashi, S.M. O'Grady, and H. Kita, *The danger signal, extracellular ATP, is a sensor for an airborne allergen and triggers IL-33 release and innate Th2-type responses.* J Immunol, 2011. **186**(7): p. 4375-87.
14. Bustamante-Marin, X.M. and L.E. Ostrowski, *Cilia and Mucociliary Clearance.* Cold Spring Harb Perspect Biol, 2017. **9**(4).
15. Dvorak, A., A.E. Tilley, R. Shaykhiev, R. Wang, and R.G. Crystal, *Do airway epithelium air-liquid cultures represent the in vivo airway epithelium transcriptome?* Am J Respir Cell Mol Biol, 2011. **44**(4): p. 465-73.
16. Idzko, M., H. Hammad, M. van Nimwegen, M. Kool, M.A. Willart, F. Muskens, H.C. Hoogsteden, W. Luttmann, D. Ferrari, F. Di Virgilio, J.C. Virchow, Jr., and B.N. Lambrecht, *Extracellular ATP triggers and maintains asthmatic airway inflammation by activating dendritic cells.* Nat Med, 2007. **13**(8): p. 913-9.
17. Idzko, M., D. Ferrari, and H.K. Eltzschig, *Nucleotide signalling during inflammation.* Nature, 2014. **509**(7500): p. 310-7.
18. Zhang, F., X. Su, G. Huang, X.F. Xin, E.H. Cao, Y. Shi, and Y. Song, *Adenosine Triphosphate Promotes Allergen-Induced Airway Inflammation and Th17 Cell Polarization in Neutrophilic Asthma.* J Immunol Res, 2017. **2017**: p. 5358647.

19. Shah, D., F. Romero, W. Stafstrom, M. Duong, and R. Summer, *Extracellular ATP mediates the late phase of neutrophil recruitment to the lung in murine models of acute lung injury.* Am J Physiol Lung Cell Mol Physiol, 2014. **306**(2): p. L152-61.
20. Riteau, N., P. Gasse, L. Fauconnier, A. Gombault, M. Couegnat, L. Fick, J. Kanellopoulos, V.F. Quesniaux, S. Marchand-Adam, B. Crestani, B. Ryffel, and I. Couillin, *Extracellular ATP is a danger signal activating P2X7 receptor in lung inflammation and fibrosis.* Am J Respir Crit Care Med, 2010. **182**(6): p. 774-83.
21. Esther, C.R., Jr., N.E. Alexis, M.L. Clas, E.R. Lazarowski, S.H. Donaldson, C.M. Ribeiro, C.G. Moore, S.D. Davis, and R.C. Boucher, *Extracellular purines are biomarkers of neutrophilic airway inflammation.* Eur Respir J, 2008. **31**(5): p. 949-56.
22. Cicko, S., T.C. Kohler, C.K. Ayata, T. Muller, N. Ehrat, A. Meyer, M. Hossfeld, A. Zech, F. Di Virgilio, and M. Idzko, *Extracellular ATP is a danger signal activating P2X7 receptor in a LPS mediated inflammation (ARDS/ALI).* Oncotarget, 2018. **9**(55): p. 30635-30648.
23. Davis, C.W. and E. Lazarowski, *Coupling of airway ciliary activity and mucin secretion to mechanical stresses by purinergic signaling.* Respir Physiol Neurobiol, 2008. **163**(1-3): p. 208-13.
24. Button, B., S.F. Okada, C.B. Frederick, W.R. Thelin, and R.C. Boucher, *Mechanosensitive ATP release maintains proper mucus hydration of airways.* Sci Signal, 2013. **6**(279): p. ra46.
25. Hao, Y. and W.H. Ko, *Purinergic P2Y receptors in airway epithelia: from ion transport to immune functions.* Sheng Li Xue Bao, 2014. **66**(1): p. 16-22.
26. Morse, D.M., J.L. Smullen, and C.W. Davis, *Differential effects of UTP, ATP, and adenosine on ciliary activity of human nasal epithelial cells.* Am J Physiol Cell Physiol, 2001. **280**(6): p. C1485-97.
27. Zhang, L. and M.J. Sanderson, *Oscillations in ciliary beat frequency and intracellular calcium concentration in rabbit tracheal epithelial cells induced by ATP.* J Physiol, 2003. **546**(Pt 3): p. 733-49.
28. Lazarowski, E.R. and R.C. Boucher, *UTP as an extracellular signaling molecule.* News Physiol Sci, 2001. **16**: p. 1-5.
29. von Kugelgen, I., *Pharmacological profiles of cloned mammalian P2Y-receptor subtypes.* Pharmacol Ther, 2006. **110**(3): p. 415-32.
30. Burnstock, G., *P2X ion channel receptors and inflammation.* Purinergic Signal, 2016. **12**(1): p. 59-67.
31. North, R.A., *Molecular physiology of P2X receptors.* Physiol Rev, 2002. **82**(4): p. 1013-67.
32. Borea, P.A., S. Gessi, S. Merighi, F. Vincenzi, and K. Varani, *Pharmacology of Adenosine Receptors: The State of the Art.* Physiol Rev, 2018. **98**(3): p. 1591-1625.
33. Idzko, M., E. Panther, H.C. Bremer, S. Sorichter, W. Luttmann, C.J. Virchow, Jr., F. Di Virgilio, Y. Herouy, J. Norgauer, and D. Ferrari, *Stimulation of P2 purinergic receptors induces the release of eosinophil cationic protein and interleukin-8 from human eosinophils.* Br J Pharmacol, 2003. **138**(7): p. 1244-50.
34. Meis, S., A. Hamacher, D. Hongwiset, C. Marzian, M. Wiese, N. Eckstein, H.D. Royer, D. Communi, J.M. Boeynaems, R. Hausmann, G. Schmalzing, and M.U. Kassack, *NF546 [4,4'-(carbonylbis(imino-3,1-phenylene-carbonylimino-3,1-(4-methyl-phenylene)-car bonylimino))-bis(1,3-xylene-alpha,alpha'-diphosphonic acid) tetrasodium salt] is a*

non-nucleotide P2Y11 agonist and stimulates release of interleukin-8 from human monocyte-derived dendritic cells. J Pharmacol Exp Ther, 2010. **332**(1): p. 238-47.
35. Seo, D.R., S.Y. Kim, K.Y. Kim, H.G. Lee, J.H. Moon, J.S. Lee, S.H. Lee, S.U. Kim, and Y.B. Lee, *Cross talk between P2 purinergic receptors modulates extracellular ATP-mediated interleukin-10 production in rat microglial cells.* Exp Mol Med, 2008. **40**(1): p. 19-26.
36. Douillet, C.D., W.P. Robinson, 3rd, P.M. Milano, R.C. Boucher, and P.B. Rich, *Nucleotides induce IL-6 release from human airway epithelia via P2Y2 and p38 MAPK-dependent pathways.* Am J Physiol Lung Cell Mol Physiol, 2006. **291**(4): p. L734-46.
37. Lazarowski, E.R., J.I. Sesma, L. Seminario-Vidal, and S.M. Kreda, *Molecular mechanisms of purine and pyrimidine nucleotide release.* Adv Pharmacol, 2011. **61**: p. 221-61.
38. Okada, S.F., L. Zhang, S.M. Kreda, L.H. Abdullah, C.W. Davis, R.J. Pickles, E.R. Lazarowski, and R.C. Boucher, *Coupled nucleotide and mucin hypersecretion from goblet-cell metaplastic human airway epithelium.* Am J Respir Cell Mol Biol, 2011. **45**(2): p. 253-60.
39. Okada, S.F., C.M. Ribeiro, J.I. Sesma, L. Seminario-Vidal, L.H. Abdullah, C. van Heusden, E.R. Lazarowski, and R.C. Boucher, *Inflammation promotes airway epithelial ATP release via calcium-dependent vesicular pathways.* Am J Respir Cell Mol Biol, 2013. **49**(5): p. 814-20.
40. Kamiya, Y., T. Fujisawa, M. Katsumata, H. Yasui, Y. Suzuki, M. Karayama, H. Hozumi, K. Furuhashi, N. Enomoto, Y. Nakamura, N. Inui, M. Setou, M. Ito, T. Suzuki, K. Ikegami, and T. Suda, *Influenza A virus enhances ciliary activity and mucociliary clearance via TLR3 in airway epithelium.* Respir Res, 2020. **21**(1): p. 282.
41. Atkinson, S.K., A.H. Morice, and L.R. Sadofsky, *Rhinovirus-16 increases ATP release in A549 cells without concomitant increase in production.* ERJ Open Res, 2020. **6**(4).
42. Shishikura, Y., A. Koarai, H. Aizawa, M. Yamaya, H. Sugiura, M. Watanabe, Y. Hashimoto, T. Numakura, T. Makiguti, K. Abe, M. Yamada, T. Kikuchi, Y. Hoshikawa, Y. Okada, and M. Ichinose, *Extracellular ATP is involved in dsRNA-induced MUC5AC production via P2Y2R in human airway epithelium.* Respir Res, 2016. **17**(1): p. 121.
43. Button, B., M. Picher, and R.C. Boucher, *Differential effects of cyclic and constant stress on ATP release and mucociliary transport by human airway epithelia.* J Physiol, 2007. **580**(Pt. 2): p. 577-92.
44. Tatur, S., S. Kreda, E. Lazarowski, and R. Grygorczyk, *Calcium-dependent release of adenosine and uridine nucleotides from A549 cells.* Purinergic Signal, 2008. **4**(2): p. 139-46.
45. Tatur, S., N. Groulx, S.N. Orlov, and R. Grygorczyk, *Ca2+-dependent ATP release from A549 cells involves synergistic autocrine stimulation by coreleased uridine nucleotides.* J Physiol, 2007. **584**(Pt 2): p. 419-35.
46. Lazarowski, E.R., L. Homolya, R.C. Boucher, and T.K. Harden, *Direct demonstration of mechanically induced release of cellular UTP and its implication for uridine nucleotide receptor activation.* J Biol Chem, 1997. **272**(39): p. 24348-54.
47. Lazarowski, E.R. and T.K. Harden, *Quantitation of extracellular UTP using a sensitive enzymatic assay.* Br J Pharmacol, 1999. **127**(5): p. 1272-8.
48. Lazarowski, E.R. and R.C. Boucher, *Purinergic receptors in airway epithelia.* Curr Opin Pharmacol, 2009. **9**(3): p. 262-7.

49. Paradiso, A.M., S.J. Mason, E.R. Lazarowski, and R.C. Boucher, *Membrane-restricted regulation of Ca2+ release and influx in polarized epithelia.* Nature, 1995. **377**(6550): p. 643-6.
50. Homolya, L., T.H. Steinberg, and R.C. Boucher, *Cell to cell communication in response to mechanical stress via bilateral release of ATP and UTP in polarized epithelia.* J Cell Biol, 2000. **150**(6): p. 1349-60.
51. Kim, K.C., H.R. Park, C.Y. Shin, T. Akiyama, and K.H. Ko, *Nucleotide-induced mucin release from primary hamster tracheal surface epithelial cells involves the P2u purinoceptor.* Eur Respir J, 1996. **9**(3): p. 542-8.
52. Kim, K.C. and B.C. Lee, *P2 purinoceptor regulation of mucin release by airway goblet cells in primary culture.* Br J Pharmacol, 1991. **103**(1): p. 1053-6.
53. Kemp, P.A., R.A. Sugar, and A.D. Jackson, *Nucleotide-mediated mucin secretion from differentiated human bronchial epithelial cells.* Am J Respir Cell Mol Biol, 2004. **31**(4): p. 446-55.
54. Deterding, R.R., L.M. Lavange, J.M. Engels, D.W. Mathews, S.J. Coquillette, A.S. Brody, S.P. Millard, B.W. Ramsey, N. Cystic Fibrosis Therapeutics Development, and G. the Inspire 08-103 Working, *Phase 2 randomized safety and efficacy trial of nebulized denufosol tetrasodium in cystic fibrosis.* Am J Respir Crit Care Med, 2007. **176**(4): p. 362-9.
55. Ratjen, F., T. Durham, T. Navratil, A. Schaberg, F.J. Accurso, C. Wainwright, M. Barnes, R.B. Moss, and T.-S.I. Group, *Long term effects of denufosol tetrasodium in patients with cystic fibrosis.* J Cyst Fibros, 2012. **11**(6): p. 539-49.
56. Song, S., K.N. Jacobson, K.M. McDermott, S.P. Reddy, A.E. Cress, H. Tang, S.M. Dudek, S.M. Black, J.G. Garcia, A. Makino, and J.X. Yuan, *ATP promotes cell survival via regulation of cytosolic [Ca2+] and Bcl-2/Bax ratio in lung cancer cells.* Am J Physiol Cell Physiol, 2016. **310**(2): p. C99-114.
57. Zsembery, A., A.T. Boyce, L. Liang, J. Peti-Peterdi, P.D. Bell, and E.M. Schwiebert, *Sustained calcium entry through P2X nucleotide receptor channels in human airway epithelial cells.* J Biol Chem, 2003. **278**(15): p. 13398-408.
58. Ma, W., A. Korngreen, N. Uzlaner, Z. Priel, and S.D. Silberberg, *Extracellular sodium regulates airway ciliary motility by inhibiting a P2X receptor.* Nature, 1999. **400**(6747): p. 894-7.
59. Winkelmann, V.E., K.E. Thompson, K. Neuland, A.M. Jaramillo, G. Fois, H. Schmidt, O.H. Wittekindt, W. Han, M.J. Tuvim, B.F. Dickey, P. Dietl, and M. Frick, *Inflammation-induced upregulation of P2X4 expression augments mucin secretion in airway epithelia.* Am J Physiol Lung Cell Mol Physiol, 2019. **316**(1): p. L58-L70.
60. Ma, W., A. Korngreen, S. Weil, E.B. Cohen, A. Priel, L. Kuzin, and S.D. Silberberg, *Pore properties and pharmacological features of the P2X receptor channel in airway ciliated cells.* J Physiol, 2006. **571**(Pt 3): p. 503-17.
61. Theatre, E., V. Bours, and C. Oury, *A P2X ion channel-triggered NF-kappaB pathway enhances TNF-alpha-induced IL-8 expression in airway epithelial cells.* Am J Respir Cell Mol Biol, 2009. **41**(6): p. 705-13.
62. Zech, A., B. Wiesler, C.K. Ayata, T. Schlaich, T. Durk, M. Hossfeld, N. Ehrat, S. Cicko, and M. Idzko, *P2rx4 deficiency in mice alleviates allergen-induced airway inflammation.* Oncotarget, 2016. **7**(49): p. 80288-80297.

63. Akdis, C.A. and K. Blaser, *Histamine in the immune regulation of allergic inflammation.* J Allergy Clin Immunol, 2003. **112**(1): p. 15-22.
64. Noah, T.L., A.M. Paradiso, M.C. Madden, K.P. McKinnon, and R.B. Devlin, *The response of a human bronchial epithelial cell line to histamine: intracellular calcium changes and extracellular release of inflammatory mediators.* Am J Respir Cell Mol Biol, 1991. **5**(5): p. 484-92.
65. Muller, T., D. Myrtek, H. Bayer, S. Sorichter, K. Schneider, G. Zissel, J. Norgauer, and M. Idzko, *Functional characterization of histamine receptor subtypes in a human bronchial epithelial cell line.* Int J Mol Med, 2006. **18**(5): p. 925-31.
66. Rada, B., H.E. Boudreau, J.J. Park, and T.L. Leto, *Histamine stimulates hydrogen peroxide production by bronchial epithelial cells via histamine H1 receptor and dual oxidase.* Am J Respir Cell Mol Biol, 2014. **50**(1): p. 125-34.
67. Clarke, L.L., A.M. Paradiso, and R.C. Boucher, *Histamine-induced Cl- secretion in human nasal epithelium: responses of apical and basolateral membranes.* Am J Physiol, 1992. **263**(6 Pt 1): p. C1190-9.
68. Zabner, J., M. Winter, K.J. Excoffon, D. Stoltz, D. Ries, S. Shasby, and M. Shasby, *Histamine alters E-cadherin cell adhesion to increase human airway epithelial permeability.* J Appl Physiol (1985), 2003. **95**(1): p. 394-401.
69. Hogan, P.G., R.S. Lewis, and A. Rao, *Molecular basis of calcium signaling in lymphocytes: STIM and ORAI.* Annu Rev Immunol, 2010. **28**: p. 491-533.
70. Prakriya, M. and R.S. Lewis, *Store-Operated Calcium Channels.* Physiol Rev, 2015. **95**(4): p. 1383-436.
71. Ma, H.T. and M.A. Beaven, *Regulation of Ca2+ signaling with particular focus on mast cells.* Crit Rev Immunol, 2009. **29**(2): p. 155-86.
72. McNally, B.A., A. Somasundaram, M. Yamashita, and M. Prakriya, *Gated regulation of CRAC channel ion selectivity by STIM1.* Nature, 2012. **482**(7384): p. 241-5.
73. Kaur, M., M.A. Birrell, B. Dekkak, S. Reynolds, S. Wong, J. De Alba, K. Raemdonck, S. Hall, K. Simpson, M. Begg, M.G. Belvisi, and D. Singh, *The role of CRAC channel in asthma.* Pulm Pharmacol Ther, 2015. **35**: p. 67-74.
74. Feske, S., Y. Gwack, M. Prakriya, S. Srikanth, S.H. Puppel, B. Tanasa, P.G. Hogan, R.S. Lewis, M. Daly, and A. Rao, *A mutation in Orai1 causes immune deficiency by abrogating CRAC channel function.* Nature, 2006. **441**(7090): p. 179-85.
75. McCarl, C.A., C. Picard, S. Khalil, T. Kawasaki, J. Rother, A. Papolos, J. Kutok, C. Hivroz, F. Ledeist, K. Plogmann, S. Ehl, G. Notheis, M.H. Albert, B.H. Belohradsky, J. Kirschner, A. Rao, A. Fischer, and S. Feske, *ORAI1 deficiency and lack of store-operated Ca2+ entry cause immunodeficiency, myopathy, and ectodermal dysplasia.* J Allergy Clin Immunol, 2009. **124**(6): p. 1311-1318 e7.
76. Eckstein, M., M. Vaeth, F.J. Aulestia, V. Costiniti, S.N. Kassam, T.G. Bromage, P. Pedersen, T. Issekutz, Y. Idaghdour, A.M. Moursi, S. Feske, and R.S. Lacruz, *Differential regulation of Ca(2+) influx by ORAI channels mediates enamel mineralization.* Sci Signal, 2019. **12**(578).
77. Picard, C., C.A. McCarl, A. Papolos, S. Khalil, K. Luthy, C. Hivroz, F. LeDeist, F. Rieux-Laucat, G. Rechavi, A. Rao, A. Fischer, and S. Feske, *STIM1 mutation associated with a syndrome of immunodeficiency and autoimmunity.* N Engl J Med, 2009. **360**(19): p. 1971-80.

78. Kaufmann, U., S. Kahlfuss, J. Yang, E. Ivanova, S.B. Koralov, and S. Feske, *Calcium Signaling Controls Pathogenic Th17 Cell-Mediated Inflammation by Regulating Mitochondrial Function.* Cell Metab, 2019. **29**(5): p. 1104-1118 e6.
79. Clemens, R.A., J. Chong, D. Grimes, Y. Hu, and C.A. Lowell, *STIM1 and STIM2 cooperatively regulate mouse neutrophil store-operated calcium entry and cytokine production.* Blood, 2017. **130**(13): p. 1565-1577.
80. Chang, W.C., C. Nelson, and A.B. Parekh, *Ca2+ influx through CRAC channels activates cytosolic phospholipase A2, leukotriene C4 secretion, and expression of c-fos through ERK-dependent and -independent pathways in mast cells.* FASEB J, 2006. **20**(13): p. 2381-3.
81. Chang, W.C., J. Di Capite, K. Singaravelu, C. Nelson, V. Halse, and A.B. Parekh, *Local Ca2+ influx through Ca2+ release-activated Ca2+ (CRAC) channels stimulates production of an intracellular messenger and an intercellular pro-inflammatory signal.* J Biol Chem, 2008. **283**(8): p. 4622-31.
82. Baba, Y., K. Nishida, Y. Fujii, T. Hirano, M. Hikida, and T. Kurosaki, *Essential function for the calcium sensor STIM1 in mast cell activation and anaphylactic responses.* Nat Immunol, 2008. **9**(1): p. 81-8.
83. Vig, M., W.I. DeHaven, G.S. Bird, J.M. Billingsley, H. Wang, P.E. Rao, A.B. Hutchings, M.H. Jouvin, J.W. Putney, and J.P. Kinet, *Defective mast cell effector functions in mice lacking the CRACM1 pore subunit of store-operated calcium release-activated calcium channels.* Nat Immunol, 2008. **9**(1): p. 89-96.
84. Toth, A.B., K. Hori, M.M. Novakovic, N.G. Bernstein, L. Lambot, and M. Prakriya, *CRAC channels regulate astrocyte Ca(2+) signaling and gliotransmitter release to modulate hippocampal GABAergic transmission.* Sci Signal, 2019. **12**(582).
85. Maneshi, M.M., A.B. Toth, T. Ishii, K. Hori, S. Tsujikawa, A.K. Shum, N. Shrestha, M. Yamashita, R.J. Miller, J. Radulovic, G.T. Swanson, and M. Prakriya, *Orai1 Channels Are Essential for Amplification of Glutamate-Evoked Ca(2+) Signals in Dendritic Spines to Regulate Working and Associative Memory.* Cell Rep, 2020. **33**(9): p. 108464.
86. Gao, X., J. Xia, F.M. Munoz, M.T. Manners, R. Pan, O. Meucci, Y. Dai, and H. Hu, *STIMs and Orai1 regulate cytokine production in spinal astrocytes.* J Neuroinflammation, 2016. **13**(1): p. 126.
87. Liu, H., A. Kabrah, M. Ahuja, and S. Muallem, *CRAC channels in secretory epithelial cell function and disease.* Cell Calcium, 2018. **78**: p. 48-55.
88. Xing, J., J.G. Petranka, F.M. Davis, P.N. Desai, J.W. Putney, and G.S. Bird, *Role of Orai1 and store-operated calcium entry in mouse lacrimal gland signalling and function.* J Physiol, 2014. **592**(5): p. 927-39.
89. Ahuja, M., D.M. Schwartz, M. Tandon, A. Son, M. Zeng, W. Swaim, M. Eckhaus, V. Hoffman, Y. Cui, B. Xiao, P.F. Worley, and S. Muallem, *Orai1-Mediated Antimicrobial Secretion from Pancreatic Acini Shapes the Gut Microbiome and Regulates Gut Innate Immunity.* Cell Metab, 2017. **25**(3): p. 635-646.
90. Concepcion, A.R., M. Vaeth, L.E. Wagner, 2nd, M. Eckstein, L. Hecht, J. Yang, D. Crottes, M. Seidl, H.P. Shin, C. Weidinger, S. Cameron, S.E. Turvey, T. Issekutz, I. Meyts, R.S. Lacruz, M. Cuk, D.I. Yule, and S. Feske, *Store-operated Ca2+ entry regulates Ca2+-activated chloride channels and eccrine sweat gland function.* J Clin Invest, 2016. **126**(11): p. 4303-4318.

91. Kreda, S.M., S.F. Okada, C.A. van Heusden, W. O'Neal, S. Gabriel, L. Abdullah, C.W. Davis, R.C. Boucher, and E.R. Lazarowski, *Coordinated release of nucleotides and mucin from human airway epithelial Calu-3 cells.* J Physiol, 2007. **584**(Pt 1): p. 245-59.
92. Kreda, S.M., L. Seminario-Vidal, C.A. van Heusden, W. O'Neal, L. Jones, R.C. Boucher, and E.R. Lazarowski, *Receptor-promoted exocytosis of airway epithelial mucin granules containing a spectrum of adenine nucleotides.* J Physiol, 2010. **588**(Pt 12): p. 2255-67.
93. Kawao, N., M. Nagataki, K. Nagasawa, S. Kubo, K. Cushing, T. Wada, F. Sekiguchi, S. Ichida, M.D. Hollenberg, W.K. MacNaughton, H. Nishikawa, and A. Kawabata, *Signal transduction for proteinase-activated receptor-2-triggered prostaglandin E2 formation in human lung epithelial cells.* J Pharmacol Exp Ther, 2005. **315**(2): p. 576-89.
94. Lazarowski, E.R., R.C. Boucher, and T.K. Harden, *Calcium-dependent release of arachidonic acid in response to purinergic receptor activation in airway epithelium.* Am J Physiol, 1994. **266**(2 Pt 1): p. C406-15.
95. Jairaman, A., M. Yamashita, R.P. Schleimer, and M. Prakriya, *Store-Operated Ca2+ Release-Activated Ca2+ Channels Regulate PAR2-Activated Ca2+ Signaling and Cytokine Production in Airway Epithelial Cells.* J Immunol, 2015. **195**(5): p. 2122-33.
96. Samanta, K., D. Bakowski, and A.B. Parekh, *Key role for store-operated Ca2+ channels in activating gene expression in human airway bronchial epithelial cells.* PLoS One, 2014. **9**(8): p. e105586.
97. Jairaman, A., C.H. Maguire, R.P. Schleimer, and M. Prakriya, *Allergens stimulate store-operated calcium entry and cytokine production in airway epithelial cells.* Sci Rep, 2016. **6**: p. 32311.
98. Leslie, C.C., *Properties and regulation of cytosolic phospholipase A2.* J Biol Chem, 1997. **272**(27): p. 16709-12.
99. Saunders, M.A., M.G. Belvisi, G. Cirino, P.J. Barnes, T.D. Warner, and J.A. Mitchell, *Mechanisms of prostaglandin E2 release by intact cells expressing cyclooxygenase-2: evidence for a 'two-component' model.* J Pharmacol Exp Ther, 1999. **288**(3): p. 1101-6.
100. Tokumoto, H., J.D. Croxtall, and R.J. Flower, *Differential role of extra- and intracellular calcium in bradykinin and interleukin 1 alpha stimulation of arachidonic acid release from A549 cells.* Biochim Biophys Acta, 1994. **1211**(3): p. 301-9.
101. Safholm, J., M.L. Manson, J. Bood, I. Delin, A.C. Orre, P. Bergman, M. Al-Ameri, S.E. Dahlen, and M. Adner, *Prostaglandin E2 inhibits mast cell-dependent bronchoconstriction in human small airways through the E prostanoid subtype 2 receptor.* J Allergy Clin Immunol, 2015. **136**(5): p. 1232-9 e1.
102. FitzPatrick, M., C. Donovan, and J.E. Bourke, *Prostaglandin E2 elicits greater bronchodilation than salbutamol in mouse intrapulmonary airways in lung slices.* Pulm Pharmacol Ther, 2014. **28**(1): p. 68-76.
103. Oppenheimer-Marks, N., A.F. Kavanaugh, and P.E. Lipsky, *Inhibition of the transendothelial migration of human T lymphocytes by prostaglandin E2.* J Immunol, 1994. **152**(12): p. 5703-13.
104. Maric, J., A. Ravindran, L. Mazzurana, A.K. Bjorklund, A. Van Acker, A. Rao, D. Friberg, S.E. Dahlen, A. Heinemann, V. Konya, and J. Mjosberg, *Prostaglandin E2 suppresses*

human group 2 innate lymphoid cell function. J Allergy Clin Immunol, 2018. **141**(5): p. 1761-1773 e6.
105. Schmidt, L.M., M.G. Belvisi, K.A. Bode, J. Bauer, C. Schmidt, M.T. Suchy, D. Tsikas, J. Scheuerer, F. Lasitschka, H.J. Grone, and A.H. Dalpke, *Bronchial epithelial cell-derived prostaglandin E2 dampens the reactivity of dendritic cells.* J Immunol, 2011. **186**(4): p. 2095-105.
106. Zhang, S., Y. Liu, X. Zhang, D. Zhu, X. Qi, X. Cao, Y. Fang, Y. Che, Z.C. Han, Z.X. He, Z. Han, and Z. Li, *Prostaglandin E2 hydrogel improves cutaneous wound healing via M2 macrophages polarization.* Theranostics, 2018. **8**(19): p. 5348-5361.
107. Loynes, C.A., J.A. Lee, A.L. Robertson, M.J. Steel, F. Ellett, Y. Feng, B.D. Levy, M.K.B. Whyte, and S.A. Renshaw, *PGE2 production at sites of tissue injury promotes an anti-inflammatory neutrophil phenotype and determines the outcome of inflammation resolution in vivo.* Sci Adv, 2018. **4**(9): p. eaar8320.
108. Vancheri, C., C. Mastruzzo, M.A. Sortino, and N. Crimi, *The lung as a privileged site for the beneficial actions of PGE2.* Trends Immunol, 2004. **25**(1): p. 40-6.
109. Simmons, D.L., R.M. Botting, and T. Hla, *Cyclooxygenase isozymes: the biology of prostaglandin synthesis and inhibition.* Pharmacol Rev, 2004. **56**(3): p. 387-437.
110. Murakami, M., Y. Nakatani, T. Tanioka, and I. Kudo, *Prostaglandin E synthase.* Prostaglandins Other Lipid Mediat, 2002. **68-69**: p. 383-99.
111. O'Banion, M.K., *Prostaglandin E2 synthases in neurologic homeostasis and disease.* Prostaglandins Other Lipid Mediat, 2010. **91**(3-4): p. 113-7.
112. Park, J.Y., M.H. Pillinger, and S.B. Abramson, *Prostaglandin E2 synthesis and secretion: the role of PGE2 synthases.* Clin Immunol, 2006. **119**(3): p. 229-40.
113. Lin, L.L., M. Wartmann, A.Y. Lin, J.L. Knopf, A. Seth, and R.J. Davis, *cPLA2 is phosphorylated and activated by MAP kinase.* Cell, 1993. **72**(2): p. 269-78.
114. Bonser, L.R. and D.J. Erle, *Airway Mucus and Asthma: The Role of MUC5AC and MUC5B.* J Clin Med, 2017. **6**(12).
115. Davis, C.W. and B.F. Dickey, *Regulated airway goblet cell mucin secretion.* Annu Rev Physiol, 2008. **70**: p. 487-512.
116. Martin, C., J. Frija-Masson, and P.R. Burgel, *Targeting mucus hypersecretion: new therapeutic opportunities for COPD?* Drugs, 2014. **74**(10): p. 1073-89.
117. Adler, K.B., M.J. Tuvim, and B.F. Dickey, *Regulated mucin secretion from airway epithelial cells.* Front Endocrinol (Lausanne), 2013. **4**: p. 129.
118. Chen, Y., Y.H. Zhao, and R. Wu, *Differential regulation of airway mucin gene expression and mucin secretion by extracellular nucleotide triphosphates.* Am J Respir Cell Mol Biol, 2001. **25**(4): p. 409-17.
119. Zhou, J., J.M. Perelman, V.P. Kolosov, and X. Zhou, *Neutrophil elastase induces MUC5AC secretion via protease-activated receptor 2.* Mol Cell Biochem, 2013. **377**(1-2): p. 75-85.
120. Takeyama, K., K. Dabbagh, H.M. Lee, C. Agusti, J.A. Lausier, I.F. Ueki, K.M. Grattan, and J.A. Nadel, *Epidermal growth factor system regulates mucin production in airways.* Proc Natl Acad Sci U S A, 1999. **96**(6): p. 3081-6.
121. Rincon, M. and C.G. Irvin, *Role of IL-6 in asthma and other inflammatory pulmonary diseases.* Int J Biol Sci, 2012. **8**(9): p. 1281-90.
122. Ullah, M.A., J.A. Revez, Z. Loh, J. Simpson, V. Zhang, L. Bain, A. Varelias, S. Rose-John, A. Blumenthal, M.J. Smyth, G.R. Hill, M.B. Sukkar, M.A. Ferreira, and S. Phipps,

Allergen-induced IL-6 trans-signaling activates gammadelta T cells to promote type 2 and type 17 airway inflammation. J Allergy Clin Immunol, 2015. **136**(4): p. 1065-73.
123. Doganci, A., K. Sauer, R. Karwot, and S. Finotto, *Pathological role of IL-6 in the experimental allergic bronchial asthma in mice.* Clin Rev Allergy Immunol, 2005. **28**(3): p. 257-70.
124. Jevnikar, Z., J. Ostling, E. Ax, J. Calven, K. Thorn, E. Israelsson, L. Oberg, A. Singhania, L.C.K. Lau, S.J. Wilson, J.A. Ward, A. Chauhan, A.R. Sousa, B. De Meulder, M.J. Loza, F. Baribaud, P.J. Sterk, K.F. Chung, K. Sun, Y. Guo, I.M. Adcock, D. Payne, B. Dahlen, P. Chanez, D.E. Shaw, N. Krug, J.M. Hohlfeld, T. Sandstrom, R. Djukanovic, A. James, T.S.C. Hinks, P.H. Howarth, O. Vaarala, M. van Geest, H. Olsson, and g. Unbiased Biomarkers in Prediction of Respiratory Disease Outcomes study, *Epithelial IL-6 trans-signaling defines a new asthma phenotype with increased airway inflammation.* J Allergy Clin Immunol, 2019. **143**(2): p. 577-590.
125. McFadyen, J.D., H. Stevens, and K. Peter, *The Emerging Threat of (Micro)Thrombosis in COVID-19 and Its Therapeutic Implications.* Circ Res, 2020. **127**(4): p. 571-587.
126. Neveu, W.A., J.B. Allard, O. Dienz, M.J. Wargo, G. Ciliberto, L.A. Whittaker, and M. Rincon, *IL-6 is required for airway mucus production induced by inhaled fungal allergens.* J Immunol, 2009. **183**(3): p. 1732-8.
127. Zhang, C., Z. Wu, J.W. Li, H. Zhao, and G.Q. Wang, *Cytokine release syndrome in severe COVID-19: interleukin-6 receptor antagonist tocilizumab may be the key to reduce mortality.* Int J Antimicrob Agents, 2020. **55**(5): p. 105954.
128. Levy, D.E., I.J. Marie, and J.E. Durbin, *Induction and function of type I and III interferon in response to viral infection.* Curr Opin Virol, 2011. **1**(6): p. 476-86.
129. Isaacs, A. and J. Lindenmann, *Virus interference. I. The interferon.* Proc R Soc Lond B Biol Sci, 1957. **147**(927): p. 258-67.
130. Ioannidis, I., F. Ye, B. McNally, M. Willette, and E. Flano, *Toll-like receptor expression and induction of type I and type III interferons in primary airway epithelial cells.* J Virol, 2013. **87**(6): p. 3261-70.
131. Meager, A., K. Visvalingam, P. Dilger, D. Bryan, and M. Wadhwa, *Biological activity of interleukins-28 and -29: comparison with type I interferons.* Cytokine, 2005. **31**(2): p. 109-18.
132. Williams, D.W., L.C. Askew, E. Jones, and J.E. Clements, *CCR2 Signaling Selectively Regulates IFN-alpha: Role of beta-Arrestin 2 in IFNAR1 Internalization.* J Immunol, 2019. **202**(1): p. 105-118.
133. Shin, A., T. Toy, S. Rothenfusser, N. Robson, J. Vorac, M. Dauer, M. Stuplich, S. Endres, J. Cebon, E. Maraskovsky, and M. Schnurr, *P2Y receptor signaling regulates phenotype and IFN-alpha secretion of human plasmacytoid dendritic cells.* Blood, 2008. **111**(6): p. 3062-9.
134. Mazzoni, A., C.A. Leifer, G.E. Mullen, M.N. Kennedy, D.M. Klinman, and D.M. Segal, *Cutting edge: histamine inhibits IFN-alpha release from plasmacytoid dendritic cells.* J Immunol, 2003. **170**(5): p. 2269-73.
135. Kalinowski, A., B.T. Galen, I.F. Ueki, Y. Sun, A. Mulenos, A. Osafo-Addo, B. Clark, J. Joerns, W. Liu, J.A. Nadel, C.S. Dela Cruz, and J.L. Koff, *Respiratory syncytial virus activates epidermal growth factor receptor to suppress interferon regulatory factor 1-dependent interferon-lambda and antiviral defense in airway epithelium.* Mucosal Immunol, 2018. **11**(3): p. 958-967.

136. Ueki, I.F., G. Min-Oo, A. Kalinowski, E. Ballon-Landa, L.L. Lanier, J.A. Nadel, and J.L. Koff, *Respiratory virus-induced EGFR activation suppresses IRF1-dependent interferon lambda and antiviral defense in airway epithelium.* J Exp Med, 2013. **210**(10): p. 1929-36.
137. Contoli, M., K. Ito, A. Padovani, D. Poletti, B. Marku, M.R. Edwards, L.A. Stanciu, G. Gnesini, A. Pastore, A. Spanevello, P. Morelli, S.L. Johnston, G. Caramori, and A. Papi, *Th2 cytokines impair innate immune responses to rhinovirus in respiratory epithelial cells.* Allergy, 2015. **70**(8): p. 910-20.
138. Moriwaki, A., K. Matsumoto, Y. Matsunaga, S. Fukuyama, T. Matsumoto, K. Kan-o, N. Noda, Y. Asai, Y. Nakanishi, and H. Inoue, *IL-13 suppresses double-stranded RNA-induced IFN-lambda production in lung cells.* Biochem Biophys Res Commun, 2011. **404**(4): p. 922-7.
139. Niwa, M., T. Fujisawa, K. Mori, K. Yamanaka, H. Yasui, Y. Suzuki, M. Karayama, H. Hozumi, K. Furuhashi, N. Enomoto, Y. Nakamura, N. Inui, T. Suzuki, M. Maekawa, and T. Suda, *IL-17A Attenuates IFN-lambda Expression by Inducing Suppressor of Cytokine Signaling Expression in Airway Epithelium.* J Immunol, 2018. **201**(8): p. 2392-2402.
140. Bauer, C.M., S.J. Dewitte-Orr, K.R. Hornby, C.C. Zavitz, B.D. Lichty, M.R. Stampfli, and K.L. Mossman, *Cigarette smoke suppresses type I interferon-mediated antiviral immunity in lung fibroblast and epithelial cells.* J Interferon Cytokine Res, 2008. **28**(3): p. 167-79.
141. Eddleston, J., R.U. Lee, A.M. Doerner, J. Herschbach, and B.L. Zuraw, *Cigarette smoke decreases innate responses of epithelial cells to rhinovirus infection.* Am J Respir Cell Mol Biol, 2011. **44**(1): p. 118-26.
142. Zhu, L., B. Lee, F. Zhao, X. Zhou, V. Chin, S.C. Ling, and Y. Chen, *Modulation of airway epithelial antiviral immunity by fungal exposure.* Am J Respir Cell Mol Biol, 2014. **50**(6): p. 1136-43.
143. Homma, T., A. Kato, B. Bhushan, J.E. Norton, L.A. Suh, R.G. Carter, D.S. Gupta, and R.P. Schleimer, *Role of Aspergillus fumigatus in Triggering Protease-Activated Receptor-2 in Airway Epithelial Cells and Skewing the Cells toward a T-helper 2 Bias.* Am J Respir Cell Mol Biol, 2016. **54**(1): p. 60-70.
144. Akbarshahi, H., M. Menzel, S. Ramu, I. Mahmutovic Persson, L. Bjermer, and L. Uller, *House dust mite impairs antiviral response in asthma exacerbation models through its effects on TLR3.* Allergy, 2018. **73**(5): p. 1053-1063.
145. Bhushan, B., T. Homma, J.E. Norton, Q. Sha, J. Siebert, D.S. Gupta, J.W. Schroeder, Jr., and R.P. Schleimer, *Suppression of epithelial signal transducer and activator of transcription 1 activation by extracts of Aspergillus fumigatus.* Am J Respir Cell Mol Biol, 2015. **53**(1): p. 87-95.
146. Nhu, Q.M., K. Shirey, J.R. Teijaro, D.L. Farber, S. Netzel-Arnett, T.M. Antalis, A. Fasano, and S.N. Vogel, *Novel signaling interactions between proteinase-activated receptor 2 and Toll-like receptors in vitro and in vivo.* Mucosal Immunol, 2010. **3**(1): p. 29-39.
147. Jartti, T., K. Bonnelykke, V. Elenius, and W. Feleszko, *Role of viruses in asthma.* Semin Immunopathol, 2020. **42**(1): p. 61-74.
148. Michi, A.N., M.E. Love, and D. Proud, *Rhinovirus-Induced Modulation of Epithelial Phenotype: Role in Asthma.* Viruses, 2020. **12**(11).
149. Contoli, M., S.D. Message, V. Laza-Stanca, M.R. Edwards, P.A. Wark, N.W. Bartlett, T. Kebadze, P. Mallia, L.A. Stanciu, H.L. Parker, L. Slater, A. Lewis-Antes, O.M. Kon, S.T.

Holgate, D.E. Davies, S.V. Kotenko, A. Papi, and S.L. Johnston, *Role of deficient type III interferon-lambda production in asthma exacerbations.* Nat Med, 2006. **12**(9): p. 1023-6.
150. Busse, W.W., R.F. Lemanske, Jr., and J.E. Gern, *Role of viral respiratory infections in asthma and asthma exacerbations.* Lancet, 2010. **376**(9743): p. 826-34.
151. Corne, J.M., C. Marshall, S. Smith, J. Schreiber, G. Sanderson, S.T. Holgate, and S.L. Johnston, *Frequency, severity, and duration of rhinovirus infections in asthmatic and non-asthmatic individuals: a longitudinal cohort study.* Lancet, 2002. **359**(9309): p. 831-4.
152. Zhu, J., S.D. Message, P. Mallia, T. Kebadze, M. Contoli, C.K. Ward, E.S. Barnathan, M.A. Mascelli, O.M. Kon, A. Papi, L.A. Stanciu, M.R. Edwards, P.K. Jeffery, and S.L. Johnston, *Bronchial mucosal IFN-alpha/beta and pattern recognition receptor expression in patients with experimental rhinovirus-induced asthma exacerbations.* J Allergy Clin Immunol, 2019. **143**(1): p. 114-125 e4.
153. Baraldo, S., M. Contoli, E. Bazzan, G. Turato, A. Padovani, B. Marku, F. Calabrese, G. Caramori, A. Ballarin, D. Snijders, A. Barbato, M. Saetta, and A. Papi, *Deficient antiviral immune responses in childhood: distinct roles of atopy and asthma.* J Allergy Clin Immunol, 2012. **130**(6): p. 1307-14.
154. Gielen, V., A. Sykes, J. Zhu, B. Chan, J. Macintyre, N. Regamey, E. Kieninger, A. Gupta, A. Shoemark, C. Bossley, J. Davies, S. Saglani, P. Walker, S.E. Nicholson, A.H. Dalpke, O.M. Kon, A. Bush, S.L. Johnston, and M.R. Edwards, *Increased nuclear suppressor of cytokine signaling 1 in asthmatic bronchial epithelium suppresses rhinovirus induction of innate interferons.* J Allergy Clin Immunol, 2015. **136**(1): p. 177-188 e11.
155. Wark, P.A., S.L. Johnston, F. Bucchieri, R. Powell, S. Puddicombe, V. Laza-Stanca, S.T. Holgate, and D.E. Davies, *Asthmatic bronchial epithelial cells have a deficient innate immune response to infection with rhinovirus.* J Exp Med, 2005. **201**(6): p. 937-47.
156. Garcia-Valero, J., J. Olloquequi, J.F. Montes, E. Rodriguez, M. Martin-Satue, L. Texido, and J. Ferrer Sancho, *Deficient pulmonary IFN-beta expression in COPD patients.* PLoS One, 2019. **14**(6): p. e0217803.
157. Singanayagam, A., S.L. Loo, M. Calderazzo, L.J. Finney, M.B. Trujillo Torralbo, E. Bakhsoliani, J. Girkin, P. Veerati, P.S. Pathinayake, K.S. Nichol, A. Reid, J. Footitt, P.A.B. Wark, C.L. Grainge, S.L. Johnston, N.W. Bartlett, and P. Mallia, *Antiviral immunity is impaired in COPD patients with frequent exacerbations.* Am J Physiol Lung Cell Mol Physiol, 2019. **317**(6): p. L893-L903.
158. Patel, D.A., Y. You, G. Huang, D.E. Byers, H.J. Kim, E. Agapov, M.L. Moore, R.S. Peebles, Jr., M. Castro, K. Sumino, A. Shifren, S.L. Brody, and M.J. Holtzman, *Interferon response and respiratory virus control are preserved in bronchial epithelial cells in asthma.* J Allergy Clin Immunol, 2014. **134**(6): p. 1402-1412 e7.
159. Hogan, P.G. and A. Rao, *Store-operated calcium entry: Mechanisms and modulation.* Biochem Biophys Res Commun, 2015. **460**(1): p. 40-9.
160. von Kugelgen, I. and K. Hoffmann, *Pharmacology and structure of P2Y receptors.* Neuropharmacology, 2016. **104**: p. 50-61.
161. Bahra, P., J. Mesher, S. Li, C.T. Poll, and H. Danahay, *P2Y2-receptor-mediated activation of a contralateral, lanthanide-sensitive calcium entry pathway in the human airway epithelium.* Br J Pharmacol, 2004. **143**(1): p. 91-8.

162. Kountz, T.S., A. Jairaman, C.D. Kountz, K.A. Stauderman, R.P. Schleimer, and M. Prakriya, *Differential Regulation of ATP- and UTP-Evoked Prostaglandin E2 and IL-6 Production from Human Airway Epithelial Cells.* J Immunol, 2021.
163. Djuric, S.W., N.Y. BaMaung, A. Basha, H. Liu, J.R. Luly, D.J. Madar, R.J. Sciotti, N.P. Tu, F.L. Wagenaar, P.E. Wiedeman, X. Zhou, S. Ballaron, J. Bauch, Y.W. Chen, X.G. Chiou, T. Fey, D. Gauvin, E. Gubbins, G.C. Hsieh, K.C. Marsh, K.W. Mollison, M. Pong, T.K. Shaughnessy, M.P. Sheets, M. Smith, J.M. Trevillyan, U. Warrior, C.D. Wegner, and G.W. Carter, *3,5-Bis(trifluoromethyl)pyrazoles: a novel class of NFAT transcription factor regulator.* J Med Chem, 2000. **43**(16): p. 2975-81.
164. Zitt, C., B. Strauss, E.C. Schwarz, N. Spaeth, G. Rast, A. Hatzelmann, and M. Hoth, *Potent inhibition of Ca2+ release-activated Ca2+ channels and T-lymphocyte activation by the pyrazole derivative BTP2.* J Biol Chem, 2004. **279**(13): p. 12427-37.
165. Trevillyan, J.M., X.G. Chiou, Y.W. Chen, S.J. Ballaron, M.P. Sheets, M.L. Smith, P.E. Wiedeman, U. Warrior, J. Wilkins, E.J. Gubbins, G.D. Gagne, J. Fagerland, G.W. Carter, J.R. Luly, K.W. Mollison, and S.W. Djuric, *Potent inhibition of NFAT activation and T cell cytokine production by novel low molecular weight pyrazole compounds.* J Biol Chem, 2001. **276**(51): p. 48118-26.
166. Vaeth, M., J. Yang, M. Yamashita, I. Zee, M. Eckstein, C. Knosp, U. Kaufmann, P. Karoly Jani, R.S. Lacruz, V. Flockerzi, I. Kacskovics, M. Prakriya, and S. Feske, *ORAI2 modulates store-operated calcium entry and T cell-mediated immunity.* Nat Commun, 2017. **8**: p. 14714.
167. Bootman, M.D., *Calcium signaling.* Cold Spring Harb Perspect Biol, 2012. **4**(7): p. a011171.
168. Choudhury, Q.G., D.T. McKay, R.J. Flower, and J.D. Croxtall, *Investigation into the involvement of phospholipases A(2) and MAP kinases in modulation of AA release and cell growth in A549 cells.* Br J Pharmacol, 2000. **131**(2): p. 255-65.
169. Lin, C.C., I.T. Lee, W.L. Wu, W.N. Lin, and C.M. Yang, *Adenosine triphosphate regulates NADPH oxidase activity leading to hydrogen peroxide production and COX-2/PGE2 expression in A549 cells.* Am J Physiol Lung Cell Mol Physiol, 2012. **303**(5): p. L401-12.
170. Kosmidou, I., T. Vassilakopoulos, A. Xagorari, S. Zakynthinos, A. Papapetropoulos, and C. Roussos, *Production of interleukin-6 by skeletal myotubes: role of reactive oxygen species.* Am J Respir Cell Mol Biol, 2002. **26**(5): p. 587-93.
171. Chang, W.C. and A.B. Parekh, *Close functional coupling between Ca2+ release-activated Ca2+ channels, arachidonic acid release, and leukotriene C4 secretion.* J Biol Chem, 2004. **279**(29): p. 29994-9.
172. Somasundaram, A., A.K. Shum, H.J. McBride, J.A. Kessler, S. Feske, R.J. Miller, and M. Prakriya, *Store-operated CRAC channels regulate gene expression and proliferation in neural progenitor cells.* J Neurosci, 2014. **34**(27): p. 9107-23.
173. Neher, E., *Vesicle pools and Ca2+ microdomains: new tools for understanding their roles in neurotransmitter release.* Neuron, 1998. **20**(3): p. 389-99.
174. Friday, B.B. and A.A. Adjei, *Advances in targeting the Ras/Raf/MEK/Erk mitogen-activated protein kinase cascade with MEK inhibitors for cancer therapy.* Clin Cancer Res, 2008. **14**(2): p. 342-6.
175. Glasauer, A. and N.S. Chandel, *Ros.* Curr Biol, 2013. **23**(3): p. R100-2.

176. Orr, A.L., L. Vargas, C.N. Turk, J.E. Baaten, J.T. Matzen, V.J. Dardov, S.J. Attle, J. Li, D.C. Quackenbush, R.L. Goncalves, I.V. Perevoshchikova, H.M. Petrassi, S.L. Meeusen, E.K. Ainscow, and M.D. Brand, *Suppressors of superoxide production from mitochondrial complex III.* Nat Chem Biol, 2015. **11**(11): p. 834-6.
177. Evans, J.H., D.M. Spencer, A. Zweifach, and C.C. Leslie, *Intracellular calcium signals regulating cytosolic phospholipase A2 translocation to internal membranes.* J Biol Chem, 2001. **276**(32): p. 30150-60.
178. Toth, A.B., K. Hori, M.M. Novakovic, N.G. Bernstein, L. Lambot, and M. Prakriya, *CRAC channels regulate astrocyte Ca2+ signaling and gliotransmitter release to modulate hippocampal GABAergic transmission.* Sci Signal, 2019. **12 eaaw5450**: p. 1-15.
179. Soberanes, S., A.V. Misharin, A. Jairaman, L. Morales-Nebreda, A.C. McQuattie-Pimentel, T. Cho, R.B. Hamanaka, A.Y. Meliton, P.A. Reyfman, J.M. Walter, C.I. Chen, M. Chi, S. Chiu, F.J. Gonzalez-Gonzalez, M. Antalek, H. Abdala-Valencia, S.E. Chiarella, K.A. Sun, P.S. Woods, A.J. Ghio, M. Jain, H. Perlman, K.M. Ridge, R.I. Morimoto, J.I. Sznajder, W.E. Balch, S.M. Bhorade, A. Bharat, M. Prakriya, N.S. Chandel, G.M. Mutlu, and G.R.S. Budinger, *Metformin Targets Mitochondrial Electron Transport to Reduce Air-Pollution-Induced Thrombosis.* Cell Metab, 2019. **29**(2): p. 335-347 e5.
180. Sena, L.A., S. Li, A. Jairaman, M. Prakriya, T. Ezponda, D.A. Hildeman, C.R. Wang, P.T. Schumacker, J.D. Licht, H. Perlman, P.J. Bryce, and N.S. Chandel, *Mitochondria are required for antigen-specific T cell activation through reactive oxygen species signaling.* Immunity, 2013. **38**(2): p. 225-36.
181. Dolmetsch, R.E., K. Xu, and R.S. Lewis, *Calcium oscillations increase the efficiency and specificity of gene expression.* Nature, 1998. **392**(6679): p. 933-6.
182. Mattila, P.S., K.S. Ullman, S. Fiering, E.A. Emmel, M. McCutcheon, G.R. Crabtree, and L.A. Herzenberg, *The actions of cyclosporin A and FK506 suggest a novel step in the activation of T lymphocytes.* EMBO J, 1990. **9**(13): p. 4425-33.
183. Macian, F., C. Lopez-Rodriguez, and A. Rao, *Partners in transcription: NFAT and AP-1.* Oncogene, 2001. **20**(19): p. 2476-89.
184. la Sala, A., D. Ferrari, F. Di Virgilio, M. Idzko, J. Norgauer, and G. Girolomoni, *Alerting and tuning the immune response by extracellular nucleotides.* J Leukoc Biol, 2003. **73**(3): p. 339-43.
185. Chung, K.F., *Evaluation of selective prostaglandin E2 (PGE2) receptor agonists as therapeutic agents for the treatment of asthma.* Sci STKE, 2005. **2005**(303): p. pe47.
186. Lommatzsch, M., S. Cicko, T. Muller, M. Lucattelli, K. Bratke, P. Stoll, M. Grimm, T. Durk, G. Zissel, D. Ferrari, F. Di Virgilio, S. Sorichter, G. Lungarella, J.C. Virchow, and M. Idzko, *Extracellular adenosine triphosphate and chronic obstructive pulmonary disease.* Am J Respir Crit Care Med, 2010. **181**(9): p. 928-34.
187. Anderson, C.M. and F.E. Parkinson, *Potential signalling roles for UTP and UDP: sources, regulation and release of uracil nucleotides.* Trends Pharmacol Sci, 1997. **18**(10): p. 387-92.
188. Elliott, M.R., F.B. Chekeni, P.C. Trampont, E.R. Lazarowski, A. Kadl, S.F. Walk, D. Park, R.I. Woodson, M. Ostankovich, P. Sharma, J.J. Lysiak, T.K. Harden, N. Leitinger, and K.S. Ravichandran, *Nucleotides released by apoptotic cells act as a find-me signal to promote phagocytic clearance.* Nature, 2009. **461**(7261): p. 282-6.
189. Diercks, B.P., R. Werner, P. Weidemuller, F. Czarniak, L. Hernandez, C. Lehmann, A. Rosche, A. Kruger, U. Kaufmann, M. Vaeth, A.V. Failla, B. Zobiak, F.I. Kandil, D.

Schetelig, A. Ruthenbeck, C. Meier, D. Lodygin, A. Flugel, D. Ren, I.M.A. Wolf, S. Feske, and A.H. Guse, *ORAI1, STIM1/2, and RYR1 shape subsecond Ca(2+) microdomains upon T cell activation.* Sci Signal, 2018. **11**(561).

190. Michelucci, A., M. Garcia-Castaneda, S. Boncompagni, and R.T. Dirksen, *Role of STIM1/ORAI1-mediated store-operated Ca(2+) entry in skeletal muscle physiology and disease.* Cell Calcium, 2018. **76**: p. 101-115.
191. Esteve, C., J. Gonzalez, S. Gual, L. Vidal, S. Alzina, S. Sentellas, I. Jover, R. Horrillo, J. De Alba, M. Miralpeix, G. Tarrason, and B. Vidal, *Discovery of 7-azaindole derivatives as potent Orai inhibitors showing efficacy in a preclinical model of asthma.* Bioorg Med Chem Lett, 2015. **25**(6): p. 1217-22.
192. Ohga, K., R. Takezawa, T. Yoshino, T. Yamada, Y. Shimizu, and J. Ishikawa, *The suppressive effects of YM-58483/BTP-2, a store-operated Ca2+ entry blocker, on inflammatory mediator release in vitro and airway responses in vivo.* Pulm Pharmacol Ther, 2008. **21**(2): p. 360-9.
193. Yoshino, T., J. Ishikawa, K. Ohga, T. Morokata, R. Takezawa, H. Morio, Y. Okada, K. Honda, and T. Yamada, *YM-58483, a selective CRAC channel inhibitor, prevents antigen-induced airway eosinophilia and late phase asthmatic responses via Th2 cytokine inhibition in animal models.* Eur J Pharmacol, 2007. **560**(2-3): p. 225-33.
194. Sutovska, M., M. Kocmalova, M. Joskova, M. Adamkov, and S. Franova, *The effect of long-term administered CRAC channels blocker on the functions of respiratory epithelium in guinea pig allergic asthma model.* Gen Physiol Biophys, 2015. **34**(2): p. 167-76.
195. Sutovska, M., M. Kocmalova, M. Adamkov, D. Vybohova, P. Mikolka, D. Mokra, J. Hatok, M. Antosova, and S. Franova, *The long-term administration of Orai 1 antagonist possesses antitussive, bronchodilatory and anti-inflammatory effects in experimental asthma model.* Gen Physiol Biophys, 2013. **32**(2): p. 251-9.
196. Sutovska, M., M. Kocmalova, S. Franova, S. Vakkalanka, and S. Viswanadha, *Pharmacodynamic evaluation of RP3128, a novel and potent CRAC channel inhibitor in guinea pig models of allergic asthma.* Eur J Pharmacol, 2016. **772**: p. 62-70.
197. Miller, J., C. Bruen, M. Schnaus, J. Zhang, S. Ali, A. Lind, Z. Stoecker, K. Stauderman, and S. Hebbar, *Auxora versus standard of care for the treatment of severe or critical COVID-19 pneumonia: results from a randomized controlled trial.* Crit Care, 2020. **24**(1): p. 502.
198. Xing, J., A. Zhang, H. Zhang, J. Wang, X.C. Li, M.S. Zeng, and Z. Zhang, *TRIM29 promotes DNA virus infections by inhibiting innate immune response.* Nat Commun, 2017. **8**(1): p. 945.
199. Ishikawa, H. and G.N. Barber, *STING is an endoplasmic reticulum adaptor that facilitates innate immune signalling.* Nature, 2008. **455**(7213): p. 674-8.
200. Ishikawa, H., Z. Ma, and G.N. Barber, *STING regulates intracellular DNA-mediated, type I interferon-dependent innate immunity.* Nature, 2009. **461**(7265): p. 788-92.
201. Kato, A., S. Favoreto, Jr., P.C. Avila, and R.P. Schleimer, *TLR3- and Th2 cytokine-dependent production of thymic stromal lymphopoietin in human airway epithelial cells.* J Immunol, 2007. **179**(2): p. 1080-7.
202. Chow, K.T., M. Gale, Jr., and Y.M. Loo, *RIG-I and Other RNA Sensors in Antiviral Immunity.* Annu Rev Immunol, 2018. **36**: p. 667-694.

203. Le Bon, A., G. Schiavoni, G. D'Agostino, I. Gresser, F. Belardelli, and D.F. Tough, *Type i interferons potently enhance humoral immunity and can promote isotype switching by stimulating dendritic cells in vivo.* Immunity, 2001. **14**(4): p. 461-70.
204. Le Bon, A., N. Etchart, C. Rossmann, M. Ashton, S. Hou, D. Gewert, P. Borrow, and D.F. Tough, *Cross-priming of CD8+ T cells stimulated by virus-induced type I interferon.* Nat Immunol, 2003. **4**(10): p. 1009-15.
205. Wu, W., W. Zhang, E.S. Duggan, J.L. Booth, M.H. Zou, and J.P. Metcalf, *RIG-I and TLR3 are both required for maximum interferon induction by influenza virus in human lung alveolar epithelial cells.* Virology, 2015. **482**: p. 181-8.
206. Le Goffic, R., J. Pothlichet, D. Vitour, T. Fujita, E. Meurs, M. Chignard, and M. Si-Tahar, *Cutting Edge: Influenza A virus activates TLR3-dependent inflammatory and RIG-I-dependent antiviral responses in human lung epithelial cells.* J Immunol, 2007. **178**(6): p. 3368-72.
207. Pritchard, A.L., M.L. Carroll, J.G. Burel, O.J. White, S. Phipps, and J.W. Upham, *Innate IFNs and plasmacytoid dendritic cells constrain Th2 cytokine responses to rhinovirus: a regulatory mechanism with relevance to asthma.* J Immunol, 2012. **188**(12): p. 5898-905.
208. Duerr, C.U., C.D. McCarthy, B.C. Mindt, M. Rubio, A.P. Meli, J. Pothlichet, M.M. Eva, J.F. Gauchat, S.T. Qureshi, B.D. Mazer, K.L. Mossman, D. Malo, A.M. Gamero, S.M. Vidal, I.L. King, M. Sarfati, and J.H. Fritz, *Type I interferon restricts type 2 immunopathology through the regulation of group 2 innate lymphoid cells.* Nat Immunol, 2016. **17**(1): p. 65-75.
209. Swieter, M., W.A. Ghali, C. Rimmer, and D. Befus, *Interferon-alpha/beta inhibits IgE-dependent histamine release from rat mast cells.* Immunology, 1989. **66**(4): p. 606-10.
210. Paller, A.S., J.M. Spergel, P. Mina-Osorio, and A.D. Irvine, *The atopic march and atopic multimorbidity: Many trajectories, many pathways.* J Allergy Clin Immunol, 2019. **143**(1): p. 46-55.
211. Iikura, Y., C.K. Naspitz, H. Mikawa, S. Talaricoficho, M. Baba, D. Sole, and S. Nishima, *Prevention of asthma by ketotifen in infants with atopic dermatitis.* Ann Allergy, 1992. **68**(3): p. 233-6.
212. Carlsen, K.H., *Therapeutic strategies for allergic airways diseases.* Paediatr Respir Rev, 2004. **5**(1): p. 45-51.
213. Wahn, U., *Allergic factors associated with the development of asthma and the influence of cetirizine in a double-blind, randomised, placebo-controlled trial: first results of ETAC. Early Treatment of the Atopic Child.* Pediatr Allergy Immunol, 1998. **9**(3): p. 116-24.
214. Teach, S.J., M.A. Gill, A. Togias, C.A. Sorkness, S.J. Arbes, Jr., A. Calatroni, J.J. Wildfire, P.J. Gergen, R.T. Cohen, J.A. Pongracic, C.M. Kercsmar, G.K. Khurana Hershey, R.S. Gruchalla, A.H. Liu, E.M. Zoratti, M. Kattan, K.A. Grindle, J.E. Gern, W.W. Busse, and S.J. Szefler, *Preseasonal treatment with either omalizumab or an inhaled corticosteroid boost to prevent fall asthma exacerbations.* J Allergy Clin Immunol, 2015. **136**(6): p. 1476-1485.
215. Djukanovic, R., T. Harrison, S.L. Johnston, F. Gabbay, P. Wark, N.C. Thomson, R. Niven, D. Singh, H.K. Reddel, D.E. Davies, R. Marsden, C. Boxall, S. Dudley, V. Plagnol, S.T. Holgate, P. Monk, and I.S. Group, *The effect of inhaled IFN-beta on worsening of*

asthma symptoms caused by viral infections. A randomized trial. Am J Respir Crit Care Med, 2014. **190**(2): p. 145-54.
216. Monk, P.D., R.J. Marsden, V.J. Tear, J. Brookes, T.N. Batten, M. Mankowski, F.J. Gabbay, D.E. Davies, S.T. Holgate, L.P. Ho, T. Clark, R. Djukanovic, T.M.A. Wilkinson, and C.-S.G. Inhaled Interferon Beta, *Safety and efficacy of inhaled nebulised interferon beta-1a (SNG001) for treatment of SARS-CoV-2 infection: a randomised, double-blind, placebo-controlled, phase 2 trial.* Lancet Respir Med, 2021. **9**(2): p. 196-206.
217. Simons, F.E., *Is antihistamine (H1-receptor antagonist) therapy useful in clinical asthma?* Clin Exp Allergy, 1999. **29 Suppl 3**: p. 98-104.
218. Graham, A.C., K.M. Hilmer, J.M. Zickovich, and J.J. Obar, *Inflammatory response of mast cells during influenza A virus infection is mediated by active infection and RIG-I signaling.* J Immunol, 2013. **190**(9): p. 4676-84.
219. Lee, I.H., H.S. Kim, and S.H. Seo, *Porcine mast cells infected with H1N1 influenza virus release histamine and inflammatory cytokines and chemokines.* Arch Virol, 2017. **162**(4): p. 1067-1071.
220. Jang, Y., M. Jin, and S.H. Seo, *Histamine contributes to severe pneumonia in pigs infected with 2009 pandemic H1N1 influenza virus.* Arch Virol, 2018. **163**(11): p. 3015-3022.
221. Hu, Y., Y. Jin, D. Han, G. Zhang, S. Cao, J. Xie, J. Xue, Y. Li, D. Meng, X. Fan, L.Q. Sun, and M. Wang, *Mast cell-induced lung injury in mice infected with H5N1 influenza virus.* J Virol, 2012. **86**(6): p. 3347-56.
222. Ivashkiv, L.B. and L.T. Donlin, *Regulation of type I interferon responses.* Nat Rev Immunol, 2014. **14**(1): p. 36-49.
223. Mathavarajah, S., J. Salsman, and G. Dellaire, *An emerging role for calcium signalling in innate and autoimmunity via the cGAS-STING axis.* Cytokine Growth Factor Rev, 2019. **50**: p. 43-51.
224. Kwon, D., H. Sesaki, and S.J. Kang, *Intracellular calcium is a rheostat for the STING signaling pathway.* Biochem Biophys Res Commun, 2018. **500**(2): p. 497-503.
225. Kuo, C.H., S.N. Yang, Y.G. Tsai, C.C. Hsieh, W.T. Liao, L.C. Chen, M.S. Lee, H.F. Kuo, C.H. Lin, and C.H. Hung, *Long-acting beta2-adrenoreceptor agonists suppress type 1 interferon expression in human plasmacytoid dendritic cells via epigenetic regulation.* Pulm Pharmacol Ther, 2018. **48**: p. 37-45.
226. Li, M., P. Xia, Y. Du, S. Liu, G. Huang, J. Chen, H. Zhang, N. Hou, X. Cheng, L. Zhou, P. Li, X. Yang, and Z. Fan, *T-cell immunoglobulin and ITIM domain (TIGIT) receptor/poliovirus receptor (PVR) ligand engagement suppresses interferon-gamma production of natural killer cells via beta-arrestin 2-mediated negative signaling.* J Biol Chem, 2014. **289**(25): p. 17647-57.
227. An, H., W. Zhao, J. Hou, Y. Zhang, Y. Xie, Y. Zheng, H. Xu, C. Qian, J. Zhou, Y. Yu, S. Liu, G. Feng, and X. Cao, *SHP-2 phosphatase negatively regulates the TRIF adaptor protein-dependent type I interferon and proinflammatory cytokine production.* Immunity, 2006. **25**(6): p. 919-28.
228. Zhan, Z., H. Cao, X. Xie, L. Yang, P. Zhang, Y. Chen, H. Fan, Z. Liu, and X. Liu, *Phosphatase PP4 Negatively Regulates Type I IFN Production and Antiviral Innate Immunity by Dephosphorylating and Deactivating TBK1.* J Immunol, 2015. **195**(8): p. 3849-57.

229. Takasaki, J., T. Saito, M. Taniguchi, T. Kawasaki, Y. Moritani, K. Hayashi, and M. Kobori, *A novel Galphaq/11-selective inhibitor.* J Biol Chem, 2004. **279**(46): p. 47438-45.
230. Sham, D., U.V. Wesley, M. Hristova, and A. van der Vliet, *ATP-mediated transactivation of the epidermal growth factor receptor in airway epithelial cells involves DUOX1-dependent oxidation of Src and ADAM17.* PLoS One, 2013. **8**(1): p. e54391.
231. Han, Y., C.G. Caday, A. Nanda, W.K. Cavenee, and H.J. Huang, *Tyrphostin AG 1478 preferentially inhibits human glioma cells expressing truncated rather than wild-type epidermal growth factor receptors.* Cancer Res, 1996. **56**(17): p. 3859-61.
232. McMahon, D.B., A.D. Workman, M.A. Kohanski, R.M. Carey, J.R. Freund, B.M. Hariri, B. Chen, L.J. Doghramji, N.D. Adappa, J.N. Palmer, D.W. Kennedy, and R.J. Lee, *Protease-activated receptor 2 activates airway apical membrane chloride permeability and increases ciliary beating.* FASEB J, 2018. **32**(1): p. 155-167.
233. Paradiso, A.M., C.M. Ribeiro, and R.C. Boucher, *Polarized signaling via purinoceptors in normal and cystic fibrosis airway epithelia.* J Gen Physiol, 2001. **117**(1): p. 53-67.
234. Ribeiro, C.M., A.M. Paradiso, M.A. Carew, S.B. Shears, and R.C. Boucher, *Cystic fibrosis airway epithelial Ca2+ i signaling: the mechanism for the larger agonist-mediated Ca2+ i signals in human cystic fibrosis airway epithelia.* J Biol Chem, 2005. **280**(11): p. 10202-9.
235. Zhu, Y., L.H. Abdullah, S.P. Doyle, K. Nguyen, C.M. Ribeiro, P.A. Vasquez, M.G. Forest, M.I. Lethem, B.F. Dickey, and C.W. Davis, *Baseline Goblet Cell Mucin Secretion in the Airways Exceeds Stimulated Secretion over Extended Time Periods, and Is Sensitive to Shear Stress and Intracellular Mucin Stores.* PLoS One, 2015. **10**(5): p. e0127267.
236. Abdullah, L.H., C. Wolber, M. Kesimer, J.K. Sheehan, and C.W. Davis, *Studying mucin secretion from human bronchial epithelial cell primary cultures.* Methods Mol Biol, 2012. **842**: p. 259-77.
237. Ciencewicki, J.M., L.E. Brighton, and I. Jaspers, *Localization of type I interferon receptor limits interferon-induced TLR3 in epithelial cells.* J Interferon Cytokine Res, 2009. **29**(5): p. 289-97.
238. Martinez-Anton, A., M. Sokolowska, S. Kern, A.S. Davis, S. Alsaaty, J.K. Taubenberger, J. Sun, R. Cai, R.L. Danner, M. Eberlein, C. Logun, and J.H. Shelhamer, *Changes in microRNA and mRNA expression with differentiation of human bronchial epithelial cells.* Am J Respir Cell Mol Biol, 2013. **49**(3): p. 384-95.
239. Carey, R.M., J.R. Freund, B.M. Hariri, N.D. Adappa, J.N. Palmer, and R.J. Lee, *Polarization of protease-activated receptor 2 (PAR-2) signaling is altered during airway epithelial remodeling and deciliation.* J Biol Chem, 2020. **295**(19): p. 6721-6740.
240. Wang, Y., L. Lin, and C. Zheng, *Downregulation of Orai1 expression in the airway alleviates murine allergic rhinitis.* Exp Mol Med, 2012. **44**(3): p. 177-90.
241. Wen, L., S. Voronina, M.A. Javed, M. Awais, P. Szatmary, D. Latawiec, M. Chvanov, D. Collier, W. Huang, J. Barrett, M. Begg, K. Stauderman, J. Roos, S. Grigoryev, S. Ramos, E. Rogers, J. Whitten, G. Velicelebi, M. Dunn, A.V. Tepikin, D.N. Criddle, and R. Sutton, *Inhibitors of ORAI1 Prevent Cytosolic Calcium-Associated Injury of Human Pancreatic Acinar Cells and Acute Pancreatitis in 3 Mouse Models.* Gastroenterology, 2015. **149**(2): p. 481-92 e7.

242. Coden, M.E., L.F. Loffredo, H. Abdala-Valencia, and S. Berdnikovs, *Comparative Study of SARS-CoV-2, SARS-CoV-1, MERS-CoV, HCoV-229E and Influenza Host Gene Expression in Asthma: Importance of Sex, Disease Severity, and Epithelial Heterogeneity.* Viruses, 2021. **13**(6).
243. Connelly, A.R., B.M. Jeong, M.E. Coden, J.Y. Cao, T. Chirkova, C. Rosas-Salazar, J.Y. Cephus, L.J. Anderson, D.C. Newcomb, T.V. Hartert, and S. Berdnikovs, *Metabolic Reprogramming of Nasal Airway Epithelial Cells Following Infant Respiratory Syncytial Virus Infection.* Viruses, 2021. **13**(10).
244. Lahey, L.J., R.E. Mardjuki, X. Wen, G.T. Hess, C. Ritchie, J.A. Carozza, V. Bohnert, M. Maduke, M.C. Bassik, and L. Li, *LRRC8A:C/E Heteromeric Channels Are Ubiquitous Transporters of cGAMP.* Mol Cell, 2020. **80**(4): p. 578-591 e5.
245. Zhou, C., X. Chen, R. Planells-Cases, J. Chu, L. Wang, L. Cao, Z. Li, K.I. Lopez-Cayuqueo, Y. Xie, S. Ye, X. Wang, F. Ullrich, S. Ma, Y. Fang, X. Zhang, Z. Qian, X. Liang, S.Q. Cai, Z. Jiang, D. Zhou, Q. Leng, T.S. Xiao, K. Lan, J. Yang, H. Li, C. Peng, Z. Qiu, T.J. Jentsch, and H. Xiao, *Transfer of cGAMP into Bystander Cells via LRRC8 Volume-Regulated Anion Channels Augments STING-Mediated Interferon Responses and Anti-viral Immunity.* Immunity, 2020. **52**(5): p. 767-781 e6.
246. Morales-Nebreda, L.I., M.R. Rogel, J.L. Eisenberg, K.J. Hamill, S. Soberanes, R. Nigdelioglu, M. Chi, T. Cho, K.A. Radigan, K.M. Ridge, A.V. Misharin, A. Woychek, S. Hopkinson, H. Perlman, G.M. Mutlu, A. Pardo, M. Selman, J.C. Jones, and G.R. Budinger, *Lung-specific loss of alpha3 laminin worsens bleomycin-induced pulmonary fibrosis.* Am J Respir Cell Mol Biol, 2015. **52**(4): p. 503-12.
247. Jeannotte, L., J. Aubin, S. Bourque, M. Lemieux, S. Montaron, and A. Provencher St-Pierre, *Unsuspected effects of a lung-specific Cre deleter mouse line.* Genesis, 2011. **49**(3): p. 152-9.